GDANSK UNIVERSITY OF TECHNOLOGY
FACULTY OF OCEAN ENGINEERING AND SHIP TECHNOLOGY
SECTION OF TRANSPORT TECHNICAL MEANS
OF TRANSPORT COMMITEE OF POLISH ACADEMY OF SCIENCES
UTILITY FOUNDATIONS SECTION
OF MECHANICAL ENGINEERING COMMITTEE OF POLISH ACADEMY OF SCIENCE

ISSN 1231 – 3998
ISBN 83 – 900666 – 2 – 9

Journal of

POLISH CIMAC

ENERGETIC ASPECTS

Vol. 3 **No. 1**

Gdansk, 2008

Science publication of Editorial Advisory Board of POLISH CIMAC

Editorial Office:

GDANSK UNIVERSITY OF TECHNOLOGY
Faculty of Ocean Engineering and Ship Technology
Department of Ship Power Plants
G. Narutowicza 11/12 80-952 GDANSK POLAND
tel. +48 58 347 29 73, e – mail: sek4oce@pg.gda.pl

This journal is devoted to designing of diesel engines, gas turbines and ships' power transmission systems containing these engines and also machines and other appliances necessary to keep these engines in movement with special regard to their energetic and pro-ecological properties and also their durability, reliability, diagnostics and safety of their work and operation of diesel engines, gas turbines and also machines and other appliances necessary to keep these engines in movement with special regard to their energetic and pro-ecological properties, their durability, reliability, diagnostics and safety of their work, and, above all, rational (and optimal) control of the processes of their operation and specially rational service works (including control and diagnosing systems), analysing of properties and treatment of liquid fuels and lubricating oils, etc.

All papers have been reviewed

ISSN 1231 – 3998
ISBN 83 – 900666 – 2 – 9

Printed in Poland

CONTENTS

Adamkiewicz A., Fydrych J.: OPERATION PARAMETER MONITORING AS A CONDITION TO CONTROLLING THE OPERATION OF THE MAIN POWER SYSTEM …….. 7

Krzysztof Balawender, Hubert Kuszewski, Kazimierz Lejda, Adam Ustrzycki: THE INFLUENCE OF MUTUAL ANGLE POSITION OF MAIN, PILOT AND PREINJECTION DOSE ON FUEL DOSING IN COMMON RAIL SYSTEM …….. 17

Bocheński D.: OPERATIONAL LOADS OF DIESEL ENGINES ON TRAILING SUCTION HOPPER DREDGERS IN THEIR MAIN SERVICE STATES ……. 25

Bocheński D.: OPERATIONAL LOADS OF DREDGE PUMPS IN THEIR BASIC SERVICE STATES ON SELECTED TYPES OF DREDGERS ……. 33

Borkowski T.: INVESTIGATIONS OF EXHAUST EMISSION OF BIOGAS SI ENGINE IN SEWAGE ELECTRIC GENERATOR PLANT …….. 41

Bzura P.: ANALYSIS AND ASSESSMENT OF THE ACOUSTIC EMISSION SUITABILITY FOR DETERMINATION OF THE ENERGY STATES OF A TRIBOLOGICAL SYSTEM IN THE FORM OF A FOUR-BALL TESTER FRICTION NODE ……. 53

Chybowski L.: ASSESSMENT OF MARINE ENGINES TORQUE LOAD WITHOUT USING OF THE TORQUEMETER …… 59

Dymarski C., Rolka G.: FOUR-STROKE ENGINE WITH CENTRAL LOCATED, DIVIDED COMBUSTION CHAMBER …….. 69

Gardulski J.: PROBLEMS CONNECTED WITH MINIMIZATION OF INTERNAL VIBRATION AND NOISE GENERATED BY POWER UNITS IN SHIPS ……. 77

Girtler J.: QUANTITATIVE INTERPRETATION OF ENERGY-BASED SYSTEMS AND INDEX OF THEIR RELIABILITY …… 87

Matuszak Z., Nicewicz G.: ASSESSMENT OF EXCESS POWER FACTOR IN MARINE GENERATING SETS …… 95

Michalski R.: THE APPLICATION OF THE EXERGETIC ANALYSIS IN DESIGNING OF WASTE ENERGY RECOVERY SYSTEMSIN MARINE DIESEL POWER PLANTS ……. 103

Monieta J., Lorek Ł.: RESEARCHES OF FRICTION FORCE OF INJECTOR NEEDLE IN INJECTOR BODIES OF MARINE DIESEL ENGINES IN THE PRESENCE OF LUBRICATING COMPOUND …….. 111

Myśków J., Borkowski T.: NON-THERMAL PLASMA REACTOR WORKING WITH EXHAUST GAS SYSTEM IN MARINE DIESEL ENGINE ……. 123

Piaseczny L., Kniaziewicz T.: STOCHASTIC MODELS OF EMISSION OF TOXIC COMPOUNDS IN MARINE ENGINES EXHAUSTS ……. 129

Piaseczny L., Władyka W.: EFFECTS OF THE THERMAL ACTIVATION OF FUEL ON ENERGY PARAMETERS AND TOXICITY OF COMBUSTION GASES IN THE MARINE DIESEL ENGINE ……. 139

Rosłanowski J.: AGGREGATION OF ENTER VARIABLES IN NEURON MODEL OF POWER REQUIRED FOR THE SEAGOING VESSEL BY MEANS OF DIMENSIONAL ANALYSIS ……. 151

Rudnicki J.: LOADS OF SHIP MAIN DIESEL ENGINE IN THE ASPECT OF PRACTICAL ASSESSMENT OF ITS OPERATION ……... 157

Walkowski M.: THE FUEL FLOW MODELLING IN THE FUEL PIPE IN MARINE ENGINE WITH CONSIDERING THE WAVE PHENOMENA …….. 167

Wirkowski P.: RESEARCH OF VARIATION OF GAS TURBINE ENGINE WORK PARAMETERS CHANGES EQUIPPED WITH CHANGEABLE GEOMETRY OF AXIAL COMPRESSOR FLOW PASSAGE ……... 177

Zeńczak W.: INVESTIGATION OF FLUIDIZED BED OF THE PHYSICAL MODEL OF THE MARINE FLUIDIZED BED BOILER …… 193

Żółtowski B.: FUME EMISSIONS IN INVESTIGATIONS OF EXPLOITATION OF DIESEL ENGINES 191

Journal of POLISH CIMAC

Faculty of Ocean Engineering & Ship Technology
GDAŃSK UNIVERSITY OF TECHNOLOGY

OPERATION PARAMETER MONITORING AS A CONDITION TO CONTROLLING THE OPERATION OF THE MAIN POWER SYSTEM

Andrzej Adamkiewicz

Szczecin Maritime Academy
Faculty of Mechanical Engineering
Institute of Technical Operation of Marine Power Plants
Wały Chrobrego 1-2, 70-500 Szczecin, Poland
e-mail: andrzej.adamkiewicz@am.szczecin.pl

Janusz Fydrych

Euro Africa Shipping Lines Co Ltd., Szczecin

Abstrakt

This paper shows possibilities and effectiveness of application of a monitoring system to control an automatic regulation system and the main power system of a chosen ship. It presents an analysis of operation states where unstable operation of the shaft takes place and there are black-outs of shaft current generators from the ship power system due to faults. It has been indicated that the possibility to follow the changes of operation parameter values and their characteristics enables a current evaluation of power processes on-line, and in such a case installation of sophisticated diagnostic systems is not vital. An example of an operational decision taken on the basis of the presented control system has been presented.

Keywords: *monitoring, main power system, diesel engine, controlling, operation parameters*

1. Introduction

Destination of a ship power system is to transform energy supplied in the fuel into mechanical operation indispensable to make the vessel sail at a defined speed and to provide electricity and heat for technological and social purposes. A ship is an independent unit which cannot be backed-up during operation by external services. Therefore, the problem of correct functioning of the elements of the main power system at voyage is very important.

Contemporary ship power systems are equipped in control-monitoring systems which transform the measured physical values of the power system into electrical signals. It helps with the transformation of signals whose coupling with automatic regulation system and control processes is monitored for the diagnostics purposes.

This paper justifies the need to monitor operation parameters of the main power system in operational states manifesting non-designed operation of its element such as significant change of rotational speed of the propeller, and black-outs of the shaft current generator, in order to find their sources [6].

2. The structure of the system monitoring operational parameters of the ship main power system

Fulfilling the requirements of the automation class, a ship power system is customized to cooperate with the system monitoring operation parameters. Thus the system becomes a basic

source of information for functional diagnosing and controlling the operation of the ship main power system [3, 5]

One of such tools is a system for remote control automatic regulation of the main engine, ABB-Remote Control System – ABB Marine Rotterdam, which together with a subsystem to monitor operational parameters, NORIS – German, and a system to control the operation of propeller and the FAMP III engine are installed on the container ship [1, 4]. It is an open system prepared to serve a one- or multi-engine power unit, the remote control of the propeller, the turbocompressor, a boiler run on thermal oil, a shaft current generator, and mechanisms cooperating with the main engines, such as: the main engine rotational speed regulator in a system coupled with the propeller, supplying air outlet valve, exhaust valve and the control of the temperature of supplying air.

In the described case the system was customized for a one-engine intermediate power system with an in-line diesel engine of the B&W MANN 8L56 type with the power of 3840 kW and rotational speed of the shaft – 750 rev/min, with a suspended shaft current generator equipped in an electronic rotational speed regulator [1, 2]. Nominal rotational speed of the propeller shaft is 147 rev/min.

Figure 1 presents a diagram of signal flow and transformation between rotational speed regulator of the main engine, the unit controlling the control pitch propeller (CCP) FAMP III and the NORIS monitoring system [1, 4]. The central control block of the automatic regulation sends the signals of the measured values to working subsystems NORIS. The system was programmed as a standard ABB Advant Controller unit to serve 110 processes. Constant monitoring of chosen parameters enables their graphic presentation as a time function with simultaneous recording of runs of the graphic parameters. Frequency of sampling and recording are set by the operator in the range from 1 to 1200 seconds, while the graphic runs can be edited in the time range from 5 minutes to 5 hours.

3. Detection of faults in the ship main power system

Figure 2 presents the runs of operation parameters of the main power system working with the turned-on shaft current generator recorded by NORIS within 2 hours. Disturbances in the main engine operation were manifested first of all as a short lasting change in rotational speed of the main engine shaft with black-outs of the shaft current generator from the rail of the main dashboard [5, 6]. The stated lack of rotational speed stability of the engine shaft was used for the analysis to find the causes of faulty operation of the ship main power system.

Current frequency disturbance accepted by classification societies for operation at constant rotational speed is (2 – 2.5)Hz. It is the condition allowing synchronization of the shaft current generator with the net and its coupling with the net. An alarming value for the shaft current generator, in regard to the frequencies generated for the net, is exceeding the 50Hz value by +/– (2.5 – 3/2)Hz. It corresponds with the rotational speed change by (5 – 6.4)% of the nominal rotational speed of the engine shaft. The limiting value at which the black-out of the shaft current generator from the main dashboard occurs at frequency fluctuations of +/– (3.5 – 3.8)Hz, which is equal to +/– (7 – 7.6)% corresponding to the change of rotational speed of (52.5 – 57.0) rev/min [4, 5]. These conditions are met by a faultlessly operating fuel supply system and the regulator of the rotational speed of the main engine at a technically usable power system.

Among the recorded runs the following showed changes in stability:1 – rotational speed of the engine shaft; 2 – fuel pressure and 3 – pressure of the supplying air. The remaining parameters did not show any significant changes. Time of disturbances was about 7 seconds. The decrease in the shaft rotational speed was so high (by 72 rev/min)that the recorded case was accompanied by shaft current generator black-out from the main dashboard. The immediate change of supplying fuel from the heavy one (International Fuel Oil 180 – IFO 180) to diesel oil (Marine Gas Oil _MGO) –

green line in figure 2 – brought about, for some time, stable operation of the power system with correct values of operational parameters.

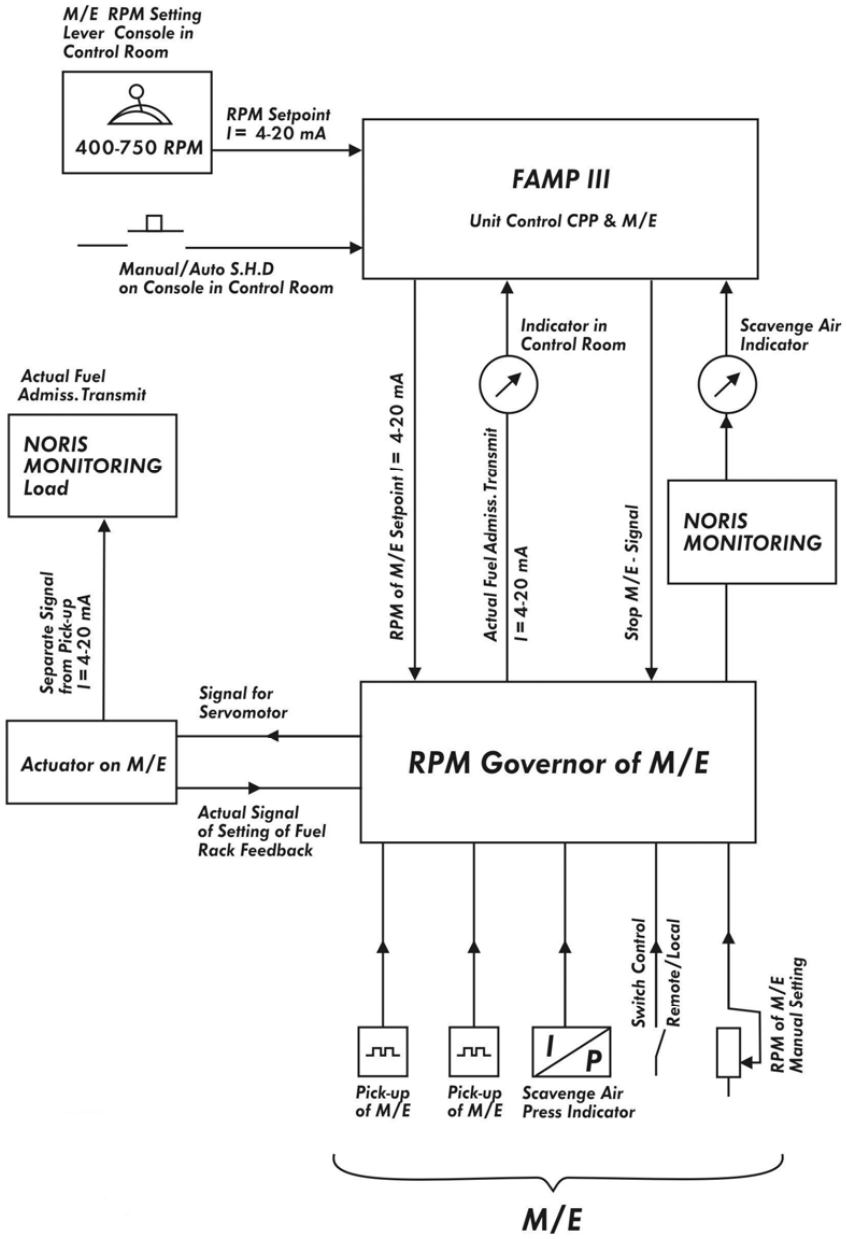

Fig. 1. A diagram of signal flow and transformation between rotational speed regulator of the main engine, the unit controlling the CCP propeller FAMP III and the NORIS monitoring system

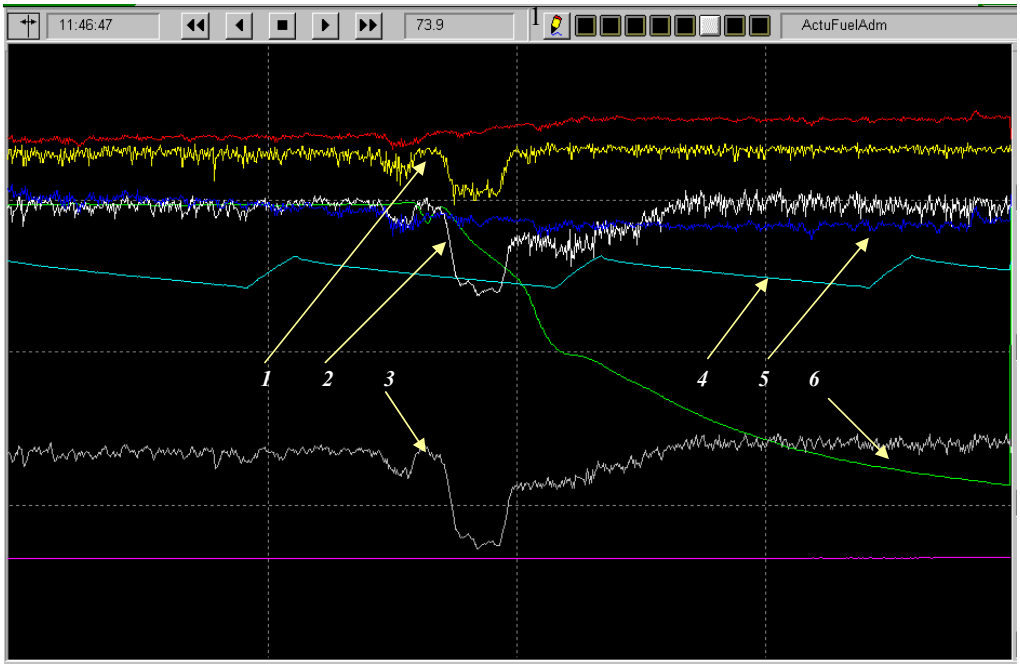

Fig. 2. Runs of operation parameters of the main power system recorded by NORIS
1 – rotational speed of main engine shaft; 2 – fuel board set-up; 3 – pressure of the supplying air;
4 – pressure of the controlling air; 5 – set up angle of the CCP propeller; 6 – temperature change of the fuel feeding the main engine at the change of fuel from the heavy one (IFO 180) to diesel oil (MGO)

As there were no external disturbances(e.g the weather, controlled load increase of the main engine) and there were no signals of internal disturbances (e.g faults in the fuel preparation unit) influencing the operation of the power unit, monitoring was directed towards operation quality of the electronic rotational speed control system (RPM Governor of ME), main engine overload controlled /monitored by NORIS MONITORING Load) block and connections between the CCP propeller control block and the main engine. (Unit Control CCP&ME, FAMP III).After stabilizing the operation of the main power system, again heavy fuel (IFO 180) was used whose temperature change can be seen in Fig 3 as green line 6 (with the two-hour edition time).

Stable operation of the ship main power unit lasted for a few days until another black-out of the shaft current generator from the main dashboard took place. In that case/situation control of signals from the CCP propeller control system and the FAMP III engine to the electronic rotational speed control system (RPM Governor of ME) was carried out, according to Fig. 1.

Their stability is guaranteed by stable operation of the system (constant rotational speed of engine shafts and shaft current generator and unchanged position of the CCP propeller of the main power system). Their values determine the response of the regulator- the change of set-up of the fuel board ensuring the required filling of the high pressure fuel pumps(Acctual Fuel Admiss. Transmit). In the studied operation state of the system monitoring of signals indicated correct values and runs of signals coming from the CCP propeller control system and the main engine (Unit Control CCP &ME, FAMP III).

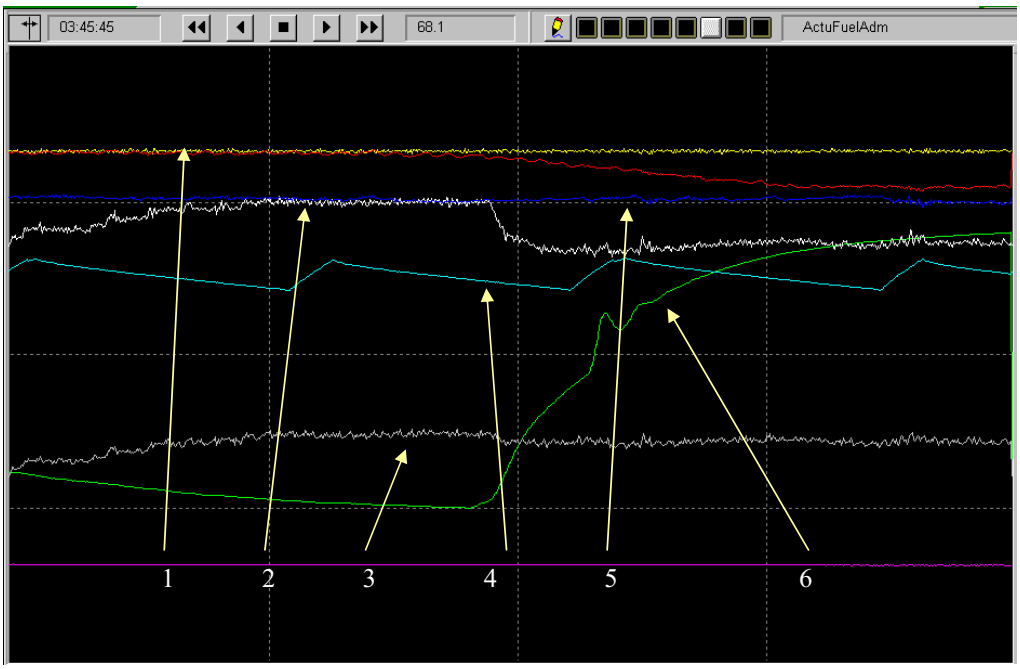

Fig. 3. Runs of operation parameters of the main power system recorded by NORIS at the come back to supplying with heavy fuel where: 1–2 as in Fig. 2.; 6 – the temperature change of the fuel supplying the main engine at switching on to heavy fuel

4. Analysis of causes of unstable operation of the main engine

The search for causes of the main engine unstable operation was carried out throughout a series of check-ups and preventive maintenance services. Detector positions for the control of rotational speed of the main engine shaft were corrected, the cooler of the supplying air was washed, the quality of operation of the hydraulic system of the CCP propeller of the ship main power system was check as well as the filling and venting of the thermo-fuel boiler. Regulation values of the set-up were checked and the time constant of the regulator was decreased. The run of parameters recorded within 2 hours was shown in Fig. 4. Although the picture was more dynamic, yet a relatively safe range of rotational speed of the main engine required for cooperation with the shaft current generator was maintained

Despite the undertaken means and switching-on to diesel fuel (MGO) when sailing at storm, the regulator worked too dynamically and its quick reactions caused instability of the rotational speed of the shaft and black-outs of the shaft current generator from the main dashboard still occurred. Such a condition and operation was unfavourable for the engine but directed the search for the cause of the lack of operational stability to the quality of functioning of the engine fuel unit. The causes of unstable operation of the main engine should be found in the faulty filling of fuel pumps or disturbances in the quality of fuel combustion in the engine.

The equipment for the high pressure fuel was checked. Faults in two precision pairs (shown in Fig. 5. and 6.) were found. Fig. 5. shows a defect on the on the working edge of the precision pair of the plunger.

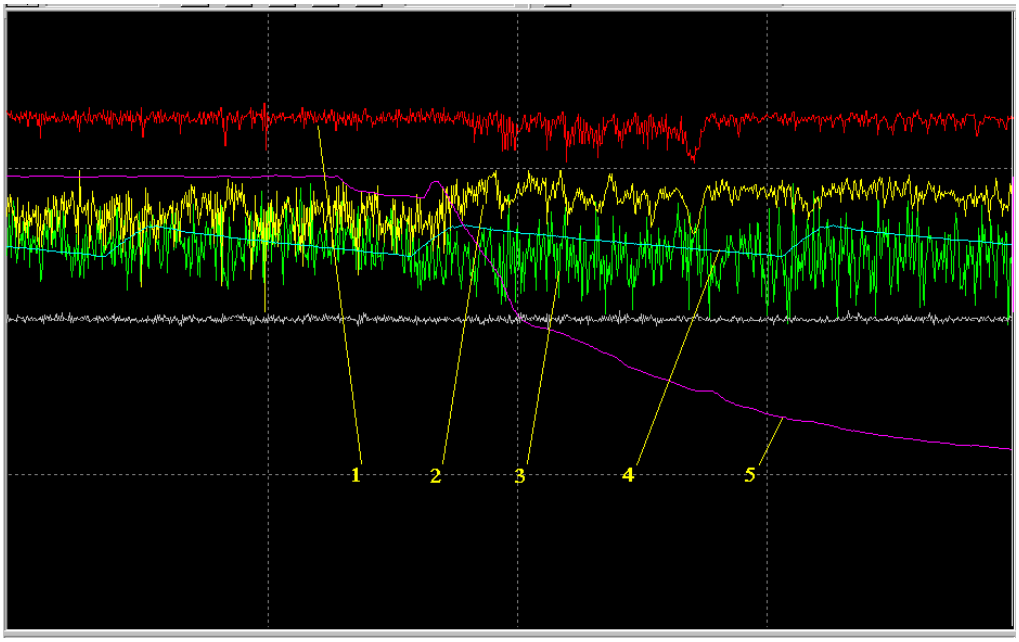

Fig. 4. Runs of operation parameters of the main power system recorded by NORIS after preventive maintenance services and corrections of set-ups:
1 – rotational speed of the main engine shaft; 2 – fuel board set-up; 3 – pressure of the fuel supplying the main engine; 4 – pressure of the controlling air; 5 – temperature of the fuel feeding the engine

Fig. 5. Defect on the working edge of the precision pair of the plunger of the fuel pump (point A)

Figure 6 shows discolouring of working surfaces of another precision pair_due to too high temperature as an effect of seizure. The faulty elements of the fuel pump were replaced with new ones. To check the effectiveness of maintenance services of the fuel equipment, resolution of edition of its recorded parameters was increased from the so-far 2 hours to 5 minutes. The picture of a screen test recording is shown in Fig 7 with the black-out and switching from heavy fuel (IFO 180) to diesel oil MGO.

Fig 6 Discoloring of working surfaces of another precision pair due to too high temperature (surface B)

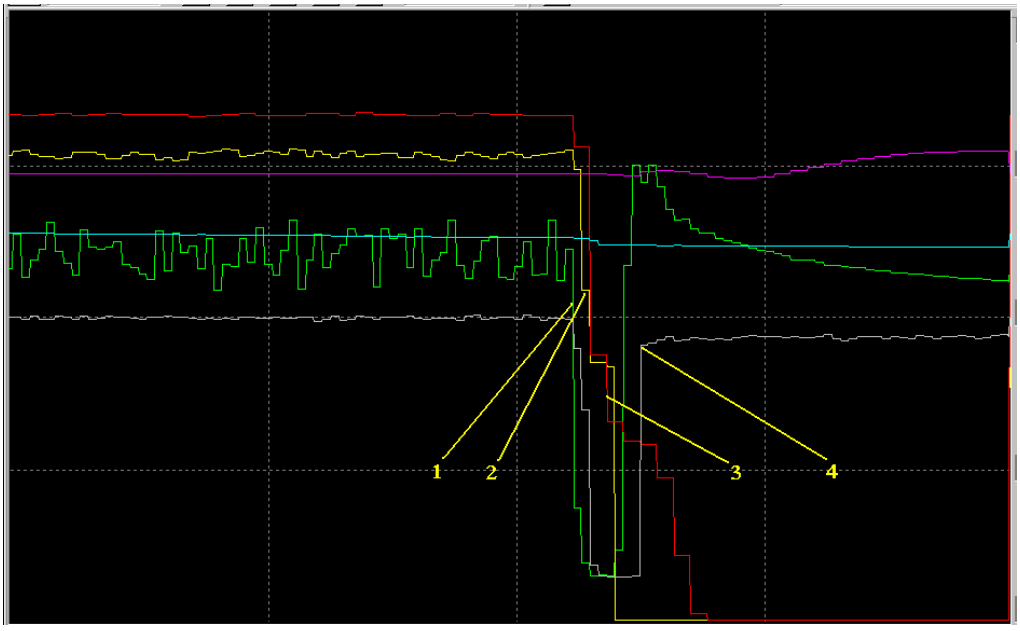

Fig. 7. Runs of operation parameters of the main power system recorded by NORIS at a black-out and with the heavy fuel (IFO 180) after servicing fuel equipment:
1 – pressure of supplying fuel; 2-fuel board set-up; 3-rotational speed of the main engine shaft; 4- pressure of the supplying air (time of edition of the recording on the monitor – 5min)

During the self- switch-off of the shaft current generator from the net, significant fluctuations of fuel pressure and decreases of pressure of the supplying air were observed. The system was unstable as if it had not responded to the programme of engine regulation n=idem (RPM constant) not taking account of the sets-up of the CCP propeller. The system searching for a new state of stable operation reduced the set-up of the fuel pump to the current load (pressure of the supplying air). In this case the runs of the following parameters were incorrect: pressure of the fuel feeding the engine, rotational speed of the engine shaft and the pressure of the supplying air. This result indicated that the unstable operation of the engine was due to the faulty operation of the engine fuel system.

With the checked-up fuel equipment, clean air and fuel filters and correct operation of the fuel preparation block, unstable operation of the main engine was still recorded. Thus its cause had to be the quality of the burnt fuel IFO 180. This assumption was supported by the fact that re-switching to MGO fuel resulted in a stable operation of the engine.

Summing up the results of fuel equipment servicing i.e. the recorded runs of operation parameters after exchanging IFO 180 fuel with MGO fuel, it can be stated that the burnt fuel did not meet the requirements of the engine manufacturer.

Fractional analysis of the applied heavy fuel IFO 180 showed its heterogeneity and tendencies to forming layers. After introducing "new" fuel, the described symptoms of unstable operation of the main power system disappeared. As a consequence sailing with a switched-on shaft generator even at stormy weather or with the waves from the stern was not a problem. The presented in Figure 8 runs of operation parameters recorded after exchanging the heavy fuel IFO 180 with the "new" one (edition time of runs on the screen –2 hours) are an evidence of removing the instability of operation of the main power system

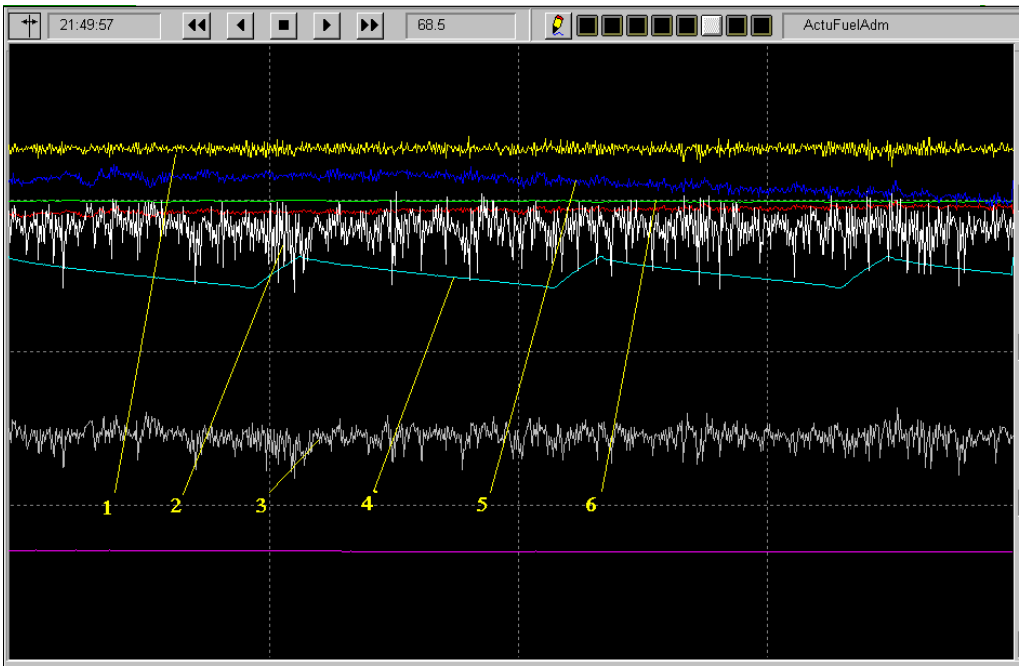

Fig. 8. Runs of operation parameters of the main power system recorded by NORIS: 1 – rotational speed of the main engine shaft; 2 – fuel boar set-up; 3 – pressure of the supplying air; 4 – pressure of the controlling air; 5 – set- up angle of the control pitch propeller; 6 - temperature change of the fuel supplying the main engine after using the "new" heavy fuel IFO 180 ("new" IFO 180)

Although the recorded run of the set up of the fuel board indicates a dynamic regulation of the main engine, stability of the rotational speed of the main engine shaft was unquestioned, met the requirements of the classification society and enabled further safe operation of the ship power system.

5. Summing up and final conclusions

The presented monitoring system of chosen operation parameters of the main power system enabled measurements, recording and evaluation of their runs/disturbances in the main engine fuel system – fuel pressure (Actul Fuel Admission Transmit) and changes of runs of parameter values which were the response of the automatic regulation system, in particular the pressure of supplying air, exhaust temperature, load of the main engine taking into account the controlled of the wings of

the CCP propeller. Thanks to them it was possible not only to state the instability of the system but also to find its causes.

Constant monitoring of proper functioning of the ship main power system carried out by the on-board monitoring system enabled regulation of set-ups in the control system of the power unit and its instant diagnosis. This diagnosing supports making maintenance decisions preventing the occurrence of more significant faults and break-downs. Supplying information in successive procedures of diagnostic concluding, a monitoring system became a tool in operation process control justifying its utilitarian position on contemporary ships.

References

[1] ABB Marine Roterdam, *Files on technical –motion control of the main power system with a propeller on the m/s Topas vessel*

[2] Krupa, A., *Electronically regulated engines, advancement, implementations.* Silniki Spalinowe. Polskie Towarzystwo Naukowe Silników Spalinowych, Nr.1/2004(118), Marzec 2004, Rok XLIII, s.20-27 (in Polish).

[3] Łosiewicz, Z., *Operational qualities of contemporary diagnosing systems for ship diesel engines on the example of CoCoS and CBM systems* W zbiorze „Wybrane problemy projektowania i eksploatacji siłowni okrętowych". Materiały XXVII Sympozjum Siłowni Okrętowych, Wydział Techniki Morskiej, Politechnika Szczecińska, Szczecin 2006, s.199-208 (in Polish).

[4] NORIS Germany, *Manual for the control system of the main power system operation for m/s Topaz.*

[5] Szcześniak, J., *Digital regulators of rotational speed of ship engines.* Fundacja Rozwoju Wyższej Szkoły Morskiej w Szczecinie, Szczecin 2003 (in Polish).

[6] Włodarski, J., K., Operational states of diesel ship engines. WyższaSzkoła Morska,Gdynia 2001 (in Polish).

Journal of POLISH CIMAC

Faculty of Ocean Engineering & Ship Technology
GDAŃSK UNIVERSITY OF TECHNOLOGY

THE INFLUENCE OF MUTUAL ANGLE POSITION OF MAIN, PILOT AND PREINJECTION DOSE ON FUEL DOSING IN COMMON RAIL SYSTEM

Krzysztof Balawender, Hubert Kuszewski, Kazimierz Lejda, Adam Ustrzycki

Rzeszow University of Technology
Al. Powstańców Warszawy 8, 35-959 Rzeszów, Poland
tel.: +48 17 8651588, +48 17 8651582, +48 17 8651524, +48 17 8651531
fax: +48 17 8543112
e-mail: kbalawen@prz.edu.pl, hkuszews@prz.edu.pl, klejda@prz.edu.pl, austrzyc@prz.edu.pl

Abstract

The common rail fuel supply systems on account of flexibility at injection characteristic shaping, are the most frequently applied fuel supply solution in Diesel engines. The most essential parameters, which have the effect on fuel dosing precision are injection duration, rail pressure and fuel temperature. Also there are other factors, which can cause fuel dosing errors. It might be also other factors caused by specific working of fuel system. The split of fuel dose into a few parts (for example into pilot dose, preinjection dose and main dose) can cause pressure fluctuation in rail and also in the whole system. Next this can cause a chang of set fuel dose. In the article research results connected with influence of mutual angle position of main, pilot and preinjection dose on the total fuel dose. The researches were conducted with test stand equipped with test bench Bosch EPS-815 with electronic measuring of fuel dose. Control of injector was realized by using worked out controller which enables to split of fuel dose into three parts.

Key words:: *Common Rail, fuel injection, injection control, injection pressure, fuel dose*

1. Introduction

The development of compression ignition engines is oriented to ecological requirement, especially in the field of emission limit of nitric oxides and particulate matters. The designers of those engine types have to be up to the challenge resulting from need to limit of fuel consumption at simultaneous to save high dynamic parameters of engine. At realization these tasks the injection system meets the most important part.

Currently, on account of flexibility at injection characteristic shaping, common rail systems are the most frequently applied fuel supply in Diesel engines [2,6]. Because another Euro standards connected with limitation of mentioned pollutions are very strict, therefore such system types have to be very precise at injection characteristic shaping. Next, course injection depends on a lot of phenomena occur in the whole system. Possibility of realization a lot of injections during the same work cycle permits flexibility shaping of injection course, but at the same time it causes arising new problems connected with interaction between injections. Especially it concerns situation, when injections are located near one another. Of course, the most essential parameters effecting on dosing precision are injection duration, rail pressure and fuel temperature. While injection duration can be precise controlled by system controller, fuel pressure and fuel temperature change dynamic effecting on fuel dose and whole injection course.

In the article the effect of mutual angle position of main, pilot and preinjection dose on fuel dosing has been presented. At keeping constant total injection duration and fuel temperature, injected fuel dose and overflow from injector were measured. A high-speed courses (fuel pressure in injection pipe behind rail and before injector) and injector control signals were recorded too. In these scope of researches demonstration test results have been presented. The researches were

conducted with test stand equipped with test bench Bosch EPS-815 with electronic measuring of fuel dose.

2. Test stand and measurement methodology

As a basic elements of test stand during researches used are: test bench with measurement system of fuel dose with heat exchanger, high pressure rail and electronic control injector. The fuel was injected into special fuel chamber which enabled observation of injected fuel spray. The scheme of test stand is showed on fig. 1.

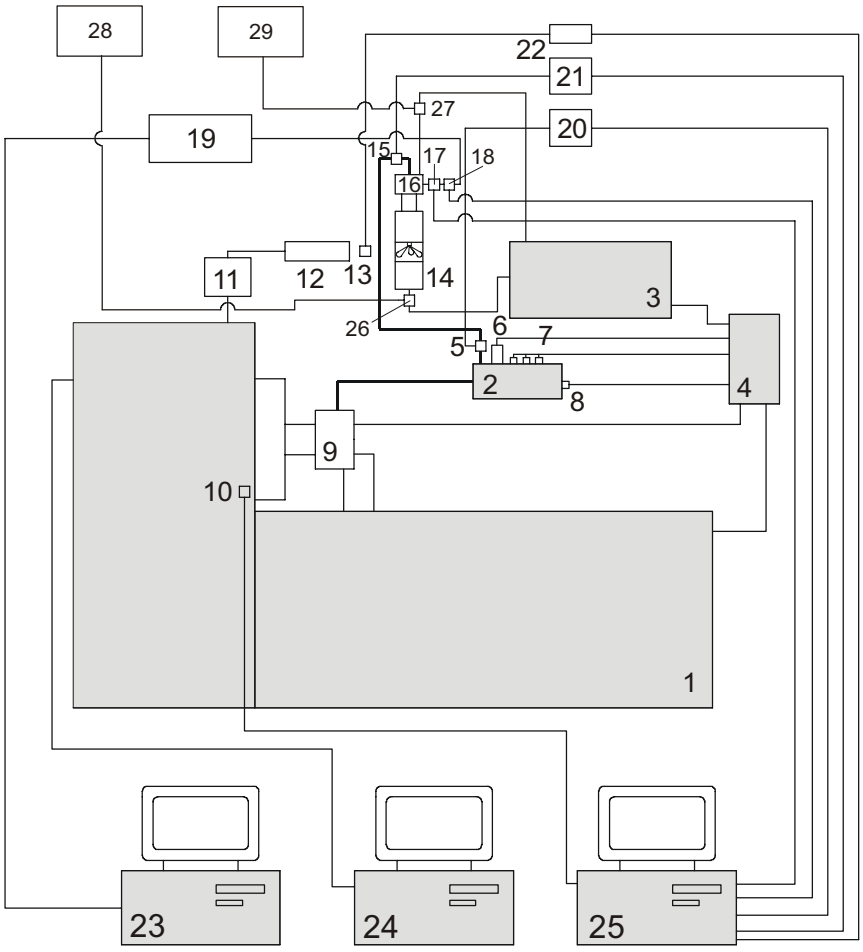

Fig. 1. Scheme of test stand: 1-test bench Bosch EPS 815, 2-rail of high pressure, 3-set of fuel dose measurement Bosch KMA 822 with heat exchanger, 4-control module of high-pressure pump, 5,15- piezoquartz pressure sensors, AVL QL21D, 6- rail pressure sensor, 7- rail pressure regulators, 8-fuel temperature sensor, 9-high pressure pump Bosch CR/CP1S3/L70/10-1V 445 010 343-02, 10-optical position and rotational speed sensor of pump shaft AVL 365C, 11-controler of stroboscopic tube Tech-Time 3300-S, 12-stroboscopic tube, 13-photoelement, 14-visualization chamber, 16-tested injector, 17-measurement connector of injector control voltage, 18-injector current sensor PA-55, 19- microprocessor controller of injector, 20, 21-charge amplifiers AVL 3057-A01, 22-voltage amplifier, 23-computer with control software of injector, 24-computer with software for test bench controlling and for measuring of fuel dose, 25-computer with data acquisition devices for high-speed courses recording, 26,27-temperature sensors, 28,29-termometers EMT 101

The description of fuel dose in dependence on its split strategy was the fundamental aim of researches. The distances between starts of injector control signals as well as a fuel doses were changed. Tests have been conducted for dose splitting into two parts (pilot dose and main dose) and for three parts (pilot dose, preinjection dose and main dose). Adjusted total injection duration $\mathbf{t_{inj}}$ was 1,0 lub 3,0 ms depending on test program. As a injection duration one should understand a duration of control signal using to injector opening. The distances between starts of control signals are as adjusted parameters and one shouldn't identify them with real injection starts. These problems were discussed accurately in the works [3,4,5,7,8].

For shorter total injection duration the researches only for pilot and main injection were conducted, while for longer duration also preinjection was used.

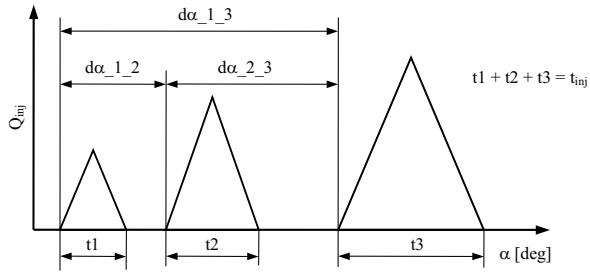

Fig. 2. Scheme of symbols described the injection strategy

Each series of test at constant injected fuel temperature $\mathbf{T_{inj}}$, fuel pressure $\mathbf{p_{rail}}$ and frequency running of injector was conducted. A frequency running of injector resulted from rotational speed **n** of the shaft of high pressure pump.

The parameter values connected with fuel injection on the figures presenting test results have been presented. The symbols described the injection strategy are showed on fig. 2.

During researches the series injector Bosch signed CR/CP1S3/L70/10-1V 445 010 343-02 was used. It was controlled by worked out controller enabling to split of fuel dose and their angle location in wide range. Detailed description of controller and set of injection system are presented in the work [1].

3. Test results

On fig. 3 the effect of distance between start of pilot injection and start of main injection **dα_1_3** on fuel dose $\mathbf{Q_{inj}}$ at various rail pressure $\mathbf{p_{rail}}$ and at rotational speed of pump **n = 600 rpm** has been presented. In this case at split of fuel dose into two parts, total injection duration amounted 1,0 ms (pilot dose 0,5 ms and main dose 0,5 ms). As showed on fig. 4, the largest dose fluctuations appear for shorter distances between doses and for lower pressures. On fig. 4 recorded course of fuel pressure $\mathbf{p_{inj}}$ before injector and control signal $\mathbf{U_s}$ for two various angle distances between pilot dose and main dose (15° and 20°) at rail pressure 75 MPa are presented. For these points, difference between obtained dose values amounted above 10 mm^3/injection (fig. 3). As showed on fig. 4, the pressure courses are shifted in phase and for 15 deg between injections the main injection is realized on descending pressure wave (solid line), while in the second case (dashed line) on rising pressure wave. Taking into consideration fact that for these conditions the changes of pressure before injector amount 30-40 MPa, it results in considerable deviation of fuel dose. The largest stabilization of fuel dose was observed for larger distances between doses and for the largest value of rail pressure $\mathbf{p_{rail}}$. Ambiguous character of fuel dose change results from random wave phenomena in injection system, which intensify at shorter distances between fuel doses. In these cases, opening of injector can occur both lower and larger values of pressure $\mathbf{p_{rail}}$ in relation to adjusted value (compare fig. 4).

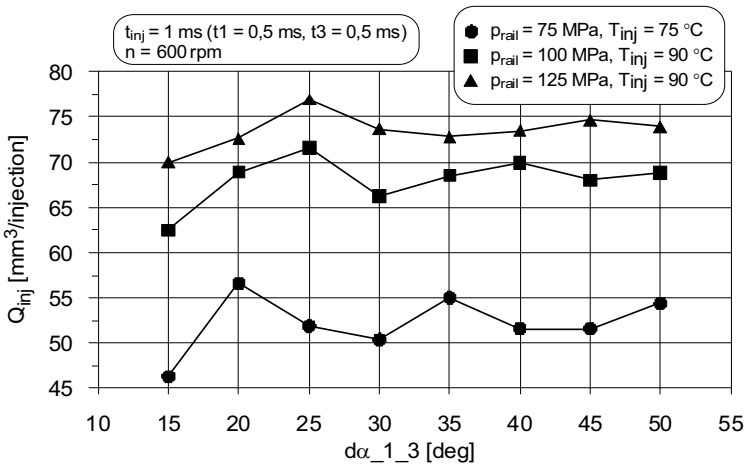

Fig. 3. Effect of distance between starts of pilot and main injection dα_1_3 and various rail pressures p_{rail} on fuel dose Q_{inj} (adjusted total injection duration t_{inj} = 1,0 ms)

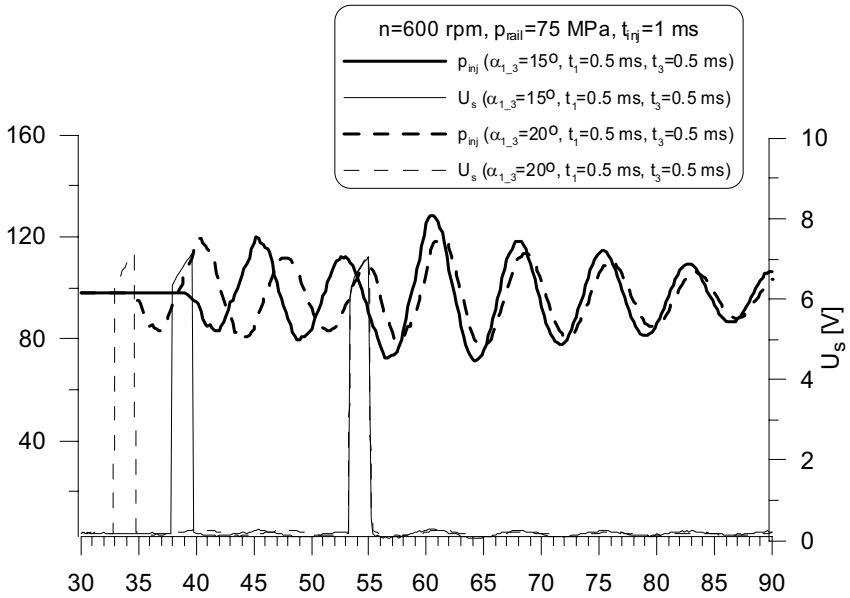

Fig. 4. Pressure courses in injection pipe before injector p_{inj} for two different ways of injector control by signal U_s, at the same total injection duration (rotational speed of pump n=600 rpm, p_{rail}=75 MPa, injection duration t_{inj}=1,0 ms)

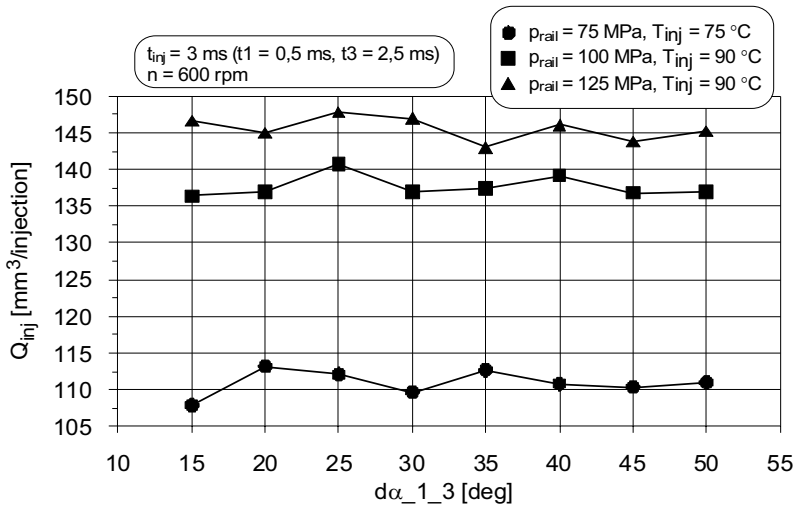

Fig. 5. Effect of distance between starts of pilot and main injection dα_1_3 and various rail pressures p_{rail} on fuel dose Q_{inj} (adjusted total injection duration t_{inj} = 3,0 ms)

On fig. 5 in similar order, as on fig. 3 test results are presented – in this case the different depends on using larger fuel dose. In this case a total injection duration amounted $\mathbf{t_{inj} = 3{,}0\ ms}$ (for pilot dose was $\mathbf{t_1 = 0{,}5\ ms}$ and for main dose was $\mathbf{t_3 = 2{,}5\ ms}$). Like in earlier analyzed case a certain stabilization of fuel dose for larger angle distances between pilot dose and main dose can be observed. Also is showed that for the lowest pressure value ($\mathbf{p_{rail} = 75\ MPa}$) a dose fluctuation are considerably lower than for lower total dose ($\mathbf{t_{inj} = 1{,}0\ ms}$, compare fig. 3).

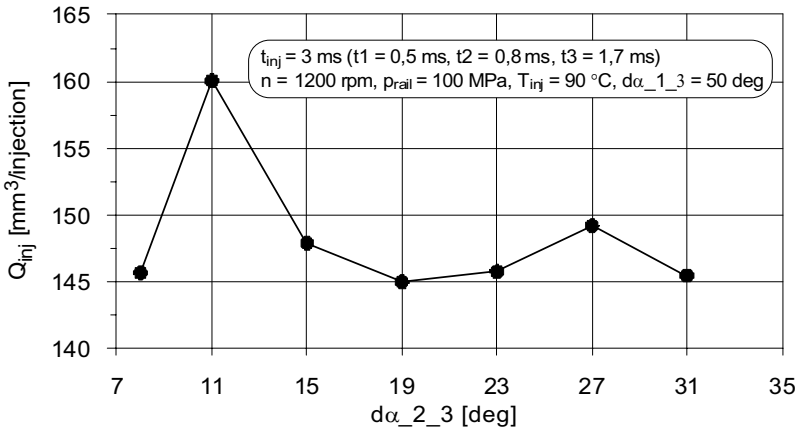

Fig. 6. Effect of distance between starts of preinjection and main injection dα_2_3 on fuel dose Q_{inj} (adjusted total injection duration t_{inj} = 3,0 ms)

On fig. 6 test results concerning the split of fuel dose into three parts are presented. The injection durations for pilot, preinjection and main dose were $\mathbf{t_1 = 0{,}5\ ms}$, $\mathbf{t_2 = 0{,}8\ ms}$ i $\mathbf{t_3 = 1{,}7\ ms}$ respectively. The distance between starts of pilot dose and main dose **dα_1_3** was constant and amounted 50 deg. However, a distance between start of preinjection dose and main dose **dα_2_3** was changed. As showed, for lower distances between preinjection dose and main dose there are considerable fluctuations of fuel dose. It results from too short time to closing of spray nozzle. In

such cases algorithm of fuel injection control has to work right correction of fuel injection duration, in order not to change adjusted total opening duration of injector.

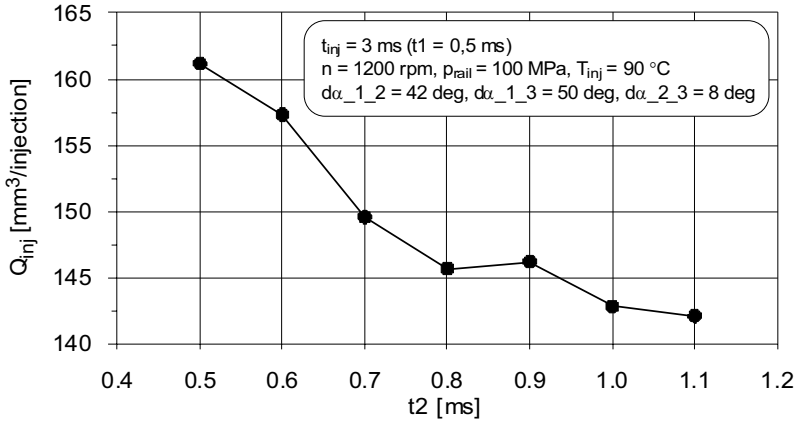

Fig. 7. Effect of preinjection duration t_2 on fuel dose Q_{inj} (adjusted total injection duration t_{inj} = 3,0 ms and pilot injecton duration t_1 = 0,5 ms)

At set of distances between fuel doses but for changing of preinjection duration, considerable decreasing of fuel dose was observed – fig. 7. Analyzing fig. 6 and 7 it can find that there are certain minimum distances between doses, after exceeding one occurs considerable decreasing of fuel dose.

4. Conclusions

Obtained test results show that change of mutual angle position of individual parts of dose at multi injection causes deviations during fuel dosing and decreases precision of control. It results from large fluctuation of pressure in injection pipe, which appear even after injection of not large doses. Because between doses (pilot dose, preinjection dose and main dose) occur not large angle distances, pressure wave isn't damping and occurring pressure fluctuations causes change of dose even though the total duration is equal. Dosing changes result from points on pressure wave where occurs injector opening. Taking into consideration that length of wave depends on a lot of factors (for example fuel property) these deviations can be difficult to compensate in controller. The changes of fuel temperature in injector, resulting from various work conditions have negative influence on dosing precision too.

To decrease a dosing deviation can be obtained by using larger pressures in the injection system and by shorting a way of flow from rail to spray nozzle. Length of injection pipes and length of fuel channels inside injector are very important also.

To sum up, it should be stated that during working of common rail system can occur considerable deviations of measure fuel dose, what can negative influence on pollution emission and functional parameters of compression ignition engine.

References

[1] Balawender, K., *Wpływ wybranych parametrów regulacyjnych procesu wtrysku na emisję cząstek stałych w silniku wysokoprężnym typu DI*, Rozprawa doktorska. Rzeszów 2007.

[2] Kuszewski, H., Lejda, K., *Wybrane metody ograniczania toksyczności spalin silnika ZS w aspekcie limitów emisyjnych*. Journal of KONES „Powertrain and Transport", Vol. 13, No.1, Warszawa 2006.

[3] Kuszewski H., Ustrzycki A., *Badania procesu dawkowania paliwa w zasobnikowym układzie wtryskowym,* Вісник Національного транспортного університету, No 14/2007, Київ 2007.
[4] Kuszewski, H., Ustrzycki, A., *Metodyka określania rzeczywistego początku wtrysku paliwa w układach zasilania silników wysokoprężnych*, Prace Zachodniego Centrum Akademii Transportu Ukrainy, Lwów 2006.
[5] Kuszewski, H., Ustrzycki, A., *Wpływ parametrów pracy zasobnikowego układu wtryskowego na rzeczywisty początek wtrysku paliwa,* Polskie Towarzystwo Naukowe Silników Spalinowych, Silniki Spalinowe, „Mixture Formation, Ignition & Combustion", 2007-SC2, 2007.
[6] Praca zbiorowa, *Zasobnikowe układy wtryskowe Common Rail,* Informatory techniczne Bosch. WKiŁ, Warszawa 2005.
[7] Ustrzycki, A., Kuszewski, H., *Badania początku wtrysku paliwa w układzie wtryskowym typu Common Rail,* Mat. XVII Konferencji Międzynarodowej SAKON'06 nt. „Metody Obliczeniowe i Badawcze w Rozwoju Pojazdów Samochodowych i Maszyn Roboczych Samojezdnych. Zarządzanie i Marketing w Motoryzacji", Rzeszów 2006.
[8] Ustrzycki, A., Kuszewski, H., *Wpływ temperatury wtryskiwanego paliwa na wielkość dawki w zasobnikowym układzie wtryskowym typu Common Rail,* Mat. XVIII Międzynarodowej Konferencji Naukowej SAKON'07 nt. „Metody obliczeniowe i badawcze w rozwoju pojazdów samochodowych i maszyn roboczych samojezdnych. Zarządzanie i marketing w motoryzacji", Rzeszów 2007.

Journal of POLISH CIMAC

Faculty of Ocean Engineering & Ship Technology
GDAŃSK UNIVERSITY OF TECHNOLOGY

OPERATIONAL LOADS OF DIESEL ENGINES ON TRAILING SUCTION HOPPER DREDGERS IN THEIR MAIN SERVICE STATES

Damian Bocheński

Gdańsk University of Technology
Ul. Narutowicza 11/12, 80-952 Gdańsk, Poland
Tel.: +48 58 3472773, fax: +48 58 3472430
e-mail: daboch@pg.gda.pl

Abstract

This paper presents results of operational investigations of eight trailing suction hopper dredgers. The investigations covered measurements of parameters which characterize service conditions of two main elements of dredger power systems, i.e. main and auxiliary engines.

Keywords*: trailing suction hopper dredgers, ship power plants, ship power systems.*

1. Introduction

Trailing suction hopper dredgers belong to the group of the largest technological ships and their power systems - to the most complex ones. Total output power of diesel engines installed on the largest dredgers of the kind exceeds 30000 kW.

Power system of suction hopper dredger consisted of diesel engines (both main and auxiliary ones) is intended for the satisfying of power demand from the side of main consumers (screw propellers, dredge pumps, jet pumps and bow thrusters) as well as of the group of auxiliary consumers. On the suction hopper dredgers a great variety of types of power systems can be found. Nevertheless the most often applied solution is the system having many variants, in which main engines satisfy the whole power demand from the side of main and auxiliary consumers in two basic service states of dredger: ”dredging work” and ”free-floating”. Then, auxiliary engines cover power demand from the side of auxiliary consumers in the service states in which main engines stand by (e.g. lying at anchor) [3,4].

In designing the power systems it is necessary to know operational loads of the diesel engines being elements of the system, first of all in the ship service state deemed crucial. In the case of the dredgers in question such state is associated with „dredging”. Service conditions which occur during the dredging are determined by the parameters assumed during design process of dredger power systems.

This paper presents characteristics of real loads of diesel engines on suction hopper dredgers during carrying out „dredging work” and also in the state of „free-floating” (in the sense of moving). The characteristics have been obtained as a result of wide operational investigations carried out on the dredgers which operated in the South Baltic, in the years 2000÷2003 and 2005÷2006 [3]. The results have been supplemented by the data dealing with three other dredgers, taken from the literature sources [5,6,7]. The main technical data of the eight dredgers, which characterize first of all their power systems, are given in Tab. 1. Two smallest dredgers: the *Kostera* and *Kronos* are fitted with the power system of the type III, which is characteristic of

separate diesel engines intended for the driving of screw propellers, separate engines for the driving of dredge pumps, as well as integrated electric generating sets to ensure driving the loosening pumps, thruster and all auxiliary power consumers. The remaining power systems of the dredgers in question belong to the type I. The type is characteristic of that one group of main engines ensure driving main power consumers of all kinds, very often in the basic service states, and auxiliary power consumers. Differences in variants of the power system type consist in different power transmission systems of given main consumers. And, the type I.a constitutes the system in which all main consumers are driven by means of diesel - electric power systems. (the dredgers *Łęgowski and Bukowski*), the type I.b is such power system in which one kind of main power consumers characterized by the largest nominal power, i.e. screw propellers, is driven by main engines working in diesel – mechanical systems (i.e. through mechanical transmission gears), and the remaining kinds of main power consumers are driven by means of diesel – electric systems , the type I.c is characteristic of that two kinds of main consumers (usually main screw propellers and dredge pumps) are driven by main engines working in diesel-mechanical systems , and the remaining kinds of main consumers - by means of diesel-electric systems (the dredger *Lange Wapper*) and the last variant of the type I , i.e. the type I.d in which as many as three kinds of main power consumers are driven by main engines working in diesel-mechanical systems (the dredger *Nautilus*).

Tab.1. Technical characteristics of power systems of the investigated trailing suction hopper dredgers

Dredger	Year built	V_{HP}	Classes of dredgers	Type of power systems	$\sum N_{ME}^{nom}$	$\sum N_{AE}^{nom}$
		m^3			kW	kW
Kostera	1968/1993	310	small	III	798	306
Kronos	1964/1985	380	small	III	885	513
Łęgowski	1975	1600	small	I.a	2640	534
Bukowski	1974	1600	small	I.a	2560	392
Nautilus	1996	4400	medium	I.d	3700	350
Gogland	1982	8200	medium	I.b	8606	1850
Geopotes 15	1985	9960	large	I.b	11160	1285
Lange Wapper	1998	13700	large	I.c	11520	2340

V_{HP} - hopper (soil hold) capacity,

$\sum N_{ME}^{nom}$ - rated output power of main engines,

$\sum N_{AE}^{nom}$ **-** rated output power of auxiliary engines.

2. Operational loads of main engines

In order to determine operational characteristics of main and auxiliary engines on dredgers to know changes of the loads during a long period is necessary. A large number of instantaneous values of the loads make their correct statistical estimation possible. To the investigations which have been carried out for long periods, the stationary measuring instruments permanently installed on dredgers have appeared most suitable. The detail description of the measuring methods applied to the service investigations in question is given a.o. in [2] and [3]. On the basis of an analysis of initial investigations concerning changes of loads of main and auxiliary engines on suction hopper dredgers [3] the every 5th minute frequency of load measurements of main engines was assumed sufficient for further investigations.

The so determined values of main engine loads were used to determine the following parameters of load distribution characteristics:

N_{ME}^{av} - average load of main engine, kW;

$\overline{N}_{ME}^{av} = \frac{N_{ME}^{av}}{N_{ME}^{nom}}$ - average relative load of main engine, -;

σ_{ME} - standard deviation of main engine load distribution, kW;

$\nu_{ME} = \frac{\sigma_{ME}}{N_{ME}^{av}}$ - coefficient of variance of main engine load distribution, -.

The four dredgers (the *Nautilus, Gogland, Geopotes 15* and *Lange Wapper*) are characteristic of that their main engines satisfy power demand from the side of auxiliary power consumers in the main service states. Hence the service effective power of the main engines is equivalent to the entire power necessary to realize technological processes by the dredger. In the case of the four remaining dredgers the service effective power of auxiliary engines should be additionally taken into account.

The characteristics of load distributions of main engines on the investigated dredgers are given in Tab. 2. The load distributions of main engines on selected dredgers are presented in Fig. 1.

Tab.2. Characteristics of load distributions of main engines on trailing suction hopper dredgers engaged in carrying out the dredging work and free-floating

Dredger	Dredging work				Free-floating				References
	N_{ME}^{av}	$\overline{N}_{ME}^{av}$	σ_{ME}	ν_{ME}	N_{ME}^{av}	$\overline{N}_{ME}^{av}$	σ_{ME}	ν_{ME}	
	kW	-	kW	-	kW	-	kW	-	
Kostera	175,1	0,22	58,8	0,336	216,1	0,271	54,6	0,252	[*]
Kronos	193,3	0,218	25,9	0,134	264,7	0,299	58,2	0,22	[*]
Łęgowski	1165,1	0,441	371,2	0,319	1249,5	0,473	282,7	0,226	[*]
Bukowski	1186,8 777,4*)	0,464 0,304	319,5 215,7	0,269 0,277	1297,3	0,507	223,7	0,172	[*]
Nautilus	1553,2	0,42	319,3	0,26	1498,4	0,405	359,9	0,24	[5]
Gogland	4735,5	0,55	943,5	0,199	5464,6	0,635	875,1	0,16	[6]
Geopotes 15	6152,4	0,551	1215,1	0,197	6752,8	0,605	1529,1	0,226	[*]
Lange Wapper	6932,7	0,602			7976,7	0,692			[7]
average		0,433		0,245		0,486		0,214	

*) – data which concern the dredging work in soft soils (silts)

[*] – self investigations

In Tab. 3 are presented calculation results concerning load characteristics of main engines during carrying out particular operations within the scope of dredging work. In all cases the calculations, irrespective of a type and power system and number of main engines, were performed jointly for all the main engines installed on a given dredger.

The performed calculations of the parameters of load distributions of main engines during carrying out the dredging work have revealed that for particular dredgers the relative average loads are contained in the range of 0,218 ÷ 0,602 at the mean value of 0,433 and variation coefficient of the range of 0,134 ÷ 0,336 at the mean value of 0,245. Simultaneously attention should be paid to the fact that for the dredgers having their power systems of the type III (the *Kostera* and *Kronos*), the relative average loads are definitely smaller and contained in the range of 0,218÷0,22. This is connected with the larger total output power of the installed main engines intended for the driving of screw propellers and dredge pumps in the power systems of the 3rd type, as compared with that for the power system of the type I. The mean values of relative loads of main engines of the dredgers having the power systems of the type I are definitely larger and contained in the range of 0,42÷0,602 at the mean value of 0,505.

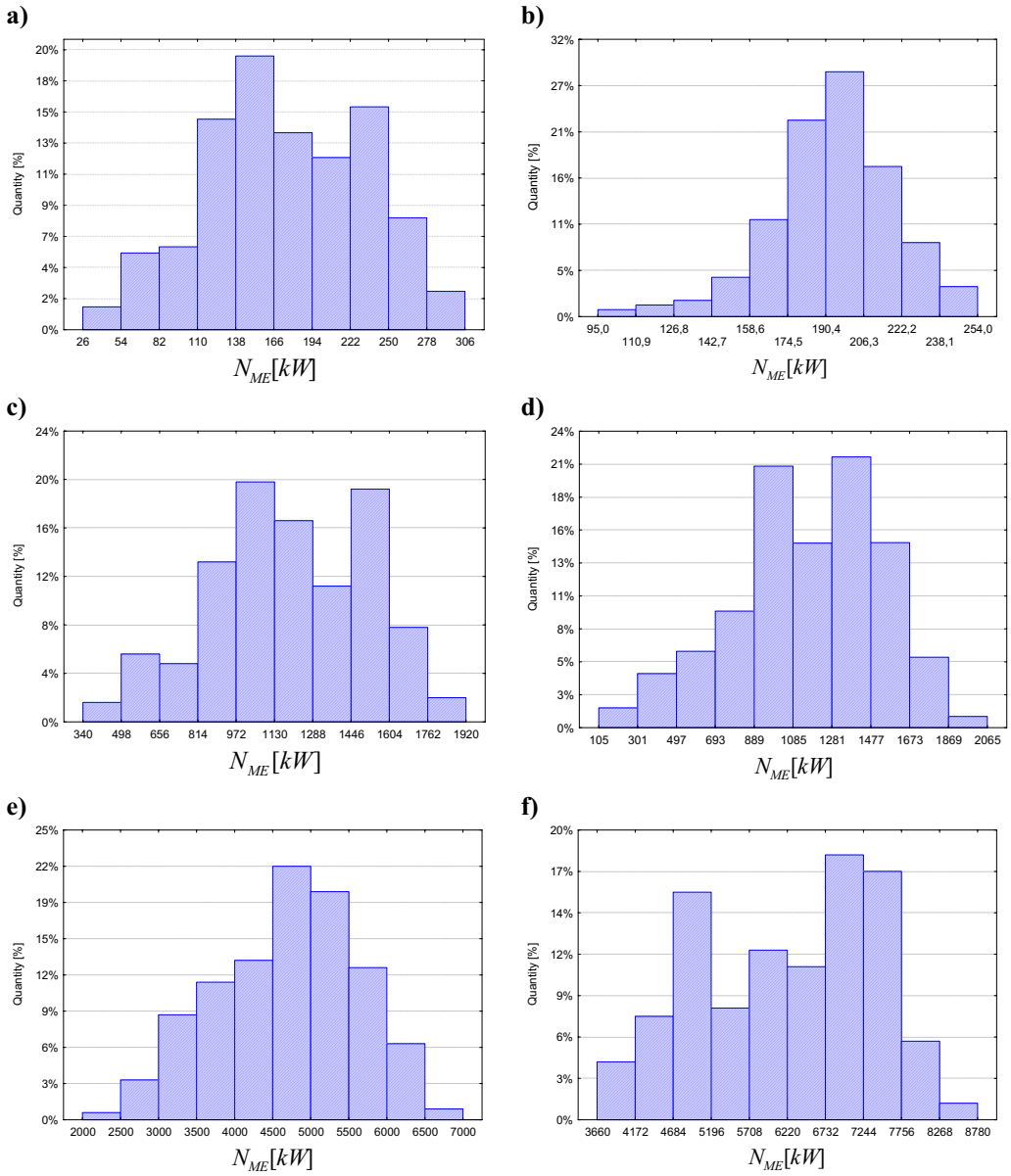

Fig.1. Load histograms of main engines on trailing suction hopper dredgers engaged in carrying out the dredging work; a) the Kostera, b) the Kronos, c) the Bukowski, d) the Łęgowski, e) the Gogland, f) the Geopotes 15

All the investigated dredgers operated in the water areas whose bed was formed of medium sandy soils, with the exception of the dredger *Inż. M. Bukowski* which additionally was engaged in maintenance work consisting in removing the silt out of bed of fairways. The silts belonged to the group of very soft soils. During operation in very soft soils other operational parameters of dredge pumps appear and jet pumps are standing by [9]. For the reasons the load distribution parameters of main engines on the dredger *Inż. M. Bukowski*, presented in Tab. 2 and 3, are given separately for the operations carried out in medium and very soft soils. As results from the data contained in Tab. 2 and 3, the loads of main engines on the dredger *Inż. M.*

Bukowski engaged in dredging work in very soft soils are smaller on average by about 30% as compared with dredging work carried out in medium soils.

For the service state of „free-floating" values of the relative average load of main engines are somewhat smaller than those for the service state of „dredging work" - their mean value is equal to 0,486. Simultaneously, relevant variation coefficients are smaller - their mean value is equal to 0,214. Like in the case of dredging work, the mean values of the relative loads of main engines of the dredgers equipped with power systems of the type III are definitely smaller and amount to 0,271÷0,299. The mean values of the relative loads of main engines of the dredgers equipped with power systems of the type I are definitely greater and are contained in the range of to 0,405-0,692 at the mean value of 0,553.

Tab.3. Characteristics of load distributions of main engines on trailing suction hopper dredgers engaged in carrying out the operations belonging to the dredging work

Dredger	Sailing from and to discharging area				Loading the spoil				Hydraulic unloading the spoil			
	N_{ME}^{av}	$\overline{N}_{ME}^{av}$	σ_{ME}	ν_{ME}	N_{ME}^{av}	$\overline{N}_{ME}^{av}$	σ_{ME}	ν_{ME}	N_{ME}^{av}	$\overline{N}_{ME}^{av}$	σ_{ME}	ν_{ME}
	kW	-	kW	-	kW	-	kW	-	kW	-	kW	-
Kostera	125,7	0,158	45,0	0,358	147,7	0,185	20,2	0,137	227,4	0,285	31,2	0,137
Kronos	190,7	0,215	37,4	0,197	196,3	0,227	13,9	0,071	193,3	0,218	21,3	0,11
Łęgowski	923,3	0,35	374,4	0,405	1479,3	0,56	182,8	0,124	1019,9	0,386	128,8	0,126
Bukowski	755,5	0,295	258,7	0,342	1551,4 827,1*)	0,606 0,323	126,6 146,8	0,082 0,177	1116,4 965,7*)	0,436 0,377	121,1 113,8	0,108 0,118
Nautilus	1452,3	0,392	225,3	0,155	1858,3	0,502	157,7	0,085	-	-	-	-
Gogland	4893,3	0,569	627,2	0,128	5692,8	0,661	340,4	0,06	3559,9	0,414	514,4	0,144
Geopotes 15	6412,9	0,575	1242,8	0,194	7057,3	0,632	397,1	0,057	4854,7	0,435	345,3	0,071
Lange Wapper	7611,6	0,661			7372,3	0,64			6210,7	0,539		
average		0,402		0,254		0,502		0,088		0,388		0,116

*) – data which concern the dredging work in soft soils (silts)

On the basis of the data given in Tab. 3 one can conclude that for six dredgers the largest average loads of main engines during carrying out the dredging work occur during loading the spoil. For the *Lange Wapper,* the largest of the dredgers, the greatest mean values of loads of main engines concern the sailing periods both in loaded and unloaded condition. The fact confirms the regularity indicated in [1,3 and 8] that for small and medium size hopper dredgers the loading of the spoil (in some cases – hydraulic unloading the spoil) is the most energy consuming operation being a part of dredging work, and for large and very large dredgers this is usually the floating both in loaded and unloaded condition.

Power system conditions and character of its work during sailing (moving) both in loaded and unloaded condition during the dredging work are close to those which occur during the state of „free-floating". As results from the data given in Tab. 2 and 3, the mean values of loads of main engines on small dredgers in sailing operation during the dredging work, $(N_{ME}^{av})_{dw}^{sl}$ constitute $0{,}58 \div 0{,}74$ of the mean load of main engines during the free-floating, $(N_{ME}^{av})_{f-f}$. For medium and large dredgers the values amount to $(N_{ME}^{av})_{dw}^{sl} = (0{,}89 \div 0{,}97)(N_{ME}^{av})_{f-f}$. It results from distances between loading and unloading sites. For small dredgers the distances reach several nautical miles, which results in a large participation of maneuver periods when sailing (moving) during the dredging work and smaller values of mean loads of main engines. The larger the dredger the larger

the distances between loading and unloading areas, and for large dredgers they reach a few dozen nautical miles [3,8].

3. Operational loads of auxiliary engines

As mentioned above, in the case of four investigated dredgers in the analyzed service states, apart from their main engines, also auxiliary engines were running as elements of the integrated electric generating sets (on the dredgers *Kostera* and *Kronos*) or the independent electric generating sets (on the dredgers *Inż. S. Łęgowski* and *Inż. M. Bukowski*). In Tab .4 the calculation results concerning load characteristics of auxiliary engines during the analyzed service states of dredger, are presented. In all the cases, regardless of a power system type and solution, and number of auxiliary engines, the calculations were performed jointly for all auxiliary engines installed on a given dredger.

Tab.4. Characteristics of load distributions of auxiliary engines on trailing suction hopper dredgers during carrying out the dredging work and free-floating

Dredger	Dredging work				Free-floating				References
	N_{AE}^{av}	$\overline{N}_{AE}^{av}$	σ_{AE}	ν_{AE}	N_{AE}^{av}	$\overline{N}_{AE}^{av}$	σ_{AE}	ν_{AE}	
	kW	-	kW	-	kW	-	kW	-	
Kostera	37,12	0,121	12,23	0,329	21,3	0,07	2,37	0,111	[*]
Kronos	56,22	0,11	26,14	0,465	24,1	0,047	3,11	0,129	[*]
Łęgowski	149,1	0,279	23,3	0,156	118,6	0,222	15,11	0,127	[*]
Bukowski	142,6	0,364	28,1	0,197	113,1	0,289	13,21	0,117	[*]

[*] – self investigations

The performed calculations of load distribution parameters of auxiliary engines during the dredging showed that for particular dredgers the relative average loads were contained in the range of 0,11 ÷0,364 at the mean value of 0,218, and the distribution variation coefficient in the range of 0,156 ÷0,465 at the mean value of 0,287. For the service state of „free-floating", the values of the relative average load of main engines are definitely smaller as compared with those in the service state of „dredging work"; their mean value equals 0,157. Also, variation coefficients are smaller; their mean value equals 0,121.

The first conclusion which comes to mind is that the relative average loads of auxiliary engines are definitely smaller as compared with those of main engines (the mean value for auxiliary engines during dredging amounts to 0,218 against that of 0,433 for main engines). This mainly results from that in the case of the designing of ship electric power plants number of auxiliary engines is usually assumed by one unit greater than that obtained from electric power balance calculations. It leads to a much greater rated power of installed auxiliary engines, and simultaneously results in smaller values of the relative average loads $\overline{N}_{AE}^{av}$.

The second conclusion is that the values of $\overline{N}_{AE}^{av}$ for auxiliary engines on the dredgers equipped with power systems of the 3rd type (the *Kostera and Kronos*) are definitely smaller than those for auxiliary engines installed on the dredgers with power systems of the 1st type (the *Łęgowski and Bukowski*). It can be explained by that on these dredgers they provide driving for two large power consumers (jet pump and bow thruster) , and by special character of work of the consumers (mainly during the loading). This results in the necessity of increasing the output power of installed auxiliary engines. The character of work of the consumers is also responsible for large values of the variation coefficients ν_{AE} for the dredgers with power systems of the type III (it concerns only the state of „dredging work").

4. Influence of size of a dredger on operational loads of its diesel engines

It is common knowledge that size of a dredger determines value of the power demanded to fulfill tasks of the dredger [8]. The average operational loads of all diesel engines N_{DE}^{av} for a given dredger represent power demand for realizing the dredger's tasks in a given service state. The main size parameter of trailing suction hopper dredger, specified as a rule in owner's design assumptions is the hopper (soil hold) capacity V_{HP}. The relation $N_{DE}^{av} = f(V_{HP})$ for the service state of „dredging work" was examined on the basis of such assumption. To this end, the data contained in Tab. 1, 2 and 4 were used. As a result the following relation was achieved (Fig. 2):

$$N_{DE}^{av} = 0{,}5264 \cdot V_{HP} + 171{,}91 \tag{1}$$

as well as the following : the coefficient of correlation $R = 0{,}981$, the standard deviation $\sigma = 291{,}5\ kW$, the value of the test $F = 154{,}3$ for the sample number $m = 8$, and $F_{kr} = 5{,}99$ for $\alpha = 0{,}05$. The range of application of Eq. (1) is : $310 \le V_{ŁG} \le 13700\,m^3$.

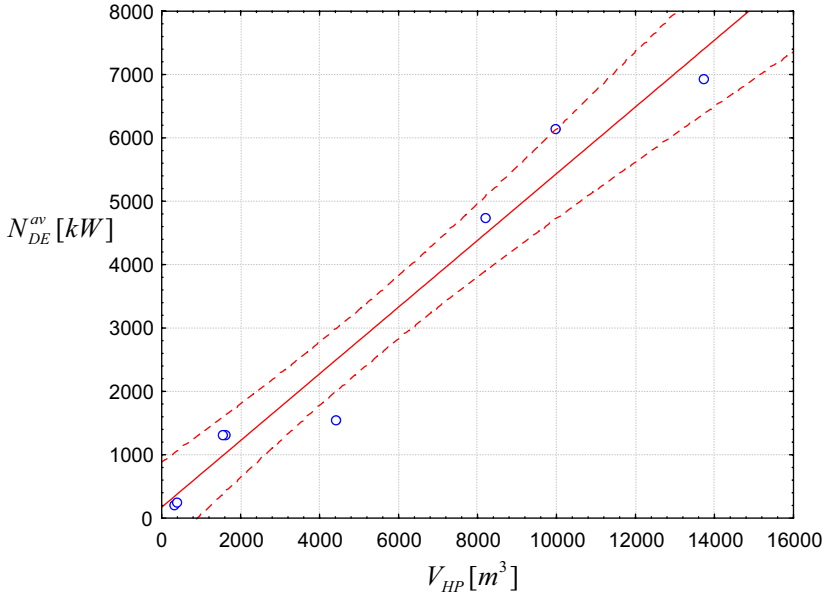

Fig .2. The relation $N_{DE}^{av} = f(V_{HP})$ for trailing suction hopper dredgers working in medium sandy soils

5. Summary

The performed investigations make it possible to formulate the following remarks and conclusions:

1) The values $\overline{N}_{ME}^{av}$ and ν_{ME} obtained from measurements can be used to determine recommended operational loads for main engines to be selected in designing dredger power systems of the 1st type, first of all. For the service state of „dredging work" in medium soils the value of $\overline{N}_{ME}^{av} = 0{,}48 \div 0{,}64$ was determined on the assumption that the maximum loads of main engines were contained in the range of $(0{,}85 \div 0{,}9)N_{ME}^{nom}$;

2) The relation (1) can be used in preliminary design stages in order to determine average power demanded for realization of tasks of a dredger of a given soil hold capacity;
3) The achieved results may be useful for solving design problems of power plants of suction hopper dredgers as well as in establishing fuel consumption standards for diesel engines on dredgers of the kind.

Bibliography

[1] Bocheński D., *Design solution and working conditions of power systems for trailing suction hopper dredgers.* Polish Maritime Research, no 2/1999
[2] Bocheński D., Kubiak A., Jurczyk L.: *Pomiary parametrów charakteryzujących pracę układów technologicznych pogłębiarek.* Materiały XXII Sympozjum Siłowni Okrętowych *SymSO200,* Szczecin 2001.
[3] Bocheński D. (kierownik projektu) i in.: *Badania identyfikacyjne energochłonności i parametrów urabiania oraz transportu urobku na wybranych pogłębiarek i refulerów*. Raport końcowy projektu badawczego KBN nr 9T12C01718. Prace badawcze WOiO PG nr 8/2002/PB, Gdańsk 2002.
[4] Bocheński D., *Analiza rozwiązań konstrukcyjnych i zależności określających parametry układów energetycznych pogłębiarek ssących nasiębiernych.* Zeszyty Naukowe Akademii Morskiej w Szczecinie, nr 73. XXIV Sympozjum Siłowni Okrętowych *SymSO2003,* Szczecin 2003.
[5] Dokumentacja prób zdawczo-odbiorczych pogłębiarki „Nautilus", GSR, Gdańsk 1996
[6] Kompleksyjne technologiczieskie issledowanija sudov popolnienija unstrukcyja po effjektiwnoj eksploatacji ziemsnarjada „Gogland". GDK, Rostow nad Donem 1984.
[7] de Vries L., *Total performance simulations of ship energy concepts*. Wondermar II Workshop, Bremen 2004
[8] Vlasblom J. W., *Designing dredging equipment*. Lecture notes, TUDelft 2003-05
[9] Volbeda J., H., *Overflow effects when trailing very soft silts and clays.* WODCON X EADA, World Dredging Congress, Singapore 1983

Journal of POLISH CIMAC
Faculty of Ocean Engineering & Ship Technology
GDAŃSK UNIVERSITY OF TECHNOLOGY

OPERATIONAL LOADS OF DREDGE PUMPS IN THEIR BASIC SERVICE STATES ON SELECTED TYPES OF DREDGERS

Damian Bocheński

Abstract

This paper presents results of operational investigations dealing with dredge pumps, one of the most important mechanical energy consumers installed on dredgers. The investigations covered measurements of parameters which characterize the loads of dredge pumps in their two basic service states, namely during loading the spoil into a soil hold – hopper (of a dredger or hopper barge) and during transferring the spoil ashore.

Keywords*: dredgers, dredge pumps, ship power systems.*

1. Introduction

Dredge pumps belong to the most important consumers of mechanical energy on dredgers. Their function is to hydraulically transport loosened soil from the sea bed into soil hold of the dredger or hopper barge (a service state called loading the spoil) as well as from the hold (sometimes directly from the sea bed) through long transfer piping to a dump on shore (a service state called transferring the spoil ashore). The states occur always on suction dredgers (e.g. trailing suction hopper dredgers, cutter suction dredgers, barge unloading dredgers), sometimes also on dredgers with mechanical dredging systems (e.g. bucket ladder dredgers) [1]. Power demand of dredge pumps depends on their use and design assumptions as well as on size of dredger. It is contained in a broad interval ranging from several hundreds kW to even a dozen or so thousands kW [1,2].

Irrespective of a type of dredger the dredge pumps can operate in two basic service states [1,3,4]:

- the loading of the spoil into the hopper (soil hold) on the dredger or assisting hopper barge; operational conditions of the pump system are characterized by the following features: the static lifting height of the system is as a rule greater than the dynamic one ($H_{st} \geq H_{dyn}$), similar values of flow drag of water-soil mixture on suction and pressure side of pump ($\Delta h_s \approx \Delta h_p$);
- the hydraulic emptying of the soil hold or transferring the spoil directly to a dump on shore (the pumping the spoil ashore); in this case operational conditions of the pump system are characterized by a much greater dynamic lifting height than the static one ($H_{st} << H_{dyn}$) and much greater values of flow drag on the pump pressure side than on its suction side ($\Delta h_s << \Delta h_p$).

The state called loading the spoil into the hold always occurs on trailing suction hopper dredgers (it concerns their own holds) , and may also occur on cutter suction dredgers (in this case it concerns hopper barge holds). The pumping-away the spoil occurs on trailing suction hopper dredgers and cutter suction dredgers, sometimes also on bucket ladder ones. Great differences in the parameters which characterize the pump systems operating in the above mentioned service states must result in great differences in the loads applied upon dredge pumps during loading and pumping-away the spoil. On the trailing suction hopper dredgers

the using of the same pumps both for the loading and pumping-away the spoil is common. Then their driving systems are fitted with multi-speed gear transmission devices.

To know service loads of dredge pumps (and also other large power consumers) is crucial in the designing of dredger power systems as it makes it possible to predict loads to be applied to pumps on a designed dredger.

This paper presents results of operational investigations which concern the driving loads of dredge pumps on 10 dredgers of various types. The investigations have been a part of a more comprehensive research on power consumption of technological processes on three main types of dredgers, carried out in the years 2000÷2003 and 2005÷2006 [5]. The results have been supplemented with those from other investigations carried out by other measuring teams, and dealing with four successive dredgers [5, 6, 7, and 8].

2. Measurement methods

The measurement methods implemented during the investigations depended on design solution of dredge pump driving system, as well as on stationary measuring instruments installed on a given dredger and their possible use for determination of instantaneous power demanded by a dredge pump. By making use of the measurement results and knowing efficiency characteristics of power transmission systems, instantaneous power values on drive coupling of a given dredge pump, were determined [9]. To this end the following methods were applied [9]:

- the method to which the measuring of the parameters of electric current absorbed from the network by electric motor driving the pump, was applied; the method was used on the dredgers of diesel-electric drive of the pumps (the dredgers : the *Inż. M. Bukowski, Inż. S. Łęgowski, Geopotes 15*),
- the method to which the measuring of the parameters characterizing operation of the pumps , i.e. their capacity (measured by means of stationary instruments) and lifting height (measured by means of manometers installed on suction and pressure side of pumps) was applied; the knowledge of values of pump lifting height as well as efficiency characteristics of a given pump (corrected with regard to the case of water-soil mixture pumping [4]) and its mechanical transmission gear (if applied), made it possible to determine the power on the pump drive coupling ; the method was applied to determination of the service loads of dredge pumps on the following dredgers and barge unloading dredgers: the *Kostera, Kronos, Trojan, Toruń, Małż II, Rozkolec* and *Raja*.

On the basis of the performed analysis of changes in loads of dredge pumps it was assumed that measurements of operational loads of the pumps will be carried out every 5th minute [9].

To determine operational load characteristics of dredge pumps, knowledge of changes of the loads for a long period is necessary. A large number of instantaneous values of the loads make it possible to perform their statistical assessment properly. The average duration time of dredging work carried out by dredgers amounts to about 2500 h/year [9]. As to carry out such investigations on every tested dredgers for so long time was not possible the service investigations were planned to cover at least 5% of the duration time of dredging work on each of the tested dredger, i.e. about 125 h [9]. Most of the service investigations were carried out in 24 h cycles.

The performed investigations made it possible to determine the load distribution characteristics of dredge pumps during loading the winning to the soil hold and during transferring the soil ashore; the characteristics contained the following:

$(N_{DP}^{av})^{ls}(N_{DP}^{av})^{sp}$ - average loads on dredge pumps during loading and transferring -away the spoil, respectively;

$(\sigma_{DP})^{ls}(\sigma_{DP})^{sp}$ - standard deviations of load distribution of dredge pumps;

$\nu_{DP} = \frac{\sigma_{DP}}{N_{DP}^{av}}$ - variation coefficient of load distribution of dredge pump;

$\lambda_{DP}^{ls}(\lambda_{DP}^{sp})$ - a coefficient which determines participation of duration time of dredge pump operation during loading and transferring the spoil ashore, respectively.

3. Load distribution of dredge pumps during loading the spoil to hopper

The analysis covered results obtained from 8 trailing suction hopper dredgers. Tab. 1 shows the data which characterize load distributions of dredge pumps of the analyzed dredgers during carrying–out operations associated with loading the spoil to soil hold , i.e. $((N_{DP}^{av})^{ls},(\sigma_{DP})^{ls},(\nu_{DP})^{ls},\lambda_{DP}^{ls}$. There are also given values of the nominal power on couplings of dredge pumps N_{DP}^{nom} as well as calculated values of the relative average loads of dredge pumps $\overline{N}_{DP}^{av}$. In Fig. 1 are showed the load histograms of dredge pumps on selected dredgers during loading the spoil to hopper (soil hold). Particular numerical values of instantaneous loads on dredge pumps were grouped into left-side open quantification intervals of identical width. The quantification interval width resulted from division of the range determined by the minimum and maximum service power of dredge pumps. With a view of accuracy of calculations 10 quantification intervals were assumed [10]. The histograms are presented together with relevant curves of normal distribution density, i.e. one of the theoretical distributions most often used for approximation of load distribution of main power consumers on dredgers [3, 9, and 10].

Tab.1. Characteristics of load distributions of dredge pumps on dredgers during loading the spoil to hopper

Dredger	N_{DP}^{nom}	N_{DP}^{av}	$\overline{N}_{DP}^{av}$	σ_{DP}	ν_{DP}	λ_{DP}^{ls}	m	References
	kW	kW	-	kW	-	-		
Kostera	125	82,1	0,657	6,9	0,084	0,98	846	[*]
Kronos	150	95,1	0,634	7,8	0,082	0,97	498	[*]
Łęgowski	2×550	774,9	0,704	62,3	0,08	0,98	1542	[*]
Bukowski	2×550	786,4 488,4*)	0,715 0,444	54,5 61,1	0,069 0,125	0,97 0,95	486 497	[*]
Nautilus	870	706,8	0,812	26,2	0,037			[6]
Gogland	2×1180	1787,1	0,757	61,2	0,034			[7]
Geopotes 15	2×1550	1987,7	0,641	71,9	0,036	0,98	592	[*]
Lange Wapper	3200	2482,6	0,776					[8]
average			0,712		0,06	0,972		

*) – pump operation connected with very soft soil (silts)

m - sample number

[*] – self investigations

All the investigated dredgers operated in spoil the medium sandy soil. Only in one case (the dredger *„Bukowski")* the dredger operated in spoil the very soft soil (the so called silts) during removing the silt from water path. For dredging the soil of the kind other values of

operational parameters of the pumps are recommended [2, 4], therefore in the case of the dredger „*Bukowski"* the respective results are given for two kinds of dredged soil.

The performed calculations of load distributions of dredge pumps during loading the spoil showed that for particular dredgers the relative average loads were contained within the range of 0,634÷0,776 at the mean value of 0,712 and distribution variation coefficient value contained in the range of 0,034 ÷0,082 at the mean value of 0,06. The presented data concern operation in medium sandy soils. The rather small values of distribution variation coefficients of pumps result from operational conditions of the pumps during loading the spoil. Power values demanded by the pumps are influenced first of all by water-soil mixture density and depth of water in a dredged area. The rather small changes of the parameters at the practically constant length of the piping (it concerns external trailing suction pipes) result just from the small values of the above mentioned coefficients.

The pump operation in light soils is associated with lower average values of pump loads. On the dredger *„Bukowski"* the average load value of the pumps dredging the light soil (silt) reached less than 65% of the loads of the same pumps during operation in medium soils.

Values of the coefficient λ_{DP}^{ls} were contained in the range of 0,95÷0,98 at the mean value of 0,972.

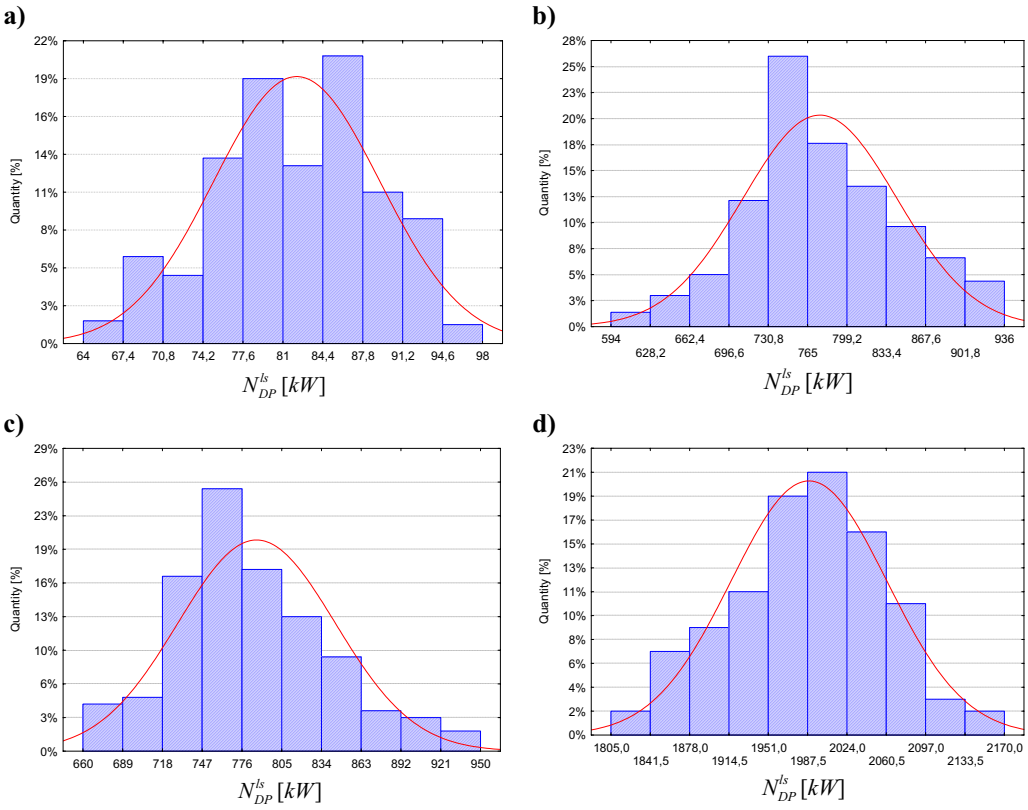

Fig.1. Load histograms of dredge pumps on trailing suction hopper dredgers during loading the spoil; a) the dredger „Kostera", b) the dredger „Łęgowski", c) the dredger „Bukowski", d) the dredger „Geopotes 15".

4. Load distribution of dredge pumps during transferring the spoil ashore

The analysis covered results obtained from 13 dredgers (including 7 trailing suction hopper dredgers, 3 cutter suction dredgers, 2 barge unloading dredgers and 1 bucket ladder

dredger) The below presented Tab. 2 shows the data which characterize load distributions of dredge pumps of the 13 dredgers during carrying –out operations associated with transferring the spoil ashore. Like in the case of the loading, in Tab. 2 are given the nominal power values of the dredge pumps intended for transferring the winning ashore. The principles for elaboration of histograms are the same as in the case of the pump service state of loading the winning.

Tab.2. Characteristics of load distributions of dredge pumps on dredgers during transferring the spoil ashore

Dredger	N_{DP}^{nom}	N_{DP}^{av}	$\overline{N}_{DP}^{av}$	σ_{DP}	ν_{DP}	λ_{DP}^{sp}	m	References
	kW	kW	-	kW	-	-		
Kostera	325	216,5	0,666	29,6	0,137	0,98	918	[*]
Kronos	420	189,4	0,451	20,6	0,109	0,99	756	[*]
Łęgowski	1100	832,9	0,757	101,4	0,122	0,99	1156	[*]
Bukowski	1100	835,7 651,6*)	0,759 0,592	52,8 82,7	0,064 0,127	0,98	465 424	[*]
Gogland	2360	1815,9	0,769	178,4	0,098			[7]
Geopotes 15	3100	2211,1	0,713	239,9	0,109	0,99	517	[*]
Lange Wapper	8900	3861,9	0,434					[8]
Trojan	1000	536,7	0,537	122,9	0,229	0,96	1437	[*]
Toruń	840	431,5	0,514	52,3	0,121	0,96	896	[*]
Scorpio	2100	1667,5	0,794	278,6	0,167			[5]
Rozkolec	3260	1188,1	0,365	334,8	0,282	0,98	636	[*]
Raja	540	240,5	0,445	32,3	0,134	0,99	576	[*]
Małż II	250	158,26	0,633	30,78	0,194	0,96	482	[*]
average			0,603		0,147	0,978		

[*] – self investigations

Like in the case of the loading, the investigated dredgers transferred ashore mainly medium soil. And, only the dredger *„Bukowski"* operated also in light soil. For this reason results for two kinds of soil are given for this dredger.

The performed calculations of distribution parameters of loads on dredge pumps during transferring the spoil ashore showed that for particular dredgers the relative average loads were contained in the range of 0,365 ÷0,794 at its mean value of 0,603 and variation coefficient in the range of 0,064 ÷0,282 at its mean value of 0,147. The above given values concern operation in medium soils.

Attention should be paid to the fact of greater absolute average values of loads on pumps during transferring the winning as compared with those in the case of loading (such situation takes place on trailing suction hopper dredgers). It results from that during transferring the spoil power value demanded by the pumps depends mainly on length of piping for transferring the winning. In the case of single dredge pump systems such values are on average 2,2÷2,3 times greater, and for the systems of two dredge pumps such values are about 1,1÷1,2 times greater in the state of transferring the winning ashore.

Values of variation coefficients of load distribution of pumps during transferring the spoil are greater than in the case of loading operations. Varying transfer piping length directly influences changes of pump loads during transferring the winning. As results from the

performed investigations the maximum transfer piping length $L_{sp}^{\max}$ reached on average $4{,}46L_{sp}^{\min}$ (where $L_{sp}^{\min}$ - minimum transfer piping length) [9].

Values of the coefficient λ_{DP}^{sp} are close to those of λ_{DP}^{ls} and are contained in the range of 0,96÷0,99 at its mean value of 0,978.

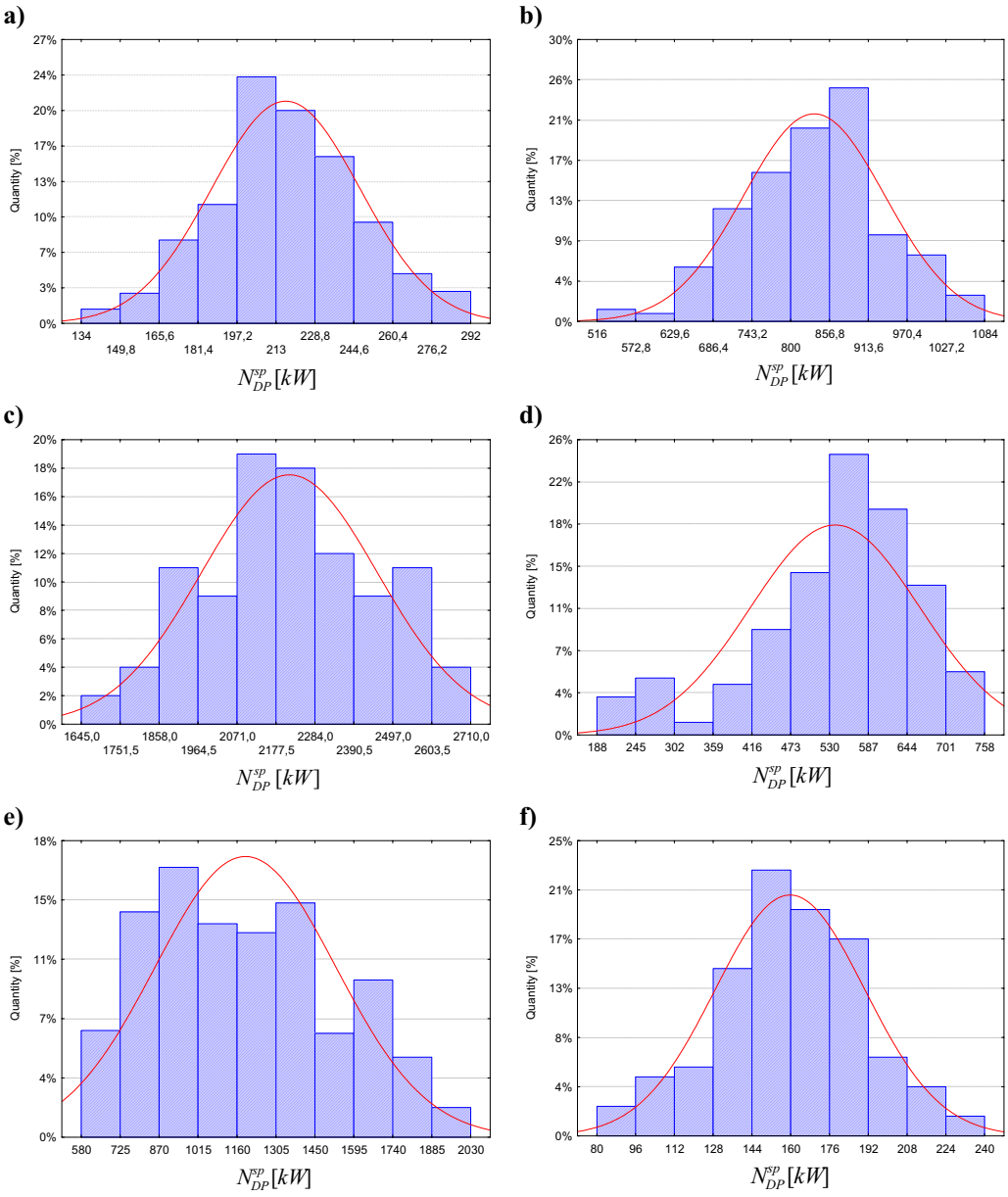

Fig.2. Load histograms of dredge pumps on dredgers during transferring the spoil; a) the tshd „Kostera", b) the tshd „Łęgowski", c) the tshd „Geopotes 15", d) the csd „Trojan", e) the barge unloading dredger „Rozkolec", f) the bld „MałżII"

Where: tshd – trailing suction hopper dredger,

csd – cutter suction dredger,
bld – bucket ladder dredger.

5. Summary

All the above presented calculation results concerning characteristics of dredge pumps and histograms of their loads represent real service conditions of such pumps on dredgers. Owing to the large number of investigated dredgers and the wide range of their size the results can be deemed representative of the entire population of dredge pumps operating on dredgers.

The presented results may be useful in predicting operational loads on dredge pumps depending on their service state on dredgers of various kinds. All that , when combined with knowledge of loads on other main power consumers and efficiency characteristics of power transmission systems of particular main power consumers, can make it possible to determine the service load characteristics of main engines installed on dredgers. This is especially important in preliminary design stages of power systems on dredgers.

Bibliography

[1] Bocheński D., Kubiak A., *Wybrane problemy eksploatacji pomp gruntowych na pogłębiarkach*. /Materiały/ XXI Sympozjum Siłowni Okrętowych SymSO 2000', Gdańsk 2000

[2] Vlasblom J. W., *Designing dredging equipment. Lecture notes*, TUDelft 2003-05

[3] Bocheński D., Kubiak A., *Analiza i ocena warunków pracy pomp gruntowych na pogłębiarkach ssących nasiębiernych*. Międzynarodowa XIX Sesja Naukowa Okrętowców NT. TECHNIKA MORSKA NA PROGU XXI WIEKU. Materiały konferencyjne, vol.2, Szczecin-Dziwnówek 4-6.V.2000r, 35-43

[4] Vlasblom J. W., *Dredger pumps. Lecture notes*, TUDelft 2003-05

[5] *Development and first production unit of the IHC Beaver WSDredger*. WODCON World Dredging Congress 1983

[6] Dokumentacja prób zdawczo-odbiorczych pogłębiarki „Nautilus", GSR, Gdańsk 1996

[7] *Kompleksyjne technologiczieskie issledowanija sudov popolnienija unstrukcyja po effjektiwnoj eksploatacji ziemsnarjada* „Gogland". GDK, Rostow nad Donem 1984.

[8] de Vries L., *Total performance simulations of ship energy concepts*. Wondermar II Workshop, Bremen 2004

[9] Bocheński D. (Kierownik projektu) i in., *Badania identyfikacyjne energochłonności i parametrów urabiania oraz transportu urobku na wybranych pogłębiarek i refulerów. Raport końcowy projektu badawczego KBN nr 9T12C01718*. Prace badawcze WOiO PG nr 8/2002/PB, Gdańsk 2002

[10] Balcerski A., *Modele probabilistyczne w teorii projektowania i eksploatacji spalinowych siłowni okrętowych*. Fundacja Promocji Przemysłu Okrętowego i Gospodarki Morskiej, Gdańsk 2007

Journal of POLISH CIMAC
Faculty of Ocean Engineering & Ship Technology
GDAŃSK UNIVERSITY OF TECHNOLOGY

INVESTIGATIONS OF EXHAUST EMISSION OF BIOGAS SI ENGINE IN SEWAGE ELECTRIC GENERATOR PLANT

Tadeusz Borkowski

Maritime University of Szczecin – Department of Engineering
70-500 Szczecin, Waly Chrobrego 1-2
tel: +48 91 4809400, fax: +48 91 4809419
e-mail: tborkowski@am.szczecin.pl,

Abstract

The heat co-generation power arrangements in which SI reciprocating engines are fed with biogas can pose a real alternative of waste energy utilization in the cleaning processes of municipal sewage. The emission of exhaust gases in sewage plant vicinity is an unavoidable characteristic of this design, which raises the issue of appraising the harmful components of the gases. The study shows the results of experimental investigations conducted on three generator sets with modern SI reciprocating Deutz engines, TBG620V12K - type. The results of complete norm tests were applied in parametric calculation of final exhaust gas emission coefficients. Due to transitory lack of national legislation on exhaust gas emission in such applications, limit values of emission were adopted from TA-Luft (Germany).

Keywords: *SI reciprocating engine, exhaust emission, biogas, heat co-generation arrangement*

Introduction

Structural transformations in Poland together with transition to new economic system helped the process of growth of renewable sources of energy utilization. The development strategy for renewable energy establishes incremental share of renewables in fuel-energy balance, where the key source of energy will be the biomass. Notion of "biomass" includes the substances of vegetal or animal origin that undergo biodegradation and come from consumer products, miscellaneous waste and remnants of agricultural and forest production, and also industries reprocessing these products down the production chain. The realization of such definite aims and the development of renewable sources of energy create a possibility of maintaining energy independence, and also a pro-ecological modernization, diversification and decentralization of national energy sector [1].

The biogas constitutes an attractive source of comparatively cheap energy. The biogas installations can be fitted to existing sewage plants that serve towns and cities. The secretion of settlings from municipal sewages is an essential part of the purifying process. Sewer settlings display a large variability in chemical composition that is dependent on property of sewage, and the technology of purification and processing. The amount of settlings in municipal sewages after purification processes is estimated in the range of 0,5÷2,0 % of unpurified sewer waters volume. The anaerobic stabilization process of sewage settlings causes the formation of biogas as a side product. Growing requirements related to the degree of sewage purification, processing and neutralization of settlings, increase demand for heat input and energy consumption at sewage plants. The high-methane biogas may be used to cover energy demands of processes in biogas plants.

The biogas handling and its degree of utilization in heating up fermentation chambers plays a very important part in plant energy balance as only the surplus biogas can be made use of for other purposes as deemed appropriate. The demand for internal heat use in the process of biogas production relates to supporting the process of fermentation (heating up sewer settlings within range of 10÷35°C). Moreover, the neutralization of biogas through burning becomes an indispensable necessity in the aspect of preservation of natural environment, particularly the

atmosphere, against the emission of un-burnt methane contained in biogas. It should be marked that the production of biogas is a side effect ensuing from the necessity of utilization of wastes in a least detrimental way for the environment.

The modern biogas installations, as a principle, should conclude with some type of energy production device. The biogas can be used in gas driven electric generators, gas boilers, heat co-generation arrangements that produce electric and thermal energy [2], [3]. The transmission of biogas for long distances is technically complex and therefore largely unprofitable. Its conversion to useable system gas is the most technologically advanced process of the utilization. The location of energy producing plants fed with biogas will therefore be in close proximity to municipal agglomerations. This calls for an assessment of their operational harmfulness mainly reflected in exhaust fumes emission. The aim of this work is an experimental appraisal of exhaust gas emission of engines operated in a modern sewage treatment plant of municipal sewage waters.

1. The biogas production installation – an analysis of feasibility of supplying SI engines with biogas

1.1. Biogas formation and composition

The mixture of gases that forms in biological processing of organic pulp, devoid of oxygen, is termed the biogas. This widespread in nature process can also be recreated in artificially altered conditions in reservoirs with organic pulp. The biogas forms as a result of anaerobic organic matter fermentation, for example biomass or sewer settlings, that is, biodegradable solid waste matter. The organic pulp transforms into biogas yielding also small amounts of heat and residual biomass. Created in this way mixture of gases consist mainly of methane and carbon dioxide. Small quantities of hydrogen, hydrogen sulfide and traces of ammonia and different vestigial gases, are not uncommon in the biogas. One of the methods of biogas production that can be applied in reference to bio-organic municipal wastes is anaerobic fermentation, which is held in three structural phases: hydrolysis, acid fermentation and methane fermentation. Participating in this process bacteria release the enzymes, which dissolve the material along biochemical reactions.

Subsequently, in the second structural phase, indirect products of these reactions decompose, with help of acid-forming bacteria, to fatty acids (acetic, butyric and propionic), hydrogen, and carbon dioxide. In the next structural phase, these products transform into substances preceding biogas formation. Methane forms in following, final phase as the result of wearing away of hydrogen. If all four phases take place in one fermentator, then this is defined as one stage process. However, dual module installations divide hydrolysis and acidification into two stages. The quantity and gas composition of emerging biogas depends on quality of output material and the quantity of organic compounds contained. The course of fermentation process is dependent on a sequence of factors of which the most important are: temperature (within range of 4÷70°C), time of reaction (at 30÷35°C it takes from 12 to 36 days, while at the temperature 52÷55°C, 12 last to 14 days) and the pH reaction (~ 7) [4].

The composition of the biogas is dependent on the chosen technological process and applied material, the universally occurring exhibits: 55÷85% CH_4, 14÷48% CO_2 with small quantities of: hydrogen sulfide, nitrogen, oxygen, hydrogen and other vestigial substances. The proportional share of methane in the biogas determines its calorific power. By means of example, biogas containing 65% methane has a calorific value of 23.0 MJ/m^3. Hydrogen sulfide, which is present in the biogas in small quantities, creates a number of technical problems [5].

1.2. Associated production of thermal and electric energy

The transformation of biogas energy into thermal energy occurs through combustion in boilers or SI engines. Due to the fact that calorific value of biogas significantly differs from universally applied natural gas, its use is not feasible with typical gas burners without prior modification, or SI engines with standard gas intake installations. The associated production of thermal and electric energy is realized through co-cogeneration system. A cogeneration unit consists of two elements: an electric system, which makes up the electric generator set (the SI engine - electric generator) and a thermal system. Electric energy is created thanks to the work of the generator set. Thermal energy, on another hand, is captured from heat exchangers built into piston engine installations: gas-air mixtures, lubricating oil, cooling water and exhaust gas.

The SI reciprocating engines are most often used in low power associated arrangements. The production of electric energy in associated arrangements from biogas requires large flexibility due to varied gas supply and unstable demand for energy. The possible occurrences of variation in gas flow or its composition during system operation greatly influence the installation design choice and the type of produced energy.

2. Project investigative foundations

2.1 Description of experimental test bench

The methane fermentation with biogas acquirement is conducted in closed fermentation chambers from where it is transmitted to a constant-pressure gas tank. During fermentation every one of four reservoirs of 5000m^3 capacity exudes biogas, with total volume of about 12000m^3 per day. Due to high concentration of hydrogen sulfide (~ 0.2%) the biogas is subjected to desulfurization until a value that meets PN-71/C-96001 standard is reached. The clearing of unpurified hydrogen sulfide takes place in a biological fluid reservoir of 60m^{3}capacity.

The biological desulfurization method relies on microbiological oxygenation of hydrogen sulfide by microorganisms of oxygenic bacteria on a biological bed. The purified gas has a concentration of hydrogen sulfide below 0.02g/m^3. Subsequently, the biogas gets accumulated in a wet type reservoir of 3000m^3 capacity in order to stabilize its flow in the supply installation, and be partially stored. The biogas is then pressed into supply system of two boilers rated 1400kW (each). Boilers are mainly used for heating up of fermentation settlings within spiral heat exchangers (technological water and fermentation settlings) up to 35÷37 centigrade Celsius, an indispensable value for realization of mesophillic fermentation. Whereas, the excess of produced gas is used for supplying the cogeneration arrangement that generates electric energy and heat. The layout of engine biogas supply installation is shown on Fig. 1. The source of the arrangement consists of SI gas engine propelling asynchronous generator, and a unit of two heat exchangers, which is shown on Fig. 2.

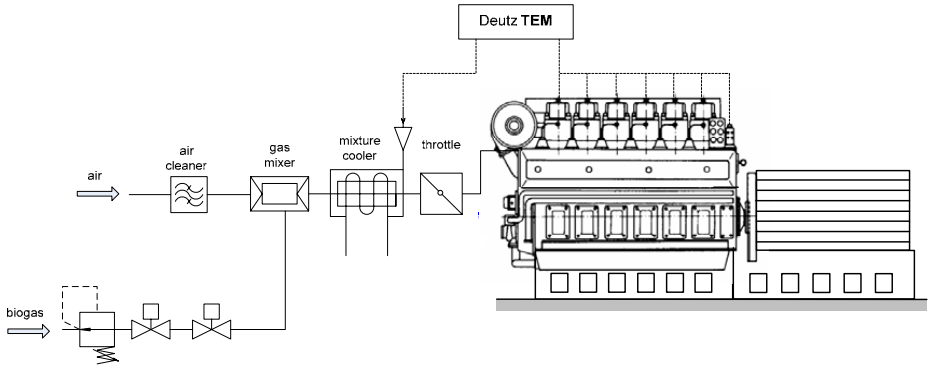

Fig. 1. Layout of generator set biogas supply system

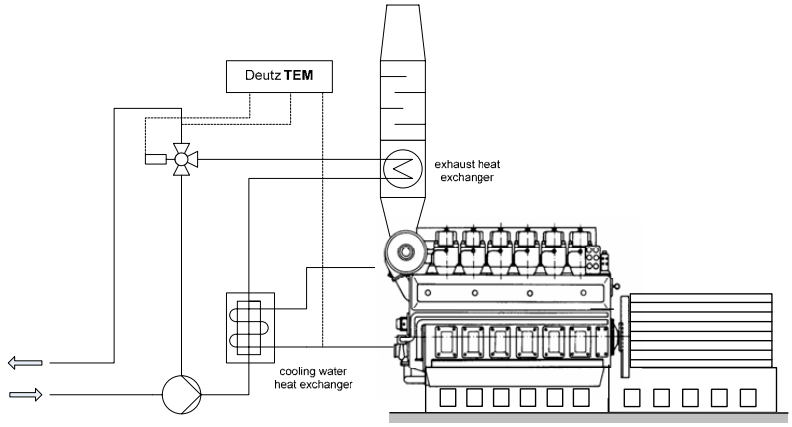

Fig. 2. Layout of generator set heat exchangers

This is a typical installation of associated power engineering CHP producing electric energy and heat, where the heat is delivered to a local distribution network. The produced electric energy largely covers plant energy demands. The production of biogas can provide heating for fermentation chambers, and supply generator set with gas also in the winter time. The biogas generator set is controlled by means of a control and monitoring system, and few automatic safety units, which cut off gas flow and arrest the engines.

2.2 The objective of investigation

The aim of the study is to assess the emission into plant surroundings of harmful gaseous exhaust components from engines in current-generating assembly at the sewage treatment plant. Standard exhaust emission coefficients were calculated and compared with the requirements of selected European standard (TA-Luft[1]) due to the lack of Polish environmental norm for this class of SI engines. The exhaust emission requirements and limits of TA-Luft do not belong to the lowest ones found in other European countries [6]. Experimental investigations were carried out during the site tests of generator units. The object of examination were three Deutz high speed engines, type TBG620V12K (12V- cylinders), whose basic parameters are presented in Table 1.

[1] 30.07.2002 - Germany

Tab.1. Test engines specification

Effective power	kW	970
Nominal speed	1/min	1500
Bore/stroke	m	0.170/0.195
Mean effective pressure	bar	14.6
Specific fuel gas consumption[2]	kWh/kWh	2.53
Exhaust flow	kg/h	5114
Exhaust temperature (max)	°C	480
Thermal efficiency	%	48.7
Electrical efficiency	%	38.5
Total efficiency	%	87.2

2.3 The method of investigation

As stated earlier, the additional aim of this investigation was a comparison of obtained exhaust emission coefficients with TA-Luft standards. The realization of following engine exhaust gas measurements of harmful components was therefore essential: NO_x, CO, SO_2, and deflagrated hydrocarbons – measured in two ways: as the sum of all deflagrated hydrocarbons (THC - Total Hydrocarbons) together with a share of methane as NMHC (Non-Methan Hydrocarbons), that is hydrocarbons without the share of methane with the use of methane separating module - NMC. Exhaust emission in this context denotes the emission of the characteristic component of exhaust gas, expressed in [mg/m^3], related to standard conditions and constituting the result of averaging for the work of engine according to the standardized test cycle. The measurement of engine exhaust emission parameters and the methodology of calculations was based on definite principles of PN-EN ISO 8178 norm. The measurements were conducted according to the standard ISO 8178 (part 4) test cycle for engines operating with constant speed - D2. The engine exhaust gas emission components were quantified through volumetric measurement with utilization of recommended by ISO 8178 (part 1) norm exhaust gas analyzers (measuring arrangement assembly is shown on Fig. 3).

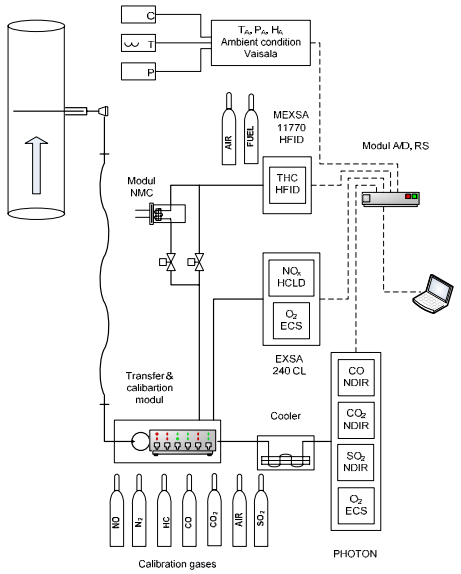

Fig. 3. Engine exhaust emission measurement setup

[2] Fuel Gas Consumption/ Electric Energy

The exhaust gas analyzers were calibrated before commencing the measurements and audited upon finish. The samples of exhaust gas were continuously taken from pipe connector placed in exhaust gas duct (in funnel above the hall's roof) of engine outlet system, after turbine and heat exchanger, by means of a heated line (192° C), all throughout test cycle duration. Observed exhaust gas component concentration values used in calculations, recorded at 1 second intervals, constitute the average value from three (one-minute) cycles of every structural constituent of test cycle program. The ambient surrounding conditions were registered with the use of an integrated device throughout measurements. Test engine parameters and indicators required for the test cycles and essential in determination of emission amount in accordance to ISO3046 (part I, II, III and IV) standard, were obtained through the registrations of engine control and supervision system.

The engines were supplied with gas fuel (biogas), proprieties shown in table 2. The fuel gas supply system was equipped with flow meters, pressure and temperature sensors, whose indications were used in assessment of fuel stream used by measurement apparatuses during the realization of engine test cycles.

Tab.2. Fuel gas specification

Factor			Value
1	Density @ 20°C	kg/m^3	1.095
2	Calorific value @ 20°C	MJ/m^3	19.74
3	CH_4	%	58.08
4	CO_2	%	34.97
5	N_2	%	3.82
6	H_2O	%	1.08
7	O	%	1.03
8	H_2S	ppm	>300

The majority of gas fuels being used to drive cogeneration arrangements is characterized by low calorific value. The usability of gas fuel in the aspect of CHP arrangements depends on a number of properties of which the most important are: calorific value, Wobbe number, knock combustion resistance, the speed of air-fuel mixture deflagration, and low content of impurities. The so-called methane number defines the knock resistance of the gas fuel. The higher the methane number is, the larger the knock resistance of the fuel. The gas fuel methane number corresponds to volumetric methane content in methane-hydrogen mixture. The value of gas fuel methane number depends on the content of methane and different hydrocarbons, and the share of inert gases such as CO_2 and N_2 [7]. The methane number drops with content growth of hydrocarbons other than methane. The low methane number raises the necessity of lowering engine compression ratio. The Wobbe number is the essential parameter characterizing gas usable properties in terms of utilization in energy-producing devices. It also defines the possibility of interchangeable application of various gas fuels. Its magnitude is equal in importance to gas calorific value and burning temperature.

In case of low-calorific gas deflagration, a deciding factor of fuel applicability in respective devices is its combustion velocity, which depends on air excess coefficient to combustion. It is accepted that the minimum combustion velocity of gas fuels in SI gas engines (without added mixtures of another flammable gas) is 0.008m/s. A number of the gas fuels applied in small engine-cogeneration arrangements are used independently, while some are enriched with natural gas.

3. The results of investigation

The emission coefficients calculations were based on representative group of data chosen from digital notation files of every test cycle load. Some examples of data used in analysis

(example in Table 3 - appendix) are visually demonstrated on graphs: Fig. 4 for the generator set no:1, and Fig. 5 for the for the generator set no: 3. The statistical analysis of measurement data was executed for estimation of errors and value dispersion. The sample results of coefficients emission calculation is shown in Table 4 (appendix). The NO_x emission was corrected according to ISO standard procedure. The emission of chosen components of exhaust gas expressed as mass concentration converted to conventional conditions with the required 5% share of oxygen, allowed for emission comparison with TA-Luft norm.

A decision was made to enlarge the error margin on SO_2 measurement to account for measurement range of one of the sensors (0-5000ppm). The measured concentration value was within 10% of lower limit for a part of measurement duration. It should be assumed that resultant error could be as high as 15% of absolute value.

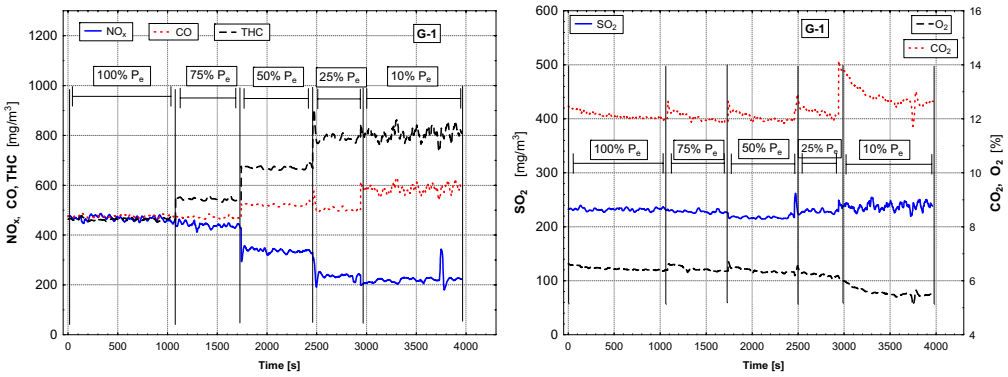

Fig. 4. NO_x, CO, THC, SO_2, CO_2 and O_2 concentration for generator set No:1 test cycle

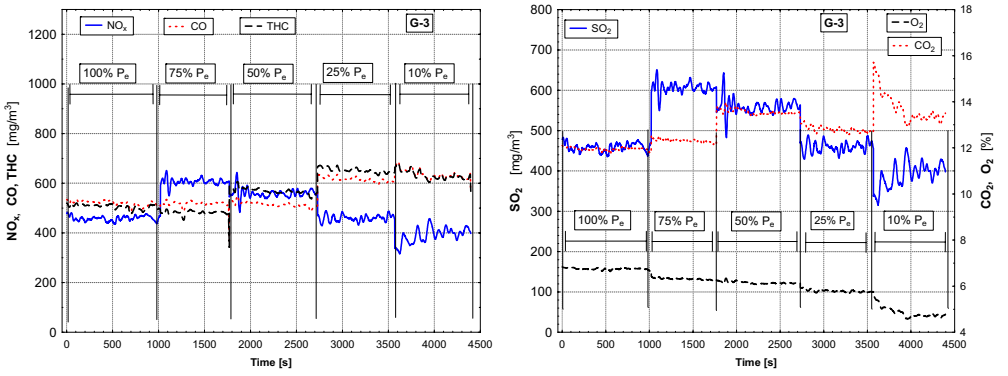

Fig. 5. NO_x, CO, THC, SO_2, CO_2 and O_2 concentration for generator set No:3 test cycle

This factor caused underestimation of SO_2 content in the exhaust gas. The inconsistency of the measured SO_2 concentration was confirmed with the qualitative content analysis of the biogas. However, it should be noted, the type - matter laboratory analysis of the biogas should not be treated as an absolute reference system for this particular setting, that is as fuel for the engines in question. Questionable methodology of gas sample uptake (plastic bags were used) was something of an issue, as well as assessment of H_2S presence only, omitting other biogas components that include sulfur. The measurement of all other exhaust gas emission components could be classified as highly accurate thanks to applied measuring devices (laboratory quality) and a fact of double measurements of NO_x and HC (two analyzers). The obtained concentration values of NO_x were

closely compatible with the results of engine delivery-acceptance certificates, validating the methodology and apparatus accuracy. The THC measurement (Total Hydrocarbons, in Poland - Volatile Organic Compounds) was made in a dual form:

- the appraisal of total sum of hydrocarbons converted into pure carbon C according to effective reference methodologies in Poland.
- the appraisal applied to engines fed with biogas, that is NMHC (Non-Methane Hydrocarbons), according to TA-Luft requirements. The value of hydrocarbons sum was converted into pure carbon C, with subtracted value of methane - CH_4. This determination, like before, was realized through reference methodology.

4. Conclusions

The concord of mass emission of chosen components in exhaust gases of engines in question with TA –Luft norm can be defined in the following way:

1. In reference to NO_x emission, two engines, GS-1 and GS-2, showed full compatibility of emission factors in dominant range of engine effective load range. Small departure was noted, emission values surpassing the limit, for engines at nominal load as follow: for GS-1, it was 13.9mg/m^3 what constitutes a 2.8% breach of limit value; for GS-2, it was 37.5mg/m^3, what constitutes a 7.5% breach of limit value. Due to the methodology of test conduction at engine installation site and taking into account industrial setting and ensuing from it limited technical capabilities for conduction of measurements, both emission values satisfy limit conditions at 500mg/m^3 level within error range. However, the GS-3 engine demonstrated NO_x emission levels way above the limit, for both partial and nominal engine load. The maximal NO_x emission value for this engine was estimated at 661.3mg/m^3 at 75% effective load, which constitutes a violation of the limit by 32.3 %. It has been stated that NO_x emission of GS-3 engine was not compliant with requirements of TA-Luft norm.
2. All three engines showed CO emission levels below the limit of 1000mg/m^3, fulfilling the TA-Luft standard.
3. The SO_2 emission of all three engines showed values below the 350mg/m^3 limit, fulfilling the TA-Luft standard.
4. The NMHC emission of all three engines showed values below the 150mg/m^3 limit, fulfilling the TA-Luft standard.

The visual comparison of exhaust emission values specified in TA-Luft norm: NO_x (expressed as NO_2 concentration), CO, SO_2, NMHC for respective engines is shown in Figure 6, and 7 below.

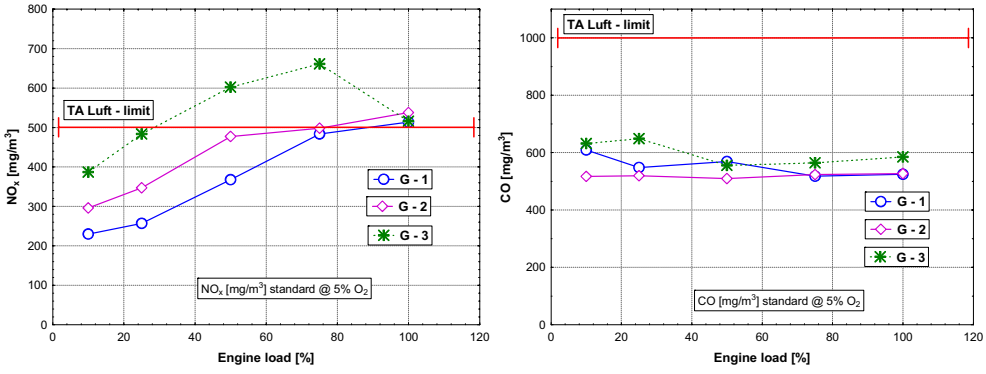

Fig. 6. Engine NO_x and CO emission values comparison against TA-Luft standards

Obtained engine NO_x emission factors could be classified as exceptionally low in comparison with adequate CI engines of corresponding power, whose NO_x emission is few times higher (weighted average specific emission coefficient). It should added that the NO emission coefficient for CI and SI reciprocating piston engines is subject to variation during operating period, as it is contingent on various factors, but it will be contained within the 10% range of absolute values reflecting engine effective load, and will remain at uniform level throughout the very long period of exploitation. It can only demonstrate considerable aberrations from the norm (growth or fall) in cases of engine damage (some functional units) or its technical modification.

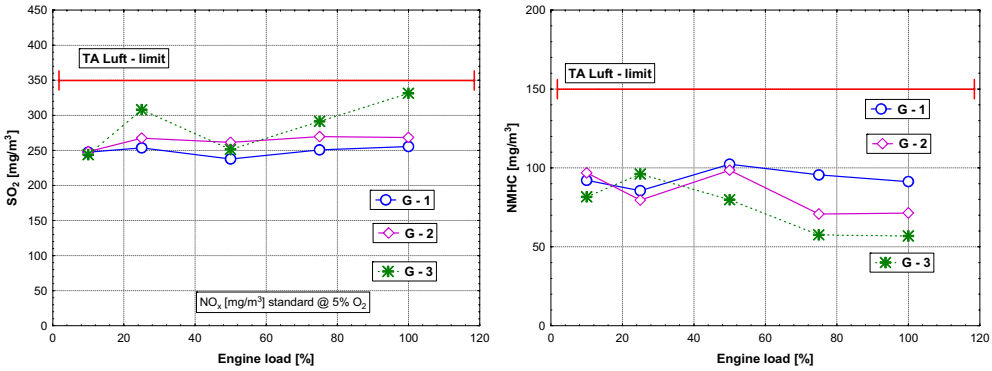

Fig. 7. Engine SO_2 and NMHC emission values compared against TA-Luft standards

In general terms, the exhaust emission performance of TBG620V12K Deutz engines can be described as correct and exceptionally low (in comparison to spontaneous ignition CI engines). The emission performance (except the GS-3 engine - the NO_x emission) is entirely in concord with TA-Luft requirements, and is very similar to modern engines of this class in analogous applications (fed with biogas). The exhaust gas component remaining in close relationship to fuel in use is SO_2, whose obtained concentration factors are burdened with relatively high uncertainty (the gas composition analysis and exhaust gas component concentration analysis). Those two reasons impinge upon the fact of accepting SO_2 emission in practice mainly relying on proven and accurate type - matter analysis of the fuel, but not on exhaust gas concentration analysis, which is less credible due to large underestimation in connection to present technology of quantitative assessment of this compound in the hot fumes.

Abbreviation

P_e	effective power,
n	rotational speed,
f_a	ambient conditions factor,
t_a	ambient air temperature,
t_c	charge air temperature,
t_b	biogas temperature,
t_g	exhaust gas temperature,
p_c	charge air pressure,
p_b	biogas pressure,
V_b	biogas flow,
w_g	exhaust gas velocity,
K_{HDIES}	Atmospheric air humidity correction coefficient for NO_x

Index
d – dry,
w – wet

Acknowledgments

The author would like to thank Budimex (Poznań) for the possibility of creating experimental part of this paper and the permission to use parts of this report in the study: Borkowski T., Zimnicki B.: Badania emisji spalin silników zespołów prądotwórczych typu TBG620V12K – Deutz, PPHU Atmoservice – Poznań, 2007

References

[1] REEH U., MØLLER J. *Evaluation of different biological waste treatment strategies*, http://orgprints.org/1924/,
[2] WALLA C. SCHNEEBERGER W. *Survey of farm biogas plants with combined heat and power production in Austria*, Proceedings International Nordic Bioenergy 2003 Conference Jyväskylä, Finland, 2003,
[3] REDDY A. K. *Lessons from the Pura community biogas Project*, Energy for Sustainable Development l Volume VIII No. 3l, articles 73, September 2004,
[4] PLÖCHL M., HEIERMANN M. *Biogas Farming in Central and Northern Europe: A Strategy for Developing Countries*, Agricultural Engineering International: the CIGR Ejournal. Invited Overview No. 8. Vol. VIII. March, 2006,
[5] WEILAND P., RIEGER CH., EHRMANN TH. *Evaluation of the newest biogas plants in Germany with respect to renewable energy production, greenhouse gas reduction and nutrient management* , Future of Biogas in Europe II, Esbjerg 2-4 October 2003.
[6] ROUBAUD A., RÖTHLISBERGER R., FAVRAT D. *Lean-Burn Cogeneration Biogas Engine with Unscavenged Combustion Prechamber: Comparison with Natural Gas*, Int.J. Applied Thermodynamics, Vol.5 (No.4), December 2002, pp.169-175,
[7] JAN K. JENSEN J. K., JENSEN A., J. *Biogas and natural gas fuel mixture fort the future*, 1st WORLD CONFERENCE AND EXHIBITION ON BIOMASS FOR ENERGY AND INDUSTRY, SEVILLA, 2000.

Appendix

Tab.3. Engine test cycle data (example)

Object - parameter			Unit	Engine effective power				
				1	2	3	4	5
1	Engine	P_e	[%]	100	75	50	25	10
2		P_e	[kW]	970	727.5	485	242.5	97.0
3		n	[1/min]	1500	1500	1500	1500	1500
4		p_c	[bar]	1.75	1.15	0.57	0.03	0.01
5		t_c	[°C]	58.6	58.1	57.4	57.7	57.8
6	Ambient conditions	p_a	[kPa]	100.27	100.29	100.29	100.30	100.31
7		t_a	[°C]	30.7	32.6	32.9	33.0	28.9
8		H_a	[%]	34.0	30.0	29.0	34.0	27.9
9		f_a	[-]	1.045	1.055	1.057	1.057	1.036
10	Supply gas	V_b	[m^3/h]	411	325	228	145	83
11		t_b	[°C]	29.5	30.4	31.0	32.4	32.9
12		p_b	[kPa]]	81	82	82	85	85
13	Exhaust emission	t_g	[°C]	218	203	181	155	141
14		p_g	[Pa]	150	79	38	16	2
15		p_s	[Pa]	221	107	43	23	3
16		w_g	[m/s]	17.28	12.64	8.81	5.26	3.18
17		t_g	[°C]	167	164	121	124	108

18		O_{2s}	[%] vol	7.70	7.27	7.11	6.77	5.73
19		CO_{2d}	[%] vol	11.95	12.32	13.56	12.81	13.72
20		CO_d	[ppm] vol	417.33	415.0	412.5	430.3	509.4
21		SO_{2d}	[ppm] vol	103.0	93.5	81.5	89.3	86.1
22		THC_w	[ppm] vol	945.8	898.8	1064.0	1218.0	1183.3
23		NO_{xw}	[ppm] vol	228.2	300.1	276.2	213.4	200.3
24		K_{HDIES}	[-]	0.981	0.986	0.987	1.005	0.952
25		NO_{xcorr}	[ppm] vol	223.9	295.8	272.5	214.5	190.6
26		O_{2w}	[%] vol	6.75	6.3	6.15	5.80	4.85

Tab.4 Engine test cycle data (example)

Measurement number					**1**	**2**	**3**	
No:	Parameter			Unit	Value			Average
1	Ambient conditions	Barometric pressure		Pa	100520	100520	100520	100520
2		Air temperature		°C	30.5	30.6	30.6	30.6
3	Exhaust gas duct	Diameter		m	0.3			0.3
4		Surface area		m^2	0.071			0.071
5	Exhaust gas	Temperature		K	434.2	434.2	434.2	434.2
6		Static pressure		Pa	233.0	233.0	233.0	233.0
7		Dynamic pressure		Pa	124.6	124.6	124.6	124.6
8		Gas moistness (water)		%	4.2	4.2	4.2	4.2
9		Gas average velocity		m/s	17.4	17.4	17.4	17.4
10		Chemical composition	O_2	%	6.5	6.4	6.4	6.5
11			CO_2	%	12.3	12.1	12.0	12.1
12		Wet gas density*		kg/m^3	0.82	0.82	0.82	0.82
13	Concentration	NO_x		mg/m3	471	466	464	467.0
14		CO		mg/m3	477	476	476	476.3
15		SO_2		mg/m3	233	232	232	232.3
16		THC		mg/m3	464	463	463	463.3
17		NMHC		mg/m3	83	83	83	83.0
18	Emission	NO_x		kg/h				1.258
19		CO		kg/h				1.283
20		SO_2		kg/h				0.626
21		THC		kg/h				1.248
22		NMHC		kg/h				0.224

* measurement conditions

Journal of POLISH CIMAC

Faculty of Ocean Engineering & Ship Technology
GDAŃSK UNIVERSITY OF TECHNOLOGY

ANALYSIS AND ASSESSMENT OF THE ACOUSTIC EMISSION SUITABILITY FOR DETERMINATION OF THE ENERGY STATES OF A TRIBOLOGICAL SYSTEM IN THE FORM OF A FOUR-BALL TESTER FRICTION NODE

Piotr Bzura

Gdansk Uniwersity of Technology
ul. Narutowicza 11/12, 80-952 Gdansk, Poland
tel. +48583472573

Abstract

The present operating safety and cost reduction requirements of the compression ignition engines make it necessary to search for new methods of detecting their defects, e.g. by the analysis of acoustic emission signals coming from the slide bearings. The paper presents non-destructive measurements of acoustic emission (AE) in order to obtain information on the processes taking place in a tribological system under the continuously increasing load.

Key words: tribological system, acoustic emission, energy state

1. Introduction

Ensuring safe sailing of a sea-going ship requires having sufficient amount of energy obtained from the chemical energy contained in the fuel combusted in compression ignition engines. That energy must be transmitted through many tribological systems to different receivers, e.g. to the screw propeller. The energy is then transformed and transmitted in the tribological systems. Therefore, it is justified to consider the tribological systems as energy expenditure devices. Operation is such an energy state of a tribological system when transformation and transmission of energy takes place [3, 4].

Maintaining a compression ignition engine in the operational state for as long a time as possible requires collecting sufficient information on the tribological system physical and chemical parameters. It is necessary to know the technical state of a tribological system for its proper operation, or for maintaining the energy state.

The paper deals with the assessment and analysis of the impact of release of the material accumulated energy by propagating micro-defects (increased micro-cracks) on the tribological system energy state. The object of investigation was a tribological system in the form of a four-ball tester friction node. Each ball has a primary distribution of the elastic energy (residual stresses) and a certain level of the structural defects and even micro and macro damage. The cause of change of the ball material state of equilibrium is the change of stress and temperature. If we assume that the bearing ball manufacturing stage structure of the external layer and the material interior was correct (i.e. in compliance with the respective standards) then acoustic emission should be considered a signal of degradation of properties of a given tribological system element.

Additionally the acoustic emission may be considered from the point of view of changes in the bearing ball material. These are, among others [2]:

- movement of vacancies and dislocations, grain boundary slip - possible in the high stress areas near the material yield point,

– connecting of dislocations, creation and development of cracks - a strong AE source.

It can be seen that AE may be a good tool for physical investigation of the material destruction process and on the other hand a tool for detecting internal defects reducing the tribological system strength.

The energy release impact investigations [1] were carried out on the T-02 four-ball tester with Vallen piezoelectric gauges (Fig.1), in the conditions defined in Section 2.

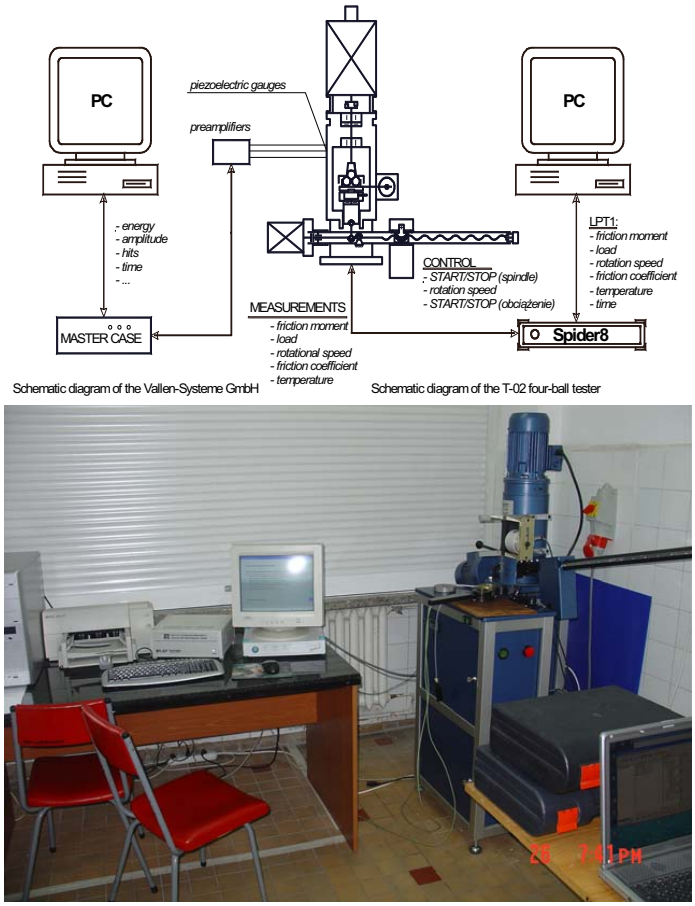

Fig.1 Schematic diagram of the ITeE Radom company four-ball tester and the Vallen-Systeme GmbH AMSY-5 apparatus measurement and control systems[1]

2. Investigation methodology

The investigations were carried out in four stages on the Marinol RG1240 lubricating oil of a Cegielski-Sulzer 8S20UD-H engine:

– clean oil (not used for lubrication),
– used oil,
– used oil with a 5% content of the MDO fuel that the engine is fed with,
– used oil with a 5% content of distilled water.

In order to obtain a broad picture of the impact of forcing intensity on the tribological characteristics, the following testing parameters were adopted [1,5]:

– spindle roational speed: 500 rpm, 1000 rpm, 1500 rpm
– load escalation rate: 409 N/s
– initial load: 0 N
– maximum load: 7400 ± 100 N
– lubricating oil temperature: 60°C

The friction node constituted dia. 12.7 mm bearing balls from the LH15 steel (iron alloy with an average content of 1% C, 0.02% S, 0.3% Ni, 0.3% Cu), accuracy class 16 in accordance with the PN-83/M-86452 standard, dipped in the tested lubricating oil.

Altogether 12 different tests were carried out and each one was additionally analysed by the AE gauges (Fig. 2).

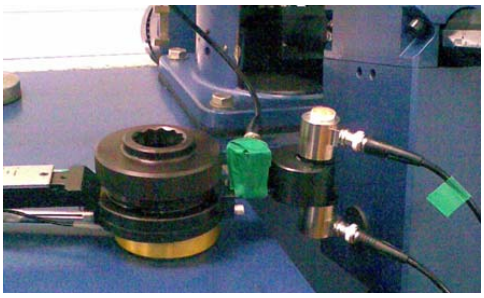

Fig. 2. Positioning of three piezoelectric gauges in the T-02 four-ball tester friction node [1]

During the AE measurements, the most often used measure of the phenomenon is the impulse (event) count or the AE rate (number of events in a time unit). Also the AE energy may be used, i.e. area under the envelope of the squared amplitude. These quantities are illustrated in Fig. 3, an example of one AE impulse.

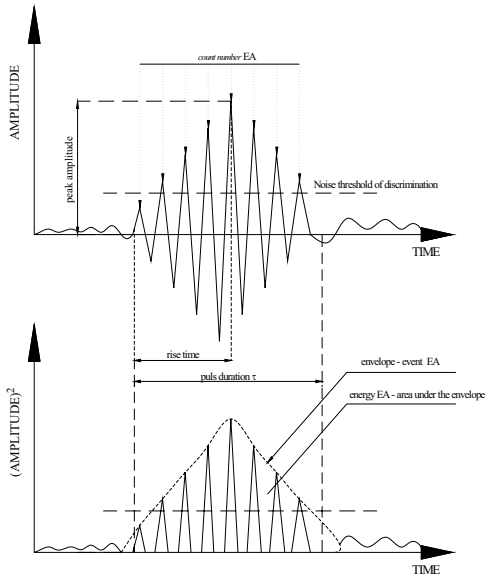

Fig.3. The AE phenomenon main description and valuation parameters, Σ = count number, event, event energy in V^2 sec [2]

3. Analysis of the investigation results

Based on the results of measurements performed by the T-02 four-ball tester and the AMSY-5 apparatus measurement and control system, an analysis was carried out of which diagnostic parameters may be useful (Table 1 and Figs. 4 to7).

Table 1. Values of the calculated diagnostic parameters

1	P_t	f_t	A_t	E_t
Clean oil: measurement at 500 rpm	1604		51	503
Clean oil: measurement at 1000 rpm	1610		48,5	193
Clean oil: measurement at 1500 rpm	1621		47,9	185
Used oil: measurement at 500 rpm	1237,2	0,72	54,7	202
Used oil: measurement at 1000 rpm	1351,2	0,66	49	200
Used oil: measurement at 1500 rpm	1380	0,62	48,7	208
Used oil + 5% MDO: measurement at 500 rpm	1156,8	0,72	55,8	8080
Used oil +5% MDO: measurement at 1000 rpm	1244,4	0,64	76,9	1970000
Used oil +5% MDO: measurement at 1500 rpm	1294,8	0,63	76,9	1970000
Used oil + 5% H_2O: measurement at 500 rpm	949,2	0,77	85,2	36900000
Used oil +5% H_2O: measurement at 1000 rpm	1017,6	0,66	72	2070000
Used oil +5% H_2O: measurement at 1500 rpm	1114,8	0,65	75,4	5090000

where:

- P_t – seizing load [N],
- f_t – maximum value of the kinematic friction coefficient [-],
- A_t – peak amplitude at the seizing load [dB],
- E_t – seizing load energy [eU].

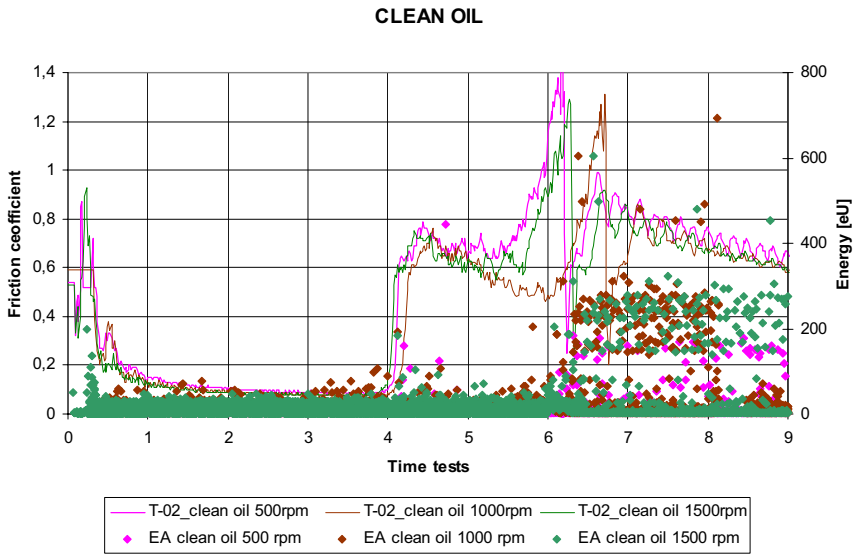

Fig. 4. Changes of the AE energy caused by the kinematic friction in the friction node dipped in clean oil, where: T-02_clean oil 500 rpm – friction coefficient change at 500 rpm curve; AE clean oil 500 rpm – AE energy distribution at 500 rpm curve; T-02_clean oil 1000 rpm – friction coefficient change at 1000 rpm curve; AE clean oil 1000 rpm – AE energy distribution at 1000 rpm curve; T-02_clean oil 1500 rpm – friction coefficient change at 1500 rpm curve; AE clean oil 1500 rpm – AE energy distribution at 1500 rpm curve;

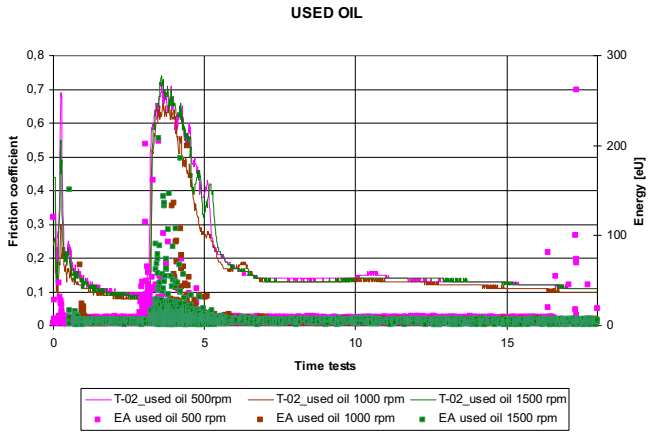

Fig. 5. Changes of the AE energy caused by the kinematic friction in the friction node dipped in used oil, (curve designations as in Fig. 4)

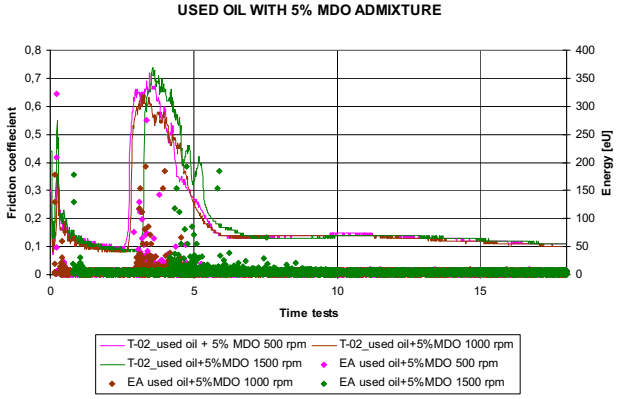

Fig. 6. Changes of the AE energy caused by the kinematic friction in the friction node dipped in used oil with 5% MDO admixture, (curve designations as in Fig. 4)

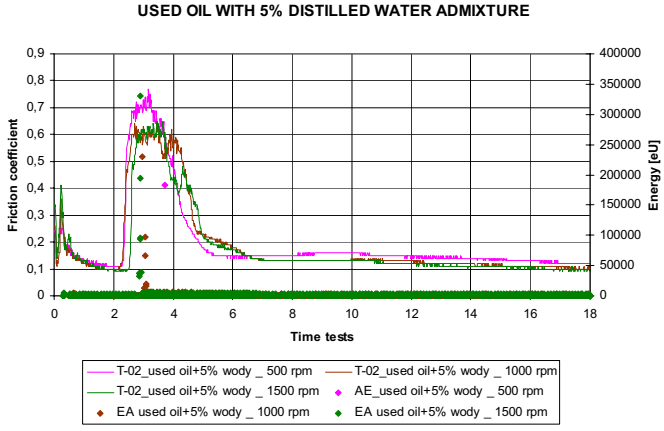

Fig. 7. Changes of the AE energy caused by the kinematic friction in the friction node dipped in used oil with 5% distilled water admixture, (curve designations as in Fig. 4)

During clean Marinol RG1240 oil testing (Fig. 4) the ball seizure and welding together occurred, therefore the maximum value of the kinematic friction coefficient is missing (Table 1).

4. Final remarks and conclusions

The compression ignition engine tribological system boundary layer action is understood as transmission of the friction node load energy in a given time, in the form of work dependent on the friction node tribological parameters. The work value may indicate the energy states of tested tribological systems, corresponding to specific technical states (i.e. fully operational, partially operational and nonoperational state).

Results of the tests carried out by the authors of reference [4] should be treated as a pilot study. The results pertain to the acoustic emission of friction node in the T-02 four-ball tester with the Vallen-Systeme GmbH company AMSY-5 apparatus set connected to it. The main purpose of the tests was analysing the lubricant interaction with the friction surface by the acoustic emission signals.

The tests indicate a significant probability of strong correlation between the kinematic friction coefficients defining the friction node technical state, and the AE signals defining the friction node energy state. The following requirements should be met in order to improve the reliability of the T-02 four-ball tester results and to facilitate the energy state separation:

- sample the lubricating oil in the whole period of a compression ignition engine operation and compile a test result biography,
- the four-ball tester friction node balls should have the same overlay structure as e.g. the main slide bearing liners,
- install in the four-ball tester friction node a number of different piezoelectric gauges in order to determine the energy released during the boundary layer destruction process.

References:

[1] H. Buglacki, P. Bzura, P. Eichert: *Analysis and assessment of wear changes in the T-02 tester friction node indicated by acoustic parameters*, (in Polish) Work performed within the Ministry of Science grant no. 08/08/PB

[2] Cz. Cempel: *Vibroacoustic Diagnostics of Machines*, (in Polish), Warszawa 1989 PWN.

[3] J. Girtler: *Analysis and synthesis of a decision-making situation in the energy system operation process*, (in Polish), Work performed within the Ministry of Science grant no. N509 045 31/3500.

[4] j. Girtler: *Concept for interpretation and assessment of slide bearings operation in diesel engines in probabilistic approach*, Eurpean Science Society of Powertrain and Transport Publication, Warsaw 2007

[5] M. Szczerek, W. Muszynski, *Tribological investigations. Seizing*. (in Polish), Radom: Biblioteka Problemów Eksploatacyjnych 2000.

Journal of POLISH CIMAC
Faculty of Ocean Engineering & Ship Technology
GDAŃSK UNIVERSITY OF TECHNOLOGY

ASSESSMENT OF MARINE ENGINES TORQUE LOAD WITHOUT USING OF THE TORQUEMETER

Leszek Chybowski

Maritime Academy of Szczecin
Ul. Wały Chrobrego 1-2, 70-500 Szczecin, Poland
tel.: +48 91 4809412, tel.: +48 607 288978
e-mail: l.chybowski@am.szczecin.pl

Abstract

One of the aspects of marine engine operation is defining its torque load. It is crucial for both the general estimation of the engine working parameters value reflecting the engine's operational condition and for comparing its current condition with the previous one (recorded during the last check of the engine performance) or its state during the trials at the engine test bed. In the paper there have been analyzed the well known and recommended by marine engine manufacturers methods of estimating marine engine torque load without any torquemeter used, based exclusively on measurable working parameters of marine engines. To most marine engines the above mentioned indirect methods apply since so far the systems of taking torque direct measure have been neither common nor standard engine room equipment. Methods based on parameters obtained during engine indicating (engine performance check), fuel rack setpoint or load indicator reading and turbocharger system working parameters have been presented. Example nomograms for engine torque load estimation for engines manufactured by famous makers have been shown. Some of the methods have been compared based on parameters obtained during engine performance check. Discussion on the advantages and disadvantages presented methods has been presented.

Keywords: *marine engine, torque load assessment, effective power, torquemeter*, indirect estimation

1. Introduction

Methods of evaluating engine effective power can be divided into direct (making use of brakes or simultaneous measure of torque and revolutionary speed) and indirect ones (approximate). Brakes are used only during the manufacturer's engine trials whereas the torque to be measured during the engine operation needs additional devices which so far have not been comprised by the standard engine room equipment. That is why engine room operators often can make use only of approximate methods.

Accessible literature presents various approximate methods of engine torque load, like in [12, 13, 14]. No synthetic analysis containing applied methods comparison has been found in the literature. There are numerous publications presenting the subject in a general way; e.g. [1, 2, 3, 5, 7, 8, 9, 10]. On the one hand there has not existed any review material summarizing the topic and on the other hand the usefulness of the engine torque load methods for the engine room operators is significant which has made the author of the paper present the most common approximate methods of estimating power.

Basic methods of engine torque load assessment without the use of torquemeters (devices using the phenomenon of intermediate shaft torsion in order to measure the engine torque) have been methods making use of energetic processes analysis results (engine indicating), reading fuel rack setpoint (load indicator) and using parameters measure of engine supercharging system. Possible calculation of effective power based on the measure of active generator power regarding marine generator sets here is not taken into account because the method is endangered to significant error connected with the lack of information concerning the alternator's efficiency

(greatly affected by the loads). Furthermore, in the paper a short characteristic of each of the methods together with selected examples have been presented.

2. Load estimation based on engine indicating results

One of more frequently applied methods of defining engine effective power P_e without the use of torquemeter is evaluation based on the results of engine indicating (determined indicated power P_i) [3, 4, 7, 11]. There is a relation between effective and indicated power:

$$P_e = P_i - P_r \ \text{[W]}, \tag{1}$$

where:

P_r – the stream of energy used to overcome friction resistance and for suspended mechanisms drive/propulsion [W].

Indicated power is the power output of the engine working spaces (of all particular cylinders) in certain established environment. For one cylinder it is:

$$P_{1i} = C_1 p_i n \ \text{[W]}, \tag{2}$$

where:

C_1 – the cylinder constant taking into consideration the piston area, its stroke and number of ignitions assigned for one crank shaft revolution [m^3],
P_i – mean indicated pressure [Pa],
n – speed of the crank shaft [s^{-1}].

The indicated power of a k-cylinder engine is calculated as a sum of particular cylinders indicated power. Using the results based on indicating values of mean indicated pressures pi or particular cylinders indicating power it is possible to determine mean effective pressure p_e or effective power P_e according to the relationships:

$$p_e = \eta_m p_i \ \text{[Pa]}, \tag{3}$$

$$P_e = \eta_m P_i \ \text{[W]}, \tag{4}$$

where:

η_m – engine mechanical efficiency [-].

Having the results of indicating the engine and possessing the knowledge of engine mechanical efficiency it is possible to evaluate the effective power of the engine. It is so much the simpler that nowadays vessels are equipped with modern marine engine control indicating systems. The systems make use of computer programs supporting working out, archiving, visualization and comparing the results of indicating with the standard (reference) state .

They often make other functions accessible which with the knowledge of the engine mechanical efficiency run in the function of load indicator or the engine rotating speed allow to estimate the engine effective power. For example the electronic cylinder pressure measuring system *Premet* [15] allows estimating the load with the use of formerly introduced data concerning the engine mechanical efficiency plot in the function of the engine load indicator (Fig. 1).

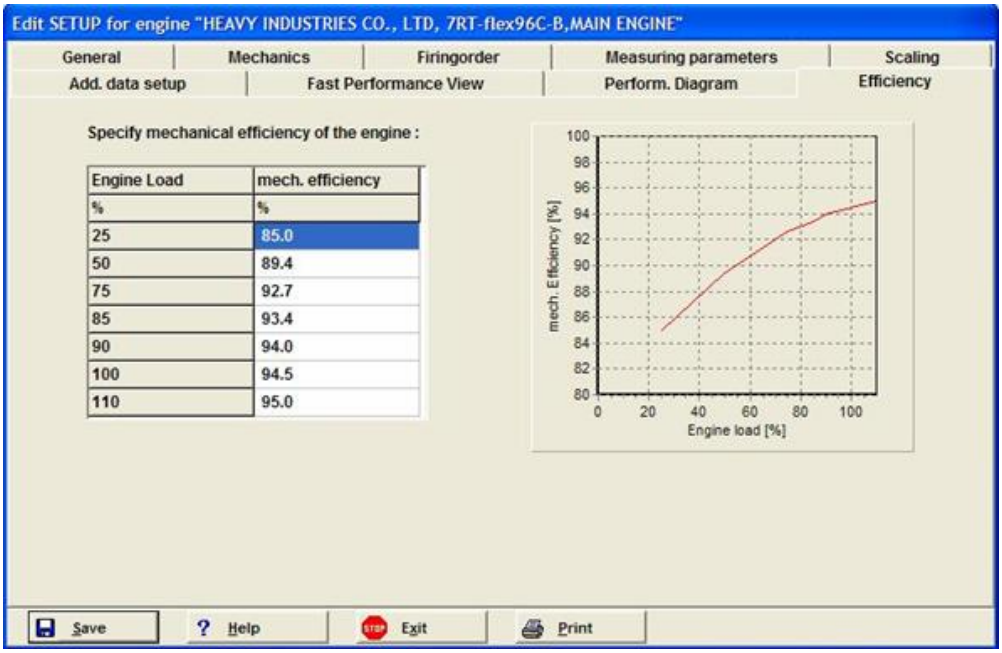

Fig. 1.Bookmark of defining the engine mechanical efficiency plot in the function of load indicator in the setup window of the computer program operating Premet system

Knowing the mean indicated pressure and the pressure of engine friction loss it is possible to assess the mean effective pressure. Assuming the mean pressure of engine friction loss C_2 as equal to 10^5 Pa (1 bar) [12, 13] in a low speed two stroke engine based on an operational experience of *MAN B&W* the mean effective pressure can be determined in relation to:

$$p_e = p_i - C_2 = p_i - 10^5 \text{ [Pa]}. \tag{5}$$

Due to the estimation approximate torque value T and effective power P_e can be calculated in relation to the following:

$$T = C_1 p_e \text{ [Nm]}, \tag{6}$$

$$P_e = C_1 p_e n \text{ [W]}. \tag{7}$$

In order to assess the possibilities of using indirect methods of defining the engine torque load it is necessary to compare the estimated values with the exact measures obtained by means of the torquemeter. This is possible only on ships with proper measuring devices. Table 1 presents the examples of power assessments with reference to (5) and (7) compared with the power estimated on the basis of the engine rotating speed and torque measured with a torquemeter. The comparison was carried out due to the results obtained from the 6 consecutive *MAN B&W 7K80 MC-C* engine performance checks. Particular data series have been arranged according to the growing value of the average (from all cylinders) mean indicating pressure.

Tab. 1. Comparison of MAN B&W 7K80 MC-C engine effective power estimations obtained by means of two selected methods

Average mean indicator pressure p_i [MPa]	Average mean effective pressure based on formula (5) p_e [MPa]	Engine rotating speed n [rpm]	Effective power determined due to the use of a torquemeter P_{e1} [kW]	Effective power determined on the basis of formulas (5) and (7) P_{e2} [kW]	$\left\|\frac{P_{e1}-P_{e2}}{P_{e2}}\right\|100$ [%]
1,57	1,47	102,1	20842	20243	2,87
1,61	1,51	101,0	20800	20,569	1,11
1,62	1,52	101,8	20100	20,870	3,83
1,64	1,54	102,0	21416	21186	1,07
1,69	1,59	103,0	22264	22088	0,79
1,72	1,62	102,1	22313	22308	0,02

The above presented results of the comparison prove high exactness of the indirect method based on (5). The percentage of the results discrepancies in this case does not exceed 4%. To a great extend such result is influenced by the torque and rotating speed exact measure as well as up-to-date precise system for carrying out engine indicating. High coherence between assessment results and the results obtained by means of the torquemeter probably refers to a certain range of engine loads close to the rated load. The presented measures were achieved in the conditions in which engine performance should be checked, that is adequately high torque load (70-80%). Error increase of effective power estimation for working at partial load does not diminish the possibility of the method application since it is usually applied during regular operation (operational load), not during a ship's maneuvering.

3. Load assessment based on the fuel rack setpoint

One of the groups of marine engines features are speed characteristics at the same/constant fuel dose. For the engine work the most important characteristic is the rated power characteristic which is done for the constant fuel dose setting corresponding with the rated power and rotary speed. Engine effective efficiency in the tested range of rotary speeds is often assumed to be constant (so called theoretical characteristic). The example of such characteristics presenting power and torque in the function of rotary speed has been shown in Fig. 2.

Change of power for certain rotary speed of an engine is possible only due to a fuel dose change [7, 10].Engine effective power at its constant effective efficiency assumed can be presented as follows:

$$P = C_3 g_w n \,[\mathrm{W}], \tag{8}$$

where:

$C_3 = zW\eta_e$ – constant value [J/kg],
z – number of ignitions inside the cylinder per one crank shaft revolution [-],
W – lower heating value of the fuel [J/kg],
η_e – rated effective efficiency [-],
g_w – fuel dose per one working cycle [kg],
n – engine rotary speed [s^{-1}].

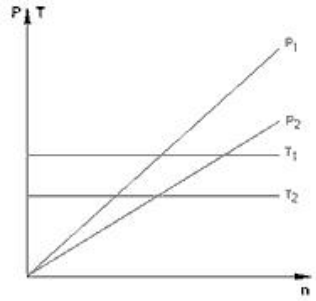

Fig. 2. An example of theoretical characteristics at the constant fuel dose in torque T and effective power P system in the function of rotary speed n for two various fuel doses $g_{w1}>g_{w2}$

Actually the engine effective efficiency is not constant so the power *P*, torque *T* and other working parameters of the engine depend not only upon the fuel dose but also upon the efficiency of energy conversion [5, 7, 10]. Effective efficiency is not constant and varies within the whole range of the engine operational rotary speeds. In Fig. 3 an example of actual characteristics of outside power and torque in the function of rotary speed have been presented.

Taking into account variable value of effective efficiency formula (8) has the following shape:

$$P = C_4 \eta_{e2} g_w n \text{[W]}, \tag{9}$$

where:

η_{e2} – effective efficiency (affected by rotary speed and the load) [-],

$C_4 = \dfrac{C_3}{\eta_e}$ – constant value[J/kg].

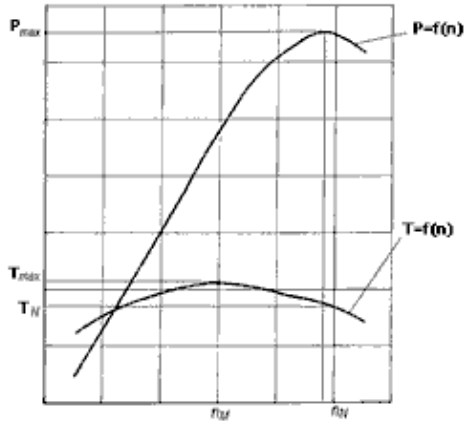

Fig . 3. Real characteristic of a constant fuel dose in power and torque system in the function of the engine rotary speed

In a considerable range of rotary speeds characteristics may be considered to be linear; thus the assumption of the engine constant efficiency value and the use of information concerning the fuel dose value is usually to be read in relative units as the fuel rack setpoints read from the load

indicator or by means of each pump reading the positions of fuel racks in millimeters a defining the mean value. In case of the main propulsion engines the reading may cause problems in bad hydro-meteorological conditions.

The fuel pump capacity h is usually read from the indicator fixed at the terminal shaft of governor or fuel pumps actuator, load indicator on the governor or it may be a remotely reading system with the use of selsyns from the indicator located in the Engine Control Room. Indications of the load indicator are usually given in percentage of the maximum fuel dose value of the fuel settings (scale 0-100%) or relative units in respect to maximum fuel dose (scale 1-10). When comparing various states of engine loads it is recommended to always apply the same way of engine load evaluation.

The torque developed by the engine depends upon fuel dose (9). In order to relate current pump settings to the setting values obtained during the trials at the engine test bench, correction of the current load indicator value to the values obtained during the trials at the engine test bench h_{ham} is based on the formula [12]:

$$h_{ham} = \frac{h\,W_{ham}}{W}\,[\%], \tag{10}$$

where :

h – current load grade [%],
W – lower heating value of the currently used fuel [J/kg],
W_{ham} – lower heating value of the fuel used during trials at the engine test bench [J/kg].

Correction of the current load indicator value may also include current fuel density ρ [kg/m^3] and the density of the fuel used during trials at the engine test bench ρ_{ham} [kg/m^3] – then the shape of the relationship is the following:

$$h_{ham} = h \cdot \frac{\rho_{ham}\,W_{ham}}{\rho\,W}\,[\%]. \tag{11}$$

Marine engine manufacturers provide engine test bench trial reports as a part of documentation also containing fuel grades of the fuel used during delivery trials which makes corrections of current load indication to the environment during the trials possible. The obtained value of the corrected load indication allows for the assessment of the engine current mechanical load.. The well known marine engine manufacturers *Wartsila* and *MAN B&W* provide their customers with nomograms allowing for approximate assessment of the power developed by the engine. Fig 4 presents an example of such a nomograms provided by *MAN B&W* allowing for approximate assessment of mechanical load based on fuel pump setting [13].

For a corrected value of load indicator the point of the crossing defined by the load indication value and the engine test bench trials curve is read. Next we read the estimated value of the average mean effective pressure which is directly proportional to the engine torque. Then from the bottom nomogram it is read the value of the effective power specified by values of the determined average mean effective pressure and the line representing current rotary speed of the engine. On the nomograms power is expressed in brake horse power (BHP), engine speed in revolutions per minute (RPM) and mean effective pressure in bar since these are units commonly used in marine engines operating practice.

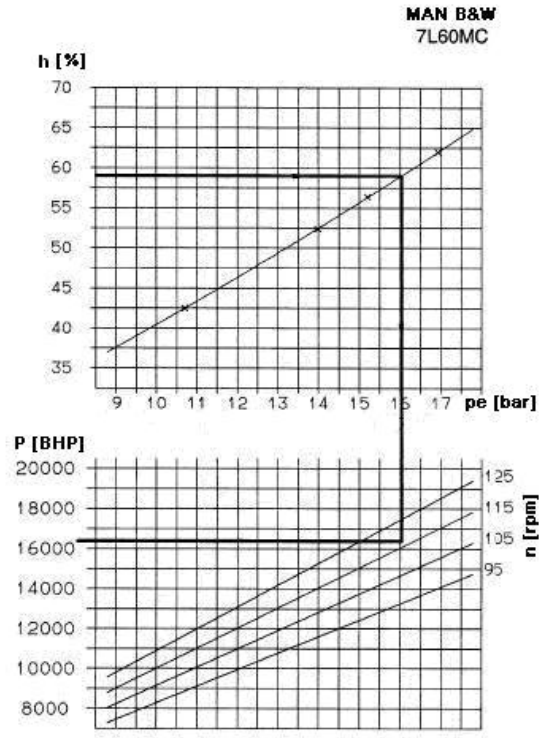

Fig. 4. The way of effective power Pe estimaton based on the load indicator value L and the rotary speed of n of MAN B&W 7L60MC engine [13]

Actually, the load indication value is affected not only by the fuel specific energy but also by other fuel properties. Lower viscosity grade shall lead to bigger leaks of fuel pumps and this shall call for increased fuel dose in order to inject the same volume of fuel. Apart from that the value of fuel dose setting shall be affected by all factors varying fuel consumption like: outside conditions, maximum combustion pressure [9,13, 14]. Thus, the varying conditions during the load assessment process in relation to the conditions at the engine test bench should be taken into account.

Wartsila company suggests a different way of assessing the engine effective power. The power value corresponds to the indication which is a product of load indicator h (directly proportional to the fuel dose g_w) and the rotary speed according to (9). Fig. 5 [14] shows an example of *Wartsila 7RT-flex 97C-B* engine diagram. Power here is also expressed in BHP and engine speed in RPM.

The comparison of approximate methods is relatively difficult due to the lack of particular parameter values for the same load states, especially when there is no exact information about actual torque load of the engine (specified by means of a torquemeter). However, the comparison of power estimations with the use of indirect methods for various fuel rack setpoints allows evaluating the tendency of changes in value differences obtained by means of various methods and the value of the differences. Table 2 presents the comparison of power estimations for which the relationship (4) and the method of nomogram presented in Fig. 5 have been used. The comparisons have been done for *Hyundai 7 RT-flex 96C-B* type of engine.

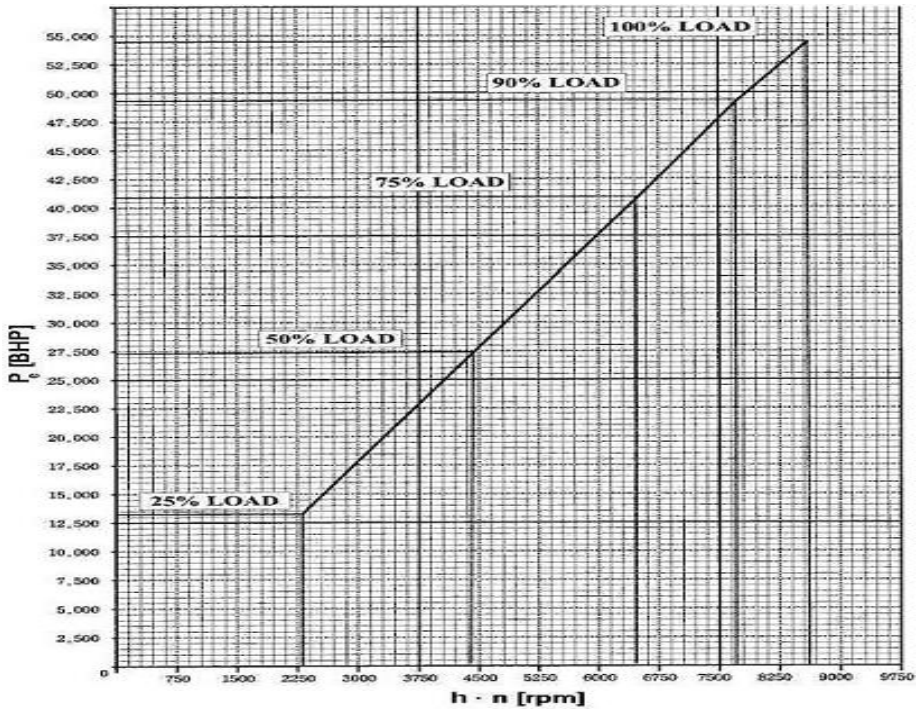

Fig. 5. The way of assessing effective power P_e based on load indication value h and rotary speed n for Wartsila 7RT-flex 97C-B engine [14]

The estimations have been carried out due to periodical reports of performance checks of a real working engine. The necessity for simultaneous register of numerous parameters, which is actually impossible because in real working conditions the parameters undergo continuous changes, makes the comparison of presented methods difficult. Another calculating error arises due to errors of measuring tools and possible reading errors concerning mainly some mean values (e.g. load indicator).

Tab. 2. The comparison of power estimations for Hyundai 7 RT-flex 96C-B engine carried out by means of two selected methods

Load indicator [%]	Rotary speed [rpm]	Power determined on the basis of indicating results from the relationship (3): P_{e1} [BHP]	Power determined on the basis of nomogram presented in Fig. 5: P_{e2} [BHP]	$\left\|\frac{P_{e1}-P_{e2}}{P_{e2}}\right\|100\,[\%]$
42,8	86	24238	22000	9,23
47,4	90	25771	26000	0,89
57,9	97	31458	35000	11,26
69,3	100	40949	44500	8,67
83,5	101	45462	52500	15,48
91,4	108	49800	55000	10,44

The value of discrepancies in power estimations with the use of relationship (3) expressed in percents range within 0,89÷15,48. The differences are relatively small and allow for the conclusion that both methods show approximate exactness of the estimation. The presented results of the estimation need to be considered as initial and depend upon numerous factors. That is why in order to draw detailed conclusions regarding the type of estimation changes in the function of real load, detailed research concerning these aspects should be carried out

4. Engine load estimation based on work charging system parameters

MAN B&W company also recommend the way of effective power estimation based on engine charging system parameters. Fig.6 presents a nomogram used for specifying the effective power based on the turbocharger rotary speed and the charging air temperature after the cooler.

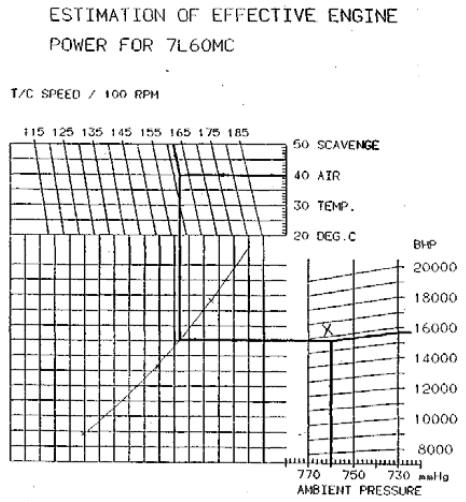

Fig. 6. The example of effective power estimation based on the turbocharger rotary speed and the charging air temperature and the atmospheric pressure of the MAN B&W 7L60MC engine [13]

The values determine the points which together with the engine trials curve the current value of the atmospheric pressure define the value of the engine effective power. The way turns out to be more precise than the formerly presented methods using the load indicator value. [13].

5. Final conclusion

In the paper the basic methods of torque engine load estimation have been presented. In fact for the main propulsion engines more and more often torquemeters have been installed. However, there have still existed many vessels without such equipment. In such cases the above presented methods are applied..

In order to verify the estimation values the methods can be connected, that is used together. Fig.7 presents the comparison of torque estimation run based on fuel rack setpoint and trial scale lines from the engine test bench and the line obtained due to the check indicating results [2]. Operational conditions undergo changes and they are often different from the conditions during the engine test bench [5, 6, 10].

Engine components including fuel pumps undergo wear causing changes of relationships between fuel rack position and the actual instantaneous fuel dose provided by the pump. That is why it is so meaningful to carry out periodical indication for the purpose of methods calibration.

Each of the presented methods has its advantages and disadvantages and a specified range of its application.. To the most universal methods belong the ones making use of indicators and readings of fuel rack setpoint values with the first ones which appear to be the most useful especially when the operator does not possess any engine test bench trial reports.

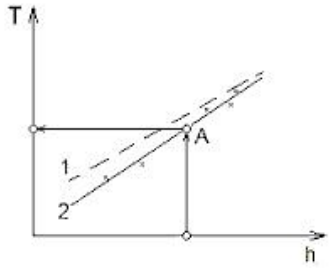

Fig. 7.General presentation of torque estimation based on of fuel rack setpoint .T –torque, h – fuel rack setpoint, 1– scaling line of engine test bench trials, 2 – scaling line based on indicator check results

Estimation based on effective power measure on the main switch board refers only to electric power generating engines. However, during the operation the method does not seem to be so significant because it requires the knowledge of generator efficiency and as a matter of fact the relative changes in engine torque load are reflected precisely enough in direct reading of the generator active power.

The method using the charging system parameters requires measure of atmospheric pressure. Its advantage is significantly higher precision of estimation when compared to other methods based on load indicator reading or fuel rack setpoint. [13].

References

1. Jędrzejowski, J., *Obliczanie tłokowego silnika spalinowego*. WNT, Warszawa 1984.
2. Kluj, S., *Diagnostyka urządzeń okrętowych*, Studium Doskonalenia Kadr WSM w Gdyni. Gdynia 2000.
3. *Komputerowe wspomaganie badań silników spalinowych*. Praca zbiorowa pod red. Z. Sroki. Oficyna Wydawnicza Politechniki Wrocławskiej, Wrocław 1996.
4. Nagawiecki, J., *Naprawy silników wysokoprężnych*. Wydawnictwo Morskie, Gdynia 1964.
5. Niewiarowski, K., *Tłokowe silniki spalinowe*. WKŁ, Warszawa 1983.
6. Niziński, S., *Elementy eksploatacji obiektów technicznych*. Wydawnictwo Uniwersytetu Warmińsko-Mazurskiego, Olsztyn 2000.
7. Piotrowski, I., Witkowski, K., *Okrętowe silniki spalinowe*. Trademar, Gdynia 1996.
8. Piaseczny, L., *Technologia naprawy okrętowych silników spalinowych*. Wydawnictwo Morskie, Gdańsk 1992.
9. Rychter, T., Teodorczyk, A., *Modelowanie matematyczne roboczego cyklu silnika spalinowego*. PWN, Warszawa 1990.
10. Wajand, J. A., Wajand, J. T., *Tłokowe silniki spalinowe średnio- i szybkoobrotowe*. WNT, Warszawa 1993.
11. Wimmer, A., Glaser, J., *Indykowanie silnika*. Instytut Zastosowań Techniki, AVL Warszawa 2004.
12. *50-108 ME Engines – Operation*. MAN B&W Instruction, Copenhagen 2005.
13. *7L60MC Engines – Operation*. MAN B&W Instruction, Copenhagen 2005
14. *Hyundai-Sulzer RT-flex96C-B Diesel Engine Operating Instruction*. Hyundai Heavy Industries. Ulsan 2006.
15. *Operator manual for the electronic cylinder pressure measuring system PREMET ONLINE SL Version 1.02.* LEHMANN & MICHELS GmbH, Hamburg 16.06.2004.

Journal of POLISH CIMAC
Faculty of Ocean Engineering & Ship Technology
GDAŃSK UNIVERSITY OF TECHNOLOGY

FOUR-STROKE ENGINE WITH CENTRAL LOCATED, DIVIDED COMBUSTION CHAMBER

Czesław Dymarski

Gdansk University of Technology
Ul. Narutowicza 11/12, 80-952 Gdansk, Poland
tel.: 48 058 3471608, fax: 48 58 3414712
e-mail: cpdymars@pg.gda.pl

Gerard Rolka

Abstract

The paper presents an original solution of the modern engine with the central located, divided combustion chamber. Such solution gives much better utilization of the warm what means that the efficiency of the engine should be higher and the fuel consumption and emission of the noxious gases such, as nitric oxides (NC), hydrocarbons (HC) and carbon dioxides (CO_2), will be reduced. The engine can work on liquid or on gas fuels. Presently the prototype of this engine is being prepared for tests and some investigation works.

Keywords: *engines, combustion chambers, emission of the noxious gases*

1. Introduction

Currently the problems with environment protection and fuel economy are significant for engine producers. The new regulations limited permissible emissions levels of noxious gases from exhaust systems. It forced engine designers and producers to develop new and modernize existing solutions of engines.

In the paper the original solution of the modern engine is presented. It already has been patented in the Patents Office in the Germany [1]. This solution is designed for high- and middle-speed engines to use in driving systems of such vehicles as: lorries, locomotives and small vessels or to driving generators and various building machines. The engine can work on liquid fuels such as petrol, alcohol, or their mixture and on gas fuels for example: LPG, natural gas or biogas. There is also possibility to work on two different kinds of the fuels (for example: petrol and gas) simultaneously.

The engine can work on diesel oil or hydrogen also, but some modifications are necessary.

The principle of the working of the engine is similar to the common diesel engine. It means that the cylinders are always filled up with maximum quantity of the air and the parameters of the work of the engine are controlled by the quantity of the injection fuel.

The most important advantage of the presented engine is the use of the centrally located, divided combustion chamber. Such solution gives much better utilization of the air and warm in the comparison with typical engines applied at present. It means that the efficiency of the engine should be higher and the fuel consumption and emission of the noxious gases such, as nitric oxides (NC), hydrocarbons (HC) and carbon dioxides (CO_2), will be reduced.

Presented in the paper drawings of the engine are simplified without details. Their aim is to show only the idea of the technical solution and the principle of the engine working.

2. Description of the engine construction

The axial section of the engine is shown on fig. 1. You can see there the main units and the elements of the engine, namely they are:

- Crankcase 1, inside which there are:
  - crankshaft, (not shown on the drawing),
  - articulated connecting-rod 2,
  - crosshead 3,
  - crosshead shoe 4,
  - sleeve packing 5,
  - piston rod 6.
- Cylinder 7, with the water jacket.
- Piston 8, inside which there are:
  - inlet valves 9,
  - pneumatic shock absorber 10,
  - bearing sleeve 11,
  - valve seat 12.
- Engine head 13, inside which there are:
  - four exhaust valves 14,
  - injection nozzle 15 of the combustion chamber,
  - injection nozzle 16 of the cylinder,
  - sparking plug 17.
- Cover 18 of the timing gear.
- Outlet pipes: left 19 and right 20.
- Inlet pipe 21.
- Circulating pipe 22 with the, located inside, control pipe 23.
- Inlet flap valve 24 with the spiral spring 25

The space inside the upper part cylinder, between the piston and the head create the main combustion chamber. The space inside the cylinder, between the piston and cover of the crankcase create the pre-compression chamber. At the upper position of the piston when its cylindrical protrusion is closing the small spherical chamber, there is created pre-combustion chamber. At the top dead centre (TDC) of the piston this chamber is practically closed.

The pneumatic shock absorber dampens the inertial forces at close by of the outermost position of the inlet valves.

3. Working principle

During the exhaust stroke (Fig.1) the piston rod 6 pushes up the piston 8, which pumps out combustion gas through the opened outlet valves 14 into the outlet pipes 19 and 20. Resistance of the flow of gas is very small because the use of four exhaust valves gives enough big their opening area.

At the moment when the flow of the air into the cylinder stops, the spring 25 closes the flap valve 24. Part of the lightly compressed air flows through the just opened inlet valves into the main combustion chamber, scavenging (blowing out) the rest of exhaust gas through the closing exhaust valves.

The piston is pulled down by the piston rod and beside of the opened inlet valves, the pressure of the air at the pre-compressed chamber a little increases and in the main combustion chamber decreases. It causes the pumping of the air through the vales in the piston and simultaneously a

small increase its temperature. Part of the air warmed by the hot surfaces of the head, the exhaust valves and the piston, mixes with the streams of the cool turbulent air, flowing into this chamber.

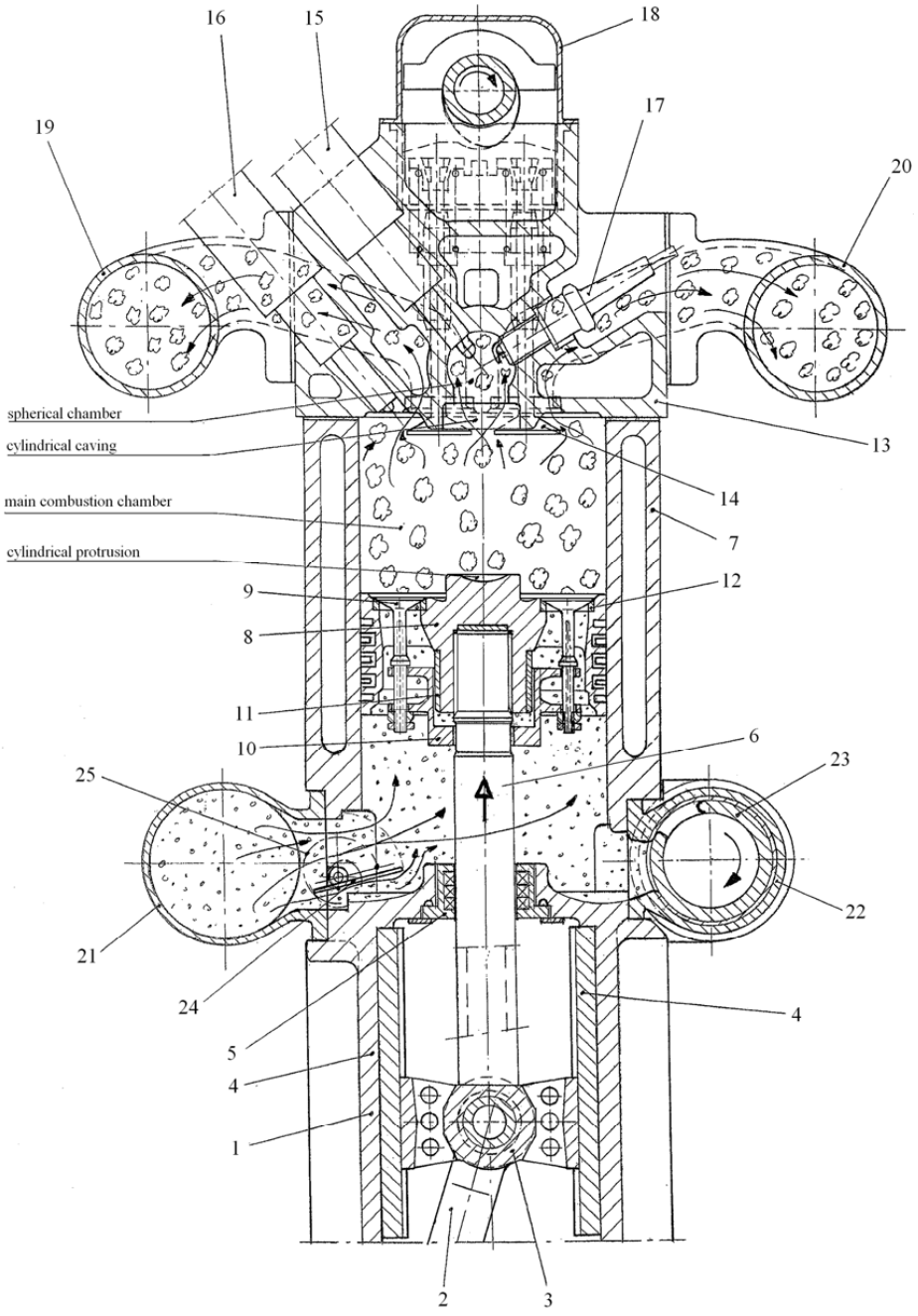

Fig.1. Axial section of the cylinder and the head of the engine

When the piston is approaching the inner dead center (IDC) its speed rapidly decreases and the inertial forces acting against the pressure forces start closing the inlet valves. Thanks to the shock

absorber the valves closes relatively smoothly just after the piston starts to move up. At this moment the compression stroke starts. The pressure and the temperature of the air quickly increase and the pressure forces keep the inlet valves in the closed position. The pressure decrease created in the lower part of the cylinder by the movement of the piston, causes an opening of the flap valve and a flow of the air from the inlet pipe into the cylinder. Resistance of this flow is very small because of the big opening area of the flap valve, what can be seen on fig.2.

4. The control of the partially loaded engine

When the distance of the piston position to TDC (during the compression stroke) amounts about 25% of the stroke, some small quantity of the fuel is injected by the injectors 15 into the pre-combustion chamber. The injection causes turbulence of the air-fuel mixture with the minimum leakages outside this chamber.

Quantity of the injected fuel should be calculated with assumption that the excess air ? number of the air-fuel mixture in the pre-combustion chamber should amounts $\lambda = 0.8 \div 1.2$ – for the petrol. After closing this chamber by the moving up piston there are very favourable condition for the intensive fuel evaporation and mixing with the air. The shape and geometrical parameters of the pre-combustion chamber are selected in such way that the increase of the pressure, the temperature and the compression ratio are bigger than in the main combustion chamber. Some losses of the pressure caused by a leakage of the mixture through the clearance into the main combustion chamber are very slight, thanks to the small value of this clearance, for example for diameter of the chamber $D = 20 \div 30$ mm the radial clearance amounts $C = 0.050 \div 0.15$ mm. The intensive flow of the mixture through this gap creates an aerodynamic lubrication layer and causes the local increase of the temperature.

Shortly after closing the pre-combustion chamber, what happens usually at the angle of the rotating crank shaft $\alpha = 32 – 30°$ before TDC, a sparking plug lights the air-fuel mixture and starts combustion process.

Just before TDC position of the piston the rotary valve 23, located inside the circulating pipe 22, starts to open the window. It enable, during a power stroke, the flow of the air from the pre-compression chamber, through the circulating pipe into another cylinder, where at this moment there is a intake stroke, what improves pressure charging effect.

When the piston reaches TDC and a power stroke starts, the spring 25 closes the flap valve 24 and as it was mentioned above, the air from pre-compression chamber is pumped out, by the moving down piston, into the circulating pipe.

At the same time inside the closed pre-combustion chamber burning process lasts. In spite of relatively high value of a compression ratio (amounts $\varepsilon = 14$ – for petrol and $\varepsilon = 14 \div 16$ – for gas) an explosive combustion does not take place.

The high pressure and temperature and sufficient quantity of the oxygen considerably limits a formation of hydrocarbons (HC) and emission of carbon monoxides (HC). On the contrary these conditions makes easier nitric oxides (NO_x) formation, but there are not too much of them, because they form from small quantity of the air closed inside the chamber. The results of the numerical simulation of these process carried out at one of the German universities allows such interpretation.

At the beginning of the movement down of the piston, the burning gas rapidly flows through encircling gap into the main combustion chamber, where it mixes with the cooler air and causes sudden increase of the its temperature. Vapours of not completely combustioned fuel and other formed combustible gases (for example CO) after contact with the air continue burning. There occur some additional chemical reactions accompany a combustion process during which a quantity of emitted nitric oxides (NO_x) decrease, as a result of the combustion gas cooling. The heating of the air by the combustion gas causes the quick increase of the air temperature and the

pressure. It improves a fuel utilization and increases the value and elasticity of the torque as well as the efficiency of the engine.

At short distance before IDC position of the piston the exhaust valves start to open and when the piston stops at IDC position the rotary valve closes and the one full cycle of the four-stroke engine is completed.

The control of the partially loaded engine is achieved by changing of a quantity of the injected fuel into pre-combustion chamber.

5. The control of the fully loaded engine

For the fully loaded engine the power obtained from the even reach ($\lambda = 0.8$ – for petrol) mixture burning inside the pre-combustion chamber is not sufficient to the demand. Because of it in the beginning of the intake stroke the injector 16 into the main combustion chamber injects the additional quantity of the fuel. This additional quantity of the fuel depends on the power demand.

The injected fuel warms, evaporates and mixes with the air. This mixture fills the upper part of the cylinder and the fresh, cooler air fills the lower part.

The compression stroke is similar to presented in chapter 4. Just before closing the pre-combustion chamber by the cylindrical protrusion of the piston, there starts fuel injection through the injector 15 and after ignition lug the burning process of the mixture takes place.

Meanwhile the pressure and temperature of the mixture inside the main combustion chamber are still rising but even at the TDC the temperature is enough lower than 1023 K, to protect from the self-ignition.

When the piston starts moving down, some losses of the combustion gases flowing into the main combustion chamber causes their mixing with the cooler mixture and its burning. This burning process proceeds smoothly and effectively with small emission of the toxic gases, similar as for the partially loaded engine.

For the maximum loaded engine the quantity of the fuel injected into the main combustion chamber should be calculated for obtain there the excess air number equal $\lambda = 1.0 \div 1.1$. For the engine load only a little bigger than it could be obtained from the pre-combustion chamber only, the quantity of the fuel injected into the cylinder should be suitable for receiving $\lambda = 5$ and even more. Meanwhile the quantity of the fuel injected into pre-combustion chamber must be calculated to obtain there the excess air number $\lambda = 1.1 \div 1.2$ – including a part of the mixture created in the cylinder during the compression stroke and closed inside this chamber.

6. The piston lubrication system

At the presented solution of the engine there was applied the pressure-circulation lubrication which is shown on fig. 2. The oil is pumped through the holes in the crankshaft, connecting rod, crosshead, piston rod and piston into the circumferential groove. The piston is equipped with two oil scraped rings: one above and second below the groove with the oil. The used oil is scraped from the internal surface of the cylinder and flows out through the holes in the piston, piston rod, crosshead, connection rod and crankshaft into the suction inlet of the cleaning circulation pump. The oil groove and the both grooves with the scraped rings are connected by at least three radial holes each with the mentioned above oil supply and drain holes.

7. The sealing of the inlet valve

The inlet valves are joined to the elastic elements of the pneumatic shock absorber, which can move axially on the piston, and is turn protected in relation to it. The valve stems are made with the axial holes for mass reduction..

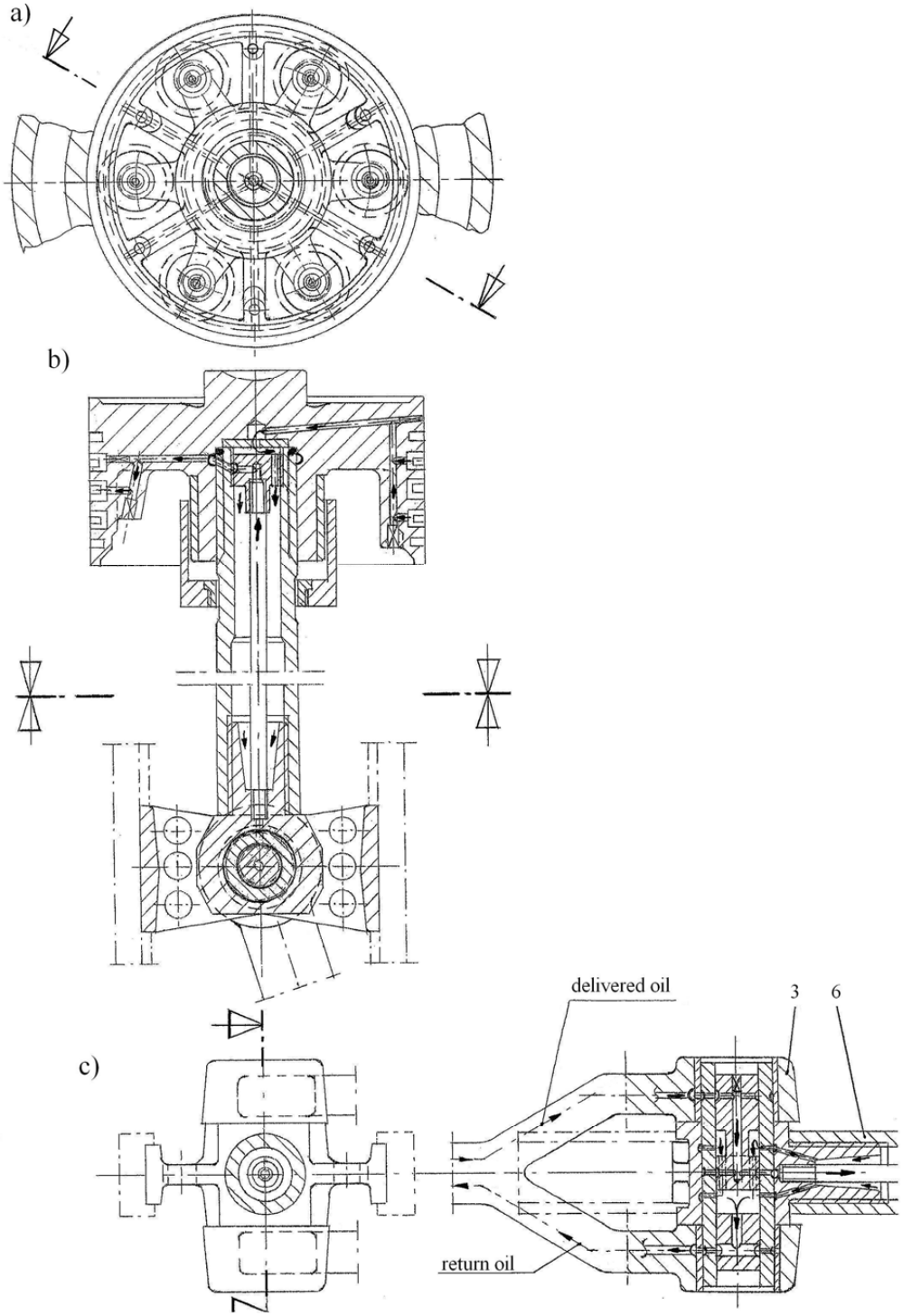

Fig. 2. The piston lubrication system: a) cross-section of the cylinder and the piston; b) axial section of the piston, the piston rod and the crosshead; c) axial section of the crosshead and the articulated connecting-rod

The stem of each valve is set in the shock absorber with same clearance. The contact spherical surface of the valve-head is made with a little smaller radius than the surface of the valve-seat. It enables better matching the valve head to the valve seat and good leak tightness.

8. Final remarks

Construction solution of the engine presented in the paper contains same original fiches and is patented [1]. Mentioned above advantages of the engine, especially such as high efficiency and low emission of the toxic gasses should be proved. It needs some research works at the laboratory stand. Presently the prototype of this engine is being manufactured in one of the Gdansk workshops.

It is quite possible that in the next year we shall be able to publish the first results of this investigation works and better assess advantages and disadvantages of the presented engine.

References

[1] Rolka G., *Verbrennungs-4-Takt-Kolbenmotor mit axialstromigem zyklischem Gaswechsel im Zylinder und zentral liegender geteilter Brennkammer*. Bundesrepublik Deutschland. Urkunde über die Erteilung des Patents Nr. 10 2004 013 461. Submitted 18.03.2004. Published 01.03.2007.

[2] *Kraftfahr technisches Handbuch*, 22.Aufl., 2004.

[3] Wajand Jan A., *Tłokowe silniki spalinowe średnio- i szybkoobrotowe*. Wydawnictwa Komunikacji i Łączności WKŁ, 2000 r.

Journal of POLISH CIMAC
Faculty of Ocean Engineering & Ship Technology
GDAŃSK UNIVERSITY OF TECHNOLOGY

PROBLEMS CONNECTED WITH MINIMIZATION OF INTERNAL VIBRATION AND NOISE GENERATED BY POWER UNITS IN SHIPS

Janusz Gardulski

Silesian University of Technology
Faculty of Transport
Department of Automotive Vehicle Construction
Ul. Krasińskiego 8, 40-019 Katowice
e-mail: janusz.gardulski@polsl.pl

Abstract

The paper discusses some problems connected with minimization of vibration and noise emitted by power units or ancillary aggregates in ships. Basic properties of the material systems are defined giving due attention to fundamental frequencies generated by these sources. Passive and active methods of noise minimization through interference with propagation path are presented. Anticipated effects are specified in the summing-up.

Key words: *power units in ships, minimization of vibro-acoustic signals*

1. Introduction

Minimization of internal noise and free vibration in sea motor yachts is a difficult task. The reasons are strongly connected with specific conditions existing in such objects, namely very small machine-room with necessary availability of transmission gear, main engine shafting and ancillary aggregates such as current generator, pumps, fans etc. These restrictions are a serious impediment to using some of the methods to minimize the vibro-acoustic effects. Generally, a multi-cylinder engine with spontaneous ignition is used where vibration is caused by variable exciting forces. The forces are induced by:
- pressure fluctuation within inlet and outlet channels,
- pressure variations in cylinders concomitant with combustion process,
- timing gear system at work,
- pressure variations in fuel system and lubrication system,
- inertia in mobile components of the engine,
- toothed gears,
- ancillary units.

Frequencies of these forces are related to rotational speed of the engine crankshaft as follows:

$$f_N = \frac{nZ_C}{60s}k \tag{1}$$

where:
n - rotational speed of the crankshaft (rev./min.),
Z_C - number of cylinders,
s=2 for four-stroke engines,
k=0.5, 1, 2, 3... exciting force harmonics.

If the frequency of rotations, induced by non-balancing of the rotating masses, is shown as:

$$f_N = \frac{n}{60} \tag{2}$$

the following frequencies connected with operation of the engine sub-assemblies will be as below:
- frequency of the camshaft

$$f_r = f_n i = 0{,}5 f_n [Hz] \tag{3}$$

where:
i - relocation of the camshaft drive;
- frequency of closing the valves.

$$f_Z = f_n \frac{Z_Z}{s} [Hz] \tag{4}$$

where:
Z_Z - number of valves working separately,
- frequency of the toothed gear.

$$f_p = f_n z [Hz] \tag{5}$$

where:
z - number of the pinion teeth,
- blade frequency of the fans.

$$f_w = f_n l [Hz] \tag{6}$$

where:
l - number of blades.
Frequency of impeller pumps, similarly to that of fans, is connected with the number of pump blades „l" and frequency of main engine revolutions „f'_n":

$$f_p = f'_n l [Hz] \tag{7}$$

Frequency of current generators is usually 50 [Hz].

As shown by the above relationships, various sub-assemblies of the engine generate the same frequencies, in particular when harmonic frequencies of the exciting forces are seen in the spectrum in result of nonlinear material systems.

Among the sources mentioned above there are low-frequency exciting sources, below 100 Hz (engine together with the exhaust, generators) and high-frequency exciting sources, above 1 kHz (fans, pumps, toothed gears etc.). Using uniform methods to minimize vibration and noise emitted by the units is very difficult in such situation.

Level of acoustic pressure in engines used for ships can be assessed approximately basing on:

$$L_p = 12 \lg N + 30 \lg n - 10{,}7 [dB] \tag{8}$$

where:
N - power of the engine [kW],
n - rotational speed of the crankshaft [rev./min.].
The level depends on many structural factors e.g. geometrical dimensions of the pistons, type of the body material etc.
Acoustic power of compression-ignition engine is about:

$$L_N = 59 + 10 \log N_Z + 10 \log N_Z - 30 \log \frac{m}{n} \pm 4 [dB] \tag{9}$$

where N_Z corresponds to rated power of the engine [kW] with its rated speed n_Z [rev./min.].

2. Methods to minimize the level of noise and vibration in machine-rooms

Minimization of vibro-acoustic signals emitted by power transmission systems can be obtained

through:

1. changing aerodynamic indicators on the inlet, outlet and working space of the units,
2. minimization of the exciting forces and their spectra.

Aerodynamic conditions can easily be changed through using covers to dampen vibration and dampers on the engine inlet and outlet and on the aggregates. Minimization of the forces: through vibration absorbers.

2.1. Minimization of vibration levels

Damping is connected with dissipation of mechanical energy converted e.g. into thermal energy, thus also with reduction of general efficiency of the unit. Therefore damping is introduced when minimization cannot be obtained through modification in structure or parameters. Such approach is typical for active methods. On the other hand, passive methods are based on changes in transmission path, namely vibroinsulation. Among the methods of structural modification there are three groups. The first of them consists in introducing additional internal connections e.g. absorbing springs (e.g. disk connections). The second of them consists in introducing additional masses (e.g. Frame type). The third is based on redevelopment of the structure continuity e.g. through intermediate flexible elements (vibroinsulators).

A major disadvantage of dynamic vibration eliminators is that they can only be used for harmonic excitations (being adjusted to strictly specific frequency). They are not useful for material systems in nonstationary conditions. Similar disadvantages are seen in parameter modification of material systems where the parameters are variables of loading vectors such as: inertia of the system „M", rigidity „K", damping „C". While at work, the true nonlinear material system is affected by exciting forces having a wide spectrum with a large number of harmonics. Wide spectrum exciting forces must necessarily be reduced in order to reduce vibration amplitude.

In mechanical conditions, the values of damping forces are usually lower than those of elasticity or inertial forces. Such forces are directed opposite to direction of speed vectors in an attempt to reduce or limit kinetic energy of the system. Type of friction (viscous, columbian or material) plays an important role here.

Minimization of vibrations in material systems is usually based on passive (relocation) or active (by force) vibroinsulation. In practice passive methods are prevalent. When fixed on vibroinsulators, the machine has 6 degrees of freedom or, in case of linear systems, 6 resonance frequencies. Vibroinsulators are so selected that the machine is prevented from working within resonance band. There are many methods to join the machine and its foundation together by way of vibroinsulators. Lifting systems or vertical, oblique, mixed types are fairly common.

A wide variety of materials can be used for vibroinsulation. With large-mass machines, usually pneumatic springs or those made of steel or rubber are used. With high loadings, steel springs are most common as they can easily be determined through computation. Most preferable types for vibroinsulation are linear springs where the force is proportional to deflection. Type of spring (helical, disk etc.) depends on the accepted vibroinsulation system.

Rubber springs are used for high-frequency exciting forces and low loadings, thus usually for springing. Rubber elements under stable loading should not exceed 15%, with coagulation 25-40% (hard blends) or 40-70% (soft blends), and their rigidity should be 50-60 Sh. Pneumatic springs are rarely used in industrial practice on account of their large geometric dimensions.

Effectiveness of vibroinsulation

Effectiveness of vibroinsulation can be defined, apart from excitation characteristics, through:

a) relocation vibroinsulation,
b) force vibroinsulation.

A model of vibroinsulation with kinematic excitation and relocation z(t) can be illustrated by a simple single-mass system with mass „m", damping „k" and elasticity „c". Such system is presented in fig.1.

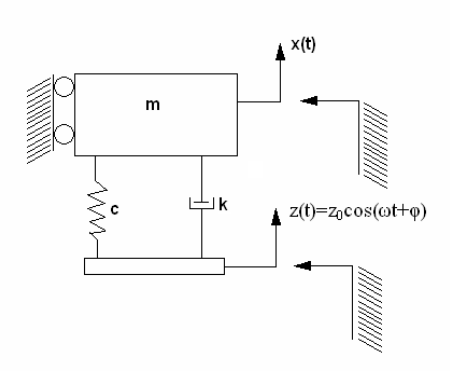

Fig.1. Model of relocation vibroinsulation

With force vibroinsulation, kinematic excitations are transformed into force type as shown in fig.2.

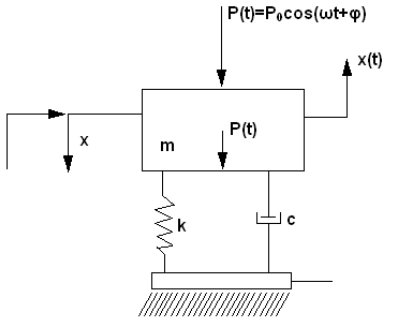

Fig.2. Model of force vibroinsulation

Vibroinsulation criterion is described by the following relationship:

$$T_x = \left| \frac{x(t)}{Z(t)} \right| \tag{10}$$

This criterion should meet the following conditions:

$$T_p \leq 1 \text{ and } T_x \leq 1.$$

If $T_p = T_x = T$, i.e. if vibration relocation factors are the same, it practically occurs for T<1 where free vibration frequency ω - to - free vibration frequency ω_o ratio is greater than 3. Upon adding a relative damping coefficient ξ to the assessment, it can be seen that if $\xi \leq 0.1$, the value of relocation factor „T" is nearly independent on damping. Such situations occur in most cases. If $\xi = 1$, the effect of vibroinsulation will disappear. Relocation factor depends almost entirely on damping.

Vibroinsulation systems can be divided into:

- passive,
- active.

Passive systems can only separate or temporarily store the energy.

Active vibroinsulation is based on generating control forces which tend to affect the unit in question. Passive systems can only dissipate or temporarily store the energy. Active systems

contain external source of energy which can provide or absorb the energy through automatic control. In general, active methods of vibroinsulation can be divided into methods controlled by excitation and methods controlled by parameters of vibratory field. This type of vibroinsulation system contains a converter to measure vibration parameters and to control both the external power source and the force element. Such vibroinsulation system is a complex automatic control system. Due to its complexity and high costs, it has fairly limited applications. Semiactive systems are far simpler. Instead of generating forces, they modify the controlled damping parameters and vibroinsulator elasticity.

2.2. Minimization of noise level

Noise level can be minimized through the following methods:
- passive,
- active.

Passive minimization methods are based on:
- reduction of noise emission generated by a sound source,
- reduction of acoustic energies on their transmission paths.

Reduction of noise source vibroacoustic energy can be obtained without interference in manufacturing process through:
- changes in aerodynamic and hydrodynamic conditions of the machines,
- reduction in relocation efficiency factor.

Changes in conditions of media flow in the source should be understood as transformation of media speed into noise (acoustic power of aerodynamic noises is proportional to 6-8th power of the gas stream speed). On the other hand, reduction in relocation efficiency is connected with a change of materials, protective covers, emission media etc. If combustion engines are considered, a modification of inlet and outlet systems through changes in their geometry is recommended upon vibroacoustic analysis in order to reduce the media energy. In this aspect it is useful to consider installation of noise eliminators, including suppressors.

Suppressors can be roughly divided into absorption and reflection types. Absorption suppressors prevent transmission of acoustic waves through absorbing a large portion of their acoustic energy. In a majority of cases such effects are obtained through using internal sound deadener lining. Such suppressors can be sucking suppressors.

Reflection suppressors are included in acoustic non-continuity channel where their acoustic resistance is either much lower or much higher than characteristic resistance of the channel. Most often it is a single or dual change in section stroke (cavity or resonator suppressors). Such suppressors can be used as exhaust silencers.

It is important to note that noise suppressors will only be highly effective if their mobility (opposite to impedance) is much higher than the sum of inlet and outlet mobilities. Apart from suppressors the following methods are recommended to minimize the level of noise:
- coverings to damp vibration in bodies,
- sound absorbing casings,
- acoustic screens,
- changes in acoustic absorptivity of the rooms,
- changes in insulating power of the barriers.

Coverings to damp vibration in engine bodies, power transmission systems and aggregates have practically no chance to be used in ships due to the requirement that they should continually undergo operating supervision. Sound absorbing casings protect the entire machine. The material should have a high sound absorption coefficient on its internal side. This can be obtained through spreading sound deadener on respective surfaces. Walls of the casing should have high insulating power of the barrier („β"). This, together with the internal sound deadener, will provide the

following effect:

$$\Delta L_u = L_1 - L_2 = \beta_u = 20\log f\rho + 10\log\alpha + \rho \tag{11}$$

where:p - surface density of the barrier,
f - frequency of the emitted sound [Hz],
ά - sound absorption coefficient,
L_1, L_2 - level of sound before and after the barrier [dB].
Effects of the casings depend on leak tightness of their components. Unlike sound insulating casings, acoustic screens are practically not used inside machine-rooms in ships.
Good effects of noise minimization in closed spaces can be obtained through changing noise absorption coefficient „ά". Effects of such changes are shown in fig.3.

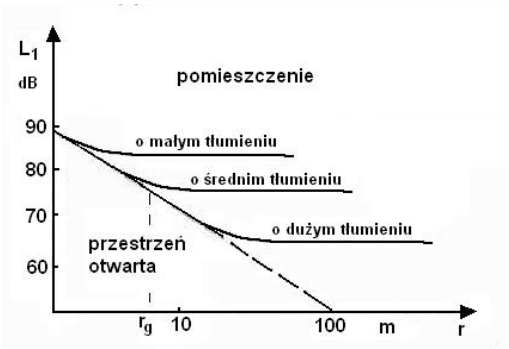

Fig.3. Reduction of noise level in open space and in rooms provided with various degrees of suppresion

If the distance from noise source is longer than „rg" (limit), the noise level will depend on acoustic absorptivity of room „A" [m²]. If „α" = mean sound absorption coefficient for a room floor „S", the definition can be as follows:

$$A=S\alpha\ [m^2] \tag{12}$$

Upon increasing the absorption coefficient from α1 to α2, the noise level will be reduced by:

$$\Delta L = 10\log\frac{R_2}{R_1}[dB] \tag{13}$$

where:

$$R_{1,2} = \frac{A_{1,2}}{1-\overline{\alpha}_{1,2}}[m^2] \tag{14}$$

Penetration of acoustic energy through barriers is a complicated phenomenon. It is generally accepted that such penetration may be affected by dynamic factors together with structure and material of the barrier. The coefficient (acoustic insulating power of the barrier) is approximate in character. Influence of material on insulating power of the barrier is presented in fig.4.

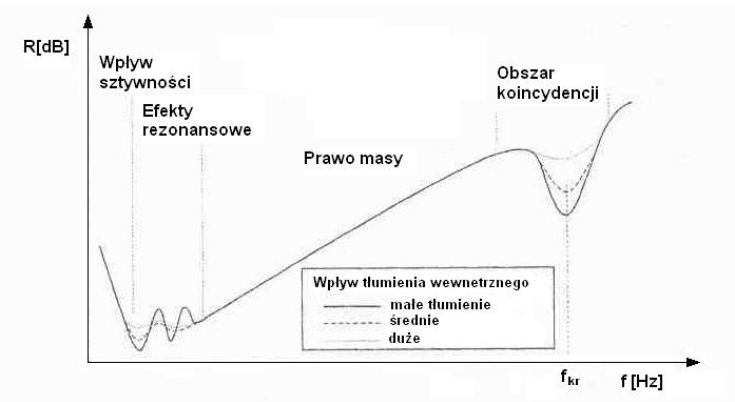

Fig.4. Influence of barrier material properties on its acoustic insulating power against air sounds

Physical properties of materials that affect insulating power include: elasticity, specific gravity, internal suppresion etc. As far as low frequencies are concerned, the insulating power depends chiefly on rigidity of the barrier. Next in importance is the influence of free vibration frequency „f_o". The influence of mass begins to work when said frequency is $2f_o$. Later stage is connected with coincidence effects. Acoustic insulating power of the barrier (homogeneous and isotropic) is:

$$R = 20\lg m + 20\lg f - C[dB] \tag{15}$$

where: f - frequency [Hz], m - surface mass of the barrier [kg/m²], C - constant coefficient (equal to 48 for normal weather conditions).

Basing on *mass law* equation, acoustic insulating power of the barrier (homogeneous and isotropic) appears to be directly proportional to surface mass of the barrier (expressed by the mass of 1m² of its surface), growing with frequency approximately by 6dB/octave.

Approaching acoustic insulating power of the barrier in terms of its surface mass only seems to be a simplification of the problem. The reason for discrepancy between the results may be that sound wave will fall, in some conditions, onto the plate with bent wave speed in the plate (c_g) being equal to sound wave speed (c_o) falling onto the plate ($c_g = c_o$).

Imput impedance of the plate becomes reduced, together with reduction of acoustic insulating power, in result of condensation. Theoretically, insulating power level for coincidental frequency should drop to zero. However, the drop is of stepwise character due to internal losses of the barrier material. In case of hard barriers, such drop can even go up to more than ten dB. Within coincidence area ($f>f_{kr}$) the insulating power will deteriorate in accordance with internal losses in the material (coefficient ŋ).

Coincidental frequency or *resonance frequency* can be determined basing on the following formula:

$$f_{kr} = \frac{c_0^2}{2\pi}\sqrt{\frac{m}{B}} = \frac{c_0^2}{2\pi h}\sqrt{\frac{12\rho(1-\nu^{2)}}{E}}[Hz] \tag{16}$$

where: c_o - sound speed in the air [m/s], m - surface mass of the plate [kg/m²], B - rigidity of the plate on bending cylindrical surface $B = Eh^3/12(1-\nu^2)$[Nm], p - density of the plate material [kg/m³], h - plate thickness [b],υ - Poisson's ratio.

Reduction in the barrier mass, without deterioration of its insulating power, can be obtained through installation of a multilayer barrier. However, the following conditions must be met in order to obtain the best possible insulating power with a multilayer barrier: number of layers,

thickness, resultant rigidity „E" of the barrier, surface mass of the barrier. The barrier should have low-degree rigidity on bending B.

When installing multilayer barriers, it is important that maximal energy suppression should be expected in soft layer (high ηh) through using materials with high factor of internal losses „η". On the other hand, it is not recommended to maximize layer „h" thickness because this would intensify the barrier rigidity thus causing relocation of coincidence to the band below 5 kHz.

Unlike passive methods of noise minimization, active methods are quite different. Active methods of noise reduction are supplementary to classical (passive) methods. In general, they employ additional (secondary) sound sources to work together with basic (primary) sources. In result, either mutual compensation or destructive interference of primary and secondary waves will occur. In order to obtain maximal (theoretically total) suppression of primary wave, it is necessary that the generated secondary wave should have the same frequency and amplitude as the primary wave but opposite phase. To give an example, in case of harmonic waves, the suppression will be approximately 20dB if the difference between acoustic pressure levels of waves is lower than 1dB and phase displacement does no deviate from 180º by more than 5º. As shown by the example, the secondary source control must obey strict regulations.

Control signal is primary signal detector, e.g. microphone. It must be placed in a different point than observation point, otherwise the system will be unstable, susceptible to self-excitation. Signal from primary detector will travel to the electronic control which in turn will excite secondary source thus changing amplitude and phase of the signal. Therefore it is a filter having appropriate amplitude-phase characteristics.

Summing-up

Main engines and ancillary aggregates used in ships are usually connected with their bodies by ancillary frames. The units are nonstationary and transient when at work. Active or passive methods are used to minimize vibration generated by these machines. Passive methods include vibration dampers, vibroinsulators, multilayer rigid plates to dissipate or partially store the energy. Active methods employ external energy sources to reduce the vibration. These methods are expensive and require complex automatic controls. Their effectiveness may be fairly poor with transient systems.

Similarly, passive methods are used to minimize noise in motor yacht machine-rooms. These methods often include sound-insulating engine casings together with ancillary aggregates or multilayer barriers for the walls.

When using sound-insulating casings it is important to remember that heat and gases must be carried away in order to ensure thermal safety of the place. Gases lighter than air require 60 x h.change of air whereas gases heavier than air require 120 x h. change of air. Correct casings provide reduction of the noise level by 15-20 dB (A). An example of correct casing is shown in fig.5.

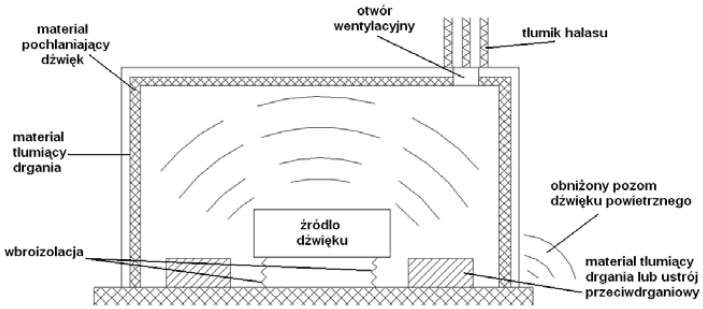

Fig.5. An example of correct sound-insulating casing

Multilayer barriers used for walls are materials of high insulating power. The materials should have the following insulating power: mean sound absorption coefficient
$\alpha_{śr} \sim 0.6$ on the side of the source. Correct insulation of the walls together with their acoustic absorptivity enable reduction of the noise level by more than 20dB(A).

With a broad approach to minimization of noise and vibration in sea motor yachts, it is quite possible to obtain a reduction in noise level by 30 dB(A) using passive methods. Each type of yacht requires an individual, unique approach to select most suitable methods for the case. Changes in acoustic environment can be introduced both for the machine-room and for crew quarters. To obtain maximal results, it is often useful to use passive and active methods jointly because active part operates within low frequencies whereas passive part operates within higher frequencies. Such approach enables obtaining the best acoustic effects.

References

[1] Z. Engel i inni, *Podstawy wibroakustyki przemysłowej*, AGH Kraków 2003 r.
[2] Z. Engels, *Ochrona środowiska przed drganiami i hałasem*, PWN Warszawa 2001 r.
[3] C. Cempel, *Wibroakustyka stosowana*, PWN Warszawa 1989 r.
[4] J. Kowal, *Sterowanie drganiami*, Gutenberg, Kraków 1996 r.
[5] S. Weyna, *Rozpływ energii akustycznych źródeł rzeczywistych*, WNT-Warszawa 2005r.

Journal of POLISH CIMAC

Faculty of Ocean Engineering & Ship Technology
GDAŃSK UNIVERSITY OF TECHNOLOGY

QUANTITATIVE INTERPRETATION OF ENERGY-BASED SYSTEMS AND INDEX OF THEIR RELIABILITY

Jerzy Girtler

Gdansk University of Technology
Faculty of Ocean Engineering & Ship Technology
Department of Ship Power Plants
ph. (+48 58) 347-24-30
fax (+48 58) 347-19-81
e-mail: jgirtl@pg.gda.pl

Abstract

The paper presents a proposal of quantitative interpretation for operation of energy-based systems (e.g. diesel engines, gas turbine engines, steam turbines, steam and water boilers), which (just like in physics: the operations of Hamilton and Maupertius and the operation resulting from changes of body momentum) is considered as a physical quantity with a joule-second [joule × second; Js] as a unit of measure. It has been also showed that interpretation of operation can be considered as a reliability index and in special cases – as a safety index of such energy-based systems' operation. To give the grounds for such usability of the mentioned energy-based systems' operation the homogeneous process of Poisson has been applied. This process enabled constructing a model of run of getting worse (decreasing) operation of a gas turbine engine with the lapse of operation time. Thus, such model is a random process of homogeneous and independent gains in drops of energy generated by the engine, as the result of using it in determined time.

1. Introduction

Ensuring safe operation of an energy-based system (e.g. installed inside a ship: diesel engines, gas turbine engines, steam turbines, steam and water boilers, etc.) needs having an adequate quantity of energy being obtained from chemical energy contained in fuel consumed by engines. Action which ensures delivering the wanted quantity of energy in proper time strictly depends on taken decisions.
Taking decisions in time of operation of energy-based systems (e.g. installed inside sea-going ships) is always realized in a stochastic decision-making situation, thus in the conditions of uncertainty (in conditions of statistic risk). That means, that there is a need of using the rules of the calculus of probability and the inductive (mathematical) statistics. Operating decisions are taken at the very beginning (before starting) and during operation of the ship. That means that these decisions are taken at least once, on the basis of primary information (obtained e.g. during reliability tests of energy-based systems and their particular elements, or from the bank of information concerning similar systems) which can be named a priori, and next on the basis of information obtained during operation of the systems (e.g. as the result of application of diagnostics, not only technical one), which can be named a posteriori information.

Decisions, taken at the beginning of operation, are indispensable to plan the process of using and operating the systems. These decisions have to take the risk into account, of which the estimation is a probability of taking a wrong decision, resulting from [1, 5]:

- impossibility of precise estimation of unknown parameters of distributions of random variables, which are the states of the process of operating the energy-based systems and their particular elements;
- lack of possibility to elaborate entirely or/and enough reliable information demanded to take the right decision.

The first case generates random mistakes of which the estimation is called *the stochastic precision of inferring* and the second one – random mistakes and such mistakes which can be considered as not random (systematic). Establishing the last kind of mistakes is a problem, that I suggest to name *a problem of accuracy or precision of inferring.* Determination of these mistakes together is *a problem of statistic precision of inferring. The accuracy of inferring* results from the current level of scientific and useful knowledge, and the precision of inferring results from not appreciating some information and leaving it out of account, although he/she could make himself/herself sure if it was really unimportant. However, in time of operating energy-based systems the reasons of taking wrong or irrational decisions are difficulties in establishing a completed and sufficiently reliable diagnosis on the technical state of the engines as well as a similar diagnosis referring to the expected outer conditions (of weather and sea) which can appear during operation [1, 4, 12, 16].

In the presented above situation for making decisions, making the rational decision is possible in case of applying the statistic theory of making decisions and thereby the expected value of consequences as the criterion for making such decision [5, 7]. Determining a set of decisions which if necessary, may be taken in agreement with the taken criterion of optimisation, needs identification of the problem of safety and reliability of the energy-based system in respect to its operation.

2. General identification of safety problem for energy-based systems

In order to avoid any threat for energy-based systems, man has to make proper decisions and take actions resulting from the decisions, both in the phase of preparing the system to perform a given task and during the course of task performance, and after the task was finished. This action, of course, has to be efficient, so – purposeful, energetic and economical [6-9]. Such action, just like another one, demands using proper quantity of energy in determined time. Thus, it can be considered as a physical value expressed with the unit of measure [joule × second; Js] and interpreted (generally, in a deterministic formulation) in the form of dependence:

$$A = Ut \tag{1}$$

where: A – action, U – energy used in the action A, t – time of energy U use.

Interpretation of action, presented by the dependence (1), has its equivalent in physics (quantum mechanics) - Planck constant (h) because [2, 10, 15]:

$$E_\nu = h\nu \rightarrow h = E_\nu \nu^{-1} \tag{2}$$

where: E_ν – energy of one quantum of electromagnetic radiation, ν – frequency of energy quantization, h – Planck constant of which the unit of measure [joule × second; Js] has been called action.

Action expressed by the formula (1) has also its equivalents in thermodynamics and tribology. In thermodynamics there may be considered two methods of changing energy in time t: work L and heat Q [11, 14]. The operation of systems can be expressed by formulas:

$$A_L = Lt, \; A_Q = Qt \tag{3}$$

In tribology the operation of tribological systems can be interpreted in a similar way considering the work of friction (W_T) [16], done in time t. Then, the work can be expressed as follows:

$$A_T = W_T t \tag{4}$$

Such understood work has to be of course, comprehensively analysed. In order to do that, proper indexes which determine efficiency of work, e.g. universal efficiency meters [8], are needed.

Action which results from tending to keep the safety of a energy-based system, in agreement with the dependence (1), can be:

- Demanded action (A_W) in the situation (in which the system find itself), so such action that ensures (enables) keeping the safety of the energy-based system;
- possible action (A_M) in the situation (in which the system find itself), so such action that may be, but doesn't have to be, sufficient to ensure (keep) the safety of an energy-based system.

In accordance with the dependence (1), the actions can be expressed by the dependencies:

$$A_W = U_W t_W \tag{5}$$

$$A_M = U_M t_M \tag{6}$$

Safe operation of a system is possible only when the possible action (A_M) amounts at least to the demanded action (A_W), so the action indispensable to keep the safety in the situation in which the operated system finds itself. That means that safe operation of a system is possible, if:

$$A_M \geq A_W \tag{7}$$

Thus, any threat for a system occurs when:

$$A_M < A_W \tag{8}$$

We can predict that action for the bigger than the wanted scale, is less efficient. Thus, the need is to tend to $A_M = A_W$.

From the considerations results that the following cases of threat for an energy-based system may be taken into consideration:

1) $t_M < t_W$, if simultaneously $U_M = U_W$;
2) $U_M < U_W$, if simultaneously $t_M = t_W$;
3) $U_M < U_W$, if simultaneously $t_M < t_W$;
4) $U_M > U_W$ if simultaneously $t_M < t_W$, but in consequence $A_M < A_W$;

5) $U_M < U_W$, if simultaneously $t_M > t_W$, but in consequence $A_M < A_W$.

The mentioned conditions can be interpreted as follows: the first of them reflects the situation when the energy-based system's operator has not time needed to ensure the safe operation of the energy-based system. The second condition reflects a situation when although having the needed time the safety of the energy-based system cannot be ensured because of lack of the proper quantity of energy. The third condition reflects the most difficult situation in which a gas turbine engine may find itself because of not only insufficient energy but also the lack of time to ensure safe operation to the energy-based system. The fourth condition reflects such situation when there is excess energy comparing with the needed quantity to ensure safe operation to the energy-based system but the time in which the energy should be made out is insufficient. The effects of this situation may be similar to the mentioned ones in the case of the first condition. The last condition reflects such situation when the needed energy to ensure the safe operation to the energy-based system is insufficient and cannot be increased although the time of action in which this energy could be increased before a threat to the energy-based system occurs, is long. This situation may be caused by extensive damages in constructional structure (damages called break-downs) of the energy-based system, being of the essential meaning for its safety.

Presented considerations concerning quantitative formulation of action to ensure the safety of a energy-based system, can be (and should be) developed by applying the theory of stochastic processes. This follows from that generating energy by a energy-based system in time of operating is a random process. This process in conditions of fixed states of the energy-based systems' operation, can be a set of random variables U_t of not large (and that's why unimportant from the practical point of view) variation. However, in the reality changes of energy in time of operating can be (and should be) considered as a stochastic process $\{U(t): t \geq 0\}$ with a defined expected value $\mathrm{E}[U(t)]$ and variation $\mathrm{V}^2[U(t)]$.

Examination of the process in any interval $(t_0, t_0 + t)$ demands considering its momentary states (for each time t) which are random variables U with expected values $\mathrm{E}(U_t)$ and variation $\mathrm{V}^2(U_t)$, dependent on the value t. It is obvious that both: the expected value and variation of the process $\{U(t); t \geq 0\}$ depend on time t because for its different values $\mathrm{E}(U_t)$ and also $\mathrm{V}^2(U_t)$ can be different. But $\mathrm{E}[U(t)]$ and $\mathrm{V}^2[U(t)]$ are not random functions because $\mathrm{E}(U_t)$ and also $\mathrm{V}^2(U_t)$ are constant quantities for a given value t and defined set of random variables values U, and they are not random variables. Thus, the dependence (1) can be presented as follows:

$$A(t) = \int_0^t \mathrm{E}[U(\tau)]d\tau \tag{9}$$

Considering the safety, it may be important to take more careful decisions or more risky ones, thus it is necessary to do estimation not only in a point but also in an interval, so in the formula (9) instead of $\mathrm{E}[U(t)]$ it should be put the value of the bottom limit of the confidence interval $E_d[U(t)]$ if the decision should be more careful or the value from the top limit of the confidence interval $E_g[U(t)]$ if the risky decision is admissible. It is obvious that when in the particular intervals Δt_i of time t (of generating energy) the expected values $\mathrm{E}(U_i)$ can be considered as constant, the mark of integral should be replaced in the formula (9) by the symbol of sum.

In a concrete use of the interpretation of action, according to the dependence (1) or (9), the operation of an energy-based system and the operation of its subsystems can be expressed in the form of different formulas according to :

- type of a subsystem which in defined time generates the energy to meet the need of the whole system for operation;
- class of stochastic processes of which changes of energy consumed during the course of the system operation, may be included to.

Taking into consideration the presented above interpretation of the energy-based systems' operation it is possible to define a reliability state in which the system finds itself.

3. Interpretation of reliability states for an energy-based system

Taking into account the dependencies (7) and (8) it may be accepted that each energy-based system is in the state of ability (and is able to perform a task) if meets the dependence (7). Otherwise, in case of inequality (8) it should be accepted that the energy-based system is in the state of disability. That means that such an energy-based system should be considered as a failed one although the energy is still transformed in it. The dependence (7) is satisfied if such a system like a gas turbine engine may be loaded according to the external characteristic of maximal power in the time interval suggested by a producer. In case when the engine may not be loaded (without any threat of failure) the dependence (7) can be satisfied only if in time of performing the task it does not occur the need to load the engine according to this characteristic. Otherwise, the dependence (7) is not satisfied and the engine (as mentioned) should be considered as damaged.
Inferring about usability of particular energy-based system for realization of exactly defined tasks can be made after comparing fields of *system's action*: the demanded one A_W and the possible one A_M. From the presented above considerations results that the *system operation* in this formulation means:

- testing changes of the demanded work L_{eW}, to be done by the energy-based system in the demanded time t_W, so in time in which a transport task should be finished;
- testing changes of the possible work L_{eM}, to be done by the energy-based system in possible time t_M, so in time in which the system can be correctly operated.

Considering *energy-based system's operation* as a measure of (full or partial) ability of an energy-based system to perform the task, demands first of all defining the classes of model states among which its technical state could be classified. According to the dependence (7) the energy-based system finds itself in the state of ability (so in the state which makes performing tasks possible), if:

$$\left.\begin{array}{l} 1)\ t_M \geq t_M \text{ if at the same time } L_{eM} \geq L_{eW}; \\ 2)\ t_M = t_M \text{ if at the same time } L_{eM} = L_{eW}; \\ 3)\ t_M \geq t_M \text{ if at the same time } L_{eM} = L_{eW}; \\ 4)\ t_M = t_M \text{ if at the same time } L_{eM} \geq L_{eW}. \end{array}\right\} \quad (10)$$

In case when none of dependencies (10) can be satisfied the energy-based system should be considered as disable to perform tasks although it is able to convert chemical energy into mechanical energy which enables performing the work L_e by it [3, 13]. Thus, operation $A_{(\cdot)}$ of any energy-based system, being analyzed with regard to the dependence (10), can be accepted as a factor of its reliability. In case when the dependencies (10) are not satisfied, so the inequality (8) takes place, the operation A_M of the given energy-based system can also be the measure (factor) of safe operation. Of course, the factors of reliability and safety for the energy-based systems' operation may also be the generally known factors referring to the *systems' operation* in the version suggested here in this paper. In this case, as the reliability

measures can be considered the probabilities of satisfying the equations (10), being the probabilities of correct operation of the energy-based system and its performance of the demanded task. For elaboration of these reliability factors (and in case of taking sea accidents into account – safety factors) the homogeneous process of Poison can be applied as the model of the process of decreasing mechanical energy (so also the work L_e) as the result of wear of the energy-based system [6, 7, 9]. Applying this process, the following physical interpretation of the process of decreasing work L_e by a constant value e can be expressed: from the moment of starting operation of a energy-based system (it can be the moment $t_0 = 0$) to the moment of recorded for the first time by a measuring device, the event E which is a decrease (as the result of wear of the system) of work L_e by the value $\Delta L_e = e$, it can be performed any value of work L_e (including the maximal one) in particular time intervals of energy-based system's operation. Further use of the energy-based system causes occurring next drops of the values of work L_e, by the next homogeneous values e, recorded by a measuring device. Therefore, in case of recording the cumulated quantity B_t of occurred events E up to the moment t described by the homogeneous process of Poison, the total decline of work L_e by the value $L_e(t)$ to the moment t can be presented by the dependence:

$$L_e(t) = eB_t \tag{11}$$

where: e – quantum of energy, B_t – cumulated number of events E appeared (recorded) up to the moment t.

at which the random variable B_t is (as it's known) of the distribution [1, 6]

$$P(B_t = k) = \frac{(\lambda t)^k}{k} \exp(-\lambda t); \quad k = 1,\ 2,... \tag{12}$$

where: λ – constant value (λ = idem) interpreted as the intensity of decreasing work L_e by the same values e, recorded in time of the research; $\lambda > 0$.

The expected value and the variation of the process of growing the quantity of events E, so decreasing the work Le by values e, recorded in turn, can be presented as follows:

$$E(B_t) = \lambda t; \quad D^2(B_t) = \lambda t \tag{13}$$

Thus, according to the dependence (11) and formulas (13) the expected value and the standard deviation of decreasing work L_e performed by the energy-based system up to the moment t, can be expressed by the formulas [6,7]:

$$E\left[\Delta L_e(t)\right] = eE(B_t) = e\lambda t \quad \sigma_L(t) = e\sqrt{D^2(B_t)} = e\sqrt{\lambda t} \tag{14}$$

Taking into account the fact that a brand new energy-based system can (when $t = 0$) perform the biggest work, so $L_e(0) = L_{e\max}$ the mathematical dependence describing the decline of this work with the lapse of time, can be expressed by the formula [6, 7]:

$$L_e(t) = \begin{cases} L_{emax} & dla \quad t = 0 \\ L_{emax} - e\lambda t \pm e\sqrt{\lambda t} & dla \quad t > 0 \end{cases} \tag{15}$$

Graphic interpretation of the dependence (15) is presented in Fig. 1.

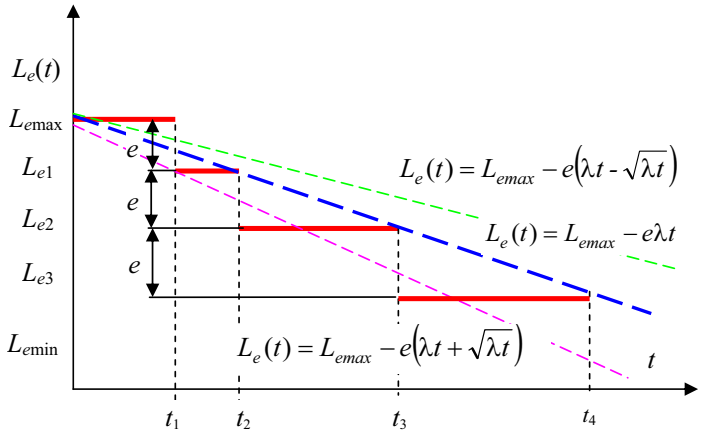

Fig. 1. Graphic interpretation of exemplary realization of useful work reduction for an energy-based system: L_e – useful work, e – quantum by which the work L_e is changed, t – time

From the formula (15) results that for any moment t the work L_e which can be performed by the system, can be determined and from the formula (12) – that it can be determined the probability of occurring such the decline of work L_e as the result of wear of the energy-based system, what makes performing the task impossible. Thus, the probability $P(B_t = k; k = 1, 2, \ldots, n)$ determined by the formula (12), can be considered as a reliability factor of the energy-based system. The probability can be also a safety factor of energy-based system's operation in case if it concerns such the decline of work L_e which may lead to an accident.

4. Summary

Operation of any energy-based system has been presented as a measure (index) of its reliability and safety. In the presented suggestion the operation is understood as generating and processing the energy by a technical system in determined time, which enables the energy-based system to perform the useful (effective) work L_e. The operation has been considered as a physical quantity which can be expressed (just like in physics – e.g. Hamilton's operation, Maupertius operation and the others [6, 7, 9]) with a number and the unit of measure: a *joule-second* [joule × second; Js].

References

[1] Benjamin R., Cornell C.A., *Probability, Statistics, and Decision for Civil Engineers*. *Wyd. polskie* Rachunek prawdopodobieństwa, statystyka matematyczna i teoria decyzji dla inżynierów. WNT, Warszawa 1977.

[2] Białyński-Birula I., Cieplak M., Kamiński J., Teoria kwantów. *Mechanika falowa*. Wyd. Naukowe PWN, Warszawa 2001.

[3] Chmielniak T.J., Rusin A., Czwiertnia K., *Turbiny gazowe. Maszyny Przepływowe* Tom 15. Polska Akademia Nauk. Instytut Maszyn Przepływowych. Zakład Narodowy im. Ossolińskich. Wyd. PAN, Wrocław- Warszawa-Kraków 2001.

[4] Dzida M., *Identyfikacja przyczyn niestacjonarności oraz niestabilności temperatury i ciśnienia gazów za komorą spalania turbiny gazowej*. Monografie Nr 16, Politechnika Gdańska 2000.

[5] Firkowicz S., *Statystyczna ocena jakości i niezawodności lamp elektronowych*. WNT, Warszawa 1963.

[6] Girtler J., *Operation of diesel engines as the index of their reliability and safety*. Journal of KONES Internal Combustion Engines. Warsaw, vol. 10, No 1-2, pp. 17-24, 2003.

[7] Girtler J., *Work of a compression-ignition engine as the index of its reliability and safety*. Proceedings of II International Scientifically-Technical Conference "Explo-Diesel & Gas Turbine'01. Gdansk-Miedzyzdroje-Copenhagen, vol. 1, pp.79-86, 2001.

[8] Girtler J., *Suggestion of interpretation of action and the rule of taking decisions with regard to safety of sea ships traffic*. Exploitation Problems of Machines. Polish Academy of Sciences Committee of Mechanical Engineering, Quartelly, vol. 35, pp.177-191, 2000.

[9] Girtler J., *Operation of diesel engine as the index of the reliability and safety*. Journal of KONES Internal Combustion Engine. Vol. 10, No 1-2. Warsaw 2003, pp.17-24.

[10] Gribbin J., *In Search of Schrodinger's Cat. Quantum Physics Reality*. *Wyd. polskie* W poszukiwaniu kota Schrodingera. Wydawnictwo Zysk i S-ka, Poznań 1997.

[11] Szargut J., *Termodynamika techniczna*. PWN, Warszawa 1998.

[12] Korczewski Z., *Diagnostyka symulacyjna okrętowego turbinowego silnika spalinowego*. Materiały XIX Międzynarodowego Sympozjum Siłowni Okrętowych (XIX-th International Symposium on Ship Propulsion Plants. WSM, Szczecin 1997, s.181−188.

[13] Kowalski A., *Okrętowe turbozespoły spalinowe*. Wydawnictwo Morskie, Gdańsk 1983.

[14] Wiśniewski S., *Termodynamika techniczna*. WNT, Warszawa 1999.

[15] Leksykon naukowo-techniczny z suplementem. Zespół redaktorów Działu Słownictwa Technicznego WNT. WNT, Warszawa 1989.

[16] Wybrane zagadnienia zużywania się materiałów w ślizgowych węzłach tarcia. Praca zbiorowa pod redakcją Wiesława Zwierzyckiego. PWN, Warszawa 1990.

Journal of POLISH CIMAC
Faculty of Ocean Engineering & Ship Technology
GDAŃSK UNIVERSITY OF TECHNOLOGY

ASSESSMENT OF EXCESS POWER FACTOR IN MARINE GENERATING SETS

Zbigniew Matuszak, Grzegorz Nicewicz

Maritime Academy of Szczecin
ul. Wały Chrobrego 1-2, 70-500 Szczecin, Poland
tel.: +48 91 4809414, +48 91 4809420
e-mail: zbimat@am.szczecin.pl, nicze1@wp.pl

Abstract

In the paper there has been presented a method of assessing auxiliary engines load based on identification tests of marine electric power systems loads of cargo vessels. The analysis has been illustrated by means of four auxiliary engines of an up-to date container ship 2200 TEU. A critical analysis of adjusting the auxiliary engines excess power factor to the active rated power of the generators of the currently operating generating sets.

Keywords: *marine power plants, marine electric power systems, generating sets, auxiliary engines*

1. Introduction

Generating subsystems of marine electric power systems consist mainly of synchronic generators driven by diesel engines which constitute independent generating sets. For most types of marine vessels they are the basic source of electric energy. Diesel engines when compared with other types of contemporary generator drive of marine electric power systems (e.g., combustible turbine engines or steam turbines) turn out to play the dominating role. The research carried out during the marine vessels operation determined the conditions for economical work of diesel engines driving the generators. The analyses presented in [8] show clearly that economical operation of generating sets to a great extend depends upon their load. According to [8] the work of the set appears to be the most economical at its load of 70% – 90%. At 50% – 70% of the load the increase of specific fuel consumption is negligible but at lower load values it is growing fast to reach the increase by 100% at the load of less than 20%. Thus, it appears to be significant that the power and the number of generating sets are adjusted in such a way that in various conditions of all vessel's characteristic operational states they can work at optimal load, that is at the load of 70% – 90%.

The issue of optimal operation of generating sets is connected with the adjustment of diesel engines power to the power of the generators. Diesel engines of power enlarged by 10% – 15% than the power of the generators have been suggested [3]. According to the research [8] the power of the diesel engines has been precisely adjusted to the rated power of the generators in marine power plants and the combustible engines excess power factor to the rated power of the generators equaled 1,05 – 1,25 (average 1,12). According to [8] at the generator's efficiency 0,92 – 0,94 the excess power of the engine appears to be negligible.

However, it should be remembered that in real operational conditions the load of the marine generating sets can be considerably lower than the rated power of the generator (installed power of generating set). It is proved by the results of the identification tests of the loads of marine electric power systems conducted by the author's of the paper on up-to-date cargo vessels partially discussed in [1, 4, 5, 6, 7, 9]. The knowledge of real need for electric energy during the vessel operation allows to assess the adjustment of excess power factor of the diesel engine to the power

of the generator of the marine generating set and evaluate the real load of the diesel engine commonly known as the auxiliary engine. The issue shall be discussed more broadly in the further part of the paper.

2. Excess power factor in up-to-date power generating sets

The data concerning excess power factor of the auxiliary engines to the rated power of the generators of the electric power generating sets enclosed in the paper [8] come from the 70's of the last century and deal with vessels which have been out of service. Table 1 presents data concerning vessels currently in service which have undergone load identification tests of marine electric power systems. The vessels were constructed in the shipyards of Bulgaria, China, France, Japan, Yugoslavia, South Korea, Norway, Poland and Taiwan. The 14 types of vessels comprise six types of various size container ships (7500 TEU – 1100 TEU), two types of semi-containers, three types of bulk carriers, one type of general cargo vessel, a tanker DP2 and a chemical cargo carrier. The total length of the ships ranges within 72 – 300 meters. Power of the vessels main propulsion ranges within 1470 kW – 69440 kW.

Tab. 1. Values of the auxiliary engines excess power factor to the active power of the generators of the generating sets on the vessels tested for loads of marine electric power systems

Type of vessel	Date of construction	Auxiliary engine excess power factor to the active power of the generators
container vessel 7500 TEU	2004	1,05 1,05
container vessel 7500 TEU	2005	1,05 1,05
container vessel 5500 TEU	1999	1,40
container vessel 3050 TEU	2001	1,05
container vessel 2200 TEU	2003	1,06
container vessel 1100 TEU	1982	1,21
semi-container	1986	1,62
semi-container	1979	1,25
bulk carrier	1993	1,60
bulk carrier	2003	1,10
bulk carrier	2000	1,09
general cargo vessel	1979	1,46
tanker DP2	1993	1,07
chemical cargo carrier	1979	1,26 1,11

Generating sets installed in marine power plants of the vessels in question vary quite considerably in auxiliary engines excess power to the active rated power of the generators. Excess power factors range within 1,05 – 1,62. The smallest values of the factors have been recorded on vessels constructed after 2000. In case when generating sets of various power have been installed in the generating subsystem, in table 1 more than one factor values have been presented.

Data concerning peak loads of electric power systems and specified generating sets collected due to identification tests carried out on the cargo vessels in question deal with all registered operational states typical for the above mentioned vessels. This allows to determine not only the range to which the installed power of the whole electric power system or the generating sets has been made use of, but also to assess the real load of auxiliary engines driving the generating sets. The values of the peak load of generating sets used to be recorded for one hour time intervals and treated as a random variable due to which an empirical time series for the variable in question has been created.

As an example for the analysis data achieved for the generating sets of a container vessel 2200 TEU constructed in 2003 have been applied. The generating subsystem consisted of four identical generating sets of relatively small value of the auxiliary engine excess power factor to the power of the generator driven by the engine, that is 1,06. The character of the achieved peak loads distributions (for the one hour time intervals) of the generating sets has been shown in fig. 1 by means of the Box-and-Whisker plot achieved for each of the sets. The plots have been numbered from 1 to 4 which is adequate to the marking of the generating sets.

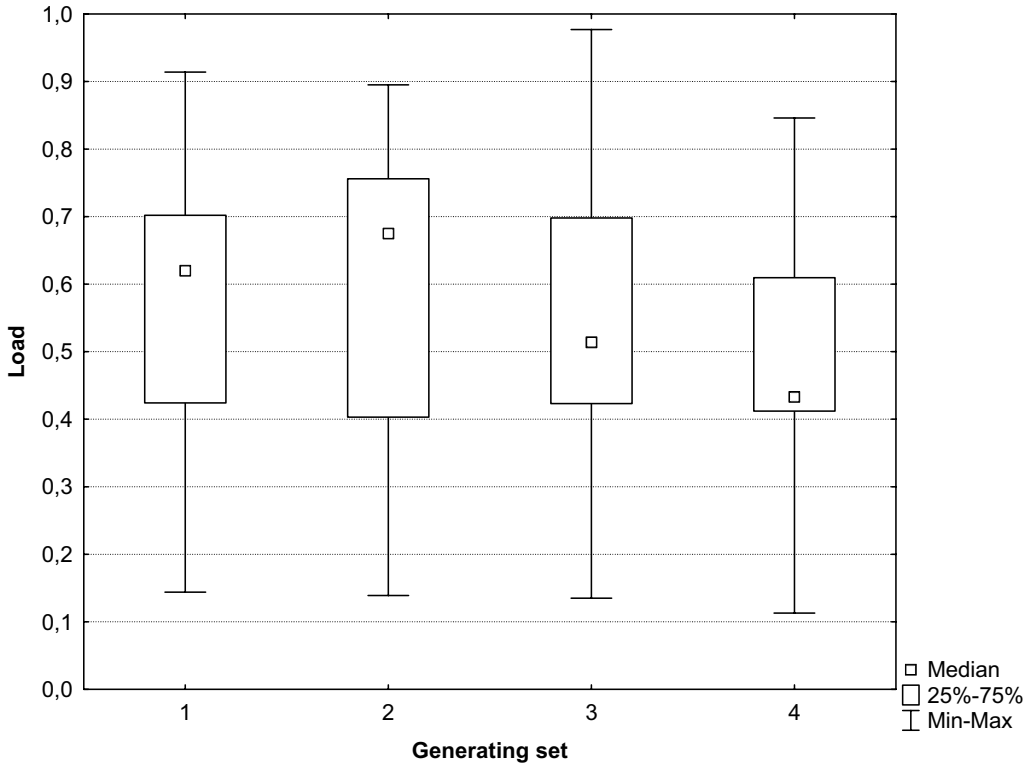

Fig. 1. Box-and-Whisker plots of generating sets loads distributions of a container vessel 2200 TEU

Due to the illustration of the achieved loads distributions of the generating sets by means of Box-and-Whisker plot introduced by Tukey in 1979 it is easy to compare their measures of location, dispersion and asymmetry, that is their minimal and maximal values, median and the upper and lower quartiles. The varied value of the peak load of the generating sets is estimated by means of comparing the length of four consecutive segments defining 25% of the registered peak load value. The variety of 50% of the most typical load values is proved by the box height of the plot adequate to the inter-quartile range. But asymmetry of the whole distribution is evaluated by comparing so called whiskers. If the upper whisker is longer than the bottom one the distribution is characterized by the right-hand side asymmetry and analogically, if the bottom whisker is longer than the upper one the distribution has left-hand side asymmetry. Asymmetry among 50% of the most typical peak load values is assessed due to the analysis of median location. If the median is closer to the upper (third) quartile, represented by the upper side of the Box-and-Whisker plot the distribution of the peak loads in the middle part is left-hand asymmetric and analogically, if the median is closer to the bottom (first) quartile represented by the bottom side of the Box-and-Whisker plot the distribution of the peak loads in the middle part is right-hand asymmetric.

The peak load distributions of the generating sets presented in fig. 1 make the basis for the analysis of auxiliary engines loads which shall be discussed in the further part of the paper.

3. The assessment of the excess power factor in the up-to-date generating sets

The peak load of the generating sets discussed in the previous chapter should be understood as the generator load – the registered peak values of the active power produced by the generator were referred to their rated active power. But there must be provided by the auxiliary engine greater power on the generator's shaft for its efficiency. And that is why in order to define the auxiliary engines load the generators' efficiency must be taken into account. If the generators' efficiency is taken on level 0,95 [2] the achieved distributions of the peak loads for the successive hours of the engine's work can be described by means of the Box-and-Whisker plots, which have been shown in fig. 2. Having the generators' efficiency on level 0,95 and the auxiliary engines excess power factor to the generators active rated power 1,06 the peak loads distributions of the generating sets and the auxiliary engines in fig. 1 and 2 differ quite insignificantly.

In fig. 2 there can be noticed considerably big differences between medians of the peak loads distributions of the auxiliary engines 1, 2 and 3, 4. This may be the result of the accepted by the ship owners technical service strategy for operating generating sets in reference to which sets 3 and 4 worked during the testing process longer than 1 and 2. Especially in the case of the generating set 2 working the shortest the influence of its switching on for the work while maneuvering which is connected with the use of 2 thrusters, whose power is approximate to the rated power of the generating sets, turned out to be very important for the value of the median.

The location of the load distributions' upper quartiles of the auxiliary engines 1, 3 and 4 in fig. 2 manifests that during 75% of the engines working time their peak load was lower than 70%, which according to [8] is regarded the lowest boundary of the auxiliary engines optimal load. The situation does not seem to be much better with the auxiliary engine 2 for which during 75% of working time the load did not exceed 75%. Thus, the auxiliary engines peak load at the presumed optimal level 70% – 90% occurred only during 25% of their working time.

Also in case of the longest working auxiliary engines 3 and 4 the location of the peak load distribution medians shows that for approximately half of the time they were working at the peak load below 50%. Apart from that for each of the auxiliary engines in question the peak load for 25% of their working time was below 40% which significantly worsens technical and economical conditions of their operation, especially because they were working on residual fuel. The smallest recorded values of the auxiliary engines peak load reached the level of approximately 15%.

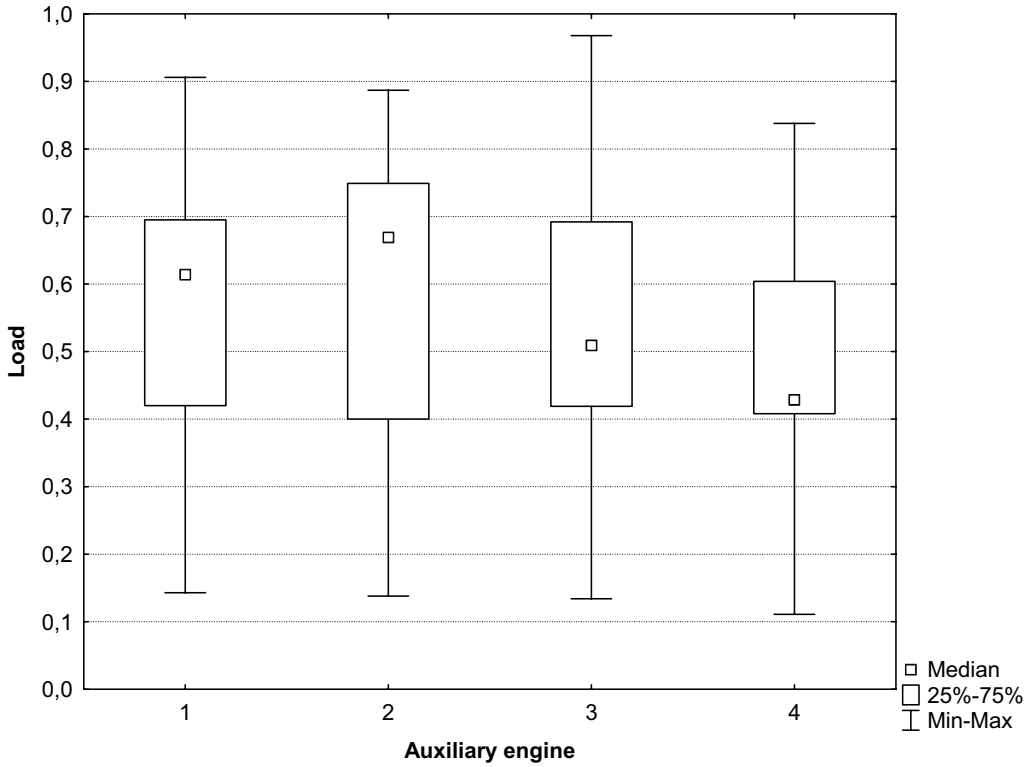

Fig. 2. Box-and-Whisker plots of load distributions of a container ship 2200 TEU auxiliary engines

It should be kept in mind that the auxiliary engines loads distributions shown in fig. 2 refer to the peak loads for the successive time intervals whose equivalent is one hour. Thus, in practice the auxiliary engines loads were even lower and the working time at the optimal loads 70 – 90% could be considerably shorter than 25% of the total working time of each of the engines.

The highest load values (more than 90%) were recorded in case of the auxiliary engine 3 (fig. 2). This was related to the malfunctioning of the diesel engine governor during manoeuvring with the use of thrusters and due to that unequal active power distribution between working in parallel generating sets – generating set 3 had its highest load then.

Due to the Box-and-Whisker plot the distributions of the auxiliary engine excess power factor to the peak power required on the generator's shaft (after the generator's efficiency has been taken into account) for the successive working hours of each of the sets can be presented. The distributions have been presented in fig. 3. In extreme cases the factor can reach even the value of 9 just as it occurred in case of the generating set 4.

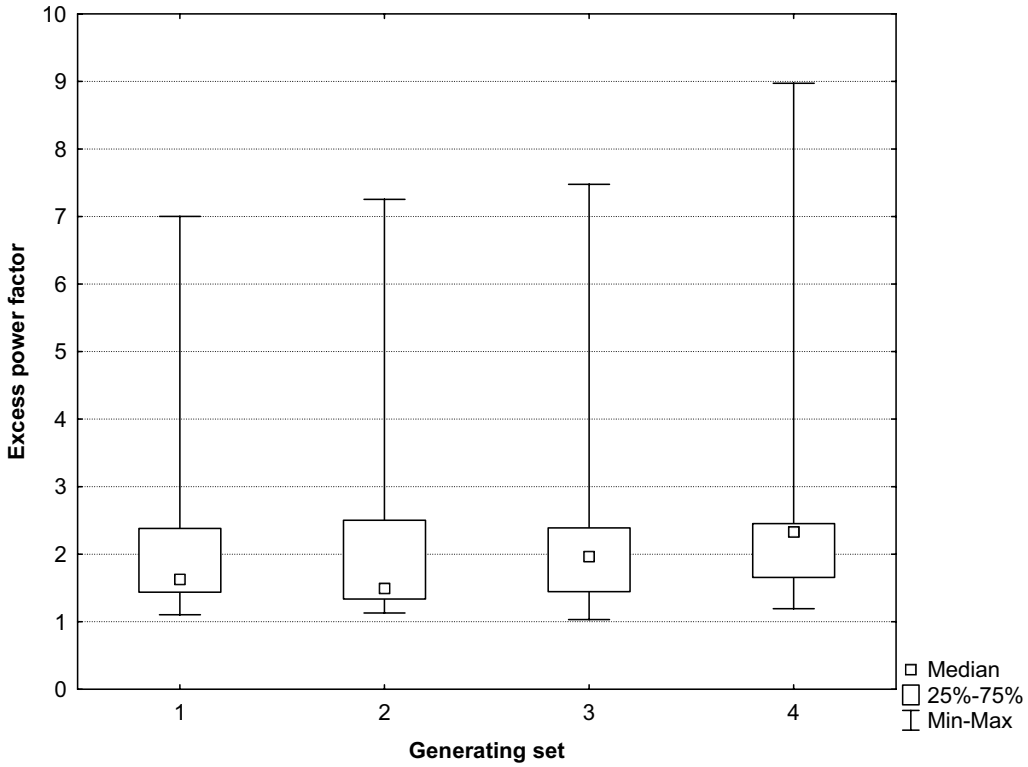

Fig. 3. Box-and-Whisker plots of the excess power factor distributions of a container ship 2200 TEU generating sets

4. Final remarks

The presented analyses deal with a vessel whose generating sets are characterised with one of the lowest auxiliary engines excess power factor to the active rated power of the generators from among the vessels referred to in table 1. At the same time the values of the generating sets peak loads registered during identification load tests of the electric power systems of cargo vessels outlined in table 1 belonged to the highest ones. In spite of that working time of the generating sets when the level of the peak load of the auxiliary engines ranged between 70 – 90 % equalled approximately 25% of their total working time during the research period covering a typically operational voyage of a ship between the ports of Europe and West Africa. Thus, it seems that no justification can be found for assuming higher values of the auxiliary engine excess power factor to the generator's active rated power of the installed generating sets when designing the cargo vessels. Identification tests of cargo vessels electric power systems loads carried out by the authors of the paper show clearly that in most cases generating sets work at considerably lower loads than the rated one and moreover too big excess power of the auxiliary engine stops its work being economical. When adjusting the number and power of generating sets statistical data concerning operation of marine electric power systems and probabilistic models of their loads in order to avoid possible design errors should be taken into consideration. Ship owning companies and their technical service have to struggle in case the generating sets of the marine power plants appear to be over dimensioned. The issue can be so essential that for example for the container vessel 1100 TEU enlisted in table 1 where the generating sets did not have the highest auxiliary engines excess power factor to the generator's rated power (1,21), residual fuel for the auxiliary engine needed to be changed for distilled fuel because of their too low load. Apart from the increase in fuel

expenses, over the years of the vessel operation, some of the fuel and steam installation connected with preparing the residual fuel oil for the auxiliary engines stopped being used although the costs of its construction had required to be paid for.

Thus, collecting statistical data during vessels operation, especially by means of the up-to-date control systems which most marine power plants of the currently constructed vessels are equipped with, shall significantly contribute to discerning real working conditions of the machinery and devices as well as the development of marine industry.

References

[1] Chybowski, L., Kijewska, M., Nicewicz, G., *Analiza obciążeń autonomicznych urządzeń prądotwórczych systemów energetycznych obiektów pływających.* II Międzynarodowa Konferencja Naukowa Systemy Wspomagania w Zarządzaniu Środowiskiem, Ekonomika i Organizacja Przedsiębiorstwa Rok LVI Nr 7 (666) Lipiec 2005, Słowacja, Zuberec 2005.

[2] Cichy, M., Kowalski, Z., Maksimow, J.I., Roszczyk, S., *Statyczne i dynamiczne własności okrętowych zespołów prądotwórczych*. Wydawnictwo Morskie, Gdańsk 1976.

[3] Figwer, J., *Zagadnienie wielkości mocy silnika napędowego w okrętowych zespołach prądotwórczych*. Budownictwo Okrętowe Nr 6, 1962.

[4] Kijewska, M., Matuszak, Z., Nicewicz, G., *Identyfikacja obciążeń systemu elektroenergetycznego siłowni okrętowych w rzeczywistych warunkach eksploatacyjnych*. SYSTEMS Journal of Transdisciplinary Systems Science Vol. 11 2006, s. 334-340.

[5] Kijewska, M., Nicewicz, G., *Analiza rozkładu obciążeń zespołów prądotwórczych elektrowni okrętowej statku transportowego dla wybranego stanu eksploatacyjnego*. Надежность и Эффективность Технических Систем. Международный Сборник Научных Трудов, KGTU, Kaliningrad 2004, s. 64-72.

[6] Kijewska M., Nicewicz G., *Estymacja gęstości rozkładu obciążeń zespołów prądotwórczych elektrowni okrętowej w wybranym stanie eksploatacji*. Zeszyty Naukowe Politechniki Gdańskiej nr 598 (seria: Budownictwo Okrętowe Nr LXV), Gdańsk 2004, s. 79-87.

[7] Kijewska M., Nicewicz G., *Rozkłady empiryczne a rozkłady teoretyczne obciążeń autonomicznych zespołów prądotwórczych elektrowni okrętowych*. Надежность и Эффективность Технических Систем. Международный Сборник Научных Трудов, KGTU, Kaliningrad 2005, s. 124-131.

[8] Kuropatwiński, S., Lipski, T., Roszczyk, S., Wierzejski, M., *Elektroenergetyczne układy okrętowe*. Wydawnictwo Morskie, Gdańsk 1972.

[9] Nicewicz G., *Obciążenie okrętowego systemu elektroenergetycznego a bezpieczeństwo statku*. Zeszyty Naukowe AMW im. Bohaterów Westerplatte Nr 168 K/1, X Konferencja Morska „Aspekty bezpieczeństwa nawodnego i podwodnego oraz lotów nad morzem", Gdynia 2007, s. 205-215.

[10] Stanisz, A., *Przystępny kurs statystyki*. *Tom 1*. *Statystyki podstawowe*. StatSoft, Kraków 2006.

Journal of POLISH CIMAC

Faculty of Ocean Engineering & Ship Technology
GDAŃSK UNIVERSITY OF TECHNOLOGY

THE APPLICATION OF THE EXERGETIC ANALYSIS IN DESIGNING OF WASTE ENERGY RECOVERY SYSTEMS IN MARINE DIESEL POWER PLANTS

Ryszard Michalski

The Szczecin University of Technology
41 Piastów Ave, 71-065 Szczecin, Poland
tel: (091) 4494941; fax: +48 91 449 44 88
e-mail : *ryszard.michalski@ps.pl*

Abstract

The efficient use of waste energy is a major element in designing the energy-saving marine power plants. The ecological aspects of the usage of this energy are of importance as well. Thus the need to perform the evaluation becomes significant – in respect of both the sources of the waste energy and the marine systems of its recovery, inter alia in terms the achievable efficiency levels. Besides the determination of the available quantity of the energy it is necessary to take into account the value characterising this energy in terms of its quality. The measure of the quality of the energy is the value of the maximum capacity of work performance referred to as the exergy. The exergetic analysis allows to determine the values of the individual jets of working media as well as, which is particularly important, allows to properly assess the proportions of losses in the individual elements of the recovery systems under investigation. Therefore it is a basis to calculate their exergetic efficiency. The article presents the balance values of the energy fluxes of the selected ship's main propulsion engines as well as, inter alia an example of the course of the changes in the specific exergy and enthalpy of the exhaust gases in the function of the load of ship's main propulsion engine. It presents also the examples of the exergetic analysis of the main propulsion engine exhaust gases recovery systems with the application of Brayton cycle, Clausius-Rankine cycle or both cycles combined.

Keywords*: designing, marine power plants, waste energy, recovery, exergetic analysis*

1. Introduction

The basic source of the waste energy in the motor power plant are the self-ignited Diesel piston engines of the main and auxiliary (Diesel generators) propulsion systems. The exhaust gases, engine cooling water, charging air and lubricating oil are the carriers of this energy.

The physical waste energy and chemical waste energy are distinguished in relation to the operation of the marine Diesel engines. The physical waste energy occurs in the temperature form resulting from the temperature deviation of the waste energy carrier from the ambient and pressure temperature that results from the increased pressure in relation to the pressure value prevailing in the environment. The chemical waste energy is the effect of the difference in the chemical composition of the waste substance which are the exhaust gases in comparison to the generally occurring components in the environment [1. 2, 3]. In the shipping practice the physical waste energy is used. The proper evaluation of the sources of the waste energy is necessary in designing the shipboard waste energy recovery systems. This evaluation should concern not only the parameters of the waste energy carriers corresponding to the nominal engine load, but also should take into account their change resulting from the change in engine load during the ship's service life.

The quantity of energy is not a sufficient measure of its practical usability. Besides the energy quantity it is necessary to consider the value characterising the energy in terms of its quality. The choice of the measure of this usability is of relative nature. It has been assumed to apply the value of the maximum capacity for work called exergy [2].

The main task of the exergetic analysis is to detect the kind and places of occurrence of the factors increasing the imperfections of the energetic processes and another chief task is the quantity assessment of the results caused by these factors.

The exergetic balance figures allow to evaluate efficiently the values of the individual energy fluxes of working media as well as, which is of particular significance, allow to properly assess the proportion of losses in the individual elements of the system under investigation. Exergy balance consists therefore the basis for the calculation of the exergetic efficiency [2, 3, 4]. It should be noted that the differences between energy balance and exergy balance are particularly large in the examination of the processes occurring in the vicinity of ambient temperatures [4].

The efficient use of waste energy is a major element in designing the marine power plants. Thus the need to perform the evaluation becomes significant – in respect of the marine systems of waste energy recovery, inter alia in terms the achievable efficiency levels.

The ecological aspects of the usage of this energy are of importance as well. Similar like in the land power engineering the transformation of the energy carriers in a ship's power plant is related with the detrimental effects on the natural environment. It chiefly consists in the emission of the harmful exhaust gases components and the thermal contamination. In such terms every action resulting in saving of the energy, including also the use of waste energy, leads to the reduction of the harmful ecological effects.

2. The Evaluation of the Sources of the Waste Energy in the Diesel Power Plants

It is necessary to know the share in % of the waste energy and the effective mechanical energy in the total energy of the burnt fuel, expressed in terms of energy balance in order to perform the evaluation of the amount of waste energy and the effective mechanical energy.

In order to evaluate the amounts of waste energy the thermal balance values of the engines are determined. The complement of the information on this energy form is the knowledge of the temperature and pressure of its carriers.

Analysing the balance structure it can be preliminarily concluded which factors are to be used in the first place and which may be regarded as the additional sources, less applicable in practice. While designing the waste energy recovery systems it should be borne in mind that the suitability of a given waste energy source is proven, besides the thermodynamic parameters, also by the physical and chemical parameters of the energy transferring medium.

Table 1 shows the balances of the energy fluxes of the MAN and Wärtsilä main propulsion low-speed Diesel engines corresponding to the maximum continuous rating value, MCR. These balances have been achieved on the basis of the catalogue data of the engines [7, 8]. The table shows the maximum and minimum figures of the share in % of the waste power and waste heat flux contained in various carriers.

Table 1. Balances of the energy fluxes of some selected marine main propulsion engines, %

Manufacturer	**MAN**		**Wärtsilä**	
Energy flux, %	max	min	max	min
Engine output	50.8	47.1	50.9	48.5
Exhaust gases	24.6	21.5	25.5	23.7
Charging air cooling water	19.5	16.5	16.3	15.6
Lubricating oil	6.3	3.8	6.0	4.5
Cylinder cooling water	9.1	6.5	10.5	7.7
Radiation	0.9	0.5	0.6	0.5

Table 2 shows on the other hand the characteristic temperature ranges of the waste energy carriers of MAN and Wärtsilä main propulsion low-speed Diesel engines corresponding to the maximum continuous rating value [7, 8].

Table 2. Waste energy carrier temperatures of some selected main propulsion engines

Manufacturer	**MAN**		**Wärtsilä**	
Temperature, K	max	min	max	Min
Exhaust gases	528.15	508.15	548.15	535.15
Charging air cooling water	331.15	318.15	331.15	329.15
Lubricating oil	324.55	323.35	347.85	334.55
Cylinder cooling water	353.15	353.15	363.15	363.15

The presented data allow to conclude that the efficiently used heat consists 47.1÷50.9% of the energy contained in the burnt fuel. The heat transferred in the exhaust gases consists 21.5÷25.5%, in charging air cooling water – 15.6÷19.5%, in cylinder cooling water – 6.5÷10.5%, and the heat contained in the lubricating oil – 3.8÷6.3% accordingly. It should be noted that the relatively high value of the heat fluxes does not always correspond to the high temperature of the heat carriers. Such is the case for instance in respect of heat contained in charging air cooling water.

The evaluation of the sources of the waste energy performed on the basis of the engine heat balance does not provide the explicit and clear information on its quality, although given in connection with the information on the energy carrier temperatures. The application of the exergetic analysis for the evaluation of the quality of the waste energy however allows to put the sources of the waste energy in the right order in terms of their quality.

An important component of the exhaust gases exergy, besides its temperature part, is its pressure part. Information on this exergy part is significant for the designing of the recovery systems with Diesel turbines.

The specific exergy of the exhaust gases, covering the temperature and pressure parts, can be determined by the equation:

$$b_s^{wl} = c_p\left(T_s^{wl} - T_o\right) - T_o c_p \, ln\frac{T_s^{wl}}{T_o} + RT_o \, ln\frac{p_s^{wl}}{p_o}, \tag{1}$$

where:

b_s^{wl} – specific exergy of the exhaust gases, kJ/kg,
c_p – mean specific heat capacity under constant pressure, kJ/kgK,
T_s^{wl} – exhaust gas temperature before turbine, K,
T_o – ambient temperature, K,
R – exhaust gas constant, kJ/kgK,
p_s^{wl} – exhaust gas pressure before gas turbine, Pa,
p_o – ambient pressure, Pa.

Figure 1 shows the engine exhaust gases exergy and specific enthalpy values with the assumed ambient temperature T_0=298 K, ambient pressure p_0=100 kPa and exhaust gas pressure p=200 kPa. In the Figure 1 the physical specific temperature and pressure exergy is marked as “bs”, the physical specific temperature exergy is marked as “bsT”, and the specific enthalpy as “isT”.

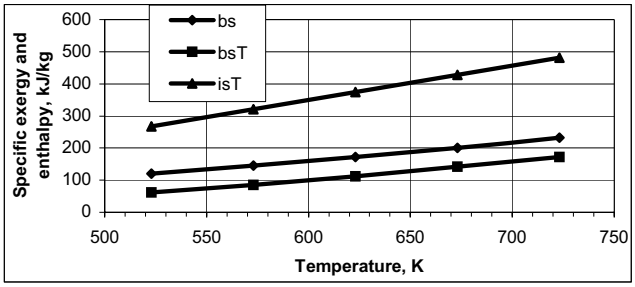

Fig 1. Specific exergy and enthalpy values of the engine exhaust gases in the function of the temperature

The figure above shows that although the exhaust gas specific enthalpy is relatively high its exergy is low. The knowledge of exergy allows to assess properly the quality of waste energy.

A significant issue in designing the waste energy recovery systems is the evaluation of the parameters of exhaust gases corresponding to engine partial loads. The available quantity of waste energy contained in exhaust gases in such conditions decreases due to their decreasing flux despite some increase in their specific exergy. At that time the total heat demand on a ship in general decreases insignificantly.

Figure 2 shows the changes of the temperatures of exhaust gases before turbocharger (before TC), after turbocharger (after TC) and the mean exhaust gas temperature after cylinders (after cyl.) in the function of 7S60 MC-C engine load according to the characteristics of the screw.

On the other hand figure 3 shows the changes of the specific exergy and enthalpy of the exhaust gases after turbocharger in the function of the load of the engine under investigation. The physical specific temperature exergy has been marked as "b(T)", and the specific enthalpy as "iT". The values of the presented parameters have been obtained pursuant to the measurements conducted on engine test bed in the H Cegielski Mechanical Works in Poznań.

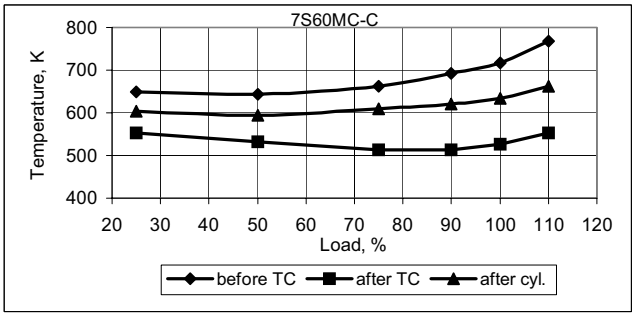

Fig 2. The change of the exhaust gases temperature of 7S60MC-C engine

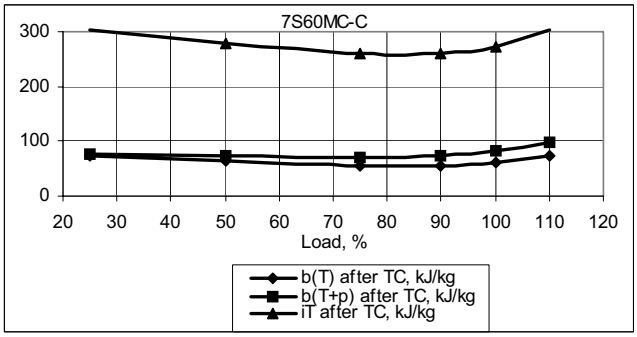

Fig 3. The change of the specific exergy (b) and enthalpy (iT) of the exhaust gases of 7S60MC-C engine

The physical exergy flux transferred by cylinder cooling water can be determined from the relation:

$$\dot{B}_w = b_e W_d N_e \alpha_w \left(1 - \frac{T_o}{T_w} \right) \cdot \frac{0{,}01}{3600}, \tag{2}$$

where*:*

$\dot{B}_w$ – physical exergy flux, kW,

b_e – specific fuel consumption, kg/kWh,

W_d – fuel lower calorific value, kJ/kg,

N_e – effective power, kW,

α_w – proportional share of heat transferred by cylinder cooling water, %,

T_0 – ambient temperature, K,

T_w – engine cooling water temperature, K.

The engine charging air cooling water physical exergy flux or the lubricating oil exergy fluxes can be determined in the similar manner.

The exhaust gases from main and auxiliary engines have high exergy level. Cylinder and charging air cooling water has significantly lower exergy level thus its applicability is indeed limited. Also the lubricating oils are characterised by low exergy and can only consist a supplementary source of the waste energy to be used in the recovery systems.

In the designing practice mainly the energy contained in main engine exhaust gases and cylinder cooling water whereas that contained in engine charging air is used less frequently and that in lubricating oil only from time to time.

3. The Exergetic Analysis of the Shipboard Systems of Waste Energy Recovery

In order to conduct the analysis of the arrangements of the waste energy recovery systems it is necessary to use a set of, among others, mathematical models concerning the thermodynamic changes occurring in their elements. These allow to analyse the processes occurring both in themselves as well as in any recovery systems – the simplest ones, single-pressure, producing saturated steam for heating purposes and multi-pressure type – used for the production of heating steam and superheated steam to supply turbo-generator and those using waste energy contained in cylinder cooling water, in engine charging air and lubricating oil. The description of the appropriate calculation models has been provided among others in paper [4]. The method of determination of the exergetic efficiency of the waste heat boilers, exergetic efficiency of the systems including the waste heat turbo-generator and the exergetic efficiency of the system producing electric power and steam for heating purposes has been presented inter alia in [5].

In the self-ignition engines the parameters of the exhaust gases leaving turbocharger are far from the ambient parameters. The heat contained therein can be used in steam turbine running according to Clausius-Rankine cycle. The progress in the increase of the charging turbocharger efficiency provides a possibility of using a part of the exhaust gases in a separate gas turbine supporting the ship's propeller propulsion system, referred to as reverse turbine, or in turbine driving the generator. Thus a problem appears to make a choice of the arrangement of the engine exhaust gas waste energy recovery system. This can involve among others the use of Brayton cycle with the waste gas turbine and Clausius-Rankine cycle with waste steam turbine. The results of the analysis of this type can be found in [9]. The author of this article has expanded the investigation scope by incorporating the complex systems where Brayton cycle has been combined

with Clausius-Rankine cycle. The more comprehensive results of the investigations are contained in [6]. The said cycles are being offered nowadays among others by MAN [10] and Wärtsilä [11].

The exergetic analysis performed for the cycles is of theoretical nature. It does not include inter alia the turbine internal efficiency values or energy consumption for own needs of both systems. On the other hand it takes into account the necessity to keep the temperatures difference in the waste heat boiler bigger than zero which is the condition for heat transfer to take place. It is of particular importance to keep at the same time the minimum temperature difference between the exhaust gases and the steam-water mixture – pinch point (ΔT_{min}).

The calculations of the unitary work of the Brayton turbo-gas cycle have been carried out according to the following model.

The specific exergy of exhaust gases before turbine b_s^{wl} has been determined according to equation (1). In the further course of this article the symbols adopted for this equation have been maintained too.

The temperature of the exhaust gases after turbine T_s^{wy} is determined by the equation:

$$T_s^{wy} = T_s^{wl}\left(\frac{p_s^{wl}}{p_o}\right)^{\frac{\kappa-1}{\kappa}}, \text{ K}, \tag{3}$$

where $\kappa = \frac{c_p}{c_p - R}$ - isentropic curve exponent in the exhaust gas expansion process in turbine.

The specific exergy of the exhaust gases after turbine b_s^{wl} is determined from the relation:

$$b_s^{wy} = c_p\left(T_s^{wy} - T_o\right) - T_o c_p \, ln\frac{T_s^{wy}}{T_o}, \text{ kJ/kg}. \tag{4}$$

The unitary theoretical work l_t of the cycle is equal to:

$$l_t = b_s^{wl} - b_s^{wy}, \text{ kJ/kg}. \tag{5}$$

The exergetic efficiency of the cycle η_b is determined by the relation:

$$\eta_b = \frac{l_t}{b_s^{wl}}. \tag{6}$$

The calculations of the Clausius-Rankine steam cycle have been performed by the use of the Util1 software [4]. In the cycle calculations the constant steam pressure in condenser has been assumed equal to 0.007 MPa, also there has been assumed the constant value of the temperature difference of exhaust gases and steam in steam heater, equal to 15 K and the exhaust gas temperature after the waste heat boiler, equal to 443 K. The calculations have been conducted for $\Delta T_{min.}$=15 K. In this situation among others the pressure of the steam generated has been changed.

The results obtained have been presented in figures 4 and 5 where Brayton cycle has been marked with B and the Clausius-Rankine cycle with C-R.

Figure 4 shows the achievable recoverable unitary work values in Brayton and Clausius-Rankine cycles as well as unitary work achieved additionally in Clausius-Rankine cycle obtained owing to the use of heat of the exhaust gas of gas turbine (in figure 4 it is marked as “dop. ob. C-R”) and the joint work of Brayton cycle together with the combined Clausius-Rankine cycle. It is significant that once a certain temperature is exceeded, the unitary work of the additional Clausius-Rankine cycle is larger than the work achieved in the basic Brayton cycle. As shown in figure 4, the unitary work increases in case of both cycles together with the growing temperature of the exhaust gases. At the same time there is an area where Brayton cycle is more useful and another where the Clausius-Rankine cycle is the better arrangement. This corresponds also to the conclusions presented in [9].

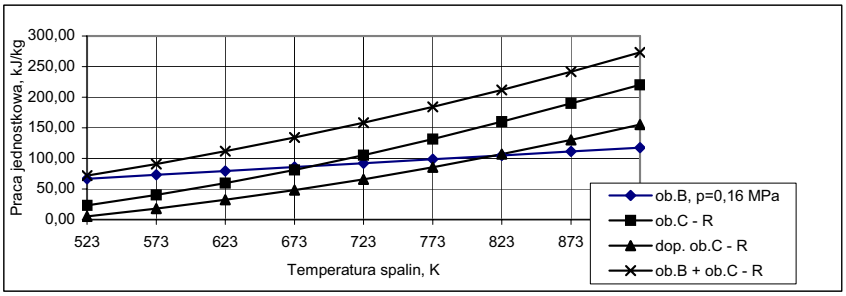

Fig. 4. Possible work to obtain due to the consideing cycles versus exhaust gas temperature after diesel engines

Figure 5 shows the course of efficiency of Brayton and Clausius-Rankine cycles in the function of exhaust gas temperature under assumption of the constant value of the exhaust gas pressure (p=0,16 MPa).

The efficiency values defined by equation (6) increase together with the temperature increase in case of Clausius-Rankine cycle and decrease in Brayton cycle. In the latter case it results from the fact of simultaneous increase of temperature of exhaust gas leaving the gas turbine which is characteristic for the expansion process in turbine. The degree of exhaust gas energy recovery in Brayton cycle increases together with the exhaust gas pressure increase and decreases for the Clausius-Rankine cycle. In every case the efficiencies of both cycles combined increase.

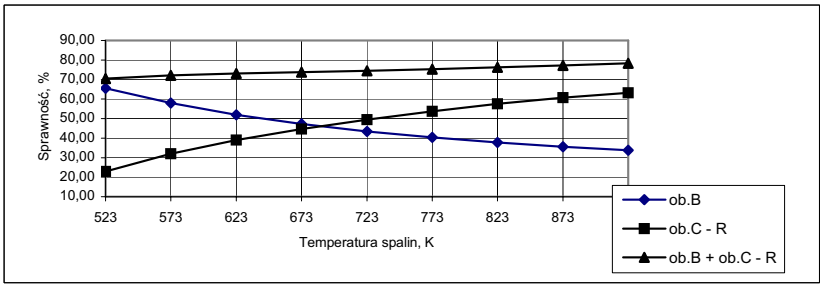

Fig. 5. The efficiency of the considering cycles versus exhaust gas temperature after diesel engines

Conclusions

The basis of the evaluation of the waste energy resources in marine Diesel power plants is their exergy whereas the basis for the evaluation of the possibility and manner of waste energy recovery is their exergetic analysis. While designing the waste energy recovery system the number and the parameters of the carriers of this energy should be of particular concern. All kinds of listing and specifications of the amounts of energy transferred, temperatures of its carriers, specific exergy or specific heat capacity are particularly useful.

The application of exergetic analysis in connection with energetic analysis allows to qualify and put in the right order the sources of waste energy in terms of their quality.

There is a possibility of large variety of the applications of the marine systems of waste energy recovery. The individual arrangement of a waste energy recovery system should depend on the appropriate kind of energy and its amount needed to keep the operation of the ship's engine room and ship herself, prevailing ambient conditions during the ship's service, planned main engine distribution loads and main engine type.

The exergetic analysis allows to evaluate the quality of the processes occurring in the waste energy recovery systems. It also allows to indicate the least effective processes thus facilitating the optimising of the designed systems.

At the same time a due attention should be paid to the specific nature of the operation of these systems which are operative only while their heat sources are active.

The final evaluation of the variants of the energy recovery arrangement in the motor ship's power plant is possible upon due consideration of the thermodynamic criteria as well as technical, service and economic criteria.

LITERATURE

[1] Szargut, J. i inni, *Przemysłowa energia odpadowa. Zasady wykorzystania. Urządzenia*, *[Industrial Waste Energy. The Principles of Recovery. Equipment]*, WNT, Warszawa 1993.

[2] Szargut, J., *Analiza termodynamiczna i ekonomiczna w energetyce przemysłowej [Thermodynamic and Economic Analysis in Industrial Power Engineering]*, WNT, Warszawa 1983.

[3] Szargut, J., Ziębik, A., *Podstawy energetyki cieplnej [The Basics of Heat Power Engineering]*, Wydawnictwo Naukowe PWN S.A., Warszawa 1998.

[4] Michalski, R., *Przykład zastosowania analizy egzergetycznej do badania procesów utylizacji ciepła odpadowego w siłowniach motorowych [An Example of the Application of the Exergetic Analysis for the Investigation of the Recovery Processes of the Waste Heat in Motor Ships Power Plants]*, XX Sympozjum Siłowni Okrętowych, Wyd. Uczeln. AMW w Gdyni, Gdynia 1998.

[5] Michalski, R., *Ocena termodynamiczna okrętowych systemów utylizacji energii odpadowej spalin [Thermodynamic Evaluation of the Exhaust Gas Waste Energy Marine Recovery Systems]*, Zeszyty Naukowe Wyższej Szkoły Morskiej w Szczecinie, Nr 66, ss. 287-299, Szczecin 2002.

[6] Michalski, R., *Porównawcza analiza termodynamiczna obiegu Braytona i Clausiusa-Rankine'a w okrętowych systemach utylizacji energii odpadowej spalin [A Comparative Thermodnamic Analysis of Brayton and Clausius-Rankine Cycles in the Exhaust Gas Waste Energy Recovery Marine Systems]*, XXII Sympozjum Siłowni Okrętowych, Szczecin 2001.

[7] ME Project Guide, MAN-B&W, 1998-2000.

[8] Engine Selection and Project Manual, Wärtsilä, 1997-2008.

[9] Woodward, J. B., *Evaluation of Brayton and Rankine alternatives for Diesel waste heat exploitation*, Journal of Engineering for Gas Turbine and Power; Vol. 116, January 1994.

[10] Thermo Efficiency System (TES) for Reduction of Fuel Consumption and CO_2 Emission, MAN B&W Diesel, Reg. No. 39 66 13 14, P.9161-00, Jul. 05.

[11] Schmid, H., *Less Emissions Trough Waste Heat Recovery*. Green Ship Technology Conference, London, 28/29 April 2004, Wärtsilä Corporation, April 2004.

Journal of POLISH CIMAC

Faculty of Ocean Engineering & Ship Technology
GDAŃSK UNIVERSITY OF TECHNOLOGY

RESEARCHES OF FRICTION FORCE OF INJECTOR NEEDLE IN INJECTOR BODIES OF MARINE DIESEL ENGINES IN THE PRESENCE OF LUBRICATING COMPOUND

Jan Monieta*, Łukasz Lorek

**Maritime University of Szczecin, Institute of Marine Power Plant Operation,*
Wały Chrobrego 2, 70-500 Szczecin, phone: (4891) 48-09-415; 48-09-479,
fax: (4891) 480-95-75, e-mail: jmonieta@am.szczecin.pl

Abstract

In article have been presented the results of researches of friction force between injection needle and body of marine diesel engines. There were injector nozzles of piston engines, which were feeding diesel oils or residual fuels. For investigations injector nozzles were chosen amongst sprayers operated in natural conditions, in which excess resistances of the spire were stated at the movement of needles in injector nozzles. There were disabilities, which importantly disturbed performance. There has been used, so passive experiment.

The investigations have been carried on two stands for measurement of friction forces in dependence on its largeness. First of they have been raised in personal range for maximum friction force appointment witch utilization of weighting of gravity forces. For investigated of course of friction forces in injector nozzles about greatest resistances to motion, has been utilisation of stand for investigations of samples of tensile strength.

An influence of angle putting the injector needle was being examined with regard to the body of the sprayer and kind of the greasing middle. They were greasing factors: fuel, applied oil it of conservation and oil applied for attempts at the stage of the production. There has been measurement of diameter clearance between frictional couple precise and researched him influence on the values of maximum friction force.

To value of the maximum friction force among the body and needle of the injector nozzle has influence the amount and the quality of the lubricating compound, the state cooperating surfaces and their mutual location.

Keywords: marine diesel engines, injector nozzles, friction force

1. Introduction

The wrong operation active of injection apparatus of marine diesel engines in the result of wear in the fundamental way influence fall in the legal validity, fuel consumption, pollutant of the exhaust fumes and the like. The scope of the correct exploitation of injectors depends on the permanence and the most precise reliabilities of assembles, which injector nozzles are.

Injector nozzles marine diesel engines are being operated in very disadvantageous conditions, at high pressures of fuel as well as they are surrendered to thermal and mechanical loads [1]. As a result of the influence of different extrinsic factors, is achieving the intense friction, the wear and tear and failures and the passage from the state of the applicability to the acceptable profession or the state unfit nesses [6, 8].

However till the here and now a sufficient knowledge about factors having the influence on correct action of the injection sub-assembles, referring to such problems is missing, as: the influence of the wear, friction and lubricating on precise steam, the influence of the turnover of the needle in the body of the injector nozzle for increasing wearing out. He exists so are needed, being influenced by scientific as well as economic accounts, of carrying examinations of life of injection apparatus and seeking different ways for increasing it.

At work one presented results of the own research on the maximum friction force, needed for moving the injector needle from the body of the injector nozzle, as well as measurements of times

of coming out were described of needle from bodies of injector nozzles for different angles of the turnover of the injector needle in the body of the nozzle. The carried researches aren't aimed at checking the dependence of the storage friction force on the angle of the turnover of injector needle in the bodies of injector nozzle, spreading the injector needle, the kind on the time of coming out and mass of the injector needle.

2. Friction of solid bodies

An outside friction is accompanying the internal friction on micro- coming into existence and the disappearance of friction bonds, are being located in outer layer regions [3]. From a point of view of the kinetics of the move an outside friction is being distinguished static and outside friction kinetic. In fig. 1 a disintegration of forces working on the body on the inclined plane is shown.

The friction measure is resistance balanced by resultant power is tangent during transferring one body towards second. At relative transferring two bodies a kinetic friction is appearing (moving), in addition, if the relative speed of areas of the friction of two bodies is equal of the naught, then a static (rest) friction is appearing.

Kinetic friction, on account of the kind of the move, it is possible to divide in the sliding, rolling and fluid friction [9]. From a technical point of view, a division of the friction is most important for dry, border and liquid. For reducing the outside friction they were trying to divide surfaces rubbing with the layer of lubricating substance that is to replace the dry friction of solid bodies with the fluid friction.

If on account of great individual pressures is layer subject to liquid “for squeezing "from the space between friction surfaces, then between them a poor thin layer of liquids remains staying there only as a result of the interaction of liquids with solid bodies, called the boundary layer. It protects against the appearance of the dry friction. In the operation of machines only are making advances a mitigated solid friction and fluid friction. On account of the fact that cooperating surfaces aren't perfectly smooth, can be found of dry or mitigated solid friction in tops of these irregularities, and in hollows fluid friction [3].

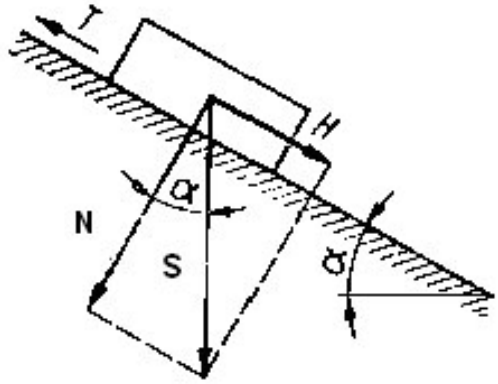

Fig. 1. Distribution of forces working on the solid body on the inclined plane: T – friction force [N], H – power transferring the body [N], N – power of the pressure [N], G – weight [N], α – indication angle of body [°]

The solid body put on the inclined plane has the weight *G*. Itself strength of the friction of the *T* is preventing of displacement from two bodies tangent to the surface and on the contrary directed as for the move and direction of power transferring the body phenomena of appearing of the joint

are *H*. The friction force *T* exists thanks of appearing of the joint of two surfaces. For the body being in a rest on the inclined plane (fig. 1) about the pitch ah, it is possible to elaborate the triangle of strength of the *G*, *N*, the *T* (*T* = *H*) [3]. Then the following dependences are appearing:

$$T = G \cdot \sin \alpha, \tag{1}$$

$$N = G \cdot \cos \alpha, \tag{2}$$

The friction force determined is formula:

$$T = \mu \cdot N, \tag{3}$$

The last relation is Amontonsa theory (law of the dry friction), which sounds: “the friction is a result of climbing of one body by irregularities second, at moving them towards oneself under the effect of the normal pressure”. There is power of the normal pressure, which is counteracting climbing in his format of friction with the deciding factor by irregularities. The border friction is appearing in the period of dawning on, when irregularities weren't still removed and they are breaking the oil wedge. Such a phenomenon can turn up at injector nozzles.

From most often kind of friction in elements of machines is a mixed friction, called the semifluid friction. It is next kind of the friction, being able to turn up at injector nozzles. It relies on the fact that in areas of the immediate joint of tops of two rubbing bodies dry or border rubbing is coming into existence, however in areas of hollows so-called spreadable microwedges are formed. The mixed friction is appearing at the swinging-turning move that is in the injector nozzle it is taking place during the movement of the injector needle in the corps. The mixed friction up is appearing in injector nozzles while reaching. At the relative move spreadable substance is filling hollows of the inequality up.

At mixed friction single areas of the metallic joint exist, where the surface is small compared with the nominal surface of the friction. There is substance greasing with air between areas of metallic joints as well as there products of the wear and tear are coming in.

At limiting friction of frictional resistance and wear of cooperating surfaces in conditions of limiting friction from coarseness of the surface and spreadable substance. In injector nozzles surfaces of the friction are lubricated by fuel [5]. Therefore a sliding, fluid or mixed friction up can here appears, if they appear great side pressures. Friction force and so will be addicted to the property of fuel, the speed slide at mixed friction up, of pressures and the coefficient of the friction.

3. The methods of friction and wear investigations of injector nozzles

With most often applied method there was a based method for measuring the storage friction force on the principle of setting power in motion under force of gravity of fixed sample from which he results, the transfer is directly proportional to needed power for transferring the sample. Applied methods of examining the wear enable the assessment of the relative resistance of materials to the wear. Value of the wear and tear, and in some cases and intensity of using up, it is possible to judge with the help of quantitative methods: of a scale, metric, of clocks, optical, of flow measurements [4, 7].

The metric method consists in the measurement of using up linear dimensions of the element checked before wearing him out and after the determined stage. The accuracy of the measurement is made conditional on measuring tools. Applying digital devices it is possible to get the accuracy of the measurement even up to 0.0001 mm [6]. To flaws in the metric method one should rank problems in measurements of the inequality on the entire examined surface. So in this method it is

possible to make the measurement of diameters of leading parts of the injector needle, diameters of the part of the body, which is piloting of the injector needle, of maximum stroke of the needle and apex angles of cones of the needle [6].

In the article research findings of the friction force were presented between the injector needle and the body of nozzles of ship's engines [5]. They were these are injector nozzles of piston internal-combustion engines, fed with diesels or residual fuels. For investigations injector nozzles were chosen around amongst exploited in natural conditions, at which immobilizing the needle was stated. In conditions of the vetting of the part constructing corps and pins of nozzles, after washing in diesel, one undergone blowing through with compressed air, i.e. for practically removing fuel.

Reliability of precise pairs of fuel apparatus, particularly injector nozzles, includes the wide range of problems of the design, production and exploitation nature. Increasing the reliability is possible through a penetrating analysis of behaving parts in all stages of making them, the assembly and the operation [4].

4. The aims of investigations

The investigations one carried in Laboratories of Institute of Power Plant Operation of Maritime University of Szczecin on several investigation stands. The aim of researches was qualified of values determining parameters essential to appoint was an aim of examinations of components of friction forces needed for moving needles from bodies of injector nozzles for different lubricating means and of all sorts of people of angles of turning the needle in the body of the injector nozzle with applying the numerical method, as well as getting of measurements of diameters leading parts the corps and the needle, what it will be possible to appoint medium ease of manner thanks to in three plains, and next to appoint its influence on value of power of rubbing for every of plains.

The tribological investigations of precise pairs should take the liberty of determining value of storage friction forces at the change of angles of needles in bodies of injector nozzles for all sorts of people of lubricating means.

5. The destinations of researches

They were an object of investigations withdrawn from operation the injector nozzles of combustion diesel engines (fig. 2). Choice of injector nozzles used to examinations was random. During the operation, the part from them was powered with residual fuel, and part with distillation fuel. These injector nozzles dated from bulk carriers of the fleet, but the part from the magazine of the shipowner.

Fig. 2. Body and needle of injector nozzle tacked in investigations

A position was the first research position for the measurement of the component of power frictions. Experiment consisted in the fact that one should check, what additional mass m_a the needle will come out from the body of the injector nozzle by [5].

On the inclined plane under angle 45° a put corpus stayed together with the pin of the injector nozzle, confirmed with the help of the fixing handle. Next, holding the bung of the needle they were checking, whether the needle would come out spontaneously, whether additional m_a mass is needed. When the injector needle didn't come out from the body of the injector nozzle, they used for burdening the weight, of which the handle was screwed with the help of the screw to the bung of needle, was put in the laboratory room of the Maritime Academy in Szczecin.

If was it is insufficient mass needed for moving the needle from the body of the injector nozzle, a string was being tied to the extender, to which a container was on an end. In order to increase mass waters were applied pouring into the container, all the way to beginning the moment and total moving the needle. Next they used scales, about different measuring scopes, in order to determine mass of injection needle and additional mass.

At very great additional masses needed for moving the needle from the body of the injector nozzle positions, were used for examinations of durability of samples to stretching.

6. Method of examinations

Measurement of the component of the friction force the position for the measurement of the storage friction force was compound of the inclined plane under the angle 45°, on which the fastened heap was for. With the help of the fixing handle of injector was put on it, directed with bung of the needle into the bottom. Before installing additionally substance was added to precise lubricating steam or they didn't add, of examinations depending on the kind carried out.

These examinations consisted on testing, whether the injector needle will come out alone from the corps under angle 45°, if this way it was, precise steam could farther be exploited, because, if the needle is coming out from the body of injector nozzle it means that he is fit for a further exploitation. Carrying out an experiment, the injector needle not always has come out under the own weight, then one should attach to the bung of the injector needle with the help especially of the made extender and the cord additional m_a mass.

In this experiment water which was gradually was additional mass titrate into the container fastened at the end of the cord, all the way to the moment, in which moving the needle from the corps followed. Next additional mass, by which the needle came out, was weighed on the scale. There were two used electronic scales depending on value of additional mass, from which one weighed with the accuracy to 1 g, and second with the accuracy till 0.001 g next after weighing additional mass, the needle was taken out of the body of the injector nozzle and weighed on the electronic scale with the accuracy till 0.0001 g.

In first experiment leading parts of injector needles were greased with vaseline-oil low setting about the following properties:

- cinematic viscosity in temperature 50°C – (6,3÷8,5) mm^2/s,
- temperature of setting – not higher than – 60 °C,
- flashpoint in the melting pot opened – not higher than 130°C,
- acid number – not higher than 0.05 mg.

White mineral oil is destined for laboratory tests on account of good properties in temperatures of surrounding the row + 20°C. Next leading parts of injector needles were greased with distillation fuel and Calibration Shell oil.

The first part of examinations focused on the relation of power of rubbing with T_{max} from greasing the kind. The second part of experiment ran similarly to first. At first injector nozzles were fixed on the heap with the presence of Calibration oil Shell after spraying, carried out investigations of using the stream of the flow to the assessment of spray holes 2 years earlier [6].

Next, when the injector needle came out, additional m_a mass was weighed, and then needle. The same injector nozzle was examined after for adding lubricating oil of needle leading parts and by analogy additional mass m_a and the needle were weighed.

The consecutive stage of examinations was aimed at checking the relation of maximum power of T_{max}, needed for moving the needle, from the angle of the turnover of the needle in the body of the injector nozzles and the time, needed for moving the needle. There were a needed stopwatch and a round made template in experiment around, which the angle scale was made of cardboard on (0÷360) °. In the initial phase of investigations the needle was turned in the body of the injector nozzle as 90°. Also a marked point of reference became the felt-tip pen on every bung of the needle.

This part of examinations was left connected with the second part of experiment, where the leading part of the needle was preserved after flow after flow investigations made is flying earlier with using Calibration Shell oil, and one make of oil at leading part of the injector needle with Calibration Shell oil. So every injector needle, in this part of examinations, was examined eight times, at the 0° angle, 90°, 180° and 270°. For each of given angles he was timed needed for moving the needle from the body of the injector nozzle. As this way as in previous experiment, additional m_a mass and the needle were weighed before and after for adding lubricating oil.

After examinations carried out stayed for the measurement of the component two injectors nozzles, in which were secured the precise pairs and in spite of trials even for hanging additional mass for value m_a = 68.137 kg, didn't manage to take needles out of bodies of injector nozzles. In order to disconnect seizured of precise steam was made a success to the position of the endurance machine, where needles were taken out of bodies of injector nozzles [5].

After installing injector nozzles in the tester gradual increasing power working on the needle followed which was put with bung of the needle vertically into the bottom. First from studied the injector needle came out at strength 1490 taking out of N (injector nozzle number 9). Second whereas, at 2200 N (injector nozzle number 43). After the outside examination of one of injector needles a distinct influence of the corrosion wear and tear was stated.

7. Research results

In experiment 46 chosen randomly injector nozzles which, were withdrawn from use, were examined. On the basis of collected results they calculated; with applying a computer program Microsoft the Excel, the maximum T_{max} friction force. Get value enabled to make the graph of maximum values of friction forces for next numbers of injector nozzles by all sorts of lubricating kinds. Fig. 8 is presenting powers needed for moving needles from bodies of injector nozzles to value.

Injector nozzles were investigated at first for lubricating from investigations made in 2 years ago, and then one make at precise pairs with Calibration Shell oil, what was every needle turned with regard to the bodies fourfold for angle 90°. Investigations were supposed to show, what value of the maximum friction force will be for lubricating from 2004 year and for spreading the from 2006 year by different locations on the needle with account of the body.

On the basis of get scores they stated, that after for adding lubricating oil of injector needle leading parts, additional mass wasn't needed for moving the needle from the body of the injector nozzle that is for adding lubricating oil reduced the surface maximum friction force.

On the attitude of collected put results graphs were made out. The 3 picture is showing value of maximum T_{max} friction forces for next numbers of injector nozzles, apart from numbers of nozzles 2, 9 and 43, by all sorts of kinds lubricating compound.

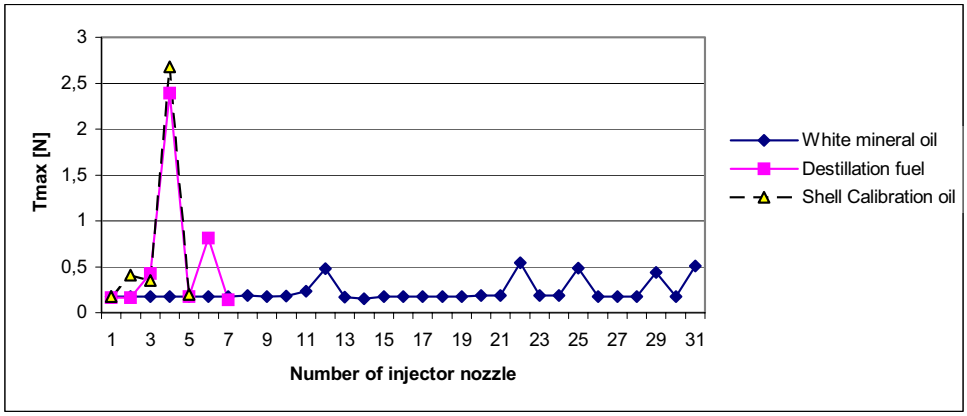

Fig. 3. The values of maximum forces of rubbing with T_{max} for next numbers of injector nozzles by all sorts o of lubricating kinds

How results from the presented fig. 3, the kind of greasing an essential influence on the maximum friction force has. For white mineral oil the maximum friction force is smallest in comparing to distillation fuel and for Calibration Shell oil, since white mineral oil is abiding for greasing devices cooperating in low temperatures. Of maximum value of strength of rubbing for distillation fuel and Calibration Shell oil are even five times bigger than for white mineral oil because of the lower viscosity in the 50°C temperature.

Next figures 4, 5 and 7 are showing the influence of "old" greasing and of adding oil of precise pairs to maximum power of rubbing for three injector nozzles.

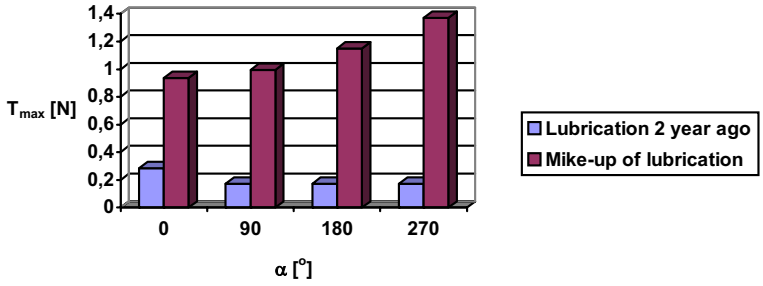

Fig. 4. The maximum values of friction power with T_{max} for the location of injector needle with account of the body of the nozzle α at spreading the from 2 year ago on precise steam and of adding oil in during investigations

He results from the presented picture 3, that "old" greasing causes increasing the maximum friction force, hence using precise steam up are increasing. After for adding oil the maximum friction force has much smaller values for the same precise steam. Examining the influence of the time of leaving the fuel or oil in the injector nozzle is pointing out to effects of leaving fuel or preservative to the technical state of precise steam.

The next 5 graph is showing maximum friction forces T_{max} from the time of coming out of needle from bodies of injector nozzles.

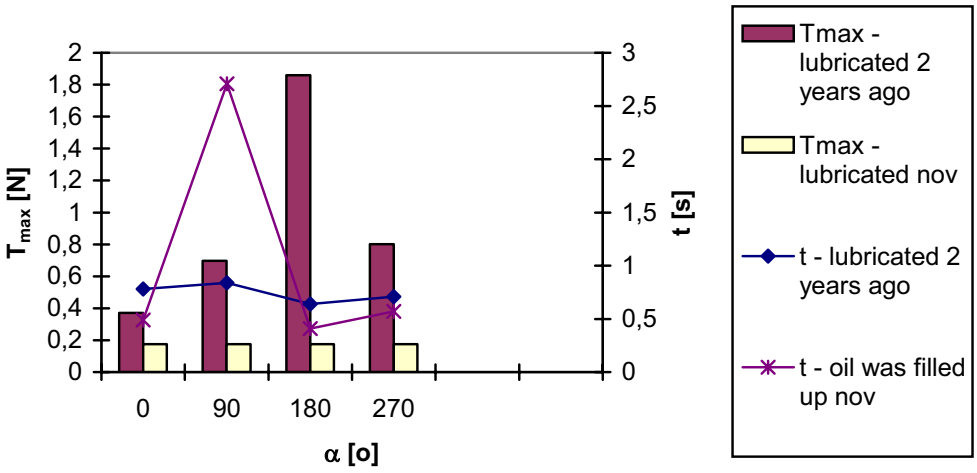

Fig. 5. The values of maximum friction power of with T_{max} for putting the needle with account of the body of the injector nozzle **α** *at spreading 2 year ago on precise steam and of adding oil in during investigations from considering times of moving needles*

Of relations on the base presented (fig. 5) it is possible to state, that time of coming out of needles from bodies of the injector nozzle largely by locations 0° and 180° is similar, as this way as for locations 90° and 270° what is providing about errors of shape of the injector needle.

The 6 picture is presenting maximum friction forces T_{max} to the relation from putting needles with account of corps for six examined injector nozzles with spreading on precise pairs with white mineral oil. The graph was made on the basis of data from the measurement table.

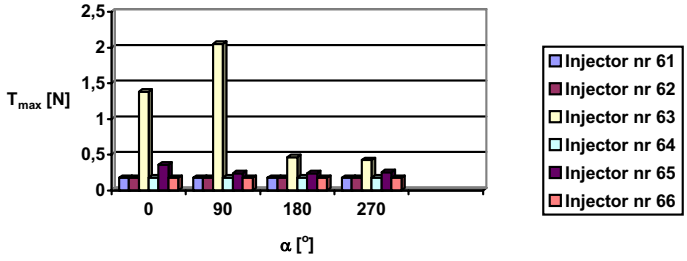

Fig. 6. Value of maximum friction power of rubbing with T_{max} from putting the needle with account of the body of the injector nozzle α

The 7 picture is presenting maximum values of T_{max} friction forces for the angle of the turnover to the needle at greasing with white mineral oil and make for the same injector nozzle. How he results from the fig. 7, new lubricated of precise steam that is increasing masses of the spread able middle, causes reducing the friction force.

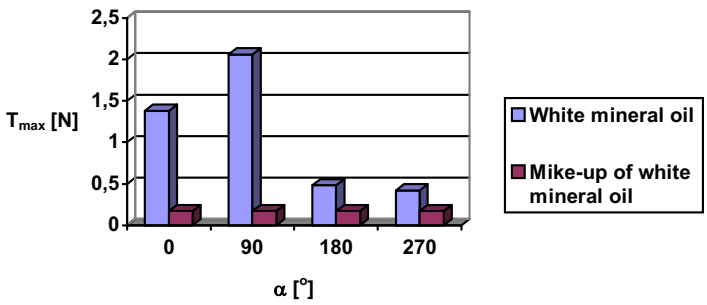

Fig. 7. The values of maximum friction power with T_{max} from putting the needle with account of the body of the injection nozzle

In the picture 8 a relation of times of moving needles from bodies of injector nozzles was presented. On the basis of the fig. 8 it is possible to state that the majority of times of coming out didn't cross needles more how for 5 s. Arranging it is biggest for the range of additional mass m_a from 0 up to 0.05 kg.

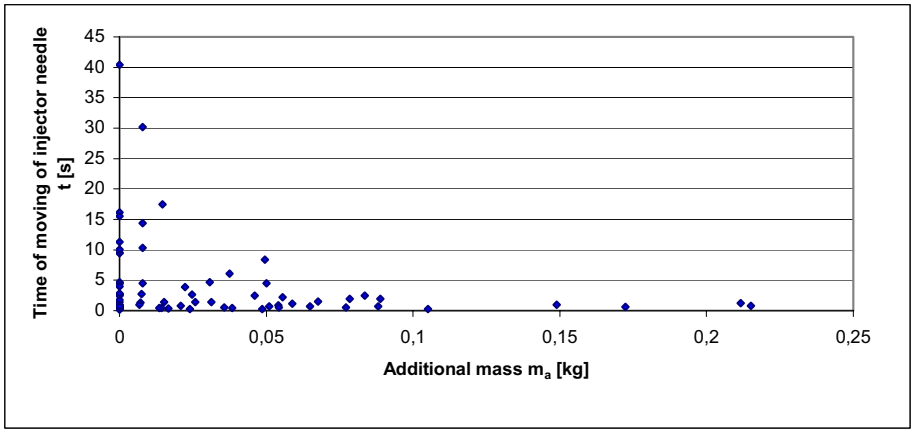

Fig. 8. Disintegration of times of coming out of inector needles t for different value of additional mass m_a

Picture 9 is showing the graph made out during the research on the course of maximum friction power on the stand for investigation of tensile strength for the injector number 43, where the position and the method of investigations were described at work [5].

On the course of the friction force at of moving the of the needle from the body of the injector nozzle at first the friction force is increasing gradually, and then a resistance, which is introduced in the picture, follows as dips and increases in the force of friction. Next moving into the right side of the picture a fall and an increase in power, by which the needle is left protruding from the body of the injector nozzle follow. Oscillations of the friction force are caused with uneven nesses of leading surfaces and randomly put pollutants.

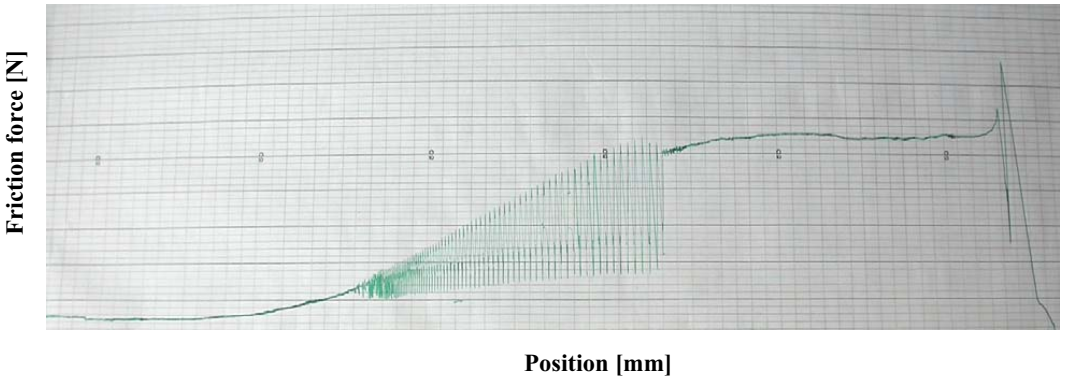

Fig. 9. Course of the friction force at of moving then needle from the body of the injector needle, made out on the machine for examining the resistance to stretching

7. Conclusions

The carried out tribological investigations of injector nozzles they allowed for checking dependences of the maximum friction force on greasing the lubricating kind, of angle of the turnover of the needle in the body of injector body and the time of coming out of needle from the body of the nozzle, as well as at the performance of geometrical measurements precise pairs of minimal and maximum diameter clearance by different angles of the turnover of the needle.

For carrying all measurements out needed using a few positions was, in addition carrying examinations out was time-consuming and it required the great accuracy. The repetitiveness of measurements was impossible on account of low ease of manner among the precise pair, as well as influence of mistakes of the shape of the needling injector nozzle and corps and being pollutants inside in lubricating.

Examinations showed that an essential influence on value of the friction force had the kind of greasing by different angles of the turnover of the injector needle. Amount of the lubricating oil influences for reducing the friction force [10]. Great value of the maximum friction force are informing about increasing using precise steam up. On the basis of turning the needle in the body of the injector nozzle uneven using up needles was stated.

On the basis of turning the needle in the body of the injector nozzle uneven using up cooperating precise couples was stated. Research findings concerning of research on friction forces in four plains they showed that the influence of the measuring plain was essential.

Get results of tribological research findings pointed to the usefulness of the research on the maximum friction force, at the assessment of the technical state of injector nozzles.

References

[1] Gąsowski W., *Wpływ zużycia na charakterystyki hydrauliczne i wzrost koksowania rozpylaczy silników wysokoprężnych.* Zagadnienia Eksploatacji Maszyn No. 3–4, pp. 527–537, Wrocław 1986.

[2] Gąsowski W., *Zawieszanie się iglic rozpylaczy silników wysokoprężnych.* Zagadnienia Eksploatacji Maszyn No. 2, pp. 245–250, Warszawa 1979.

[3] Hebda M., Wachal A., *Trybologia.* WNT, Warszawa 1980.

[4] Leszek W., *Metodologiczne podstawy badań trybologicznych.* PWN, Poznań 1981.

[5] Monieta J., *Badanie siły tarcia spoczynkowego w rozpylaczach wtryskiwaczy silników okrętowych z unieruchomionymi iglicami*. Zagadnienia Eksploatacji Maszyn No. 4, pp. 63–77, Radom 2007.
[6] Monieta J., Łukomski M., *Metody i środki oceny stanu technicznego rozpylaczy wtryskiwaczy silników okrętowych typu AL20/24.* Zeszyty Naukowe Akademii Morskiej, No. 5, pp. 383–391, Szczecin 2005.
[7] Monieta J., Wasilewski M., *Wykorzystanie strumienia przepływu do oceny zużycia otworków rozpylaczy silników okrętowych.* Tribologia No. 5, pp. 947–959, Radom 2001.
[8] Monieta J., Wójcikowski P.: *Badanie osadów koksowych rozpylaczy wtryskiwaczy silników okrętowych.* PTNSS Kongres 2005, s.86; CD pp. 1–6, Szczyrk 2005.
[9] PN–91/M–04301. Tribologia. Terminologia podstawowa. Wyd. Normalizacyjne „Alfa".
[10] Szczerek. M., Wiśniewski M.: *Tribologia i tribotechnika*, Wyd. PTT, ITE i SITMP, Radom 2000.

Journal of POLISH CIMAC

Faculty of Ocean Engineering & Ship Technology
GDAŃSK UNIVERSITY OF TECHNOLOGY

NON-THERMAL PLASMA REACTOR WORKING WITH EXHAUST GAS SYSTEM IN MARINE DIESEL ENGINE

Jarosław Myśków, Tadeusz Borkowski

Maritime University
Wały Chrobrego Street ½, 70-500 Szczecin, Poland
tel: +48 91 4809400, fax: 48 91 4809575
e-mail: jmyskow@am.szczecin.pl, tborkowski@am.szczecin.pl

Stanisław Kalisiak, Marcin Hołub

Technical University
Sikorskiego Street 37, 70-313 Szczecin, Poland
tel.: +48 91 4494129, fax: +48 91 4494561
e-mail: kal@ps.pl, mholub@ps.pl

Abstract

Recently, we HAVE BEEN faced with the regulation of NO_x from combustion exhaust gases, because it have caused smog, acid rain, and some diseases. The largest pollution sources in the world belongs to big seagoing vessels. The vessels are responsible for an estimated 14% of emission of nitrogen from fossil fuels and 16% of the emissions of sulfur from petroleum uses into the atmosphere. The Protocol adopted in 1997 includes the new Annex VI of Marpol 73/78, which entered into force on 19 May 2005. Nitrogen oxide emissions from ships were put at around 5 million tons per year – about 7% of total global emissions. This paper describes the experimental method – using non-thermal plasma reactor to clean exhaust gases. NTP reactor was built as the aftertreatment module in exhaust gas system in marine diesel engine. The main aim is to analyze exhaust gas compounds during steady load of engine, before and after NTP module.

Keywords: *marine diesel engine, exhaust emission gas treatment, non-thermal plasma reactor.*

1. Introduction

Maritime transport plays a significant role while considering transfer of materials and products. Intensified ship traffic near shoreline areas causes considerable changes to ecosystems. It is assumed that maritime economy uses about 3% of worldwide amount of produced fuels, which in most of the cases are of inferior quality, with higher contents of sulphur. As a result of the combustion process of this type of fuel, the following amounts of overall air pollution are released to the atmosphere: about 7% of with sulfur oxides and 11÷13% of nitrogen oxides. A proposal of International Maritime Organisation rules, concerning limiting of NO_x emission to the atmosphere, within "Prevention Of Air Pollution From Ships" program, aims at constraining nitrogen oxides emission by 30% comparing to 1990 levels.

In September 1997 Appendix VI was accepted at the MARPOL Convention 73/78, which incorporates regulations such as rules concerning emission of nitrogen oxides, sulfur oxides and Volatile Organic Compounds:

- Regulation 13 determines the maximum level of nitrogen oxides in exhaust gases produced by ship engines of power above 130kW, depending on engine speed;
- Regulation 14 concerns restrictions of sulfur oxides SO_x emission. The accepted content of sulfur in fuel was established at 1,5% for closed sea areas, such as the Baltic. In case of using on such areas a type of fuel exceeding this norm, a ship should be equipped then with a specialist installation limiting of SO_x emission to the level of 6g/kWh.
- Regulation 15 is related to Volatile Organic Compounds in tanker loading bases.

Exhaust gases emission sources in sea-going vessels are devices installed on board. Among them, there are mainly diesel ship engines of main propulsion, auxiliary engines, gas turbines, incinerators and main and auxiliary boilers. As a result of fossil fuels combustion, toxic compounds are released to atmosphere, such as carbon dioxide CO_2, carbon monoxide CO, sulfur oxides SO_x, nitrogen oxides NO_x, hydrocarbon HC and particulate matter PM.

Exhaust gases include particles originating from:
- incompletely combusted fuel,
- fuel ashes,
- residual materials from combustion chamber and exhaust duct.

Incompletely combusted particles of fuel delivered to combustion chamber sediment as residual materials inside the combustion chamber and in exhaust ducts. The majority of them is conveyed to atmosphere with exhaust gases. Hydrocarbon chains of some fuel particles are disintegrated in high temperatures, releasing hydrogen but not being oxidized. The rest of the matter left after hydrocarbon disintegration forms soot, mainly composed of carbon. The amounts of particulate matters are diverse, depending on the contents and properties of fuel (ash content, Condradson number).

2. Non-thermal plasma reactor

Nowadays, continuous research is being conducted on limiting the emission of harmful substances released to atmosphere. There are numerous methods of emission suppression. They can be divided into three groups:
- methods connected with preliminary fuel treatment,
- methods leading to construction changes of combustion chamber, ways of fuel injection, etc.
- methods connected with exhaust gases treatment.

Non-thermal plasma is currently a promising field of research when considering its application in exhaust gases purification process [3, 5]. In the described experiment, a reactor with cylindrical electrodes with barrier discharge is used – DBD. The advantage of the barrier discharge is a low relation between discharge parameters and chemical compound of gases. The disadvantage is a small distance between electrodes (a few mm) and therefore - small capacity of reactor. An electrode of high voltage is a plate made of stainless steel, and a low voltage electrode – a rod, made also of stainless steel. A barrier is a quartz glass pipe. Exhaust gases flow inside and outside the pipe, through the area of discharge between electrodes. A single element of the reactor is presented on Fig 1.

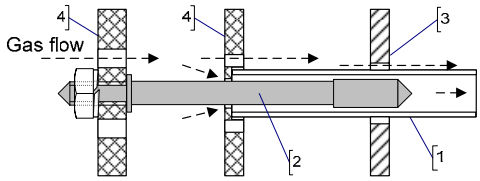

FIG.1 Basic element of non-thermal plasma reactor: 1 – quartz glass tube; 2 – rod – low voltage electrode; 3,4 – plate – high voltage electrode; arrows – gas stream direction.

The phenomenon of discharge occurs when the voltage through the plate exceeds the insulating effect of the quartz tube. The duration of these discharges is measured in nano-seconds. In a DBD field, the oxygen molecules split into two atoms of oxygen O^+ and O^+. The elemental oxygen radical, being very reactive, will form ozone - O_3. Oxygen radicals react with carbon monoxide – CO – to form carbon dioxide - CO_2, sulfur dioxide - SO_2 – and nitrogen oxide - NO_x – to form nitric acid - HNO_3 in the presence of moisture. Particulate matters – PM – could be reburned in discharge zone of DBD reactor [1, 2, 4], according to following reaction:

- soluble organic fraction - SOF:

$$SOF + NO \rightarrow NO_2 + (\text{neutral products}) \quad (1)$$

- particulate matters - PM:

$$C_x + OH \rightarrow C_{x-1} + CO + 1/2H_2 \quad (2)$$
$$C_x + 2OH \rightarrow C_{x-1} + CO_2 + H_2 \quad (3)$$
$$C_x + O \rightarrow C_{x-1} + CO \quad (4)$$
$$C_x + 2O \rightarrow C_{x-1} + CO_2 \quad (5)$$
$$C_x + 2NO_2 \rightarrow C_{x-1} + CO_2 + 2NO \quad (6)$$
$$C_x + NO_2 \rightarrow C_{x-1} + CO + NO \quad (7)$$

Due to the reason mentioned above – predicted chemical reactions, the reduction of particulate matters was expected after leaving the discharge zone of DBD reactor.

3. Test bed and apparatus set up.

In the described experiment, the exhaust gas from marine engine was measured. Engine specification data is shown below:

type	Sulzer 6AL20/24, 4 – stroke, turbocharged;
nominal power	P_{nom}=324 kW,
nominal revolution	n_{nom}=720 rev/min,
specific fuel consumption	b=218,3 g/kWh,
cylinder diameter	200 mm,
piston bore	240 mm.

NTP module was built on a by-pass system – a part of a real exhaust system from marine diesel engine. DBD plasma reactor could work as:

- gas by-pass system,
- ozone doze to exhaust gas,
- hybrid equipment with catalyst module.

Emission measurements were carried out on an engine at steady-state operation. Sampling gas was distributed to all analyzers. The performance measurement procedure of marine engines on test beds was performed in accordance with Annex VI of Marpol 73/78 convention - with the specification given in the IMO NO_x Technical Code and ISO-8178 standard. All tests were covered by test-cycles procedure D-2 and E-2. The test performed with the selected marine distillate fuel DMX in accordance with ISO-8217 standard. All engine performances were carried out continuously and simultaneously together with exhaust gas components concentration recorded by means of measurement assemble:

- AVL-Pierburg CEB II Combustion Emission Bench (NO_x, CO_2, CO, O_2, THC),
- MIR FT – Fourier Transform Infrared spectroscopy multigaz analyzer (NO, NO_2, N_2O, NH_3, CH_4, C_2H_4, C_2H_6, C_3H_6, C_7H_8, H_2O, SO_2, CO, CO_2, O_2),
- HORIBA MEXA-1230PM – (PM – particulate matter, SOF – soluble organic fraction and SOOT).
- Ambient pressure, temperature and humidity,
- Monitoring and acquisition data from marine engine by Kongsberg DCC system.

4. Experiment results.

The engine test was provided in two stages: idle and part engine load (25% of the of nominal). On each measurement stage, the engine was in steady state of operation and all parameters were examined without NTP plasma operation (plasma off) and with NTP plasma operation (plasma on). As the first step of experiment, attention was focused on non-thermal plasma reactor influence on PM-particulate matters, SOF-soluble organic fraction and soot.

Figures 2, 3 and 4 show changes of above components during engine work (all ranges), and figures 6, 7 and 8 only in idle and 25% load. Figure 5 shows the effect of unstable charge air temperature transferred on PM concentration resulting from NTP reactor operation. Electric power delivered to reactor was 200W and was kept on the same level during the test. Electrical system was working in automatic mode.

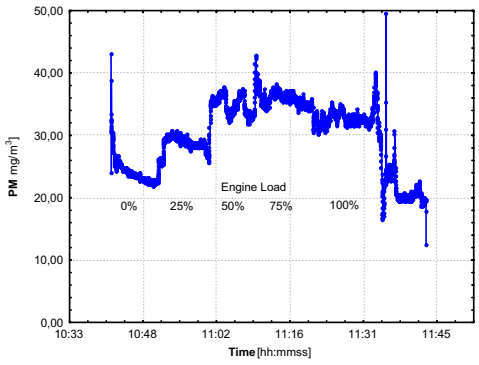

Fig.2 PM concentration during test under variable engine load, without NTP reactor operation.

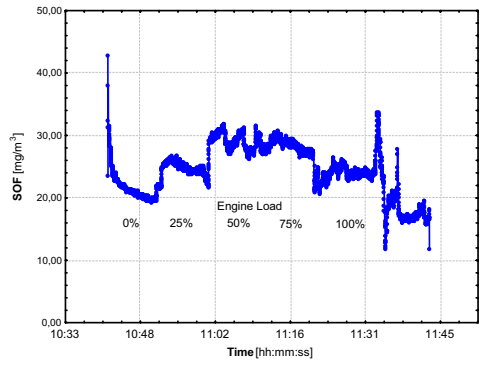

Fig.4 SOF concentration during test under variable engine load, without NTP reactor operation.

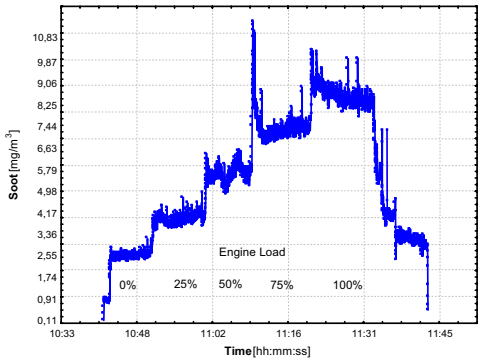

Fig.3 Soot concentration during test under variable engine load, without NTP reactor operation

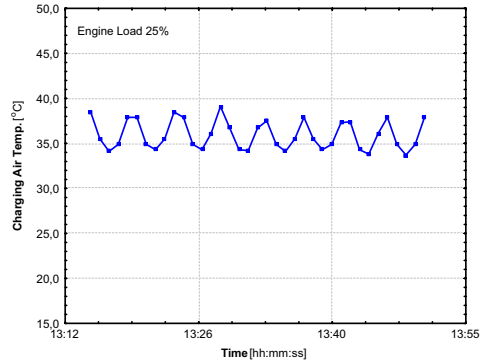

Fig.5 Air temperature at 25% engine load.

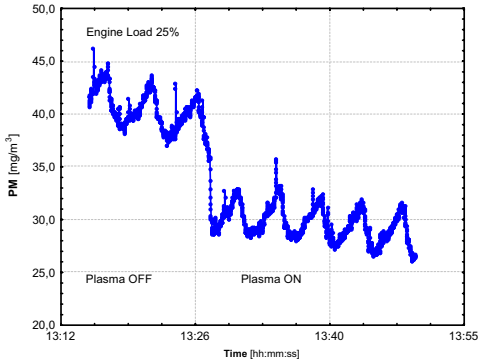

Fig.6 Changing PM parameters during test at 25% of engine load.

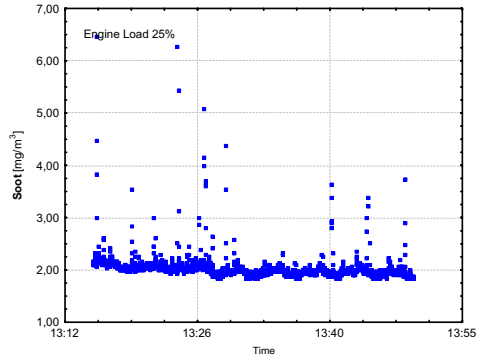

Fig.8 Changing Soot parameters during test at 25% of engine load.

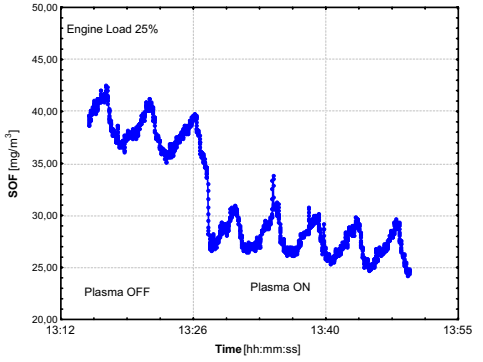

Fig.7 Changing SOF parameters during test at 25% of engine load.

5. Conclusions and observations.

During test at 25% of engine load, the reduction of PM concentration was recorded at 28% with working DBD plasma reactor. The increase in PM efficiency removal was associated with the main PM component – SOF. The other PM constituent – soot reduction degree was much slower and weaker. The increased coefficient rate of PM oxidation resulting from exhaust gas temperature increase has additional influence on CO concentration rise. The CO concentration rise was noticed in both engine loads. Some fluctuations of PM concentration were recorded - to establish the reason, the engine operational parameters were investigated. It has been found that there is strong influence of temperature of charging air on simultaneous PM concentration changes. The charge air temperature is controlled by means of external water cooling system with thermostatic valve with single value set-point.

Experimental study involving a NTP reactor operation with a realistic exhaust gas of marine engine was performed. Technical condition of the reactor after experimental trials (approximately 150 running hours) was excellent. As the next step it is proposed a two-stage plasma-chemical process for the control of harmful compounds: non-thermal plasma reactor and catalyst. This combination should be more effective and probably give the reduction with more efficiency of harmful exhaust gas compounds.

6. References

[1] Dan Y., Dengshan G., Gang Y., Xianglin S., Fan G. *An investigation of the treatment of particulate matter from engine exhaust using non-thermal plasma.* Journal of Hazardous Materials B127, 2005 p. 149-155.

[2] Du Ch. M., Yan J. H., Cheron B. G. *Simultaneous removal of polycyclic aromatic hydrocarbons and soot particles from flue gas by gliding arc discharge treatment.* Plasma chem. Process 2006 page 517÷525.

[3] Hughes D. E., McAdams R., *Non-thermal plasma for marine diesel*, International Council on Combustion Engines CIMAC Congress 2004, 7-11 June, Kyoto (Japan) 2004, Paper No. 231, p. 15.

[4] Singh G. *Additional combustion and emission control Project, heavy truck engine progra and performance measures for the engines team.* OHVT Annual Review, 12.04.2000

[5] Penetrante B., Schultheis S. E., *Non-Thermal Plasma Techniques for Pollution Control: Part B - Electron Beam and Electrical Discharge Processing*, Springer-Verlag, Berlin Heidelberg New York, 1993.

Journal of POLISH CIMAC
Faculty of Ocean Engineering & Ship Technology
GDAŃSK UNIVERSITY OF TECHNOLOGY

STOCHASTIC MODELS OF EMISSION OF TOXIC COMPOUNDS IN MARINE ENGINES EXHAUSTS

Leszek Piaseczny
Tomasz Kniaziewicz

The Polish Naval Academy
Ul. Śmidowicza 69, 81-103 Gdynia, Poland
Tel.: +48 58 626 23 82

Jerzy Merkisz

Poznań University of Technology
3, Piotrowo St., 60-965 Poznań

Abstract

Development of marine transport and projected increase of emission of toxic compounds formed when combusting marine fuels enforces, apart from the emission research, the need of modelling those pollutants dispersion their immission in coastal regions of city agglomerations. The area of Gdansk Bay, just like sea ports or coastal regions, is vulnerable to the effect of pollutants present in exhaust gases coming from industrial plants, power plants, vehicles and vessels. The last source of pollution concerns the vessels both in port areas and in the roads.

In order to determine the share of vessels in environmental pollution and counteract the harmful effects of toxic compounds in marine engine exhaust gases, it is necessary to know the emission values of these compounds from particular vessels. This is possible with the knowledge of their movement parameters, concentration values of particular compounds for these parameters and the atmospheric conditions.

The first step towards formulating the emission models of toxic compounds in marine engines exhaust gases is determination of mathematical models of vessels movement, which can be later used when formulating dispersion and immission models of those pollutants.

In the paper there were presented conditions concerning modelling the emission of toxic compounds in vessels exhausts as well as the possibilities of using the queuing theory and Monte Carlo methods in order to formulate simulated model of vessels movement in a given area.

1. Introduction

Emission E and intensity (mainly mass) of pollutants dispersed in atmospheric air – immission I, in the urban areas are the subject of intensive research conducted in many research institutions in Poland and abroad. The relation between emission of toxic compounds in exhausts and their immission can be written down as follows [1]:

$$I(t) = \aleph[E(t)], \tag{1}$$

where $\aleph$ means a mathematical operator (e.g. functional).

The intensity of emission E being a function of time $m_t(t)$ from a particular source in relation to time t:

$$E(t) = \frac{dm_t(t)}{dt}, \tag{2}$$

where m_t – mass of a given toxic compound.

Road emission is defined [1] as emission derivative, being a function of the road $m_s(s)$ from a source, which is the vessel, in relation to road s covered by her

$$b_s = \frac{dm_s(s)}{ds} \tag{3}$$

On the basis of equation (3) it can be written down that emission on road S will be equal to

$$m_s(S) = \int_0^S b_s(s)ds \tag{4}$$

and in time T

$$m_t(T) = \int_0^T b_t(t)v(t)dt\,, \tag{5}$$

where v(t) – vessel speed.

Road emission [2] can be written down as the functional of value courses describing the combustion engine work state i.e. of torque M_o, rotational speed n and the vectors describing the thermal state of the engine **R**(t), conditions of the surroundings **G**(t) (e.g. temperature of surrounding, pressure, air humidity) and the changing vessel resistances **O**(t) (vessel resistance in shallow waters, vessel resistance during movement in a canal, air resistance and wave effect):

$$b_t = \wp[\, M_o(t), n(t), \mathbf{R}(t), \mathbf{G}(t), \mathbf{O}(t)] \tag{6}$$

where $\wp$ - operator transforming torque, rotational speed and the vectors of the engine's thermal state, movement resistance and conditions of the surroundings into average road emission from a vessel.

The current research, concerning atmosphere pollution caused by emission of harmful compounds from traction engines, mainly concern vehicle engines [1,3,4,5,6] and aircraft engines [7]. They constitute a very large input into the development of modelling the immission of toxic compounds emitted from combustion engines, however, because of both different topographic, hydrometeorologic conditions and the specificity of vessel operation, they cannot be applied for immission estimation in coastal regions.

2. Factors determining exhausts emission

The subject of balancing the emission of the compounds in exhausts of vehicles and vessels engines, are the processes of global emission, averaged in sufficiently long period of time [2,8]. This time is determined first of all by the effectiveness of averaging variable conditions of the objects operation.

Main factors determining the global emission of substances present in the exhausts of marine engines can be classified as follows:

- vessel structure (with respect to their size and destination), engine size and kind, number of particular engine kinds on the vessel (main and auxiliary engines), and with respect to the vessel's technical condition, taking into consideration technical solutions, state of the hull and the wear of propulsion system elements as well as their number,
- vessel operational intensity,
- vessel movement model,

- conditions of the surroundings: atmospheric conditions (waving, strong winds, icing), navigational water areas (ports, straits, canals and other dangerous and difficult to navigate areas, open waters), sailing in ice,
- vessel economic properties with respect to operational fuel consumption,
- ecologic properties of engines applied on vessels,
- fuel properties (*inter alia,* with respect to fuel kind, composition and content of pollutants).

3. Determination of a vessel trajectory

In order to describe the trajectory of a vessel moving in a given shipping lane from point P_{i-1} to point P_i in time interval (t_0, t_k], it is necessary to formulate a suitable mathematical model. There should be taken into account two options: a deterministic model and a stochastic one. Both models must consist of a track function describing the track of the individual vessels and a probability law on the total number of vessels en route during (t_0, t_k], the position of those vessels at the initial time t_0, as well as their speed. It is necessary to assume that the times at which the ships depart each point P_{i-1} are Poisson distributed and the ship speeds and the routes the ships travel are statistically independent.

Description of a ship trajectory is possible if we formulate the function of the track the ship covers, function of the ship movement and function of the ship trajectory described by the first two functions.

The function of the track of a vessel describes a set of all possible roads from point P_{i-1} to point P_i, where the point P_{i-1} means the beginning of the journey, e.g. the departure port, and point P_i - the end of the journey, e.g. the port of destination. The bigger area is taken into account, the more pairs of points (P_{i-1}, P_i) must be considered. All possible routes between any two points are the function of distance x, measured from point P_{i-1} along the route that the vessel covers.

Vessels generally move along the shipping lanes, which means the areas of a given length and width [8,9]. Knowledge of the shipping lanes in a given area causes that for the majority of vessels, such as merchant vessels or passenger ferries travelling between ports, it can be assumed that the distance covered by them is along a known trajectory. However, there exist a group of ships, e.g. fishing vessels or recreational vessels or naval vessels, which can operate beyond shipping lanes. For these categories of vessels it can be necessary to formulate a more complicated model of ship trajectory.

Assume Δ_N is an ordered set of points $t_i, i \in \overline{1,N}$ dividing the interval $[\alpha,\beta]$ on N subintervals, where $\alpha = t_0 < ... < t_N = \beta$. To this division [9] corresponds a set $N+1$ points $P_0, P_1, ..., P_N$ on arc. These points form a broken line, which approximates the route of a vessel. The length of the segment joining points $P_{i-1}, P_i, \quad i = 1,...,N$ can be expressed by a formula:

$$| P_{i-1}P_i | = \sqrt{[x(t_i) - x(t_{i-1})]^2 + [y(t_i) - y(t_{i-1})]^2} \tag{7}$$

Applying the Lagrange's theorem about average value, the investigated length of the segment joining points $P_{i-1}, P_i, \quad i = 1,...,N$ is:

$$| P_{i-1}P_i | = \sqrt{[x'(\theta_i)]^2 + [y'(\vartheta_i)]^2}\,\Delta t_i, \tag{8}$$

where θ_i , ϑ_i are the points from interval $[t_{i-1}, t_i)$, and $\Delta t_i = t_i - t_{i-1}$.

The knowledge of ship trajectories and statistical data obtained via AIS (*Automatic Identification System*) [11,12] for marine vessels passing through given test segments situated perpendicularly to shipping lanes approaching the ports of Gdynia and Gdansk, as well as the shipping lane splitting into those two shipping lanes (in the proximity of Hel port), it is possible to describe the marine vessels flow (fig.1) [9] and then to formulate models of emission of toxic compounds in these vessels exhausts.

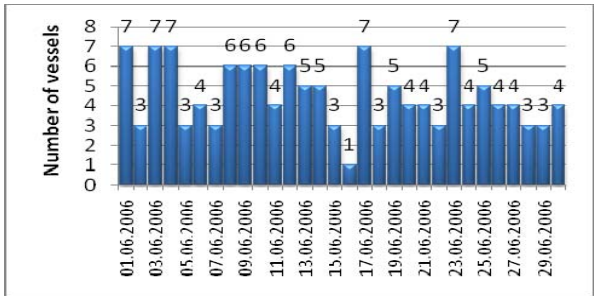

Fig. 1. A twenty-four hours distribution of the number of vessels outward bound passing through the 'gate' GD (01-30.06.2006) [9]

4. Models applying the queuing theory

In modelling the movement of ships going along the shipping lane from point P_{i-1} to point P_i, it is possible to apply the queuing theory, which is based on the characteristics of the stream of incoming vessels ('incoming traffic') to the analysed area ('service canal') and the stream of vessels leaving the 'canal' [9]. For the vessels that entered the 'canal' (the shipping lane', service time means the time of the vessels journey in the analysed route.

If the moment of entering the first vessel to the system (moment of arrival at the queue) in the analysed time interval, e.g. a day, is the initial time t_0=0, then it seems to be extremely difficult or even impossible to predict the exact time of the next arrival (entering next vessels on the shipping lane), and also times of all following arrivals (the same day and the next days). The moments of all the following arrivals will not overlap. Therefore, both the moments of each incoming arrival, and the number of arrivals during a day, week, etc. are the random variables.

The process of incoming arrivals is stochastic process, and the incoming traffic can be described by a function *X(t),* describing the number of arrivals requiring 'servicing' at the time interval *(0, t)*. The function *X(t)* is the random variable for each value of *t* [10]. In the figure 2 there is presented one of the realisations of the random function *X(t)* characterising the process of traffic incoming to the 'gate' GD in a given time period (48 hours) [9].

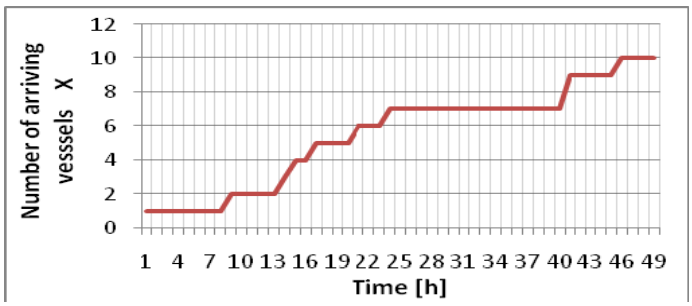

Fig. 2. Realisation of a random function *X(t)* of vessels arriving at the 'gate' GD [9]

In order to determine fully the `incoming traffic`, it is sufficient to know the probability of that in time $(0, t_1)$ there will come k_1 arrivals, in time $(0, t_2)$ there will come k_2 arrivals etc. If this probability is known for any group of positive integral numbers k_1, k_2,.., k_n and positive t_1, t_2,…, t_n, then the incoming traffic will be fully described.

A significant attribute of many real incoming traffic is their stationary character, which significantly simplifies the formulated model. The analysed incoming traffic of the vessels arriving to the shipping lane is also stationary. Moreover, this incoming traffic possesses also the character of the *traffic without sequence* or the *traffic of independent increm*ents (cumulative distribution function of a group $X(t_i+a)-X(a)$, where $(i = 0, 1, 2, ..., n)$ at $t_i > 0$ and any $a > 0$ does not depend on the value of $X(t)$ at $t < a$).

Apart from determining the probability of the number of arrivals to the shipping lane, it is also important to determine the time of their journey, which in the light of the queuing theory can be considered as *service time.* Of course, the time of their service is different for different vessels and depends on many factors: first of all, their speed, but also on random disturbances, such as conditions of the surrounding conditions, which means the atmospheric conditions (wind power and direction, state of the sea, sea currents, atmospheric pressure, air temperature), and the areas of the vessels operation (open sea, ports, straits, etc.), as well as the conditions referring to a particular vessel (hull resistances, technical state, nautical possibilities etc.).

Taking into account the above, in the analysed case for the vessels, the service time is the random variable, so it can be described by the cumulative distribution function: $F(t) = P\{\gamma < t\}$ for $t \geq 0$, where γ is the service time. The function $F(t)$ describes the probability of that the service time γ will be shorter than previously determined t. (Function $F(t)$ should be a positive function monotonically increasing and should not be greater than one).

5. Models applying Monte Carlo methods

In practice there are situations where incoming traffic does not possess the characteristic of prime traffic or is not stationary and non-homogeneous, there can be any distribution of service time, or organisation in service time is complex and consists of many stages. Problems of this kind are very difficult or impossible to solve with the analytic methods.

Simulation models of Monte Carlo methods permit to solve these problems. Simulations of the vessels 'service' [9], which means the traffic of vessels arriving at the analysed shipping lane, the time spent on the lane, can be performed with the assumption (previously preceded with the identification research) that the incoming traffic is a homogeneous Poisson process of parameter λ, and time spent on the lane is of normal distribution. In simulation performed with so-called *method of uniform step of a stationary*

system 'without waiting', the incoming traffic is simulated in an assumed period of *M* days, e.g. with the step of 24 hours. Probability of occurrence of *l*-arrivals in each time interval of 24 hours can be calculated from the following formula:

$$P(l) = \frac{\lambda^l}{l!}\exp(-\lambda) \qquad for\ l = 0,1,2,3,...,D\,. \tag{9}$$

For the calculated values of probabilities there can be assigned e.g. 10 000 pseudorandom numbers of steady distribution, which results from the accuracy of computation. If λ = 6 vessels/24 h, the probability of that an arrival will not occur during that time (l = 0) is equal to 0.0025 and to that probability there are assigned the 25 consecutive numbers, as it is presented in the fig. 3 (λ_{p1} = 0.0025).

For simulation of the process of the arrivals 'servicing', there can be analysed the distribution of speeds of vessels moving along the analysed shipping lane or distribution of time spent on that shipping lane. It is also possible to simulate the number of vessels leaving the shipping lane in the analysed period of time.

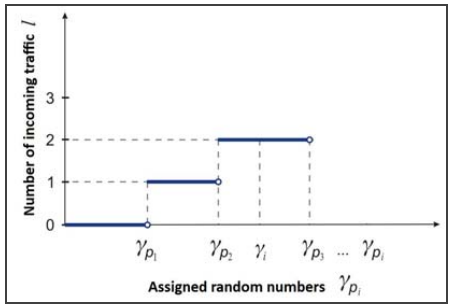

Fig. 3. An example of the simulation of the number of incoming traffic to the system [9]

The capacity of the 'service canal', expressed by the number of vessels leaving the shipping lane at *i*-unit of time, can be calculated from the formula:

$$W_i = \alpha_i \cdot \sigma + a\,, \tag{10}$$

where:

α_i – sampled random number of normal distribution *N(0,1),*

σ – standard deviation of the number of vessels leaving the shipping lane,

a – average value of the number of vessels leaving the shipping lane (being serviced by the 'canal') at a time unit.

If the average number of vessels 'serviced' in a unit of time is μ, then 1/μ means the average time of 'servicing'. And if the length of the 'canal' is known, then it is possible to determine the average speed of vessels operating in the analysed shipping lane.

In the *method of consecutive occurrences*, time of each consecutive arrival to the 'canal' and its time of 'servicing' in that 'canal' are simulated. Consecutive values of time τ_i intervals between arrivals can be computed by generating the random numbers of steady distribution. The following relation is used:

$$\int_0^{\tau} \lambda \exp(-\lambda t)dt = \xi\,, \tag{11}$$

from which it results that:

$$\tau = -\frac{1}{\lambda}\ln(1-\xi)\,. \tag{12}$$

As the distribution of value *1-*ξ is the same as the value ξ, it can be written down that:

$$\tau = -\frac{1}{\lambda}\ln\xi\,. \tag{13}$$

The formula (13) is directly helpful when computing values of τ_i, at different values of sampled random numbers ξ_i.

Time of 'service' of each arrival is simulated by sampling separately the consecutive random numbers α_j of normal distribution $N(0,1)$ and computing simulated time spent by j^{th} arrival (j^{th} vessel) in the area (on the shipping lane) with the formula:

$$t_j = \sigma \cdot \alpha_j + t_o^{śr}\,, \tag{14}$$

where:

σ – standard deviation of the time spent by a vessel on the shipping lane,

$t_o^{śr}$ – average value of time spent by vessels in the area,

$j = 1,2,3,...,m$ – a consecutive random number of 'servicing' the j^{th} arrival,

Course of computation starts at the moment of occurrence the first arrival (arriving a vessel to the entry to the shipping lane). Time spent on the shipping lane is calculated from the formula (14).

6. Modelling emission of toxic compounds in marine vessels exhausts

To determine the toxic compounds emission in exhausts on the basis of data obtained via AIS, there were formulated some statistical models describing the momentary power $\boldsymbol{P_e}$* for the momentary speed $\boldsymbol{v}$*, regarding the vessel size, its time spent in the area of research, and emission of toxic compounds. These values permit to estimate the emission intensity $\boldsymbol{E}_{NOx}$ at that point at the level of (0,6 – 576) kg/h [13].

However, it should be noticed that the time a vessel spends in a region of a "gate" is only a few minutes, and the absolute time a vessel requires for covering the distance Hel – Gdynia, depending on the vessels speed, accounts for 20-144 minutes.

Thus, determining the value of emission intensity $\boldsymbol{E}_{NOx}$ in kilograms per nautical mile [kg/Mm] (fig.4) or in grams per nautical mile during one hour [g/(Mm·h)] (fig. 5), seems to be more expedient in this case (fig.3).

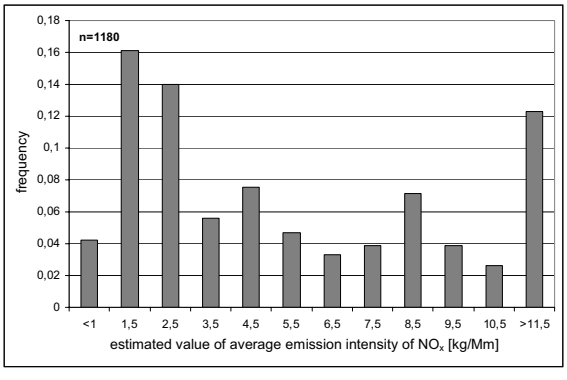

Fig.4. Distribution of estimated value of average emission intensity $\boldsymbol{E}_{NOx}$ [kg/Mm] for vessels operating in the approach area of Hel – Gdynia

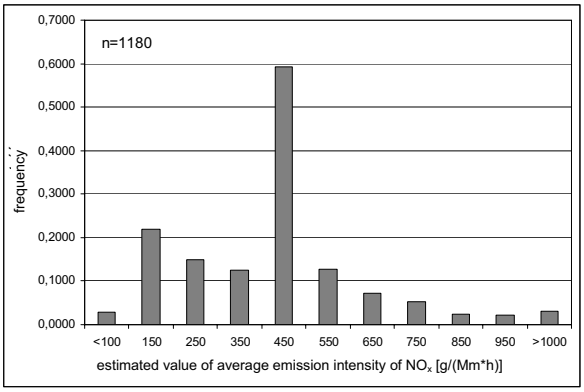

Fig.5. Distribution of estimated value of average emission intensity $\boldsymbol{E}_{NOx}$ [g/(Mm·h)] for vessels operating in the approach area of Hel – Gdynia

7. Conclusion

Modelling emission, and then dispersion and imission of toxic compounds in marine engines exhausts constitutes a very important and very complex issue. Currently conducted research devoted to the pollutants dispersion, refer mainly to motorization, which because of, among other things, the size of marine engines, disqualifies them in modelling emission of toxic compounds from marine engines, as the model structure depends not only on its destination, but also on the quantity and quality of input data.

Additionally, apart from the problems appearing when modelling the toxic compounds emission from road vehicles, in case of marine vessels, among the parameters disturbing the appropriate determination of particular compounds emission (due to the lack of data or its changeability) are also technical state of engine, and especially of fuel apparatus, as well as atmospheric conditions (mainly wind power and direction).

References

[1] Chłopek Z.: *Modelowanie procesów emisji spalin w warunkach eksploatacji trakcyjnych silników spalinowych.* ZN Politechniki Warszawskiej, Mechanika, z.173, Warszawa 1999.

[2] Kniaziewicz T.: *Problemy modelowania imisji szkodliwych składników spalin z silników okrętowych w rejonach miejskich aglomeracji nadmorskich.* Zeszyty Naukowe Politechniki Częstochowskiej 162, MECHANIKA 26, Częstochowa 2006.

[3] Brzozowska L., Brzozowski K.*: Komputerowe modelowanie emisji i rozprzestrzeniania się zanieczyszczeń samochodowych.* Wydawnictwo Naukowe „Śląsk" *,* Katowice 2003.

[4] Brzozowska L., Brzozowski K., Wojciech S.*: Computational Modeling of Car Pollutant Dispersion.* Wydawnictwo Naukowe „Śląsk" , Katowice 2001.

[5] Drąg Ł.*: Modelowanie emisji i rozprzestrzeniania się zanieczyszczeń ze środków transportu drogowego.* Archiwum Motoryzacji nr 1/2007.

[6] Joumard R.*: Methods of estimation of atmospheric emission from transport.* European scientific state of the art, Action COST319 final report, LTE 9901 report, 1999.

[7] Kotlarz W.: *Turbinowe zespoły napędowe źródłem skażeń powietrza na lotniskach wojskowych.* Wyższa Szkoła Oficerska Sił Powietrznych, Katedra Płatowca i Silnika*,* Dęblin 2003.

[8] Kniaziewicz T., Piaseczny L.: *Model of NO_x emission by sea-going vessels navigating in the gulf of Gdańsk region.* Silniki Spalinowe PTNSS – 2007-SC3. Poznań. 2007.

[9] Pawlak M., Piaseczny L.: *Evaluation of suitability of existing harmful compounds dispersion models for assessment of land pollution with marine engines exhaust gases.* Silniki Spalinowe/Combustion Engines, No. 2007-SC3, p. 62 – 71
[10] Pawlak M., Piaseczny L.: *Modele symulacyjne ruchu jednostek morskich.* Konstrukcja, badania, eksploatacja, technologia pojazdów samochodowych i silników spalinowych. Teka Komisji Motoryzacji. Oddziału PAN w Krakowie, Zeszyt Nr 33-34, s.325 – 334, Kraków 2008.
[11] Felski A., Piaseczny L*.: Monitoring of the movement of the objects on the Gdansk bay in order to recognize the characteristics of their main propulsion systems.* Silniki Spalinowe/Combustion Engines, No. 2007-SC1, p. 377 – 382.
[12] Felski A.: *Implementation of AIS in air pollution investigations.* Materials of European Navigation Conference Global Navigation Satellite Systems. Geneva 2007.
[13] Kniaziewicz T., Piaseczny L.: *Model symulacyjny emisji NOx w spalinach jednostek pływających.* Konstrukcja, badania, eksploatacja, technologia pojazdów samochodowych i silników spalinowych. Teka Komisji Motoryzacji. Oddziału PAN w Krakowie, Zeszyt Nr 33-34, s.185 – 198, Kraków 2008.

Journal of POLISH CIMAC
Faculty of Ocean Engineering & Ship Technology
GDAŃSK UNIVERSITY OF TECHNOLOGY

EFFECTS OF THE THERMAL ACTIVATION OF FUEL ON ENERGY PARAMETERS AND TOXICITY OF COMBUSTION GASES IN THE MARINE DIESEL ENGINE

Leszek Piaseczny
Wojciech Władyka

The Polish Naval Academy
Ul. Śmidowicza 69, 81-103 Gdynia, Poland
tel. +48 58 626-26-03,
e-mail: l.piaseczny@amw.gdynia.pl

Abstract

This paper concerns theoretical basis of the influence of temperature of fuel on its main parameters, which affect the efficiency and toxicity of combustion gases in the marine diesel engine. It also presents the results of own research, carried out on a single-cylinder test engine on the engine test stand. These researches aimed to determine the efficiency of applying the thermal activation of fuel to improve energy and ecological properties of the engine. Heating of fuel up to 150°C for the various values of torque and engine speed was applied. The test results indicated generally beneficial influence of fuel heating on the energy indexes and the decrease of exhausts emission.

1. Introduction

More and more restrictive legal regulations make severe requirements about the emission of toxic compounds from piston combustion engines and it is necessary to apply different methods of reducing these emissions to the permissible level. Significant group of methods reducing level of emission of those compounds in exhausts constitute the methods directly affecting the combustion processes, which are the main source of the toxic compounds. [1]

This group contains the conception of thermal activation of injected fuel, which consists in heating up fuel before it is injected to the combustion chamber. Such heating of fuel in assumption should accelerate the evaporation of fuel, and just ahead the cylinder it should initiate the destruction of nuclear bonds in hydrocarbon molecules that fuel contains, which in consequence will shorten the time of self-ignition delay and limit the amount of injected and prepared to combust fuel. In consequence, both speed of combustion just after self-ignition and size of the post flaming zone increase, which should result in the decrease of temperature in that zone. Due to the significant relation between the temperature and the nitrogen oxides formation, lowering the temperature at that zone will definitely decrease the intensity of these compounds formation and their emissions to the atmosphere. [2].

In the view of the influence of temperature on fuel properties, the most important physical values of fuel are viscosity, density and surface tension. These values affect in the significant extend on a course of fuel injection, but mostly they affect the volumetric change of fuel pumped in the injection pipe. This leads to the change in injection pressure and, in consequence, some modifications in the place of injector opening. Changes of the physical and chemical properties of fuel cause further effects, such as modification of time of injection, range of the fuel stream, and angle of fuel pulverization.

Empirical dependence [3] describes the relation between *dynamic viscosity* μ_{pal} [Pas], fuel temperature t_{pal} [°C] and pressure P [bar]:

$$\mu_{pal}\left(P,t_{pal}\right)=\mu_{pal(20)}\left(\frac{20}{t_{pal}}\right)^{k}e^{B\cdot P} \tag{1}$$

where: k – temperature coefficient; k = 0,73,

B – pressure coefficient; $B = 10^{-3}$.

Having known the values of $\mu_{pal}\left(P,t_{pal}\right)$ and $\rho_{pal}\left(P,t_{pal}\right)$, which depend on pressure and temperature, it is possible to describe kinetic viscosity, also depending on these two parameters:

$$\nu_{pal}\left(P,t_{pal}\right)=\frac{\mu_{pal}\left(P,t_{pal}\right)}{\rho_{pal}\left(P,t_{pal}\right)}\left[\frac{m^2}{s}\right]. \tag{2}$$

Rapid decrease in both dynamic and kinetic viscosities of fuel along with the temperature increase occurs in the range of 50÷100°C. Then the rate of decrease is lesser.

Therefore, it can be stated that the viscosity determines the values of resistance of fuel flowing through conductors, filters, calibrated jets of pulverizator, and also the course of process of pumping and dosing the fuel and process of lubricating mobile elements of the injection system.

Density is a characteristic feature of every group of fuel, including Diesel fuel. The decrease in density and viscosity of fuel causes the decrease in engine power, a volumetric increase in unit fuel consumption and change of the amount of toxic compounds in exhaust gases. Density of fuel (Diesel fuel) is also a significantly changing parameter along with the change of temperature. At higher temperatures, the density decreases, according to the linear dependence given in literature [2].

Surface tension has a direct influence on the size of injected fuel droplets. Mean diameter of fuel droplets should be lesser at the higher temperatures, which facilitates the pulverization of droplets. Surface tension of hydrocarbon fuels depends on its chemical composition and it linearly decreases along with the increase of temperature and pressure.

Despite the development of mathematical models of combustion processes and production of toxic exhaust gases, they do not allow to define the influence of fuel temperature on these processes. Therefore, there is a need of conducting the research on engine test beds.

2. Own research

2.1. Organisation and course of research

The research was conducted in Naval Academy of Gdynia on the engine test stand on a 1-cylinder research test engine WOLA DMVa type, which technical parameters are presented in Table 1. In order to increase the temperature to the demanded level, there was prepared an appropriate heating system ahead the feed pump. Thermal energy used for heating was taken from another source, which was the calorimeter. Temperature of the injected fuel was measured in injected pipe just ahead the injector.

Table 1. Basic technical parameters of the engine

Type	Four-stroke, right-rotary
Cylinder Diameter	150 mm
Piston Stroke	180 mm
Engine speed	1500 rev/min

Nominal power (on the brake crank)	18 kW
Maximum torque	125 N·m
Unit fuel consumption at nominal power	185 g/(kW·h)
Compression ratio	15
Mean stroke speed	9 m/s
Pressure of the injector opening	21 MPa

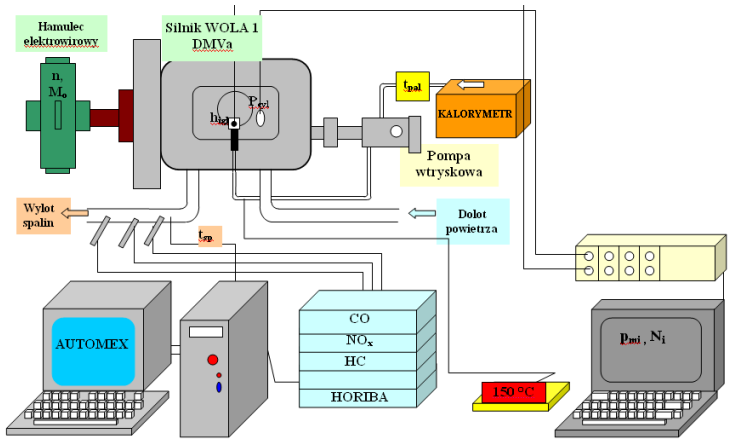

Fig 2. Scheme of engine measurement systems

Conducting the experiment, the theory of test planning was applied. Fig. 3 presents values that characterize the object of research.

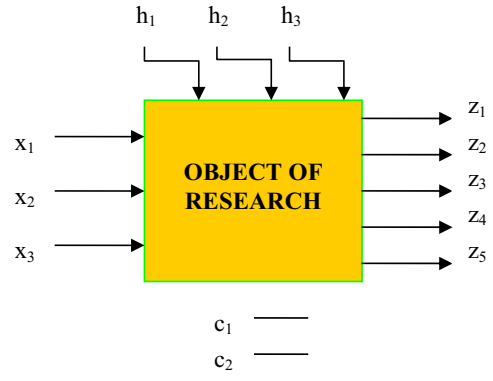

Fig 3. Model of the test engine WOLA (DMVa type), x - input values , z - output values, c-constant values, h- interferences

Among the above values, there were differentiated:

1. Set of input values X:
   - x_1 – temperature of fuel dosen to cylinder t_{pal} [°C];
   - x_2 – engine speed n [rev/min];

- x_3 – torque T [N·m];

2. Set of output values Z:
   - z_1 – concentration of emitted carbon monoxide C_{CO} [ppm];
   - z_2 – concentration of emitted nitrogen oxides C_{NOx} [ppm];
   - z_3 – concentration of emitted hydrocarbons C_{HC} [ppm];
   - z_4 – mean indicated pressure p_{mi} [MPa];
   - z_5 – indicated power N_i [kW]
3. Set of values C, which can appear during the test, were accepted as constant (fuel type).
4. Set of interfering values H, which can be modified (ex. ambient temperature, atmospheric pressure, relative ambient air humidity).

Due to the low number of input values in the research, there was applied a complete three-valued 3^3 plan with 3 independent variables and 27 measurements carried out in a single measurement block. It is presented in Table 2. The scope of three fuel temperature values covered two extreme values, imposed by physical and chemical parameters of fuel as well as by the safety conditions during increasing the fuel temperature. The third value was the mean value of the two extreme temperature values. Other input values, such as engine speed and torque, were limited by the engine construction parameters. The extreme values and their arithmetical mean were accepted as in case of fuel temperature.

*Table 2. Plan of the experiment 3** - fractal complete three-valued plan 1 block, 27 systems and received results of measurements*

Number of measurement system	Input data			Output data				
	x_1	x_2	x_3	z_1	z_2	z_3	z_4	z_5
	t_{pal} [°C]	n [obr/min]	T [N·m]	C_{CO} [ppm]	C_{NOx} [ppm]	C_{HC} [ppm]	p_{mi} [MPa]	N_i [kW]
1	20	800	25	937.8	191.7	137.4	0.410	9.00
2	20	800	75	1079.3	208.9	173.9	0.577	12.67
3	20	800	125	3023.3	405.5	210.8	0.751	16.47
4	20	1000	25	654.6	206.4	118.5	0.381	10.41
5	20	1000	75	1320.8	247.9	182.1	0.573	15.68
6	20	1000	125	2801.9	287.0	202.7	0.756	20.69
7	20	1200	25	848.1	165.9	129.8	0.383	12.58
8	20	1200	75	1890.2	231.5	179.5	0.537	17.63
9	20	1200	125	2045.9	290.1	162.3	0.695	22.81
10	85	800	25	557.7	160.1	60.5	0.409	8.96
11	85	800	75	597.1	303.4	75.4	0.588	12.81
12	85	800	125	1261.7	444.8	111.5	0.767	16.79
13	85	1000	25	519.1	167.9	48.2	0.413	11.29
14	85	1000	75	943.4	269.0	133.2	0.587	16.11
15	85	1000	125	1663.9	423.45	127.8	0.789	21.54
16	85	1200	25	715.2	147.5	99.5	0.488	16.01
17	85	1200	75	1296.4	239.1	171.2	0.683	21.41
18	85	1200	125	1544.4	294.6	163.4	0.731	24.07
19	150	800	25	525.71	182.1	56.1	0.433	9.47
20	150	800	75	643.2	272.3	75.5	0.631	13.81

21	150	800	125	1242.3	442.9	126.5	0.801	17.57
22	150	1000	25	517.7	175.4	53.7	0.481	13.13
23	150	1000	75	828.9	278.2	80.9	0.626	17.11
24	150	1000	125	1693.4	378.1	93.5	0.849	23.22
25	150	1200	25	765.1	139.1	112.6	0.533	17.49
26	150	1200	75	1294.8	248.9	159.2	0.670	21.99
27	150	1200	125	1431.3	298.2	149.1	0.850	24.66

2.2. Statistical and content-related analysis of the test results

Registered parameters were statistically analyzed at confidence interval $\alpha = 0.05$. After performing analysis of match measures of the significant statistic coefficients, there was selected an interaction L-L (linearly-linear) that had the most beneficial values of the quotient of regression coefficient and mean error of estimation the regression coefficient $t = b_i/S_{bi}$.

For the accepted model there were plotted some graphs presenting the estimation of match effects and the influence of the respective input values on a considerate output value. The graph of standardised effects is an effective tool presenting which factors have the greatest influence on the output value. As an example, Fig. 4 shows the influence of fuel temperature on the concentration of HC in exhaust gases.

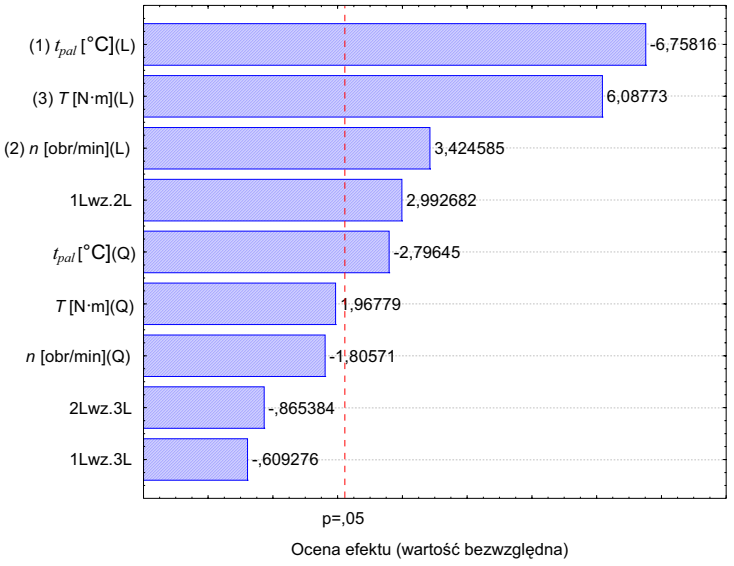

Fig 4. The graph of the standardised effects of HC concentration in an outlet manifold of the engine tested

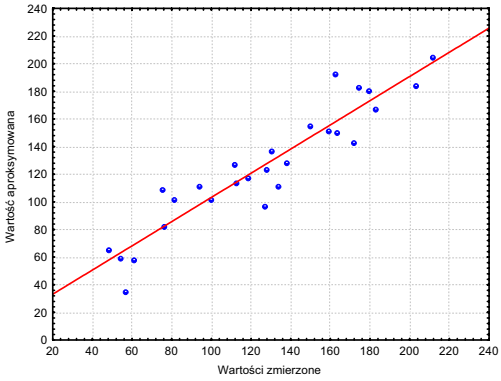

Fig 5. Dependence of the measured and approximated values of HC concentration in an outlet manifold of the engine tested – total of residues MS = 423,2653

As it results from Fig 4, the greatest influence on the HC concentration have: fuel temperature, followed by torque and the engine speed.

Torque in the first place and engine speed in the second one, are the most significant parameters that affect the NO_x concentration. Fuel temperature does not play an important role in the NO_x formation in the combustion process. The greatest influence on mean indicated pressure has torque and, in the definitely lower extends – the fuel temperature. The greatest influence on mean indicated pressure and indicated power has in order: torque, engine crankshaft speed and fuel temperature. Fig 5. illustrates the dependence of the measured and approximated values of HC concentration in a outlet manifold of the engine tested.

Engine torque has the most significant influence on CO concentration in a outlet manifold. At torque boost, the dose of fuel increases, air excess coefficient λ decreases and it results in the complete and incomplete combustion. Increase in torque T at constant air excess coefficient λ goes with the decrease of CO concentration. The decrease in torque T causes decrease in combustion temperature, which also involves the decrease in CO concentration.

Decrease in t_{pal} results in deterioration of the quality of fuel pulverization and injected fuel droplets diameters worsen the condition of fuel evaporation, which is caused also by the temperature decrease in the centre of fuel injection. Then, self-ignition delay increases, which causes interferences in the combustion course and as a result increases the amount of products of incomplete combustion, including the increase of CO in the engine exhaust gases.

The amount of toxic compounds in exhaust gases in the test engine increases along with engine load as a result of decrease in λ and increase in combustion temperature. When torque T (from T = 25 N·m to T = 125 N·m), at n = 800 [rev/min] increases, CO concentration increases as well – Fig 6.

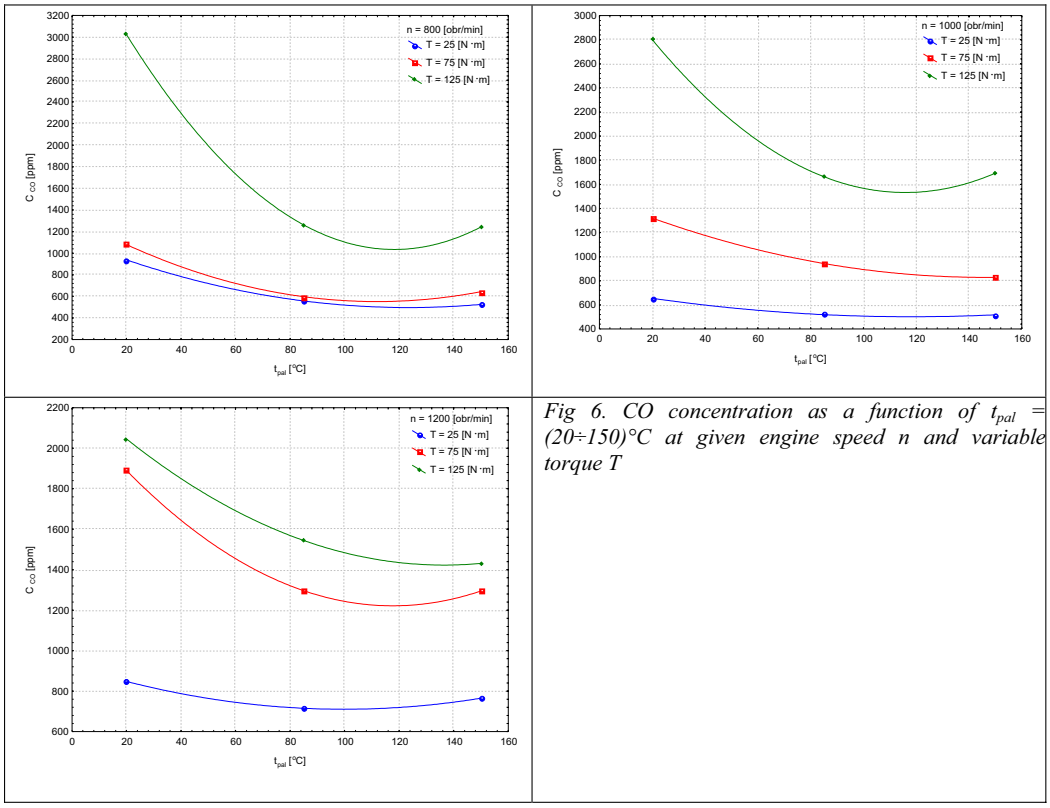

Fig 6. CO concentration as a function of t_{pal} = (20÷150)°C at given engine speed n and variable torque T

The greatest influence on the increase in NO_x concentration in four cycle engine has the torque (T). It results from the fact that two factors: temperature and amount of oxygen, playing a significant role in NO_x formation, affect one another. Along with the increase in torque *T, the value of* λ decreases, which results in temperature increase at the simultaneous decrease in oxygen concentration Along with the increase of toque T (from T = 25 to T = 125 [N·m]) at n = 1000 rev/min, the air excess coefficient λ decreases., which results in the increase in oxygen concentration in exhaust gases.

In general, an increase in temperature of injected fuel leads to decrease in NO_x concentration in exhaust gases, which is the most noticeable in the temperature range 50÷100°C. Thermal activation of fuel is the most efficient at low loads, because along with the increase in engine load, the effectiveness of this procedure radically changes and leads to a completely inverse situation, which is illustrated in Fig 7

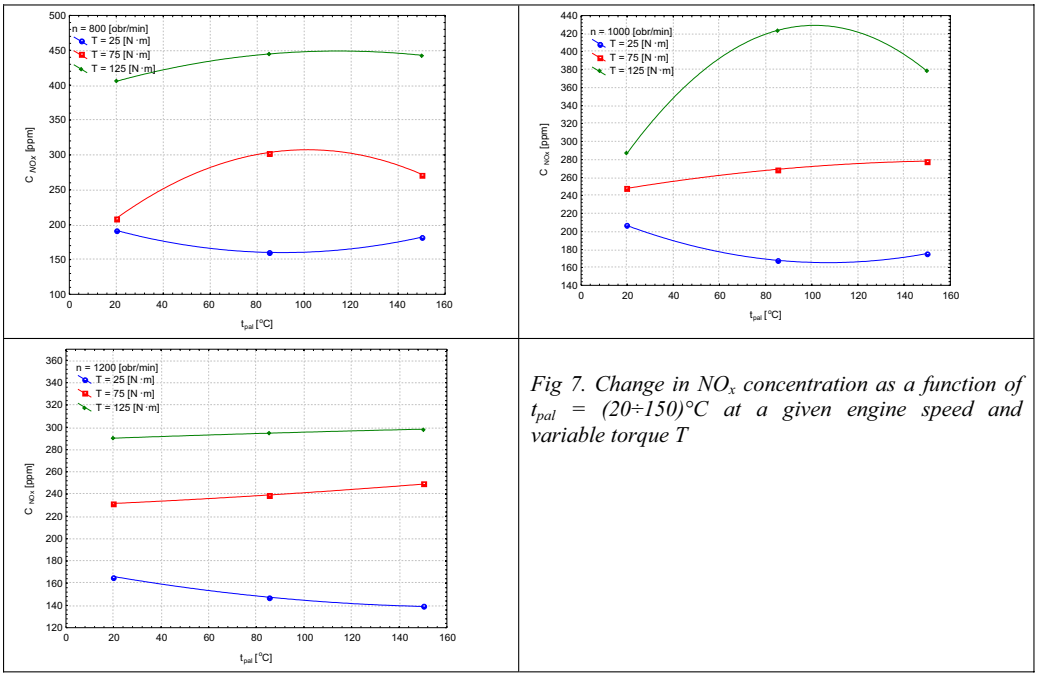

Fig 7. Change in NO_x concentration as a function of t_{pal} = (20÷150)°C at a given engine speed and variable torque T

As it was mentioned above, the principal influence on the increase in *HC* concentration in a outlet manifold has the temperature, what was verified in the statistical analysis. It is shown in Fig. 8.

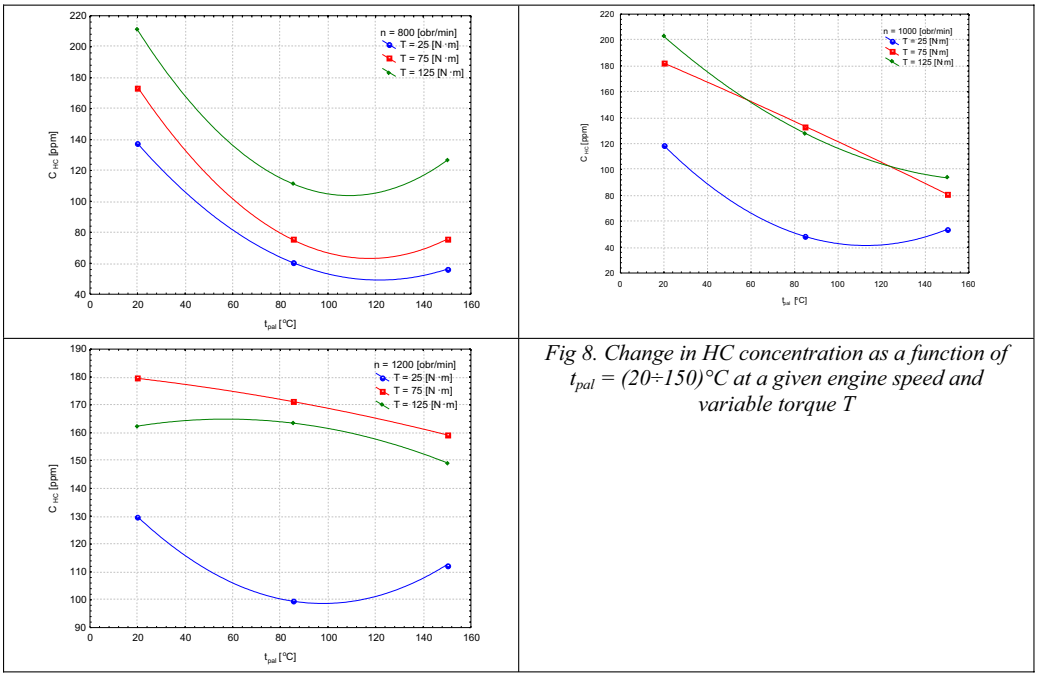

Fig 8. Change in HC concentration as a function of t_{pal} = (20÷150)°C at a given engine speed and variable torque T

It was possible to receive the decrease in uncombusted hydrocarbons along with the increase in t_{pal} (even to approx. 55% of the values received at t_{pal} = 20°C). However, it depends on engine work conditions: an increase in both its load and torque powers that beneficial effect.

The increase in *HC* concentration in exhaust gases, as a result of increase in torque T, at a given engine speed n, results from the decease in air excess coefficient λ. It is assumed, that in some areas of the combustion chamber there can appear local decrease in λ to value (λ<<1), which has the significant influence on increase in the number of uncombusted fuel particles. As a result, it leads to increase in *HC* concentration in exhaust gases. It is noticeable that *HC*, similarly to *CO*, mainly forms as a result of heterogeneous air-fuel mixture. This heterogeneity, in high extend depends on the structure of combustion chamber and its system of air filling and fuel feeding.

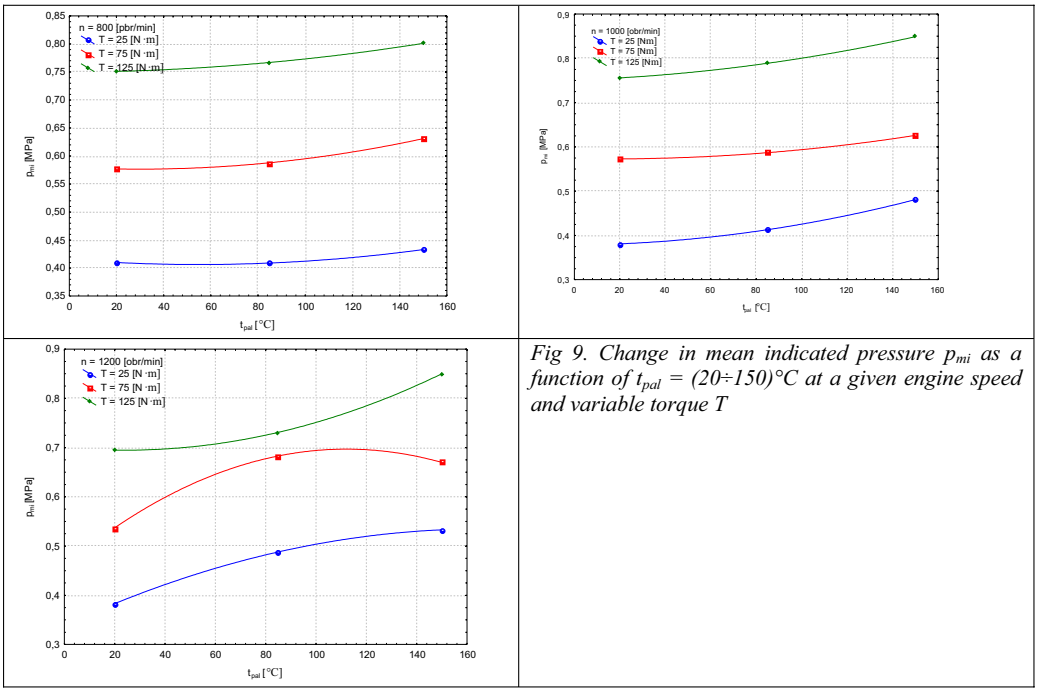

Fig 9. Change in mean indicated pressure p_{mi} as a function of t_{pal} = (20÷150)°C at a given engine speed and variable torque T

Torque has the main influence on the increase in mean indicated pressure in engine cylinder. Second in order is the fuel temperature t_{pal} (Fig 9).

Equation of the regression of *CO, NO_x* and *HC* concentration, mean indicated pressure p_{mi} and indicated power N_i in the range of t_{pal} = (20 ÷ 150)°C, n = (800 ÷ 1200) rev/min and T = (25 ÷ 125) N·m are the following:

$$[C_{CO}] = +252.8545 - 19.8306t_{pal} + 0.0703t_{pal}^2 + 0.8471n - 0.0003n^2 + 15.0177T + 0.0658T^2 + 0.0086t_{pal}n - 0.0736t_{pal}T - 0.0068nT$$

$$[C_{NOx}] = -228.7217 + 0.9116t_{pal} - 0.0033t_{pal}^2 + 0.6561n - 0.0003n^2 + 3.5422T + 0.0045T^2 - 0.0006t_{pal}n + 0.0053t_{pal}T - 0.0027nT$$

$$[C_{HC}] = 479.2674 - 2.7329t_{pal} + 0.0056t_{pal}^2 - 0.7529n + 0.0004n^2 + 2.1907T - 0.0066T^2 + 0.0014t_{pal}n - 0.0011t_{pal}T - 0.0005nT$$

$$[p_{mi}] = 0.3246 - 0.0014t_{pal} + 0.0000t_{pal}^2 - 0.0001n + 0.0000n^2 + 0.0050T - 0.0000T^2 + 0.0000t_{pal}n + 0.0000t_{pal}T - 0.0000nT$$

$$[N_i] = -6.3612 - 0.0278t_{pal} - 0.0000t_{pal}^2 + 0.0171n - 0.0000n^2 + 0.0844T - 0.0001T^2 + 0.0001t_{pal}n - 0.0001t_{pal}T + 0.0000T$$

Dependence of NO_x concentration on the values of input values (including fuel temperature) is presented in Fig 10, whereas the dependence of mean indicated pressure on these values is presented in Fig 11.

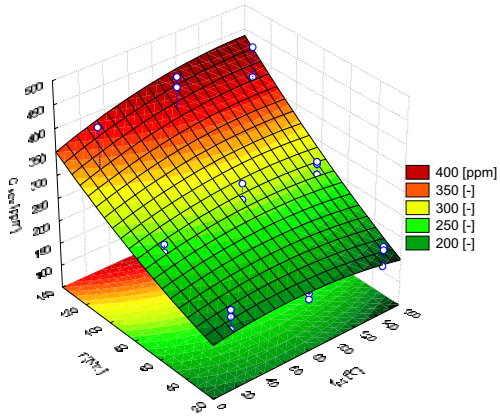

Fig 10. NO_x concentration as a function of t_{pal} and T

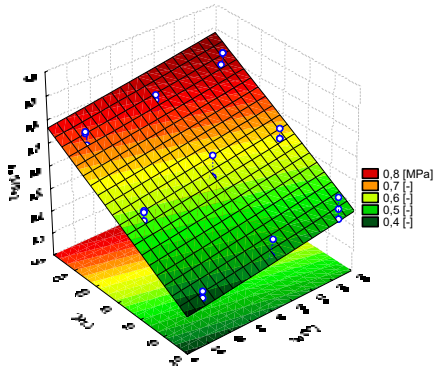

Fig 11. Mean indicated pressure p_{mi} as a function of t_{pal} and T

The highest increment of mean indicated pressure value (28%) for heated fuel is at n =1200 rev/min and T = 25 N·m. Low increments of this pressure are registered at low engine speed and high load. The increment is low and it reaches only (6%) in regard to the same load at unheated fuel.

3. Conclusions

The main aim of the use of thermal activation of fuel was to estimate energy and ecological effects of heating fuel in the feed system of vessels combustion engine. Considering the influence of temperature of injected fuel on analysed engine performance index, it is rational to search its optimal value.

Mentioned above factors must be considered up to the arbitrary decisions while making an attempt of finding the optimal values t_{pal},. Also engine work conditions must be taken under consideration while comparing the results for particular values t_{pal}.

On the basis of test results it can be stated that:

1) Along with the increase in engine load, there is a decrease in fuel temperatures, required for the most beneficial effects of heating the fuel.
2) Optimal fuel temperature in the range of $(80\div120)^{o}$C apparently decreases the power input necessary to its receiving in proportion to the input required at $t_{pal} = 150^{o}$C (they comprise at average (80÷90)% of the input at heating up to 150 ^{o}C). The range of temperature given above constitutes also the most beneficial range in proportion to the decrease in toxic compounds emission.

Feeding the engine by heated fuel brings on generally beneficial results. During proceeded tests there were obtained the following decreases in:

- *HC* concentration for about 44% (100 ppm)
- Carbon monoxide *CO* concentration for about 40% (1200 ppm)
- NO_x, concentration for about 22% (50 ppm), but only at low load, because at high load NO_x, concentration increases for about 20% (50 ppm).

Considering energy parameters of the engine fed by heated Diesel fuel in comparison with cool fuel, there was remarked the increment of:

- mean indicated pressure for about 14% (0.1 MPa)
- indicated power N_i for about 13% (3 kW).

Comparing research conducted on the test stand in LEUO with tests carried out by I. Pielecha from Poznan University of Technology it is possible to state that the obtained results do not differ much, although in the research of Poznan University of Technology the fuel was heated up to 220°C, while in the research of Naval Academy of Gdynia it was heated up to 150°C.

Literature

[1] Merkisz J.: *Ekologiczne problemy silników spalinowych, tom 1,2*, Wydawnictwo Politechniki Poznańskiej, Poznań 1999.

[2] Kowalewicz A.: *Podstawy procesów spalania.* Wydawnictwa Naukowe-Techniczne, Warszawa 2000.

[3] Baczewski K., Kołdoński T.: *Paliwo do silników o zapłonie samoczynnym*. WKiŁ, Warszawa 2004.

[4] Teodorczyk A.: *Teoria silników spalinowych.* Wydanie 1. Warszawa 2006.

[5] Piaseczny L.: *Zastosowanie teorii planowania doświadczeń w badaniach okrętowych silników spalinowych,* Zeszyty Naukowe Akademii Marynarki Wojennej, Rok XLIV nr 1 (152) 2003.

[6] Kafar I., Merkisz J., Piaseczny L.: *Model rozpylania paliwa w średnioobrotowym silniku okrętowym i jego badania symulacyjne*. Silniki Spalinowe, nr 3/2006 (126).

[7] Kowalczyk M.: *Diesel engine exhaust emmission control through pre-injection fuel thermal activation,* Archivum Combustionis. No. 1-4, Vol. 17 (1997).

[8] Pielecha I.: *Badania nad możliwością obniżenia emisji tlenków azotu silnika wysokoprężnego przez zastosowanie zewnętrznej aktywacji termicznej wtryskiwanego paliwa.* Praca doktorska. Politechnika Poznańska, 2000.

Journal of POLISH CIMAC
Faculty of Ocean Engineering & Ship Technology
GDAŃSK UNIVERSITY OF TECHNOLOGY

AGGREGATION OF ENTER VARIABLES IN NEURON MODEL OF POWER REQUIRED FOR THE SEAGOING VESSEL BY MEANS OF DIMENSIONAL ANALYSIS

Jan Roslanowski

Gdynia Maritime University
Faculty of Marine Engineering
81-87 Morska str.
81-225 Gdynia, Poland
e-mail:rosa@am.gdynia.pl

Abstract

The following article presents the possibility of enter variables aggregation in neuron models required power for the seagoing vessel by means of dimensional analysis. Such aggregation simplifies significantly the model, on the basis of which, the required power for ship propulsion is defined. The algebraical diagram of dimensional analysis constructed by S. Drobot is a good instrument for this goal. What is more, such diagram allows to control, in respect of mathematics, the correctness of conclusion rules used in neuron models.

Keywords: *aggregation of variables in conclusion rules, neuron models, dimensional analysis*

1. Introduction

Power for ship propulsion is selected on the basis of hull resistance analysis in different conditions of sailing. At present it is possible to observe more and more the use of artificial neuron networks in selecting power for ship propulsion [1,2].

In diagram 1 we can see an exemplary structure of neuron network allowing to determine power for ship propulsion in different conditions of sailing.

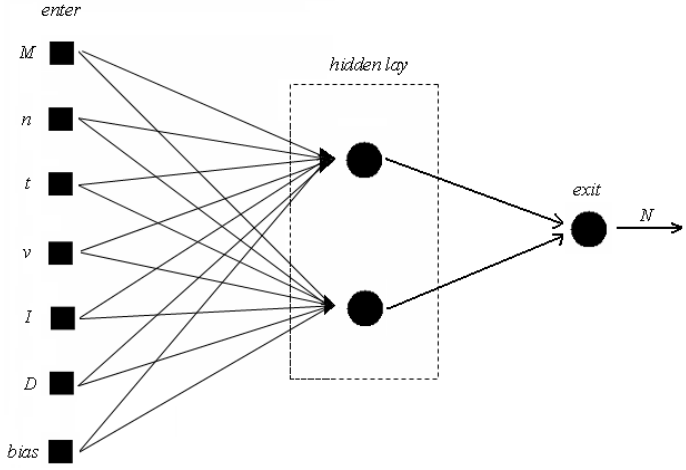

Fig.1 Structure of neuron network determining required power for ship propulsion in different conditions of sailing: M- torque of the propeller tail-end, n- revolution of the propeller, t- time of change of respective parameters, v- speed of ship, I- inertia moment of whirling propulsion elements, D-mass of ship

Therefore ship models are created using activity of neuron networks. Such networks have a complex structure putting into practice power selection for ship propulsion on this basis in a very wide range of variable parameters. The power of ship propulsion depends on dimensional quantities given to enter part of network which is put into activities respective practice. These activities involve checking premises of rules enclosed in respective bases of measurement data.

Conclusions of rules concerning power selection for ship propulsion are defined by neuron network. The number of power selection rules for ship propulsion increases violently according to the increase of the number of entrances [3].

In order to reduce the number of enter signals being dimensional quantities it is possible to use their aggregation by means of dimensional analysis. Aggregation involves the replacement of enter signals by the signal which is a respectively selected product, and their functional combination.

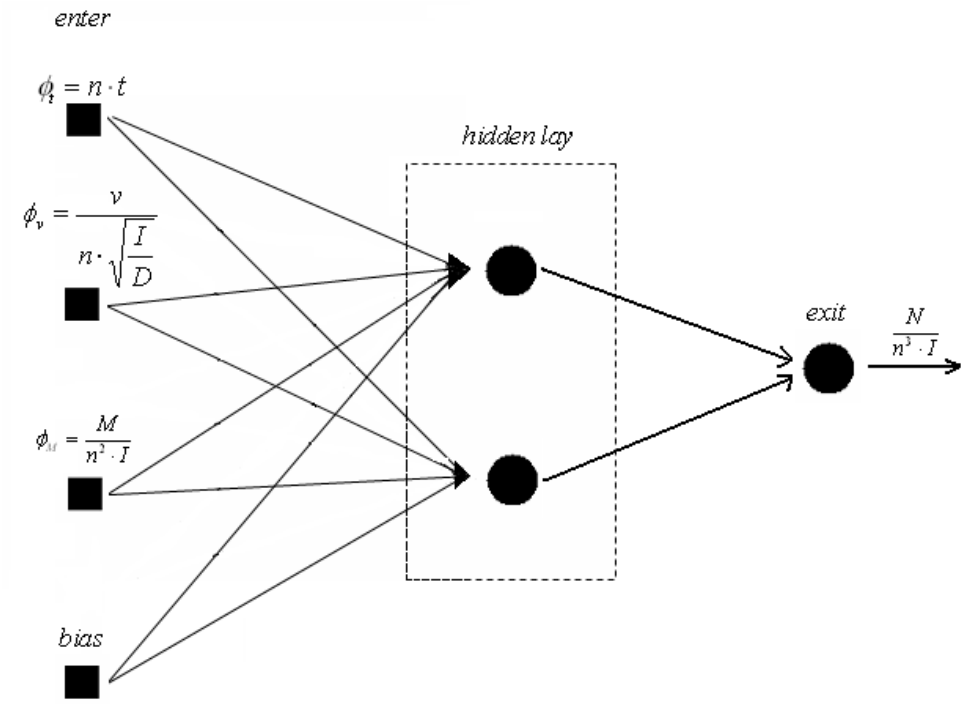

Fig.2 Structure of neuron network determining ship propulsion power followed by their aggregation of enter quantities: φ_t-nondimensional number of time,, φ_v–nondimensional number of speed, φ_M–nondimensional number o propeller torque, $\varphi_N = \frac{N}{n^3 \cdot I}$ -nondimensional number of power requirement

To achieve good results from aggregation it is primary important to select proper dimensional function combining enter variables. At the same time full use is being made in physical relations between power required for ship propulsion and ship resistance. Ship's hull resistances in different conditions of sailing are enter quantities into neuron network. In fig.2 the diagram of neuron structure network determining propulsion power of the ship after aggregation of its enter quantities, has been presented.

2. Aggregation of dimensional quantities describing requirement of power for ship propulsion

Power requirement for ship propulsion can be described by means of the following dimensional function [4,5] :

$$N = \Phi(M, n, t, v, I, D) \tag{1}$$

where:

N – required power for ship propulsion in [kg m^2 s^{-3}],
M – torque at the tail-end of the propeller in [kg m^2 s^{-2}],
n- rotational speed of the propeller in [s^{-1}],
t – time of change of respective parameters in [s],
v – speed of the ship in [m s^{-1}],
I – inertia moment of whirling mass of the ship propulsion system in [kg m^2],
D – mass of the ship in [kg].

The function defined by the formula (1) is a dimensional function in a dimensional space, whose arguments are its quantities. Such function cannot be treated as ordinary numerical function in the set of real numbers. Dimensional function (1) fulfils the conditions of invariance and dimensional homogeneity (6). Such conditions do not limit the form of numerical function where arguments as well as the value of the function are nondimensional quantities.

Six argument of dimensional function of required power for ship propulsion (1) have respective dimensions in an adopted system of measurement units SI. The matrix of exponents of the dimensions in this case, has the form:

	Kg	m	S
M	1	2	-2
N	0	0	-1
T	0	0	1
V	0	1	-1
I	1	2	0
D	1	0	0

The above matrix is of the third order, which means that among arguments of dimensional function three arguments are dimensionally independent.

Dimensional analysis does not provide any method which could make it possible to ascertain which quantities can be chosen as dimensionally independent. Generally, if six quantities define propulsive power of the ship and three quantities are dimensionally independent so the number of possibilities of their selection equals three elements combination out of the six elements set resulting in the number of twenty. Those combinations are, by way of example, the following quantities dimensionally independent of the remaining ones:(n, I, D), (t, v, D), (n, I, t), ... etc. After selection of arguments dimensionally independent of the remaining ones, we can, on the grounds of Buckingham's theorem (tw Π) write down the dimensional function (1) in the following forms:

$$N = f\ (\varphi_t, \varphi_v, \varphi_M) \cdot n^a \cdot I^b \cdot D^c \qquad (2)$$

where:

f – numerical function defined in the domain of real numbers,
$\varphi_t, \varphi_v, \varphi_M$ – nondimensional element of respective dimensional quantities,
a,b,c,d – real numbers,
- the remaining denotations as in the formula (1).

Exemplary relations between dimensional quantities dependent: t, v , M on independent quantities: n, I, D have the following form:

$$t = \varphi_t \cdot n^{\alpha} \cdot I^{\beta} \cdot D^{\gamma} \qquad v = \varphi_v \cdot n^{\alpha}{}_1 \cdot I^{\beta}{}_1 \cdot D^{\gamma}{}_1 \qquad M = \varphi_M \cdot n^{\alpha}{}_2 \cdot I^{\beta}{}_2 \cdot D^{\gamma}{}_2 \qquad (3)$$

where:

$\alpha, \alpha_1, \alpha_2, \beta, \beta_1, \beta_2, \gamma, \gamma_1, \gamma_2$ – real numbers,
- the remaining denotations like in the formulas (1) and (2).

Real numbers being the exponents of dimensional quantities are determined by comparison of dimensions of quantities taking part in relations (3) and (2) in the following way:

$$[\,s] = [\,s^{-1}\,]^{\alpha} \cdot [\,kgm^2\,] \cdot [\,kg\,]^{\gamma} \quad \Rightarrow \quad \alpha = -1; \quad \beta = 0 \quad \gamma = 0$$

$$[\,ms^{-1}\,] = [\,s^{-1}\,]^{\alpha}{}_1 \cdot [\,kgm^2\,]^{\beta}{}_1 \cdot [\,kg\,]^{\gamma}{}_1 \quad \Rightarrow \quad \alpha_1 = 1; \quad \beta_1 = \frac{1}{2}; \quad \gamma_1 = -\frac{1}{2}$$

$$[\,kgm^2s^{-2}] = [\,s^{-1}]^{\alpha}{}_2 \cdot [\,kgm^2]^{\beta}{}_2 \cdot [\,kg]^{\gamma}{}_2 \quad \Rightarrow \quad \alpha_2 = 2; \quad \beta_2 = 1; \quad \gamma_2 = 0$$

$$[\,kgm^2s^{-3}] = [s^{-1}]^{a} \cdot [\,kgm^2]^{b} \cdot [kg]^{c} \quad \Rightarrow \quad a = 3; \quad b = 1; \quad c = 0\,.$$

Calculated values of numerical exponents taking part in equations (2) and (3) allow us to write down the equation (2) in the following way:

$$\frac{N}{n^3 \cdot I} = f\left(n \cdot t; \frac{v}{n \cdot \sqrt{\frac{I}{D}}}; \frac{M}{n^2 \cdot I} \right) \qquad (4)$$

where:

- denotations like in formulas (1).

The formula (1) proceeding in the same way as above we can obtain different numerical forms of dimensional functions (1) while selecting other quantities as dimensionally independent. So, selecting the quantities: t, v, D as dimensionally independent of the remaining ones, we can obtainces:

$$\frac{N \cdot t}{v^2 \cdot D} = f\left(\frac{M}{v^2 \cdot D}; n \cdot t; \frac{I}{t^2 \cdot v^2 \cdot D}\right) \tag{5}$$

where:

- denotations like in formulas (1) and (2).

Forms of numerical dimensional function (4) and (5) with the same exactness define power required for ship propulsion. There are as many such forms as there are possibilities of selecting quantities dimensionally independent, correct in respect of mathematical precision.

In the case under investigation there are twenty of them. That means that during selecting numerical form of dimensional function we should concentrate on the way which makes it possible to carry out an experiment and train of the network on the set of measuring data. Definition exactness of such functions depends on evaluation of constant coefficients during experimental research by means of regression.

Form of above named numerical function define base for perennial day and night data recording the state parameters of vessel movement in task: „ Realization of systematic investigations of ship energy propulsion demand ” government department problem [8]. An exponential form of numerical function in which constant coefficients determine measuring data by means of least square method is selected.

Demand of power for ship propulsion determined by means of neuron model taking advantage of dimensional function (1) is in possession of six enter quantities and the same number of conclusion rules. Neuron model of ship propulsion system contains bases of rules making use of numerical form of dimensional functions which can be easily interpreted and modified.

Application of algebraical scheme of dimensional analysis constructed by S. Drobot allows to aggregate conclusion rule defined by the function (1) to form (4) or (5) in which three enter signals take place. So we can see that by means of dimensional analysis it is possible to reduce in an essential way the number of entrances into the neuron model of ship propulsion system and thus considerably simplify its structure. In the model under investigation there are only three enter variables instead of six.

At the time of identification and also estimation of enter signal in the mode on-line of such models there is the Reed preliminary calculation of the value of aggregated variables.

3. Conclusions

Determining power required by the ship means of neuron models allows to train the network in the set of measuring data. Such models are represented by the base of rules for which algebraical scheme of analysis can be used.

It allows to aggregate the model in different ways depending on the need aggregation of neuron model by means of dimensional analysis leads to a considerable reduction of the number of its entries.

In this way the structure of neuron networks is simplified and used in aggregated neuron models.

Precision of numerical function estimation (5) used in aggregated neuron models equals the exactness of determination of its parameters by way of experiment.

Besides the dimensional analysis allows to ascertain the structure of conclusion rule, and being numerical function, it is properly constructed in respect of mathematical correctness.

References

[1] Abramowski T., *Application of artificial neural networks for determination of propeller's crash-ahead, crash-back, banking performance*. Ship Technology Research, Vol. 48, pp154-160, 2001.

[2] Mesbahi E., Atlar M., *Artificial neural networks: applications in marine design and modelling*. 1st International Conference Computer Applications and Information Technology in the Maritime Industries. Potsdam 2000.

[3] Horikawa S., Furuhashi T., Uchikawa Y., Tagawa T., *A study on fuzzy modelling fusing fuzzy neural networks*. Fuzzy engineering toward human friendly systems IFES'91, pp 562-573, 1991.

[4] Roslanowski J., *Modelling of ship movement by means of dimensional function*. Radom University of Technology, Transport No 3(23), pp 443-448,2005.

[5] Roslanowski J., *The methodology of energetical process model construction in ship propulsion systems by means of dimensional analysis defining their dynamical features*. International Conference Technical, economic and environmental aspects of combined cycle power plants. Gdansk University of Technology2004, pp 59-66.

[6] Drobot S., *On the foundation of dimensional analysis*. Dissertation Mathematic, Vol. XIV,1954.

[7] Drobot S., Warmus W., *Dimensional analysis in sampling inspection of merchandise*. Mathematic, Vol. 5, 1954.

[8] Research Works of Marine Power Plant Institute Merchant Marine College in Gdynia: „*A day and night recording of state movement parameters of training vessel m/s A. Garnuszewski* " (work task No. 106.5.03.05).

Journal of POLISH CIMAC
Faculty of Ocean Engineering & Ship Technology
GDAŃSK UNIVERSITY OF TECHNOLOGY

LOADS OF SHIP MAIN DIESEL ENGINE IN THE ASPECT OF PRACTICAL ASSESSMENT OF ITS OPERATION

Jacek Rudnicki

Gdansk University of Technology
ul. Narutowicza 11/12, 80-950 Gdańsk, Poland
tel.: +48 58 3472430, fax: +48 58 3472430
e-mail:jacekrud@pg.gda.pl

Abstract

This paper presents a concept of method intended for the assessing of operation of engine which works under partial load. A valuation (quantitative) approach to the operation interpreted as a physical quantity was applied to determine existing margins of operational parameters of engine as well as additional costs associated with degradation of its technical state, born by engine's user.

Keywords: *operation, diesel engine*

Introduction

From the point of view of operation aims generated by operational system in the form of transport tasks for ship considered as a technical system, ship propulsion system is intended for realization of assumed sailing speeds of the ship within a given period and determined range of changeability of external conditions.

Hence the functioning of the ship in steady motion with speed v is determined by description of a system of forces acting on ship's hull, that can be analytically represented (on assumption of neglecting the gravity and buoyancy forces) as follows [3, 10]:

$$T = R_T + \Delta T \tag{1}$$

gdzie:
T – thrust of the propeller,
ΔT – thrust deduction,
R_T – total hull resistance.

The interdependence of ship resistance and effective power of main propulsion engine for steady sailing speed is described by the following equation [3, 10]:

$$N_e = \frac{R_T \cdot v}{\eta_{lw} \cdot \eta_s} \tag{2}$$

where:
v – speed of ship,
η_{lw} – efficiency of shaftline,
η_s – propeller efficiency.

Knowledge of the quantities appearing in Eq.(2) makes it possible to properly select all elements of propulsion system in the designing stage [9, 10]. Considering the sailing speed to be an independent variable which definitely determines two main factors associated with realization of objective function, namely :

- duration time of realization of transport task, which definitely influences costs of its realization and potential profits to ship's owner,
- possibility of maintaining an assumed ship course in heavy weather conditions, which first of all influences occurrence probability of an emergency situation,

one should observe that during ship operation all remaining quantities undergo changes due to degradation processes which involve evolution of the process of technical state changes towards technical unserviceability states. It obviously influences serviceability of system's elements and ,consequently, of the entire system.

On assumption that main propulsion system of ship has been correctly selected, the hull resistance characteristics $R_T = f(v)$ constitute the factor which generates demand for effective power developed by propulsion engine for reaching a given sailing speed of the ship [4]. The characteristics determine, for assumed conditions, value of developed effective power of engine neccessary to reach a demanded sailing speed. If a relatively short period is taken into account then it can be assumed , without any large error, that the representation is invariable.

In practice, an important change of the relation $R_T = f(v)$, resulting from influence of the environment and physical ageing processes (especially of wear, e.g. corrosion), occurs , whose external symptom is a rise of value of the force R_T at given values of the speed v in comparable sailing conditions. Long time intervals between successive ship hull docking surveys (possible repairs) are of special importance because such intervals , depending on a type (class) of ship and given classification rules, vary from 3 to 5 years [e.g. 12].

In selecting the main engine in the stage of ship designing the above desrcibed processes are taken obviously into account, that is manifested by skillfully selected design characteristics of ship hull resistance as well as by application of the so-called sea margin during determination of the main engine contractual power N_x [9, 10], which makes that the main engine usually has certain power surplus as compared with assumed design values of hull resistance. It means that in the case of typical transport task for a given ship its main engine will be used in a load state lower than rated one [1].

However, the existing power margin which guarantees ship safety, is systematically decreasing due to the above described phenomena and the worsening of operational characteristics of engine itself.

Hence, it seems rational to elaborate a method for determining the existing margin of operational engine parameters associated with degradation of its technical state, and the additional costs born by its user.

Influence of change of technical state of engine on its operation

Worth mentioning, in the light of the above described power surplus of main propulsion engine, that for the engine running under partial loads the process of decreasing the available output power will develop in two phases:

- in the first phase hourly fuel oil consumption will rise solely (at a relatively constant value of developed torque), and in consequence operational costs will be also higher;
- in the second phase a limitation of value of effective power developed by the engine will occur because of constructional constraints and lack of possibility to increase fuel charge.

The described phenomena result from control action of fuel apparatus which will increase, within a given range of values, the instantaneous fuel charge $g_p^{i\%}$ ($g_p^{i\%}$ - fuel charge for *i%* load of engine being in the technical serviceability state under assumption that the maximum engine load

amounts to 110% of its rated value, $i<110$) up to the instant of reaching its maximum value G_{pmax}. Every successive decrease of value of engine total efficiency will result in a recordable decrease of its torque M_o.

If to assume the engine partial load to be constant (e.g. for 9RT–flex60C–B engine : 85% engine load, the contractual output power $N_x = 80\%\ N_{R1} = 17370$ kW, the contractual engine speed $n_x = 90\%\ n_{R1} = 102{,}6$ rpm [13]) the phenomenon in question can be presented in the form of the diagram (Fig. 1) of the following interpretation :

- the time-dependent drop of the engine's total efficiency (in the case in question by about 9%) results , in the first phase, mainly in an increased hourly fuel oil consumption (specific fuel oil consumption). It can be represented as the occurrence of the successive recordable events F which consist in increasing the fuel charge $g_p^{i\%}$ by the value Δg_p at a relatively constant , relevant to a given engine load state, value of the torque M_o. This way, increased operational costs are generated rather without imposing limitations on the ship motion parameters described by Eqs. (1) and (2).
- the degradation processes progressing along with time of further use of engine result in occurrence of the recordable events U which consist in decreasing values of the engine torque M_o at constant fuel oil consumption (at $g_p = G_{p\,max}$). Further long-lasting use of the engine results in the significant worsening of its characteristics which definitely impose limitations on ship motion at an assumed speed or course. In heavy weather conditions such situation will obviously form an important circumstance for occurrence of state of danger to ship safety.

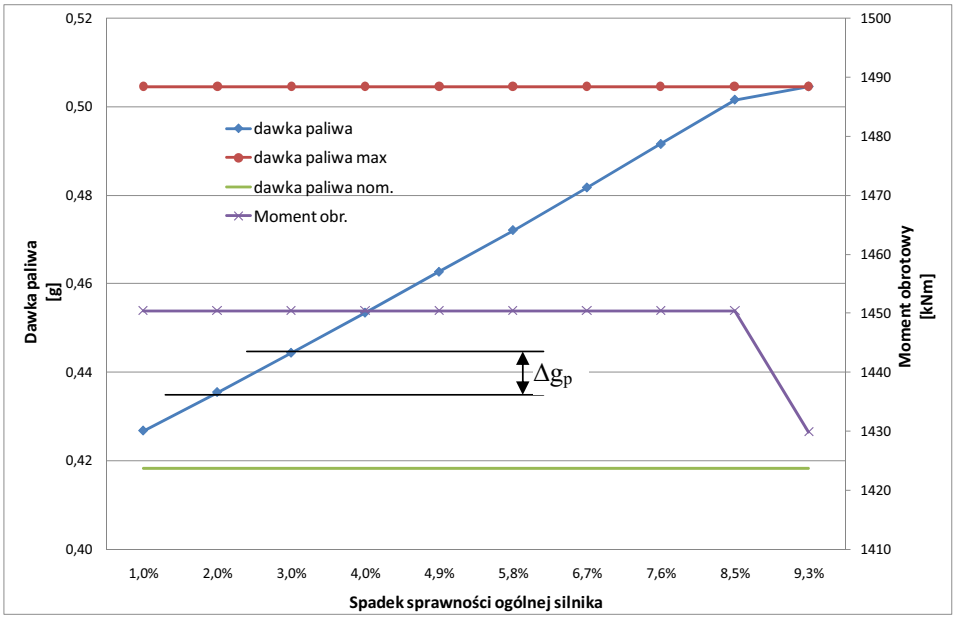

Fig. 1 Changes of engine fuel charge and torque , which result in changes of total efficiency of the engine running under partial load

Assessment of available power margin and additional operational costs of engine

The number of repetitions of the event F, $N_{\Delta gp}$, within the time interval (0, t) is a random variable of non-negative integral values. The dependence of the random variable on time constitutes the stochastic process $\{N(t): t \geq 0\}$. On the assumption on its stationarity, lack of

consequences and flow singularity [5] the Poisson homogeneous process [2] can be applied to description of the process of increasing the fuel charge $g_p^{i\%}$ (6) resulting from the decreasing of the total engine efficiency η_e (in maintained engine load conditions).

Hence, in the case if the number of the events F ,$N_{\Delta gp}$, occur up to the instant *t*, the total increase of the fuel charge $g_p^{i\%}$, up to the instant, can be expressed as follows:

$$\Delta G_p = \Delta g_p \cdot N_{\Delta gp} \tag{3}$$

where:

ΔG_p - total increase of the fuel charge g_p after occurrence of $N_{\Delta gp}$ number of the events F,

Δg_p – elementary recordable fuel increment by which the fuel charge $g_p^{i\%}$ increases , whereas the random variable $N_{\Delta gp}$ has the following distribution [1]:

$$P\left(N_{\Delta gp} = k\right) = \frac{\left(\lambda_f \cdot t\right)^k}{k} \exp\left(-\lambda_f t\right); \quad k = 1,2,...,n \tag{4}$$

where:

λ_f – a constant interpreted as the intensity of occurrence of the event F (i.e. increase of the fuel charge $g_p^{i\%}$ by Δg_p value).

Assuming that the unit fuel charge increase by Δg_p value generates the additional unit cost φ (realization of the same task at an increased fuel oil consumption) one can determine its total value Φ, up to the instant *t* , as follows:

$$\Phi = \varphi \cdot \Delta g_p \cdot N_{\Delta gp} \tag{5}$$

For the engine load smaller than maximum, the summary fuel charge increase $\Delta G_{p\max}$ and occurrence of certain number , $N'_{\Delta gp}$, of the events F affecting solely the increasing of the unit fuel oil consumption g_e and hourly fuel oil consumption B_h , can be determined by the following relation :

$$\Delta G_{p\max} + g_p^{i\%} = \Delta g_p \cdot N'_{\Delta gp} + g_p^{i\%} = G_{p\max} \tag{6}$$

where:

$g_p^{i\%}$ – fuel charge relevant to a given engine load *i* % (under assumption that the maximum engine load is equal to 110% of its rated load, i.e. $i<110$)

$G_{p\max}$ - maximum fuel charge possible to be realized by injection apparatus within existing constructional and control limitations.

Occurrence of the successive event F ($N_{\Delta gp} = N'_{\Delta gp} + 1$) for the current engine load *i %* will be associated with occurrence of certain limitation in developing the demanded power of the engine , and in consequence limitations for motion of the entire ship, will occur.

As the effective output power of engine can be expressed as follows [11]:

$$N_e = \frac{\eta_e \cdot w_d \cdot g_p^{i\%} \cdot n}{\tau} \tag{7}$$

where:

η_e – effective efficiency of engine,

w_d – fuel lower calorific value,

$g_p^{i\%}$ - temporary fuel charge (for i% engine load),

n – rotational speed of engine,

τ - a coefficient which takes into account number of strokes realized during one engine working cycle,

as well as on assumption that the changing process of engine technical state is continuous over time and states, the situation can be illustrated in the way shown in Fig. 2.

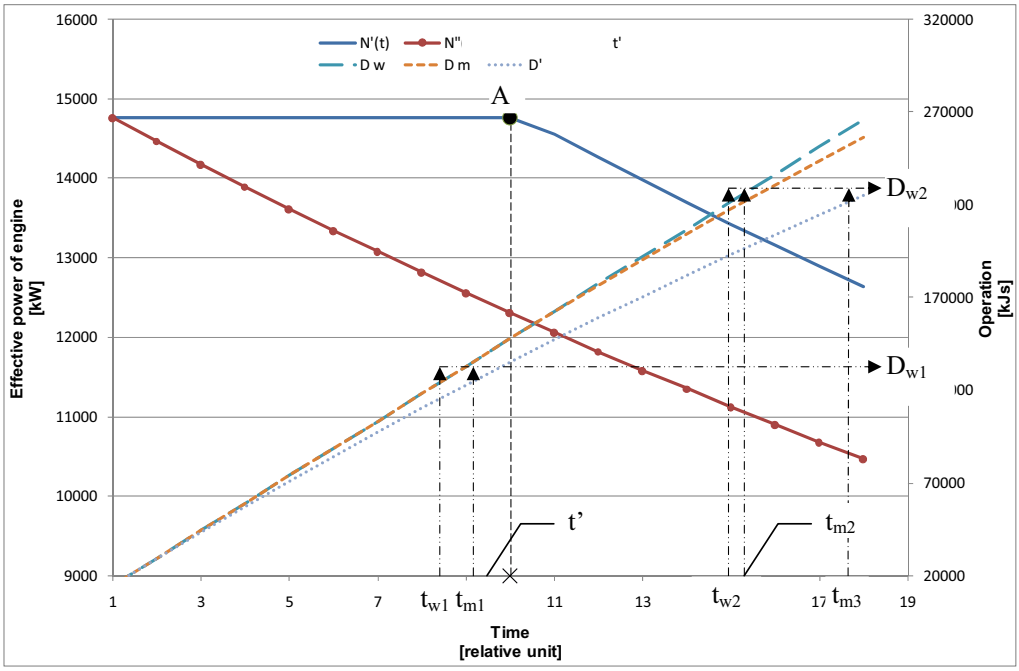

Fig. 2 *Change of engine operational characteristics, which results from degradation of its technical state.* t_{w1} *– demanded time of realization of the task 1,* D_{w1} *– demanded value of operation for realization of the task 1,* t_{w2} *– demanded time of realization of the task 2,* t_{m1} *– possible time of realization of the task 1 in the situation A (described in the text),* t_{m2} *– possible time of realization of the task 2 in the situation B (described in the text),* t_{m3} *– possible time of realization of the task 2 in the situation A (described in the text),* D_{w2} *– demanded value of operation for realization of the task 2,* D_m *– possible operation of engine in the situation 2 , D' – possible operation of engine in the situation A.*

By introducing the notions of the demanded operation D_w and the possible operation D_m , whose detail interpretation can be found in [6, 7, 8], the phenomena graphically presented in Fig. 2 can be highlighted as follows:

- in the case of a hypothetical lack of possibility of increasing the fuel charge (the situation A) a drop of total engine efficiency will result in a sudden drop of its effective power – the line N"(t) – that , apart from producing a situation hazardous to ship safety , during further degradation of technical state of engine , will cause extending the realization time of transport task from the instant t_{w1} to t_{m1},
- if at engine partial load it is possible to increase the fuel charge within the interval of values $\left\langle g_p^{i\%}, G_{p\max} \right\rangle$ (the situation B) , and up to the instant of reaching its maximum value (the point A, instant t') no noticeable drop of power occurs– the line N'(t), then only an additional cost resulting from increased fuel oil consumption will be generated. Hence it can be stated that if a transport task lasts shorter than up to the instant t' any lengthening of its realization time will not occur.
- begining from the instant t' (corresponding with the point A) a limitation of the possible engine operation D_m [6, 7, 8] occurs , that is associated on one hand with the lengthening of realization period of transport task (or lack of possibility of its realization during a given period) on the other hand – with increased costs of engine's use.

By using the relation (4) and (6) the number of the events F , *k'*, corresponding with that of $N'_{\Delta gp}$ can be expressed as follows :

$$k' = \frac{G_{p\max} - g_p^{i\%}}{\Delta g_p} \tag{8}$$

and its occurrence probability as :

$$P\left(N_{\Delta gp} = k'\right) = \frac{\left(\lambda_f \cdot t\right)^{\left(\frac{G_{p\max} - g_p^{i\%}}{\Delta g_p}\right)}}{\left(\frac{G_{p\max} - g_p^{i\%}}{\Delta g_p}\right)} \exp\left(-\lambda_f t\right) \tag{9}$$

Practically possible determination of stochastic process parameters

From practical point of view the crucial problem is to determine Δg_p and λ_f values. This will be possible if two complementary conditions are satisfied:

- to have access to results of operational investigations carried out with application of standard control measuring instruments and a system for diagnosing the process in question by recording and analyzing changes in values of fuel flow rate within time intervals when engine load is relatively constant;
- to analyze technical documentation of the engine and carry out simulation investigations in order to elaborate a mathematical model of influence of the occurring events F on operational fuel system parameters.

In the presented case Δg_p can be much easier determined , because of its small value, under the assumption that :

$$g_p^{i\%} = \frac{B_h \cdot \tau}{n} \tag{10}$$

where:
B_h – unit fuel oil consumption of engine,
n – rotational speed of engine,
τ - a coefficient which takes into account number of strokes during one engine working cycle.

The relation (10) at assumed class of accuracy (e.g. 0,5) of commonly applied flow meters makes it possible to determine Δg_p value with an accuracy sufficient for practical purposes.

Much greater difficulties are associated with determination of λ_f value, which results first of all from lack of empirical research in this area of engine functioning. However such value can be determined, in a way sufficiently accurate from practical point of view, by means of the following procedure:

- on the assumption that a typical (most frequently occurring) load state of engine is x% [1], the difference between its maximum load and the above mentioned state determines the changeability range of instantaneous fuel charge $\left\langle g_p^{x\%}, G_{p\max} \right\rangle$, hence on the basis of Eqs. (3) and (6) it yields :

$$\Delta G_{pmax} = G_{pmax} - g_p^{x\%} \tag{11}$$

- the period $T_{\Delta Gpmax}$, during which ΔG_{pmax} value is reached, should be assessed on the basis of technical documentation of engine and its producer's recommendations for overhauls and repairs, as results of relevant empirical research are usually lacking;
- taking all the above into account one can state that within the considered period about

$$N'_{\Delta g_p} = \frac{G_{p\max} - g_p^{x\%}}{\Delta g_p} \tag{12}$$

number of the events F will occur, hence :

$$\lambda_f = \frac{N'_{\Delta g_p}}{T_{\Delta G_{p\max}}} = \frac{\frac{G_{p\max} - g_p^{x\%}}{\Delta g_p}}{T_{\Delta G_{p\max}}} \tag{13}$$

Finally , making use of the above presented procedure and basing on the relation (8) one can determine at first the number of the events F, k' , and the probability of their occurrence:

$$P\left(N_{\Delta gp} = k'\right) = \frac{\left(\frac{\frac{G_{p\max} - g_p^{x\%}}{\Delta g_p}}{T_{\Delta G_{p\max}}} \cdot t\right)^{\left(\frac{G_{p\max} - g_p^{i\%}}{\Delta g_p}\right)}}{\left(\frac{G_{p\max} - g_p^{i\%}}{\Delta g_p}\right)} \exp\left(-\frac{\frac{G_{p\max} - g_p^{x\%}}{\Delta g_p}}{T_{\Delta G_{p\max}}} \cdot t\right) \quad , \tag{14}$$

and, the application of the relation (14) is this much practical that in the case of lacking results of empirical research one can approximately (but with a sufficient accuracy) determine $P\left(N_{\Delta gp} = k'\right)$value , basing solely on engine's technical documentation.

For example, for the above mentioned 9RT – flex60C – B engine (at the contractual output power N_x = 80% N_{R1} = 17370 kW, the contractual engine speed n_x = 90% n_{R1} = 102,6 rpm , G_{pmax} = 42,3 g, $T_{\Delta Gpmax}$ = 8000 h, Δg_p = 0,004 kg/s [13]) the values calculated by means of the relations (10) and (14) are the following:

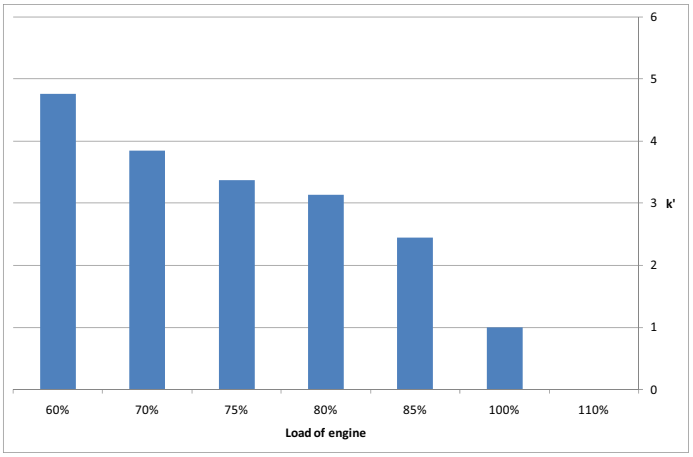

Fig. 3 *Values of the number k' of the events $N_{\Delta gp}$ in function of considered engine load values*

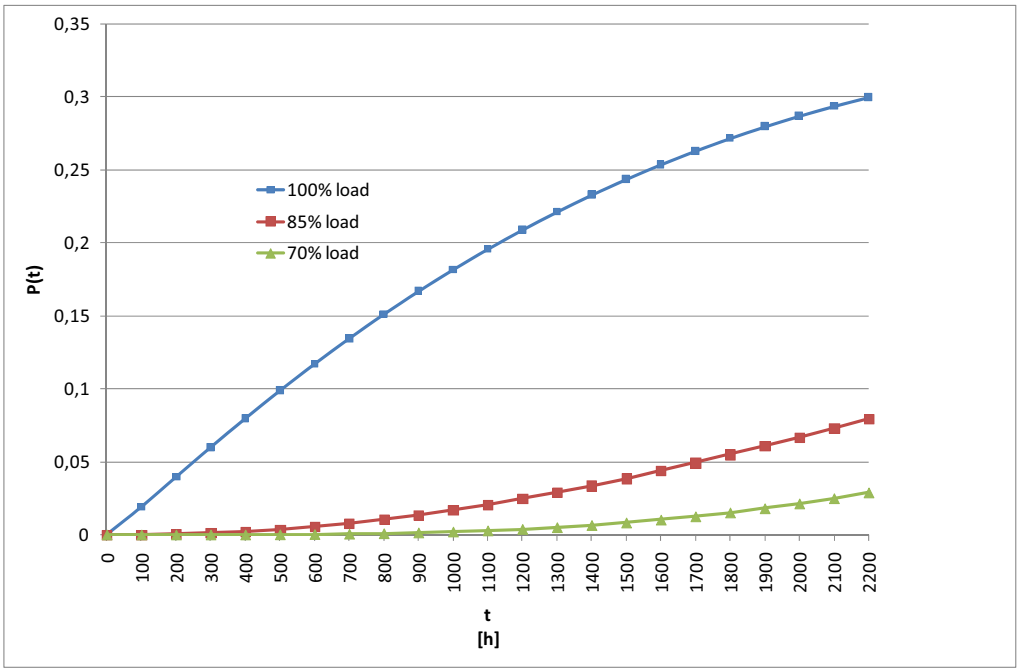

Fig. 4 *Occurrence probability of the number k' of the events $N_{\Delta gp}$ in function of considered engine load values and engine use duration period*

Summary

As already stated, the worsening of operational characteristics of an engine which operates under partial load up to the instant t' (Fig. 2), does not directly influence ship motion parameters.

However such situation generates additional cost born by engine's user , which finally lowers his profit Z resulting from realization of the task. To determine potential losses due to increased fuel oil consumption is possible by assuming that for t = 0 the additional cost Φ = 0 and the profit Z takes its maximum value $Z(0) = Z_{\max}$. By determining the expected value and standard deviation of the random variable which describes the lowering of the profit Z (the increasing of financial losses) as:

$$E[\Delta Z(t)] = \varphi \cdot \Delta g_p \cdot E(N_{\Delta gp}) = \varphi \cdot \Delta q \cdot \frac{\frac{G_{p\max} - g_p^{x\%}}{\Delta g_p}}{T_{\Delta G_{P\max}}} \cdot t$$

$$\sigma_Q = \varphi \cdot \Delta q \sqrt{D^2(N_{\Delta q})} = \varphi \cdot \Delta q \sqrt{\frac{\frac{G_{p\max} - g_p^{x\%}}{\Delta g_p}}{T_{\Delta G_{P\max}}} \cdot t} \qquad (15)$$

the relation which describes the lowering of the profit Z along with time *t* can be expressed as follows:

$$Z(t) = \begin{cases} Z_{\max} & dla \quad t = 0 \\ Z_{\max} - \varphi \cdot \Delta g_p \left(\dfrac{\dfrac{G_{p\max} - g_p^{x\%}}{\Delta g_p}}{T_{\Delta G_{p\max}}} \cdot t \pm \varphi \cdot \Delta g_p \sqrt{\dfrac{\dfrac{G_{p\max} - g_p^{x\%}}{\Delta g_p}}{T_{\Delta G_{p\max}}} \cdot t} \right) & dla \quad t > 0 \end{cases} \tag{16}$$

Making use of the relation (16) one can determine , for a given instant t , costs generated as a result of increased fuel oil consumption; and the relation (14) makes it possible to determine occurrence probability of such number of the events F which will generate additional limitations during realization of the task (e.g. lack of possibility of arbitrary loading the engine within its working area), or will make its realization impossible at all.

References

[1] Balcerski A., *Modele probabilistyczne w teroii projektowania i eksploatacji spalinowych siłowni okrętowych,* Fundacja promocji Przemysłu Okrętowego i Gospodarki Morskiej, Gdańsk 2007.

[2] Bielajew, J. K., Gniedenko, B. W., Sołowiew, A. D., *Metody matematyczne w teorii niezawodności*, Wydawnictwa Naukowo – Techniczne, Warszawa 1968.

[3] Chachulski, K., *Podstawy napędu okrętowego,* Wydawnictwo Morskie, Gdańsk 1988.

[4] Chachulski K., *Metody i algorytmy rozwiązywania problemów eksploatacyjno – ruchowych okrętowych układów napędowych,* Wydawnictwo WSM w Szczecinie, Szczecin 1992.

[5] Fidelis E., Firkowicz S., Grzesiak K., Kołodziejski J., Wiśniewski K., *Matematyczne podstawy oceny niezawodności,* PWN, Warszawa 1966.

[6] Girtler, J., Kuszmider, S., Plewiński, L., *Wybrane zagadnienia eksploatacji statków morskich w aspekcie bezpieczeństwa żeglugi*, Wyższa Szkoła Morska w Szczecinie, Szczecin 2003.

[7] Rudnicki, J., *Energy – Time Method for Assessment of Main Diesel Engine Operation,* Journal of KONES. Powertrain and Transport. - Vol. 14, nr 3 (2007), Warszawa 2007.

[8] Rudnicki J., *Ocena działania siłowni okrętowej w aspekcie energetyczno - czasowym* XXVIII Sympozjum Siłowni Okrętowych Gdynia 15-16 listopada 2007,Wydawnictwo Akademii Morskiej Gdynia 2007.

[9] Watson D.G.M., *Practical Ship Design*, Elsevier 1998.

[10] Urbański, P., *Podstawy napędu statków,* Fundacja Rozwoju Akademii Morskiej w Gdyni, Gdynia 2005.

[11] Włodarski J.K., *Okrętowe silniki spalinowe. Obciążenia eksploatacyjne,* Wydawnictwo Wyższej Szkoły Morskiej w Gdyni, Gdynia 1995.

[12] Przepisy klasyfikacji i budowy statków morskich. Część I, Zasady klasyfikacji. Wyd. PRS, Gdańsk 2006.

[13] *General Technical Data. WinGTD ver. 2.9,* Wärtsilä Switzerland Ltd 2004.

Journal of POLISH CIMAC

Faculty of Ocean Engineering & Ship Technology
GDAŃSK UNIVERSITY OF TECHNOLOGY

THE FUEL FLOW MODELLING IN THE FUEL PIPE IN MARINE ENGINE WITH CONSIDERING THE WAVE PHENOMENA

Mirosław Walkowski

Akademia Marynarki Wojennej
Instytut Konstrukcji i Eksploatacji Okrętów
81 – 103 Gdynia, ul. Śmidowicza 69
tel.: (58) 6262653, 6262665
email: mwal@interia.eu

Abstract

In the paper has been make an attempt to replace the conventional system of fuel dose control and injection passing angle with elecrtronic control system, which has been realized this manner, that selected hydraulic accumulator, injector C-R type and fuel dose controller has been attached the the marine engine.

It has been assumed, that by controlling the current impulse of controller it is possible to model whichever/any size of fuel dose, injected to the combustion chamber and to control the injection lasting time.

The wave phenomenon and the flow loss in the fuel pipe of high pressure have been presented.

Keywords: *common rail, fuel pipe, wave phenomena.*

1. Introduction

In the conventional and dividing injection pumps and in the fuel injection unit, the relation of pressing and fuel dosing process and the shaft or ring of bend rotation brings unfavorable change of the course of fuel injection parameter along with the change of the pumpshaft rotational speed.

Broadening the scope of optimal engine operation becomes possible, thanks to applying the electronic control system, which enables controlling the course of basic dosing and fuel injection parameters in the whole scope of engine operation, in the various surrounding conditions, considering also fuel properties.

The replacement of a conventional control system of fuel dose control and injection passing angle with the electronic control system in the test engine was realized this manner:

- in the place of location the conventional injector was fixed selected in advance C-R injector produced by the Bosch Company
- controlling the injection passing angle, size and multiplicity of the dose is realized thanks to the controller with the amplifier
- fuel at demanded pressure is delivered by the pump through the hydraulic accumulator (Fig. 1).

In the paper have been presented selected phenomena, which occur in the fuel pipe of high pressure at the moment of fuel injection.

2. Scheme of the CR feeding system in the laboratory/test engine JSB type.

The scheme of fuel system with attached common rail and fuel dose_controller Fig 2.1. Similar feeding system was applied in the Sulzer RT – flex60C engine. By controlling the current impulse

of controller it is possible to obtain the whichever modelling of size and multiplicity of fuel dose, which flows to the combustion chamber in engine cylinder.

The scheme of feeding system Common Rail in the one-cylinder test engine (JSB), which will replace the conventional fuel system, is presented below:

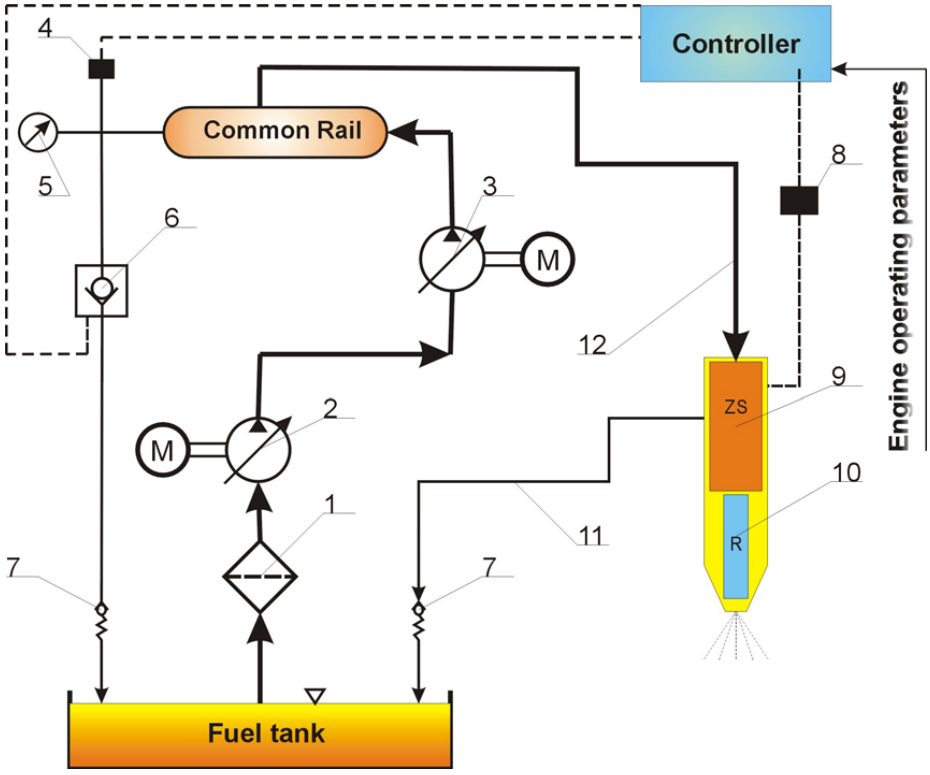

Fig. 2.1. Scheme of the injection system CR of JSB engine: 1 – filter, 2 – low pressure pump, 3 – high pressure pump, 4 – pressure sensor in the hydraulic accumulator, 5 – manometer, 6 – reversive valve with the opening control, 7 – overflow valve, 8 – signal amplifier, 9 – fuel dose controlling valve, 10 – pulverizer, 11 – low pressure fuel pipe (overflow), 12 – high pressure fuel pipe.

3. Impact waves dispersion in the fuel pipes

The wave flow in the centre, which fills the variable-section long pipe, is taken under consideration to describe the impact wave dispersion. The purpose is to explain the influence, which has the change of wave surface on the impact wave velocity.

It was assumed, that the surface A(x) of pipe section slowly changes along its length (axis x) – little at a length in order of the pipe dimension, it is called hydraulic. It offers a possibility of applying appoximation (called hydraulic), so it can be assumed that all values in the stream are constant along every cross-section pipe, and velocity is directed along its axis, in other words, the flow is treated as a quasi-one-dimension.

Such flow is defined by the equations:

$$\frac{\partial v}{\partial t} + v\frac{\partial v}{\partial x} + \frac{1}{\rho}\frac{\partial p}{\partial x} = 0 \tag{3.1}$$

$$\frac{\partial p}{\partial t} + v\frac{\partial p}{\partial x} - c^2\left(\frac{\partial \rho}{\partial t} + v\frac{\partial \rho}{\partial x}\right) = 0 \tag{3.2}$$

$$A\frac{\partial \rho}{\partial t} + \frac{\partial}{\partial x}(\rho v A) = 0 \tag{3.3}$$

The first of them is Euler equation, the second – adiabatic equation, and the third – continuity equation.

To explain this problem, it is enough to consider the pipe, where the change of surface A(x) is not only slow, but absolute value of the change is low at the whole pipe length as well.Then, the stream disorder, related to the variable section, would be also low and equations (3.1) – (3.3) could be linearized. At last, the initial conditions should be imposed to eliminate appearing any foreign disorder, which could affect on the impact wave motion; only disorders related to the change A(x) are taken under consideration. The purpose will be accomplished/achieved, if it would be assumed, that impact wave initially moves at constant velocity through constant-section pipe and section surface changes only on at/on the right from certain point (which is assumed as x = 0).

The linearized equations (3.1) – (3.3) have following form:

$$\frac{\partial \delta v}{\partial t} + v\frac{\partial \delta v}{\partial x} + \frac{1}{\rho}\frac{\partial \delta p}{\partial x} = 0$$

$$\frac{\partial \delta p}{\partial t} + v\frac{\partial \delta p}{\partial x} - c^2\left(\frac{\partial \delta \rho}{\partial t} + v\frac{\partial \delta \rho}{\partial x}\right) = 0$$

$$\frac{\partial \delta \rho}{\partial t} + v\frac{\partial \delta \rho}{\partial x} + \rho\frac{\partial \delta v}{\partial x} + \frac{\rho v}{A}\frac{\partial \delta A}{\partial x} = 0$$

where symbols without indexes mean constant values in the homogenous stream in the homogenous part of the pipe, and symbol δ means a change of these values in the variable-section pipe. Multiplying the first and the third of these equations adequately by ρa and a^2 and summing up all three equations, can be written:

$$\left(\frac{\partial}{\partial t} + (v+a)\frac{\partial}{\partial x}\right)(\delta p + \rho a \delta v) = -\frac{\rho v a^2}{A}\frac{\partial \delta A}{\partial x} \tag{3.4}$$

The general result of this equation is a sum of the general result of homogenous equation and the result of specific equation, which has non-zero right side. The first result is F(x – vt – at), where F is any function; it describes the sound disorder, approaching from the left side of the point, a – speed of sound. However, there are no disorders in the homogenous area, for $x < 0$, that is why it should be assumed that $F \equiv 0$. So, the result amounts to the non-homogenous equation integral:

$$\delta p + \rho a \delta v = -\frac{\rho v a^2}{v + a}\frac{\partial A}{A} \tag{3.5}$$

The impact wave moves from a left to the right side at velocity $v_1 > a_1$ in the immobile centre with given values p_1, ρ_1. However, the motion of centre at the back of impact wave is defined by the result (3.5) in the whole pipe area at left side from the point, which discontinuity has reached at particular moment. After the wave crossing, all values in every of the pipe section remain constant in time, i.e. equal to the values, which they obtain at the moment of discontinuity crossing: pressure p_2, density ρ_2 and velocity $v_1 – v_2$ (acoording to the symbols accepted in this paper, v_2 means velocity of gas in relation to the moving impact wave; its velocity in relation to the walls of

pipe is then equal to $v_1 - v_2$). In these symbols (after dispering various terms of these values) identity could be formulated as follows:

$$\frac{\partial A}{A} = -\frac{v_1 - v_2 + a_2}{\rho_2 (v_1 - v_2) a_2^2} \left(\delta p_2 + \rho_2 a_2 (\delta v_1 - \delta v_2) \right) \tag{3.6}$$

All values δv_1, δv_2, δp_2 could be defined by one of them, for instance δv_1. To this end dependence variations could be described as $\rho_1 v_1 = \rho_2 v_2$ and $p_1 + \rho_1 v_1^2 = p_2 + \rho_2 v_2^2$ for the discontinuity (at given p_1 i ρ_1) in the form of:

$$\rho_1 \delta v_1 = v_2 \delta \rho_2 + \rho_2 \delta v_2, \quad 2j(\delta v_1 - \delta v_2) = \delta p_2 + v_2^2 \delta \rho_2$$

where $j = \rho_1 v_1 = \rho_2 v_2$ is an undisordered stream value. The following relation should be also included

$$\delta p_2 = \frac{dp_2}{d\rho_2} \delta \rho_2$$

where derivate is calculated along the Hugoniot adiabatic curve. The calculations lead to a relation, which combine the change of impact wave velocity δv_1 in regard to the immobile gas before this change with the change of pipe section area, which means:

$$-\frac{1}{A}\frac{\delta A}{\delta v_1} = \frac{v_1 - v_2 + a_2}{v_1 a_2} \left(\frac{1 + 2 v_2 a_2^{-1} - h}{1 + h} \right) \tag{3.7}$$

where the symbol is introduced again

$$h = -\frac{j^2}{\rho_2^2}\frac{d\rho_2}{dp_2} = j^2 \frac{dV_2}{dp_2} \tag{3.8}$$

The coefficient w, standing before the square bracket, is positive. Thus, the quotient symbol $\delta v_1/\delta A$ depends on the expression symbol in this brackets, for every stable impact wave is positive and when $\delta v_1/\delta A < 0$. However, if any of discontinuity conditions $j^2 \frac{dV_2}{dp_2} < -1$ and $j^2 \frac{dV_2}{dp_2} < 1 + 2\frac{v_2}{a_2}$, which are caused by corrugation, is fulfilled, the expression in brackets becomes negative and when $\delta v_1/\delta A > 0$.

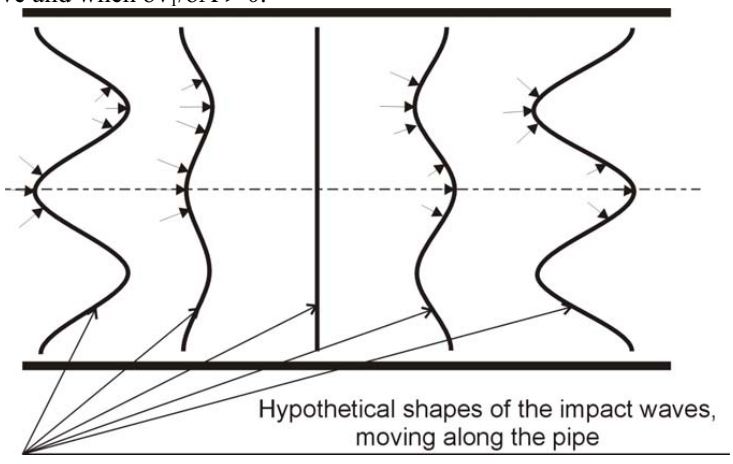

Fig. 3.1

The result offers possiblities of outlook explaining the origin of intability. Fig. 3.1 presents the "corrugated" surface of impact wave, moving to the right side; the directions of current lines are schematicly described by the pointers. During the impact wave crossing on the front protruding parts of the surface, the area δA increases and on the back parts of the surface it decreases. In case, if $\delta v_1/\delta A < 0$, it leads to the delay of the protruding parts and to the acceleration of the back parts and in relation to this the surface aims at smoothing.

On the contrary, in case if $\delta v_1/\delta A > 0$ the disorder of surface shape would demand: the protruding parts will be more protruding and the back parts will stay behind in higher extend.

4. Fuel flow in the elements with constant axis-symmetrical-section area

The d'Alembert solution, which was used by Allievi in the form of equations [5], was assumed to describe the unstable one-dimension fuel flow:

$$p(x,t) = P_0 + f_d\left(t - \frac{x}{a}\right)exp\left(-k_x\xi\frac{x}{a}\right) - f_u\left(t + \frac{x}{a}\right)exp\left(-k_x\xi\frac{x}{a}\right) \tag{4.1}$$

$$u(x,t) = u_0 + \frac{1}{a\rho}f_d\left(t - \frac{x}{a}\right)exp\left(-k_x\xi\frac{x}{a}\right) + \frac{1}{a\rho}f_u\left(t + \frac{x}{a}\right)exp\left(-k_x\xi\frac{x}{a}\right) \tag{4.2}$$

term, complemented byW. Bosch:

$$exp\left(-k_x\xi\frac{x}{a}\right) \tag{4.3}$$

taking under consideration the flow loss with the momentum at length x.

Symbols:

$$f_d\left(t - \frac{x}{a}\right) = P_d\left(t - \frac{x}{a}\right) = a\rho u_d\left(t - \frac{x}{a}\right) \tag{4.4}$$

- is an amplitude of pressure wave, which moves in the same direction as the flow at velocity **a** at length **x**;

$$-f_u\left(t + \frac{x}{a}\right) = P_u\left(t + \frac{x}{a}\right) = -a\rho u_u\left(t + \frac{x}{a}\right) \tag{4.5}$$

- is an amplitude of pressure wave, which moves in the other direction than the flow at velocity **a** at length **x**;

$$a = x/t \tag{4.6}$$

– speed of sound in the fuel;

$$k_x = \frac{4\pi}{A}\nu\rho \tag{4.7}$$

– is a flow loss coefficient, considering the fuel mass momentum according to W. Bosch.

$\mathbf{P_0}$ – constant pressure before the disorder [N/m²];
$\mathbf{u_0}$ - initial fuel velocity [m/s];
ρ - fuel density [kg/m³];
ν - kinematic viscosity of fuel [m²/s];
A - flow section area[m²];
ξ - fuel flow momentum coefficient (according to Burman and Deluca [1]).
By introducing the same symbols as in the scheme, it is obtained:
- in case of $l = x_m - x = 0$

$$P(x_m,t) = P_m(t) = P_0 + P_{dm}(t) + P_{um}(t) \tag{4.8}$$

$$u(x_m,t) = u_m(t) = u_0 + u_{dm}(t) + u_{um}(t) \tag{4.9}$$

- if $l = x_n - x = 0$

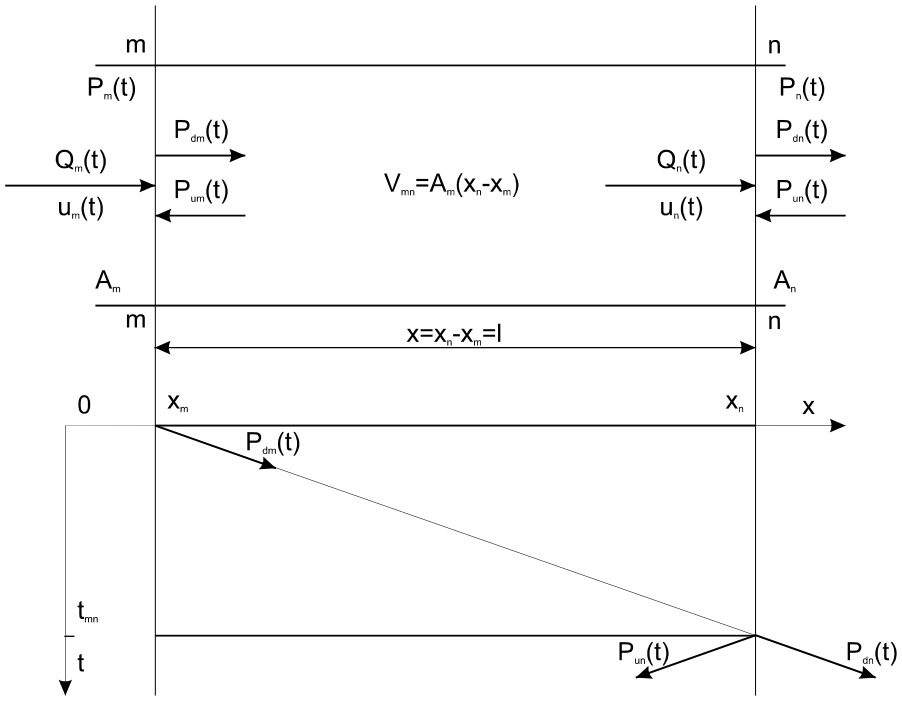

Fig. 4.1. Scheme of unstable fuel flow in the axis-symmetrical pipe.

$$P(x_n,t) = P_n(t) = P_0 + P_{dn}(t) + P_{un}(t) \tag{4.10}$$

$$u(x_n,t) = u_n(t) = u_0 + u_{dn}(t) + u_{un}(t) \tag{4.11}$$

- where $l = x_m - x_n > 0$,

$$P_n(t) = P_0 + exp\left(-k_{mn}\xi\frac{l}{a}\right)\cdot P_{dm}\left(t-\frac{l}{a}\right) + \\ + exp\left(-k_{mn}\xi\frac{l}{a}\right)\cdot P_{um}\left(t+\frac{l}{a}\right) \tag{4.12}$$

$$u_n(t) = u_0 + exp\left(-k_{mn}\xi\frac{l}{a}\right)\cdot\frac{1}{a\rho}P_{dm}\left(t-\frac{l}{a}\right) - exp\left(k_{mn}\xi\frac{l}{a}\right)\cdot\frac{1}{a\rho}P_{um}\left(t+\frac{l}{a}\right) \tag{4.13}$$

from the equations (8.60) and (8.62) follows relations:

$$P_{dn}(t) = exp\left(-k_{mn}\xi\frac{l}{a}\right)\cdot P_{dm}\left(t-\frac{l}{a}\right) \tag{4.14}$$

$$P_{un}(t) = exp\left(k_{mn}\xi\frac{l}{a}\right)\cdot P_{um}\left(t+\frac{l}{a}\right) \tag{4.15}$$

$$P_{un}(t) = exp\left(-k_{mn}\xi\frac{l}{a}\right)\cdot P_{um}\left(t-\frac{l}{a}\right) \tag{4.16}$$

Volumetric stream of fuel, flowing through the sections m-m and n-n is defined by relations:

$$Q_m(t) = \frac{A_m}{a\rho}\left[P_{dm}(t) - P_{um}(t)\right] \tag{4.17}$$

$$Q_n(t) = \frac{A_n}{a\rho}\left[P_{dn}(t) - P_{un}(t)\right] \tag{4.18}$$

$$Q_n(t) = Q_m(t - t_{mn}) - \frac{V_{mn}}{E}\frac{dP_n}{dt}(t) \tag{4.19}$$

$$Q_n(t) = \frac{A_m}{a\rho}\left[P_{dm}(t - t_{mn}) - P_{um}(t - t_{mn})\right] - \frac{V_{mn}}{E}\frac{dP_n}{dt}(t) \tag{4.20}$$

where E is a fuel compressibility module [N/m^2].

4.1. Fuel flow through the intermitten axis-symmertical-section of elements [2]

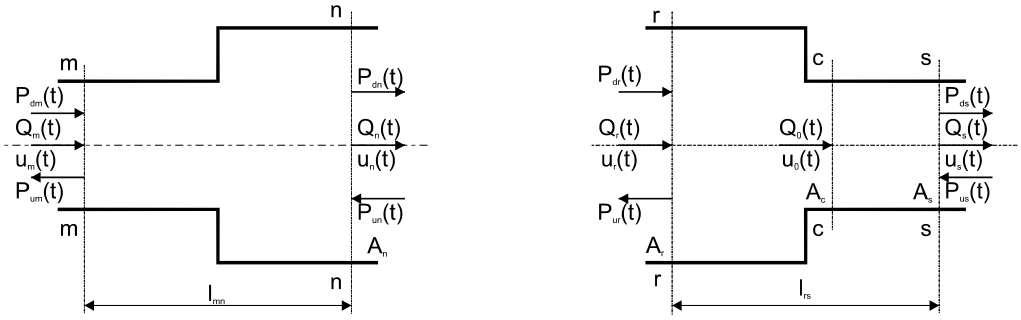

Fig. 4.2. Scheme of unstable fuel flow in the axis-symmetrical pipe.

The courses of pressure waves in the appropriate sections are equal to:

$$P_{um}(t) = P_{dm}(t) + C_m\left\{1 - D_m\left[P_{dm}(t) - P_{um}(t - t_{mn})\right]\right\}^{0.5} - C_m \tag{4.21}$$

$$P_{dn}(t) = P_{um}(t) - C_n\left\{1 - D_m\left[P_{dm}(t - t_{mn}) - P_{un}(t)\right]\right\}^{0.5} + C_n \tag{4.22}$$

$$P_{ur}(t) = P_{dr}(t) + C_r\left\{1 - D_r\left[P_{dr}(t) - P_{us}(t - t_{rs})\right]\right\}^{0.5} - C_r \tag{4.23}$$

$$P_{ds}(t) = P_{us}(t) - C_s\left\{1 - D_r\left[P_{dr}(t - t_{rs}) - P_{us}(t)\right]\right\}^{0.5} + C_s \tag{4.24}$$

Substitutions:

$$t_{mn} = \frac{l_{mn}}{a} \qquad t_{rs} = \frac{l_{rs}}{a} \tag{4.25}$$

$$C_m = 0.5\,a^2\rho\,k_m\frac{k_m + 1}{k_m - 1} \tag{4.26}$$

$$C_n = 0.5\,a^2\rho\frac{k_m + 1}{k_m - 1} \tag{4.27}$$

$$C_r = 2\,a^2\rho\frac{K + 1}{3K^2 - \left(K^2/k_r\right) - 2} \tag{4.28}$$

$$C_s = 2\,a^2\rho K\frac{K + 1}{3K^2 - \left(K^2/k_r\right) - 2} \tag{4.29}$$

$$D_m = \frac{8(k_m - 1)}{a^2 \rho (k_m + 1)^2} \tag{4.30}$$

$$D_r = 2\frac{3K^2 - \frac{K^2}{k_r} - 2}{a^2 \rho (K+1)^2} \tag{4.31}$$

$$k_m = \frac{A_n}{A_m} \quad k_r = \frac{A_r}{A_s} \quad K = \frac{u_s}{u_r} = \frac{A_0 u_0}{A_s u_r} \tag{4.32}$$

Symbols:

$\mathbf{A_0, A_m, A_n, A_r, A_s}$ – surface area of appropriate sections [m²];

$\mathbf{u_0, u_r, u_s}$ – mean velocity of fuel flow[m/s].

Fig. 4.3. The volumetric stream of fuel, flowing through the variable sections, is defined by equations:

- throttles:

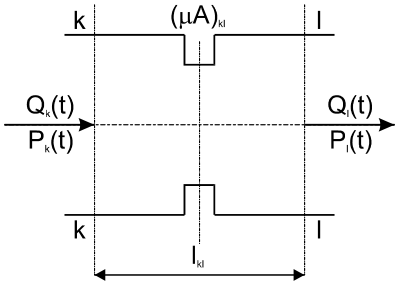

Fig. 4.3.

$$Q_l(t) = \left(\frac{2}{\rho}\right)^{0.5} (\mu A)_{kl}\, sgn\, kl \left[P_k(t) - P_l(t)\right]^{0.5} \tag{4.33}$$

where:

$$sgn\, kl \begin{cases} 1 & dla \quad P_k(t) > P_l(t) \\ 0 & dla \quad P_k(t) = P_l(t) \\ -1 & dla \quad P_k(t) < P_l(t) \end{cases} \tag{4.34}$$

$(\mu A)_{kl}$ - is an equivalent flow section between the sections k-l [m²];

Q_{kn}, Q_{ln} – are volumetric streams of fuel, which follows from the leak [m³/s].

4.2. Mild change of direction – bend

The Weisbach formula of loss coefficients for the circular-section bends is following:

$$\xi = \left[0{,}131 + \left(\frac{d}{\rho}\right)^{3{,}5}\right] \frac{\alpha^o}{90^o}$$

In the table are given loss coefficient values, which are calculated according to above given formula for various angles α and relation d/ρ.

The more detailed researches proves, that loss coefficient ξ depends not only on the relation d/ρ and the angle α, but also on the Reynolds number and the roughtness of the bend.

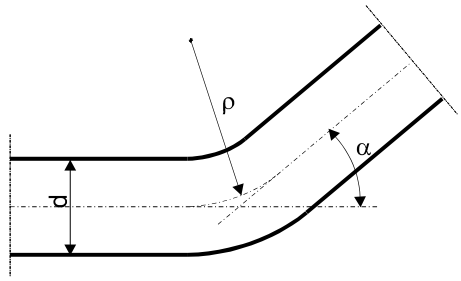

Fig. 4.4. Circular-section bend

5. Conclusions

Adapting the individual elements of electronic control system , which means an electronic control injector, a fuel dose controller with the amplifier and a common rail – for the conventional JSB engine there is a possibility of obtaining fully controlled process of electronic control.

By controlling the current impulse it is possible to control size of fuel dose and also to model the manifold injection, which is characteristic of the electronic control injection systems.

The simulation calculation were conducted basic of theoretical and empirical relations without verification and tests on actual model of valve and that is why they should be treated as a rated results.

To verify the accepted model it would be necessary to perform empirical studies on the actual valve and use obtained results to revise the approved calculation model.

Literature

[1] Burman P.G., Deluca F.: *Fuel injection and controls for internal combustion engines*. The technical Press LTD, Londyn 1962.

[2] Gałąska M., Kaczmarczyk J., Maruszkiewicz J.: *Hydromechanika stosowana.* Wojskowa Akademia Techniczna im. J. Dąbrowskiego. Warszawa 1972

[3] Guillon M.: *Teoria i obliczanie układów hydraulicznych*. WNT. Warszawa.

[4] Landau L. D., Lifszyc E. M.: *Hydrodynamika*. Wydawnictwo Naukowe PWN. Warszawa 1994

[5] Ochocki W.: *Numerycznie sterowane systemy wtrysku paliwa silników wysokoprężnych*. Wydawnictwo Poznańskiego Towarzystwa Przyjaciół Nauk. Poznań 1994.

[6] Walkowski M.: *Modelowanie działania zaworu sterującego dawką paliwa w układzie wtrysku typu common rail*. VII Międzynarodowa Konferencja Naukowa SILNIKI GAZOWE 2006. Zeszyty Naukowe Politechniki Częstochowskiej 162. MECHANIKA 26. Wydział Inżynierii Mechanicznej i Informatyki. ISSN 0867 – 3462; ISBN 83 – 7193 – 302 – 9; ISBN 978 – 83 – 7193 – 302 – 8, Str. 550 – 560. Częstochowa 2006.

[7] Walkowski M.: *Selected problems of modelling the working of container injection systems of common rail type.* (str, 477 – 485). Journal of POLISH CIMAC, EXPLO – DIESEL & GAS TURBINE '07. VINTERNATIONAL SCIENTIFIC – TECHNICAL CONFERENCE. Gdańsk – Stockholm – Tumba POLAND – SWEDEN 11 – 15 May 2007. ISSN 1231 – 3998.GDAŃSK UNIVERSITY OF TECHNOLOGY, Faculty of Ocean Engineering and Ship Technology, Department of Ship Power Plants.

[8] Walkowski M.: *Determining the characteristics of control valve in a common rail injection system of a combustion engine*. (str. 94 – 100). SILNIKI SPALINOWE. Czasopismo naukowe Nr 2007 – SC2, PL ISSN 0138-0346. Wydawca: Polskie Towarzystwo Naukowe Silników Spalinowych.

Journal of POLISH CIMAC
Faculty of Ocean Engineering & Ship Technology
GDAŃSK UNIVERSITY OF TECHNOLOGY

RESEARCH OF VARIATION OF GAS TURBINE ENGINE WORK PARAMETERS CHANGES EQUIPPED WITH CHANGEABLE GEOMETRY OF AXIAL COMPRESSOR FLOW PASSAGE

Paweł Wirkowski

The Polish Naval Academy
ul. Śmidowicza 69, 81-103 Gdynia, Poland
tel.: +48 58 6262756, fax: +48 58 6262963
e-mail: pawir@o2.pl, p.wirkowski@amw.gdynia.pl

Abstract

The paper deals with problem influence of changes variable stator vanes axial compressor settings of gas turbine engine on work parameters of compressor and engine. Incorrect operation of change setting system of variable vanes could make unstable work of compressor and engine. This paper presents theoretical analysis of situation described above and results of own research done on real engine. The next there are presented results of mathematical modelling of changes of gas turbine engine work parameters during change of angle setting of axial compressor variable stator vanes but in the most wide angle range than in real research.

Keywords: *gas turbine engine, axial compressor, variable stator vanes, modelling*

1. Introduction and purpose of research

When in compressor construction is assembled system of setting change of variable stator vanes its task is made optimal cooperation engine units during permanent improvement of compressor characteristic. Perturbations in operation of this system could cause changes in work of compressor and engine similar like changes caused by changes of rotational speed or polluted interblades ducts of compressor.

Compressor stage unitary work on radius is defined on base of equitation of angular momentum and has form (Fig. 1):

$$l_{st} = \omega r(c_{2u} - c_{1u}) = u\Delta c_u = u\Delta w_u \tag{1}$$

where:

ω – angular velocity, u – tangential velocity, r – rotor radius,
c_{1u}, c_{2u} – circumferential components of air stream absolute velocity on inlet and outlet rotor blades on radius r,
Δc_u, Δw_u – air stream whirl in rotor.

That work is constant on whole depth of rotor blade. The sum of works is unitary work of stage. Involved change of variable stator vanes angle setting during kept at a constant level rotational velocity (constant u) caused change of air stream inlet angle in rotor vane β_1 (Fig. 1). It caused change of axial component of air stream absolute velocity on inlet c_{1a} what is equivalent with change of air mass flow $\dot{m}$ and change of air stream whirl Δw_u in rotor. It influences on efficiency and work of stage [2].

Purpose of investigations made on real engine was determination influence of incorrect operation of axial compressor inlet guide variable stator vanes control system of gas turbine engine

on compressor and engine work parameters.

Compressor characteristic is relationship between compression ratio π^*_S, compressor efficiency η_S and air flow mass $\dot{m}$ and compressor rotational velocity n. It makes possible to determine the best condition of compressor and another engine units mating. The characteristic is using to select optimal conditions of air flow regulation and assessment of operational factors on compressor parameters.

Therefore compressor should be so controlled in operational range of rotational velocity that the compressor and engine mating line has a stock of stable work. The main rule of compressor control during change of their rotational velocity or flow intensity is to keep up the stream inlet angles i value near zero. One of the most popular ways of axial compressor control is changing their flow duct geometry by application of inlet guide stator vanes or variable stator vanes of several first compressor stages [2].

This solution makes possible to change of air stream inlet angle on rotor blades of compressor stages by change of stator vanes setting angles during change of compressor rotational velocity. Fig. 1 illustrates, on example one stage of compression, rule of regulation of variable stator vanes.

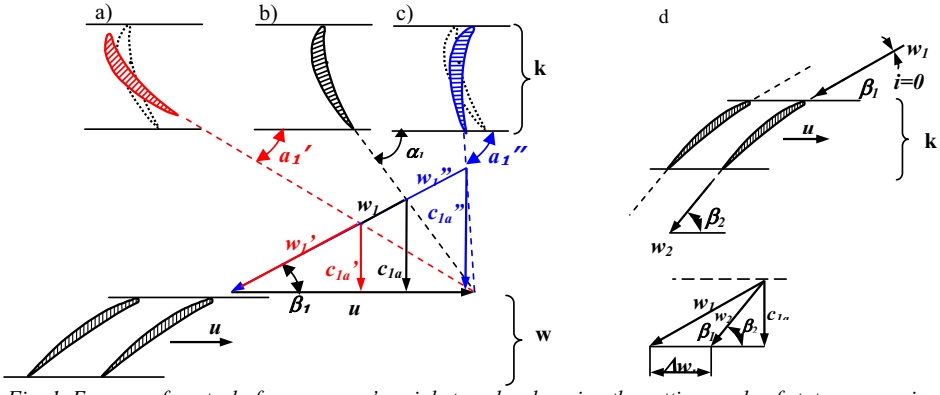

Fig. 1. Essence of control of compressor's axial stage by changing the setting angle of stator vanes ring at changeable air flow velocity; a) decreased axial velocity, b) calculation axial velocity, c) increased axial velocity, d) schema of flow round of axial compressor rotor blades during constant rotor speed and constant air stream inlet angles; ***k*** *– variable stator vanes ring,* ***w*** *– rotor vanes ring*

For average values with operational range of compressor rotor speed is situation on Fig. 1b – speed values and directions with subscript „*1*". In this situation is intermediate angle setting of stator vanes. Air stream inlet angle on rotor blades do not cause disturbance of stream flow by interblades ducts. For lower values of compressor rotor speed and in consequence lower values of absolute axial component velocity c_{1a}', it is necessary to reduce the stream outlet angle of variable stator vanes α_1 (Fig. 1a). The angle reduction range should allow keeping the same value of stream inlet angle on rotor blades. Analogical situation takes place during work of compressor with higher rotational speed. For higher rotational speed absolute axial component speed c_{1a}'' increases. In this situation for keeping stable work of compressor and in consequence constant value of stream inlet angle on rotor blades, it is necessary to increase the value of stream outlet angle of variable stator vanes – Fig. 1c. Application in gas turbine engine construction of control system of flow ducts geometry has a bearing on run inertance of unstable processes.

2. Object of research

The object of researches is type DR77 marine gas turbine engine, which is part of power transmition system of war ship. It is three-shaft engine with can-ring-type combustor chamber and reversible power turbine.

In compressor construction configuration of this engine there are used inlet guide stator vanes which make possibilities to change setting angle incidance (change of compressor flow duct geometry) in depend on engine load. This process is operated by control system which working medium is compressed air received from last stage of high pressure compressor. On Fig. 2 is presented block diagram of flow control signal of variable stator vanes system.

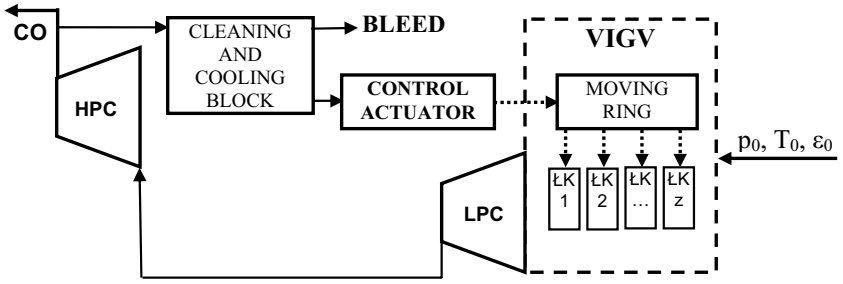

Fig. 2. Block diagram of stator vanes change setting mechanism LPC; CO – combustor, HPC – high pressure compressor, LPC – low pressure compressor, ŁK – variable stator vane, VIGV – variable inlet guide vanes

Compressed air from last stage of high pressure compressor is supllied to working space of control actuator by cleaning and cooling block. Compressed air exerts pressure on control actuator elements. It causes moving of control piston which is connected with moving ring. This ring moves on circumference of low pressure compressor body. Ring is connected with variable stator vanes by levers. When the ring is moving stator vanes realize rotational motion changing the air stream outlet angle α_1 (Fig. 1).

In cleaning and cooling block are holes. During researches air stream was bleeded by holes and less air was supplied to actuator. It caused change of setting angle α_{KW} of variable stator vanes. In consequence of that change flow duct geometry was changed.

Experiment was carry out an engine load $0{,}5P_{nom}$. For this load setting angle of variable vanes has value $\alpha_{KW} = -4^o$. During change engine load in whole range from idle to full load setting angle α_{KW} of variable vanes changes in range from -18^o to $+18^o$. Realizing experiment a few parameters of engine work was measured and registered for three different setting angle α_{KW} of variable vanes: A— $\alpha_{KW} = -4^o$, B— $\alpha_{KW} = -11^o$, C— $\alpha_{KW} = -18^o$. Tab. 1 presents measured and registered in this same time parameters of engine work.

Tab. 1. Parameters of engine DR77 work measured during researches

Parameter	Measurement range	Unit	Parameter name
n_{LPC}	0 – 20000	[min^{-1}]	low pressure rotor speed
n_{HPC}	0 – 22000	[min^{-1}]	high pressure rotor speed
n_{PT}	0 – 10000	[min^{-1}]	power turbine rotor speed
p_1	-0,04 – 0	[MPa]	subatmospheric pressure on compressor inlet
p_{21}	0 - 0,6	[MPa]	air pressure on low pressure compressor outlet
p_2	0 - 1,6	[MPa]	air pressure on high pressure compressor outlet
p_p	0 - 10,0	[MPa]	fuel pressure before injectors
T_1	203 - 453	[K]	air temperature on compressor inlet
T_{42}	273 - 1273	[K]	exhaust gases temperature on inlet power turbine

3. Results of research

Fig. 3 presents results of experiment. There are presented those parameters which are the most sensitive on change of LPC guide vanes setting angle. Change vanes setting from position *A* to

position *C* caused increase air flow resistance by stator vanes. In consequence of that subatmospheric pressure on compressor inlet p_1 decreases. It causes pressure decrease in next parts of compressor and engine flow duct (Fig. 3bc). In this way reduced air density flowing by compressor, for stable quantity of stream fule supllied to combustor, causes increase of compressors rotor speed. The most visible is increase of low pressure compressor rotor speed (Fig. 3a) caused by directly influence on this compressor incorectly setting variable guide stator vanes.

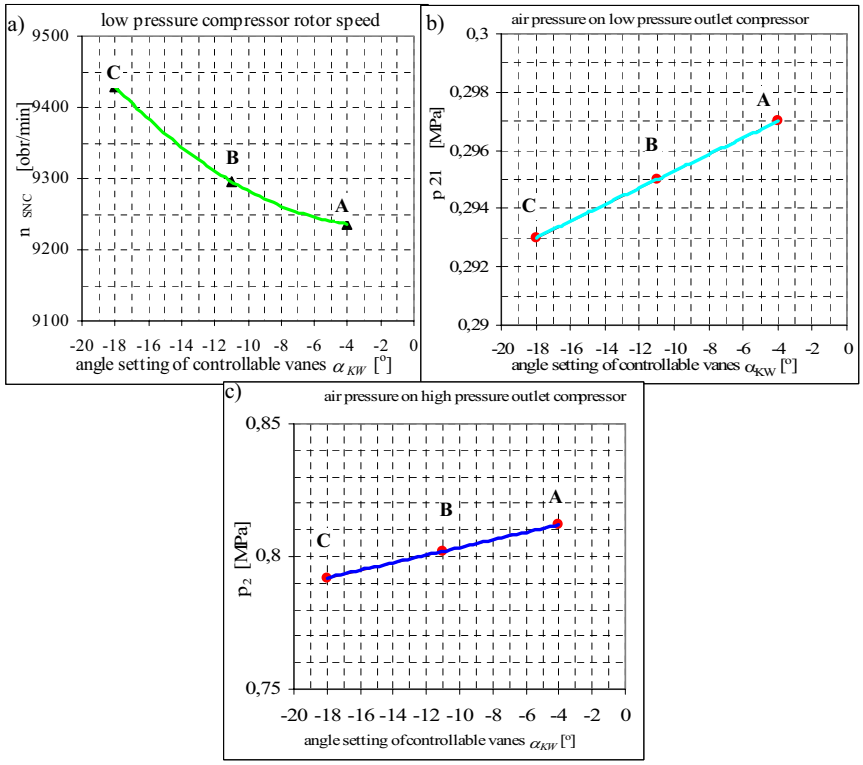

Fig. 3. Change of engine work parameters values in function of variable inlet guide stator vanes setting angle: A - α_{KW} = - 4°, B - α_{KW} = - 11°, C - α_{KW} = - 18°

Gasodynamical connection between low pressure compressor and high pressure compressor absorbs disturbances work of low pressure compressor which are transferred on high pressure compressor. Therefore range of change high pressure compressor rotor speed is lower than low pressure compressor. In this experimental it is below 1% and it is in measuring error range.

Change of subatmospheric pressure is above 5% stable value of this parameter. Changes of low and high pressure compressor outlet presure are adecuately above 1,3% and above 2,4% undisturbed value of angle setting α_{KW} = - 4°.

Changes of pressure and air mass flow intensity values accompanied disturbing work of compressor, during constant fuel mas flow intensity in combustor, caused enrichment of fuel mixture. As a result of that, temperature combustor outlet gases increases. In experiment was confirmed tendency changes of gases tempertaure values even though range of thoses changes is in measuring error range.

On the base of results of experiment there were determined mathematical equations modelling changes of particular engine work parameters in function of variable inlet guide stator vanes setting angle α_{KW} :

$$n_{SNC} = 0{,}7449\alpha_{KW}^{\ 2} + 2{,}602\alpha_{KW} + 9234{,}5 \quad (2)$$

$$n_{SWC} = 0{,}0204\alpha_{KW}^{\ 2} - 1{,}1224\alpha_{KW} + 12598 \quad (3)$$

$$p_1 = -10^{-6}\alpha_{KW}^{\ 2} - 10^{-6}\alpha_{KW} + 0{,}0077 \quad (4)$$

$$p_{21} = 10^{-16}\alpha_{KW}^{\ 2} + 0{,}0029\alpha_{KW} + 2{,}9814 \quad (5)$$

$$p_2 = 2\cdot 10^{-16}\alpha_{KW}^{\ 2} + 0{,}0143\alpha_{KW} + 8{,}1771 \quad (6)$$

$$T_{42} = 0{,}0204\alpha_{KW}^{\ 2} + 0{,}1633\alpha_{KW} + 526{,}33 \quad (7)$$

Fig. 4 presents results of solution of an mathematical equations describing of changes of engine work parameters values. Modelling was cary out an state engine load what was equivalent unchangable fuel mass flow. In this case range of change of variable inlet guide stator vanes setting angle α_{KW} was widen from -18° to +18°. Researches in range α_{KW} from -4° to +18° were not possilble to realize on real engine. It is caused by technical restrictions on the engine.

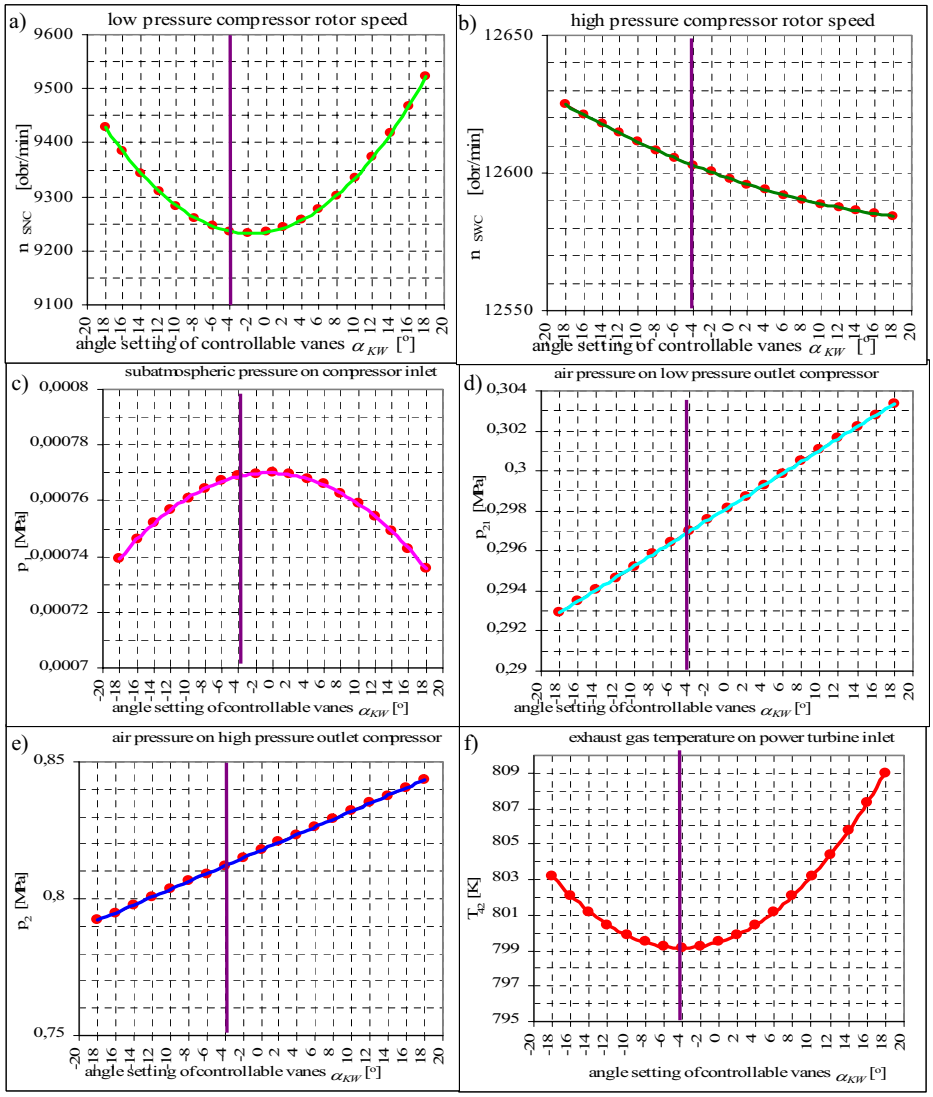

Fig. 4. Change of engine work parameters values in function of variable inlet guide stator vanes setting angle gotten during mathematical simulation

4. Conclusions

Change of variable inlet guide stator vanes setting angle α_{KW} from -4° to +18° caused increase of flowing air stream outlet angle α_1 (Fig. 1). It decreases air flow drag on low pressure compressor inlet that caused decrease of subatmospheric pressure. During keeping constant engine load (constant fuel mass flow) absolute axial component velocity c_{1a} increases. It exerts an influence on air mass flow $\dot{m}$ increase. Simultaneously the absolute axial component velocity c_{1a} increase caused decrease of air stream whirl in rotor Δw_u. The effect of above is reduction of the compressor stage unitary work – equation (1). In consequence of that low pressure compressor rotor speed increases (Fig. 4a). In connection with decrease of subatmospheric pressure it caused increase of air pressure on low pressure outlet compressor (Fig. 4d). In spite of slight decrease of high pressure compressor rotor speed the increase of air pressure on low pressure outlet compressor involves increases of air pressure on high pressure outlet compressor (Fig. 4e). This slight decrease of high pressure compressor rotor speed caused increase of gases flow drag in next gas turbine engine units for the combustor. The effect of above is slight increase of exhaust gas temperature on power turbine inlet.

Multi-shaft construction of gas turbine engine reduces effects of incorrectly setting of variable stator vanes. Therefore compressors of three-shaft gas turbine engine do not require variable stators vanes as many stages as compressor of two-shaft engine with the same achievements.

Preliminary researches confirm necessity for making inspection of correct operation of variable stator vanes system control. It makes possibility of elimination this factor from group of factors informing about deteriorating technical state of engine which are identified during diagnostic inspections.

References

[1] Charchalis A.: *Diagnostics of marine gas turbine engines* (in Polish). Published by Polish Naval Academy, Gdynia, 1991.

[2] Dżygadło Z. et al.: *Rotor units of gas turbine engines* (in Polish). Transport and Telecommunication Publishing House (WKiŁ), Warszawa, 1982.

[3] Korczewski Z.: Wirkowski, P., *Modelling gasodynamic processes within turbine engines' compressors equipped with variable geometry of flow duct*, IV International Scientifically-Technical Conference "Explo-Diesel & Gas Turbine '05", Gdańsk-Międzyzdroje-Kopenhaga, Wyd. Politechnika Gdańska, Gdańsk 2005, 227-236.

[4] Marschal D.J., Muir D.E., Saravanamuttoo H.I.H.: *Health Monitoring of Variable Geometry Gas Turbines for the Canadian Navy*, The American Society of Mechanical Engineers 345 E, 47 St., New York, N.Y.10017.

[5] Wirkowski, P., *Influence of changes of axial compressor variable stator vanes setting on gas turbine engine work*, V International Scientifically-Technical Conference POLISH CIMAC "Explo-Diesel & Gas Turbine '07", Gdańsk-Stockholm-Tumba, Published by Gdańsk University of Technology, Gdańsk 2007, 511-518.

[6] Wirkowski P.: *Modelling the characteristics of axial compressor of variable flow passage geometry, working in the gas turbine engine system*, Polish Maritime Research, No 3/2007, Published by Gdańsk University of Technology, Gdańsk 2007, 27-32.

[7] Wirkowski P.: *Gas turbine engine work parameters in conditions of changeable geometry of axial compressor flow duct,* 11TH International Conference „Computer systems aided science, industry and transport"- TRANSCOMP 2007, ZAKOPANE 3-6 December 2007, Published by Radom University of Technology, Radom 2007, 383-388.

Journal of POLISH CIMAC
Faculty of Ocean Engineering & Ship Technology
GDAŃSK UNIVERSITY OF TECHNOLOGY

INVESTIGATION OF FLUIDIZED BED OF THE PHYSICAL MODEL OF THE MARINE FLUIDIZED BED BOILER

Wojciech Zeńczak

Szczecin University of Technology
41 Piastów Ave, PL 71-065 Szczecin, Poland
tel.: +48 91 4494431, fax: +48 91 449 4737
e-mail: wojciech.zenczak@ps.pl

Abstract

The article provides the specification of the experimental testing method of the heat exchange between the fluidized bed and the heating surface immersed therein during ship's movements on the waves causing interference. The research works have been conducted on physical model of fluidized bed boiler positioned in the cradle simulating the vessel's motion on regular wave of sinusoidal type. The design features of the test stand make it possible to conduct the testing for the processes occurring in the boilers both with bubbling and the circulating fluidized beds. The method of determination of the heat transfer coefficient has been specified. The presented research results of the heat transfer coefficient have proven that the conditions of heat transfer are of explicitly local nature strongly related with the mass of the material present in the fluidizing column, flow-through conditions, fluidizing column inclination angle from vertical and swinging movement of the platform. The testing results encourage to continue the research works on a larger scale aiming to verify the hypothesis that in the shipboard conditions the circulating fluidized bed is less susceptible to the ship's rolling than the bubbling fluidized bed and that the significant conditions of heat exchange are not impaired.

Keywords*: environment protection, heat exchange, ship, fluidized bed boiler, coal*

1. Introduction

Diesel engines prevail in the modern shipboard propulsion systems. This predominant position results from their high efficiency which in case of two-stroke low-speed engines exceeds 50% as well as the possibility of burning low quality cheaper fuels. However, while developing the future ship's propulsion systems one needs to account for the decreasing oil resources and the experience proving the strong influence of some political events or natural disasters on the oil prices. Thus the research in the field of application of the alternative fuels is of urgent nature at present. The basic role here is played by coal which already in the past fuel crises proved to be a sound alternative fuel. Its resources are sumptuous as according to the USA Energy Information Administration with the current global energy consumption maintained the coal resources would suffice for 600 years. Also in terms of price the present cost of energy production from coal is approximately 6 times less than that from oil [6].

However, a serious deficiency of coal as a fuel is high emission of CO_2. As much as 41% of global emission of this compound in the energy production comes from coal combustion. Within the land power engineering it is planned therefore to apply systems separating CO_2 to store it in the earth and to apply advanced power engineering technologies. The fluidizing reactors within IGCC are considered as particularly attractive in view of their high efficiency and purity of the energy production [5]. Because of the size of the installations and degree of complexity of the system, it is not suitable at the present stage to be applied on board ships. However, coal application can be assumed as fuel on ships by its combustion in high efficiency fluid-bed boilers. The problem of CO_2 emission may be solved on the other hand in the future by its separation from exhaust gases and subsequent release into the water [4]. The studies of the possibility of application of these

boilers on ships have been assumed by the end of the 1980' of the last century in Germany [3]. In view of the shortage of the information on the experimental research in this respect a test stand for the pilot testing of the physical model of the "shipboard" fluidized bed boiler has been built in the Department of Heat Engines and Marine Power Plants of the Faculty of Maritime Technology of the Szczecin University of Technology [1].

2. Measurement Apparatus and Technique

The specially designed and executed test stand enables the testing to be conducted for the processes occurring in the boilers both with the bubbling and circulating fluidized beds in the conditions simulating the ship's motion on waves. The detailed diagram and the specification of the stand has been provided by the author in the study [1]. The Fig. 1 shows the view of the stand while the column is inclined (a) and the interior of the fluidizing chamber (b).

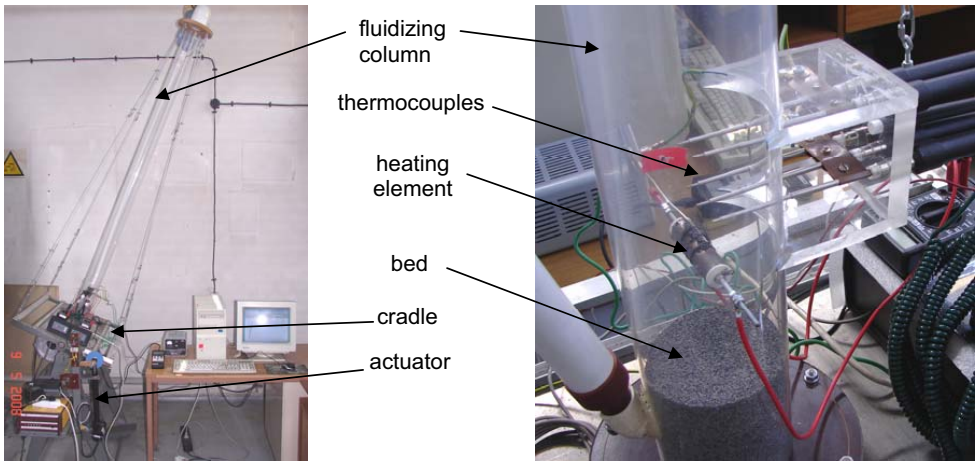

a) b)

Fig.1. View of the stand

A static method has been adopted for the investigation of the local heat transfer coefficients between the fluidized bed and the heating surface immersed therein. This method is based on the energy balance in the stabilised condition of the set-up: heating surface – fluidized bed. A pipe with electric spiral (electric heater) forms the heating surface. The determined value of the local coefficient of heat transfer α_{av} is a mean value that can be obtained from the Newton's equation

$$\alpha_{av} = \frac{\dot{Q}}{A\Delta t}, \tag{1}$$

where:

$\dot{Q}$ – heat stream supplied to the set-up,

A – heating pipe surface,

Δt – difference of the mean temperatures of heating pipe surface and fluidized bed.

The heat stream is determined on the basis of the measurement of the electric current supplying the heating spiral placed inside the pipe. In the preliminary investigations the provision has been made for the temperature readout in 6 points of the bed above the heater, the points located in two rows in the plane of symmetry of column and heater. In the row situated closer to the heater three thermocouples are positioned, and in the farther row three remaining ones. The temperature of the

heater wall is measured by use of thermocouple made fast to its surface from the top. As the pipe is made of copper thus the material of high heat conductivity coefficient, a uniform temperature distribution all over its surface has been assumed. Additionally the interior of the pipe where the electric spiral is placed has been filled with sand thus increasing its thermal inertia and the uniform heating of the wall. Teflon bar/plugs have been inserted in both ends of the pipe to reduce the heat losses from the fore walls. Heat transfer coefficients have been calculated as average values from at least three temperature readouts upon reaching the stable condition by the set-up. The layout of heater and thermocouples inside the column which are also visible in the Fig. 1b is shown in Fig. 2.

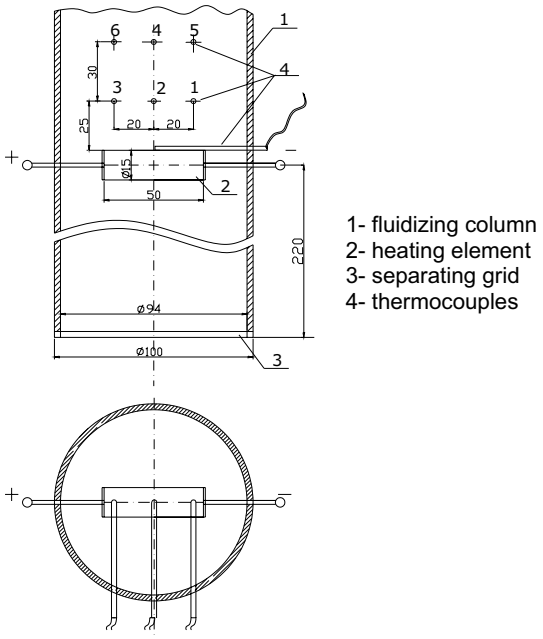

Fig. 2. The positioning of heater and thermocouples in fluidizing column

Poppy seeds have been used for the purpose of the pilot testing of heat transfer coefficient at the stand in question. The seeds have the shape similar to ball of diameter d = 1 mm and the density nearly three times less than sand, ie ρ_S = 714 g/m^3. The velocity of the beginning of the fluidizing (v_{lkr}) for poppy seeds is 0.17 m/s. Owing to this it has been possible to apply lower capacity blower and eliminate the risk of scratching the column.

3. The Results of Testing and their Analysis

The described method has been used at the erected stand to conduct several pilot measurements in respect to various aspects of bed behaviour. These allowed to evaluate the model suitability for conducting the experiments on a larger scale in the future. The first test aimed at determination of the local heat transfer coefficients for the bed of stationary height H=12 cm , in the function of fluidizing air jet velocity. The bed transition into fluidized state has been observed at air velocity of v_f=2.2 m/s. The air velocity has been increased in steps until the moment when the grains were raising from the column which was observed at the velocity of 6.2 m/s. Since that moment the transition to the circulating fluidized bed took place owing to the system of grain reverse in the model. The heat transfer coefficients have been determined on the basis of the measurements for each velocity, upon reaching the stabilised condition by the set-up. The power of the heater during

the experiment has been maintained at the constant level of $\dot{Q}$= 45 W. Figure 3 presents the values of the local heat coefficients in the column axis at the height of 25 and 55 mm above the heater (points 2 and 4 in diagram in Fig. 2).

Initially the coefficient value increase followed by the marked decrease has been observed along with the increase of the air velocity. The moment of the rapid drop in the values of the heat transfer coefficients occurred as the deposited material arose and began to circulate. This is explained by the fact that air velocity increase is accompanied by a large decrease of material concentration [2]. As evident from the graph of the local values of the heat transfer coefficients in points 2 and 4 differ slightly. Still somewhat bigger value of the coefficient in the point closer to the heater prevails

For the comparison the same figure shows the values of the local heat transfer coefficients in clean air without poppy seeds (H=0). As can be seen the heat transfer coefficients in the bubbling phase are significantly higher and only upon its dilution and transition into the circulation phase these get closer to the values achieved in clean air. The heat transfer coefficients in air grow in the obvious manner together with velocity, the value of the coefficient being somewhat higher at the point closer to the heater.

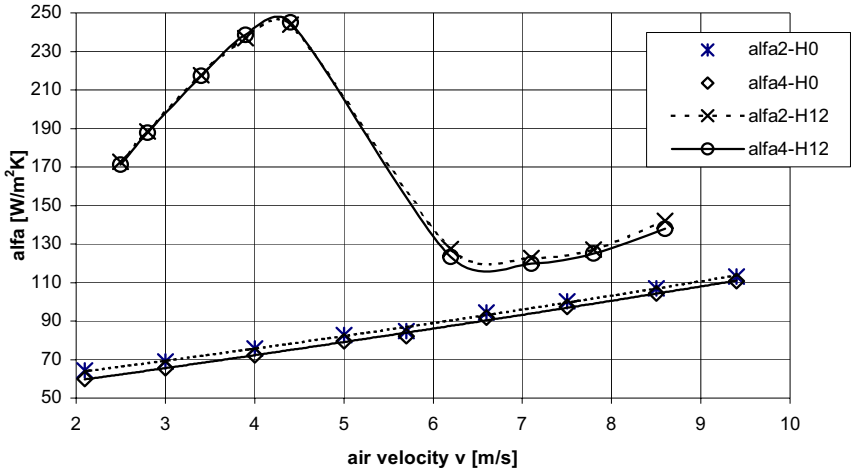

Fig.3. Local heat transfer coefficients for the fluidized bed and air in the function of air velocity

A similar experiment has been conducted for H=9 cm in order to establish the influence of the ratio of the stationary bed height to the column diameter (H/D) so as to allow in the future to record the test results pursuant to the theory of similarity by means of the dimensionless equation, eg of the following type:

$$Nu = f(Re, \frac{H}{D}), \tag{2}$$

where:
Nu – Nusselt's number,
Re – Reynold's number.

The results of the measurements of the local heat coefficients for the beds of stationary heights H=9 cm and H=12 cm are shown in Fig. 4.

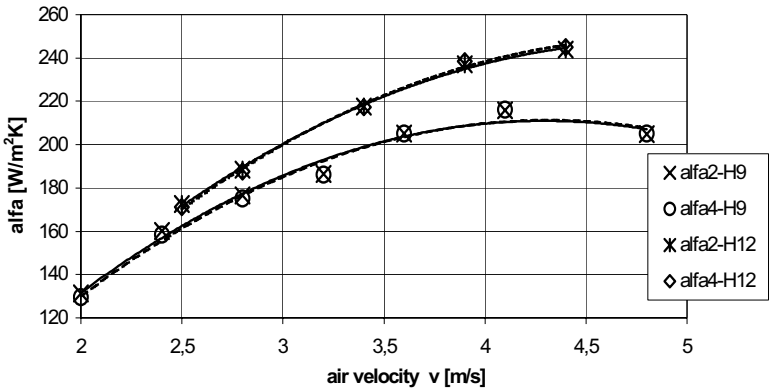

Fig. 4. Local heat transfer coefficients for fluidized bed in the function of the air velocity for poppy seeds for the stationary bed heights of H=9 cm and H=12 cm.

It shows that for bigger stationary height of the bed in the same points higher values of local heat transfer coefficients occur. This can be explained by the higher poppy seed concentration in way of the measurement points. Because of the scarce number of experiments done so far with various stationary heights this tendency cannot be regarded as a lasting or permanent one. With bed heights even bigger the fluidizing nature is likely to be altered, e.g. channelling would occur which would influence the conditions of heat exchange.

The investigation of the fluidized bed during the constant inclination of the column has been an experiment related to the conditions likely to occur in the boiler operation on ship. Figure 5 presents the hydrodynamic characteristics of 9 cm high (in vertical) stationary bed for the constant inclination angle of 30°. In these conditions the bed gets fluidized faster. This is caused by the out-of-parallel location of the bed surface in relation to the grid. The bed movements have been observed already at the velocity of approximately 1.4 m/s in its "more shallow" part. A distinctive circulation of the grains has been noticed as the fluidizing air velocity has been increased upon the bed reaching the full bubbling fluidized condition. The produced circulating movement is of the dextrorotary type (right-sided) with the column inclined to the right and just the opposite – levulorotary type (left-sided) with the inclination to the left. Figure 6 demonstrates the movement of the material in column during inclination to the right.

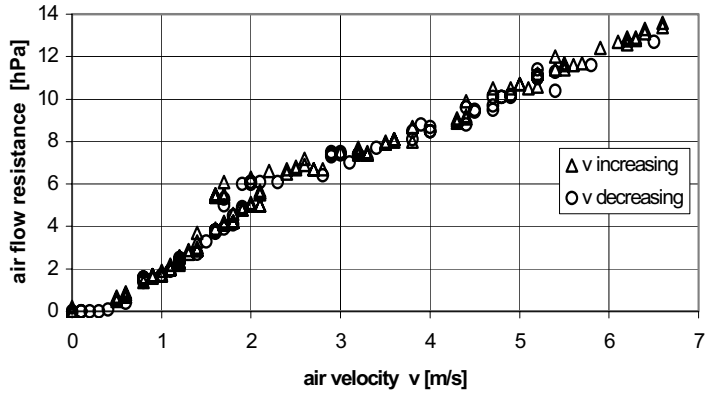

Fig. 5. Hydrodynamic characteristics of the bed (H=9cm) with the column inclined by 30°

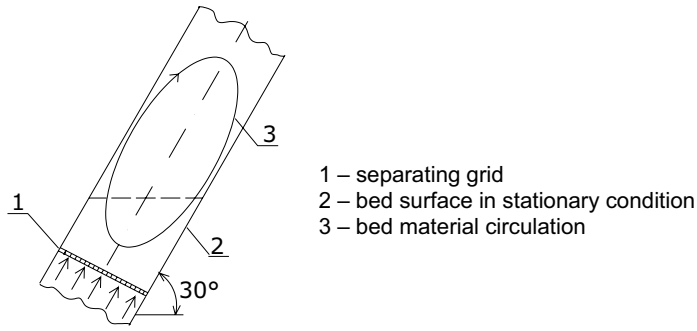

Fig. 6. Diagram of the grain movement in bed

For the purpose of comparison the investigation of the local heat transfer coefficients has been conducted for the column both position in vertical as well as inclined for the bubbling bed. The results of these tests are shown in Fig. 7.

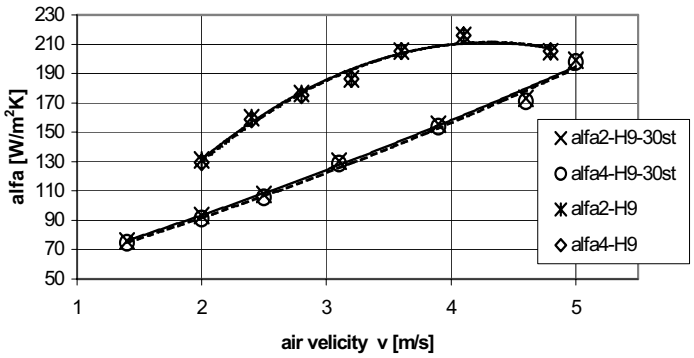

Fig. 7. Local heat transfer coefficients for the fluidized bed in the function of velocity for poppy seeds with the column positioned in vertical and inclined by 30°

The experiment indicates a marked decrease of the local heat transfer coefficients in all measurement points for the column inclined. For the sake of clarity the coefficient values are presented in the axis of column, i.e. in points 2 and 4. The decrease in the value of the coefficients is caused most probably by the poppy seeds circulating movement which has been produced in the bed.

The figures 8, 9 and 10 present on the other hand the values of the local heat transfer coefficients determined along the parallel line to heater axis at the distance of 25 mm above it (measuring points 1, 2 and 3) for the vertical column (Fig. 8), column inclined by 30° to the right (Fig. 9) and inclined by 30° to the left (Fig. 10). In every case values are presented for two different air velocities. The mass of the loose material in both cases has been the same and corresponded to the height of stationary bed in the vertical column H=12 cm. In all cases it can be seen that the biggest value is reached by the heat transfer coefficients in the column axis thus over the heater centre. Slightly less values achieved at the walls may result from the circulation inside bed caused by wall-related effect.

Comparison of the values of the heat transfer coefficients for three column positions looks interesting. Column inclination from the vertical results in reduction of the value of the heat

transfer coefficient at the side towards which the inclination took place. This may be the effect of the differentiation of poppy seeds concentration on both sides of the inclined column.

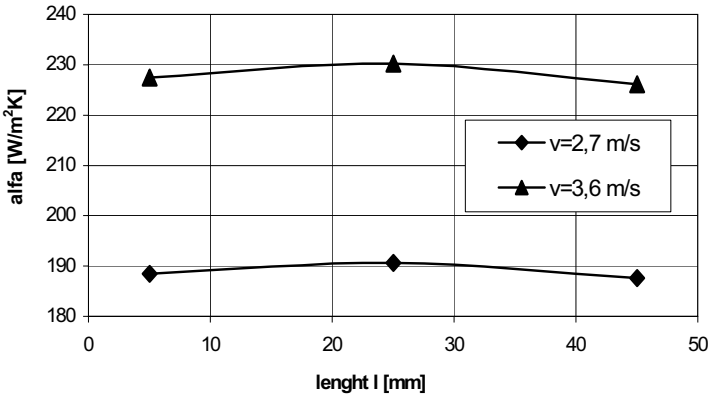

Fig. 8. Values of the local heat transfer coefficients at the line of 25 mm above heater for the vertically positioned column

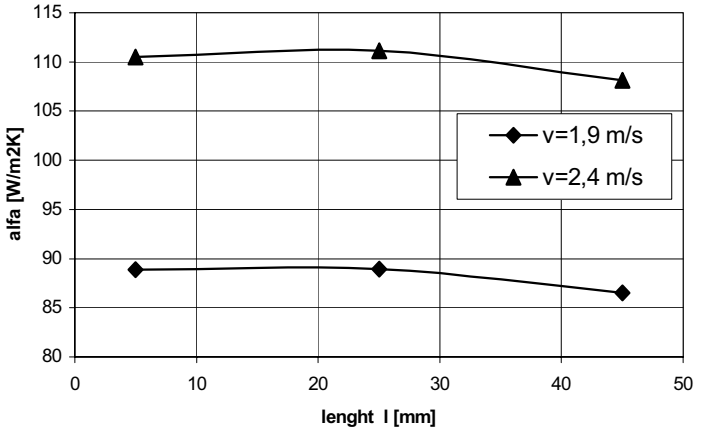

Fig. 9. The values of the local heat transfer coefficients along the line 25 mm above the heater for the column inclined by 30° to the right

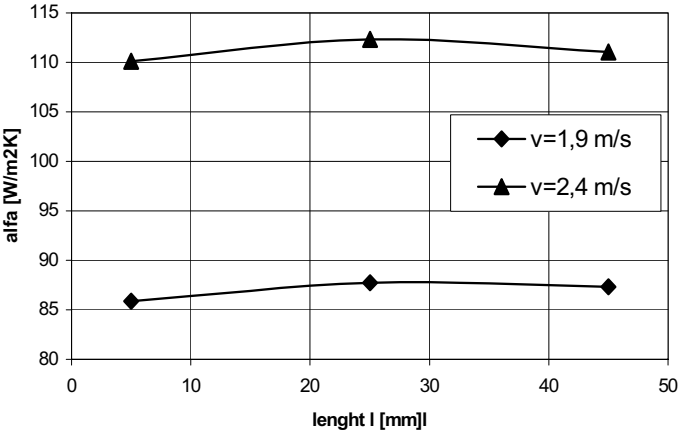

Fig. 10. The values of the local heat transfer coefficients along the line 25 mm above the heater for the column inclined by 30° to the left

The last testing of the bed the results of which are illustrated in Fig. 11 consisted in the determination of the mean values of the local heat transfer coefficients at the parallel line to heater axis 25 mm above it (measuring points 1, 2 and 3) during constant pendular motion of the column in the period of 28 seconds and with the air velocity 3.5 m/s. Getting the column into pendular motion caused the decrease in the mean values of heat transfer coefficients in these points. This is explained by the temporary cyclical dilution of the bed in accordance with the column swing period.

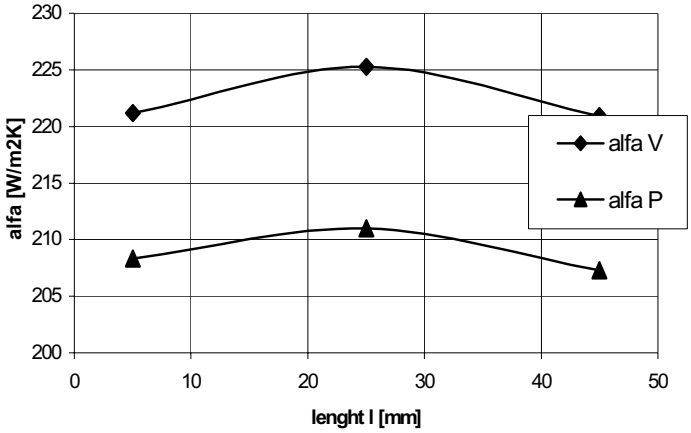

Fig. 11. The values of the local heat transfer coefficients along the line 25 mm above the heater for the column constantly positioned vertically (alpha V) and during constant pendular movement with the 28 s period (alpha P)

4. Conclusions

The presented results of the pilot testing confirm the suitability of the model and the applied method for the bigger scale research. The conditions of the hear transfer are of visibly local nature depending on the mass of the loose material present in the column, on flow-through conditions, on the angle of column positioning and its pendular movement. Further investigations are necessary to determine the relation for the specification of the heat transfer coefficient. From the results obtained for the vertically positioned column which are confirmed in literature it is deemed purposeful to conduct research works mainly for various column positions as well as for the column being in constant motion both with bubbling and circulating fluidized bed.

References

[1] Adamkiewicz, A., Zeńczak, W., *Koncepcja badań modelowych kotłów fluidalnych w aspekcie możliwości ich zastosowania na statkach morskich*, Systems, Vol.11, Special Issue, 1/1 pp. 112-119, Wrocław 2006.

[2] Ciborowski, J., *Fluidyzacja*, Państwowe Wydawnictwo Techniczne, Warszawa 1957.

[3] Geisler, O., Cousin, R., *Untersuchung der zirkulierenden Wirbelschicht im Hinblick auf ihre Eignung für den Schiffsbetrieb*, Abschlußbericht, TU Hamburg-Harburg 1987.

[4] Herzog, H., Drake, E., Adams, E., *CO2 Capture, Reuse and Storage Technologies for Mitigating Global Climate Change*, A White Paper Final Report, Energy Laboratory Massachusetts Institute of Technology, Cambridge 1997.

[5] Nowak, W., *Ograniczenie emisji CO_2*, Archiwum spalania, nr 1-4, Vol. 6, Warszawa 2006.

[6] Probert, T., *Don't coal it a comeback*, Power Engineering International, Vol. 15, Tulsa 2007.

Journal of POLISH CIMAC

Faculty of Ocean Engineering & Ship Technology
GDAŃSK UNIVERSITY OF TECHNOLOGY

FUME EMISSIONS IN INVESTIGATIONS OF EXPLOITATION OF DIESEL ENGINES

Bogdan ŻÓŁTOWSKI

University of Technology and Life Sciencie, BYDGOSZCZ
bogzol@utp.edu.pl

Abstract

The results of the investigations of exploitation emissions the harmful components of the fumes of diesel engines were introduced in the work. Obtained results were subjected to a statistical study according to new computer procedures. Qualitative and quantitative reports were established for the level and kind of emission in reference to the changes of the state of studied engines.

Keywords: combustion engines, toxic fume components, exploitation investigations, environmental protection

1. Introduction

The assumption for researches of this work was the performance of the analysis influence of engine warming on the harmful emission at these states of engine's work, especially concerning climate conditions in Poland. In the range of researches, the analysis of the emission of harmful compounds was performed during the warmed up engine in the neutral race at different temperatures of the environment.

The conducted considerations indicate that researches of the work of high-pressure engines of different destination in the conditions of exploitation take place usually in changeable unsettled conditions, or are a majority of its working time, which considerably influences the general emission of harmful components of fumes.

The contribution of harmful components of fumes diesel engines into total atmosphere pollution is as follows: there are mostly solid particles (PM) and nitro oxides (NOx) in fumes, whilst in smaller amounts there is carbon oxide (CO) and not burned hydrocarbons (HC).

The results of realized in exploitation tests on a chosen group of diesel engines allow to determine, practically and cognitively, important premises in the field of toxic effects of diesel engines on the environment.

2. Research objects

The researches of his work, in the field of recognizing toxic components generated by diesel engines for different technical states and change able external temperature, were performed on a engine S-359. Results of these researches in the range of quality changes of the toxic components of fumes in operation conditions was performer during 2 years of exploitation on the group of 20 vehicles with such engines. The units of the investigative position were showed on Fig. 1.

Fig. 1 General view of test stations

The object of research in this work was S-359 engine with self-acting fusion whose basic technical data is presented in Table 1. It is an engine of a wide practical application, and characterized by small unitary fuel use, good dynamic characteristics and small damageability.

Tab.1. Basic technical data of the engine S- 359 [105]

Cylinder formation	row, vertical
Number of cylinders	6
Cylinder diameter	110 mm
Piston stroke	120 mm
Swept capacity	6,842 dm^3
Compression degree	17
Order of cylinder work	1-5-3-6-2-4
Maximum Power	110 KW with 2800 min^{-1}
Maximum turning moment	438Nm with 1800-2100min^{-1}
Minimum unitary fuel use	224 g/kWh
Statistical angle of pumping beginning	18,5^{0}OWK before GMP
Injection system	Direct
Injection pump	P-76G10
Injection pressure	22MPa

The engine is a running unit for trucks: Star 200 – street, Star 266 – cross-country, produced in Factory in Starachowice (at present: Star Trucks Sp.z o.o). These cars are widely used in the national industry, as well as military service.

The tested combustion engines belong to the group of exploitation objects, used in difficult training conditions of military service. Large and changeable loads of engines implied by inexperienced drivers diversified their technical state, which for the researches of his work posed a challenge in the range of preparing the experiment, its proper realization, and careful concluding and statistical work.

3. The conditions of exploational investigations

It mattered considering the acquisition of different temperatures, in which the engine S-359 was thermally stabilized, and considering the temperature of the air used for running the engine.

Before proceeding with the tests, the following were checked and regulated:

a. technical state of the engine,
b. injection pump at the probing station type PW-8, predestined for testing fuel equipment of high-pressure engines with regard to dosage, performing, according to BN-88/1301-16 velocity characteristics of fuel injection,
c. injectors used for the tests were checked and regulated on an injector probe type PRW-3, performing the evaluation of pressure of the injector's opening, tightness and trickling of the sprayer, and the correctness of fuel spraying,

d. suction and exhaustion valves – according to the manufacturer's suggestions.
e. During the test, the following were registered:
f. multicomponent composition of exhausted fumes of the engine,
g. smoking of fumes with a smokemeter AVL.

Fume tests with respect to the quantity of toxic substances were performer with the use of a multicomponent analyzer of fumes LANCOM, whose general image is presented on the Fig. 2. The analyzer LANCOM enables the measurements of: CO, CH, NO_x, SO_2, fumes temperature and environment temperature.

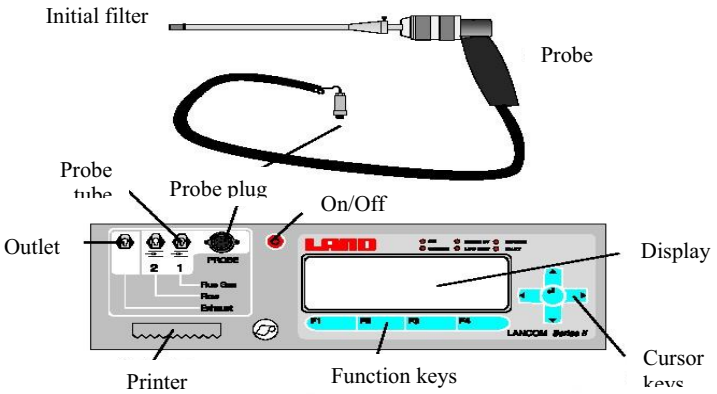

Fig. 2. General image of fume analyzer LANCOM with fume acquisition probe

The measurements of smoking degree of fumes diesel engines were performer with the use of a smokemeter AVL-4000 for the need of further statistical processing, the measured values were saved in a sheet (Excel). Exploitation tests were performed in real conditions on the group of 20 vehicles.

3.1 Testing conditions

The engine, before each test, was subjected to thermal stabilization, thanks to which all elements of the engine and exploitation liquids and exhaust system had the same temperature (for every test) equal to the environment temperature. Environment temperature and motor oil temperature were measured directly prior to each measurement, and if the temperature differences did not exceed 1°C, the measurement began. Also performed were tests in the conditions of a hot start-up. i.e. during a start-up of an engine beforehand warmed up to a normal temperature (oil temp. 80°C) in certain environment conditions. During the measurement, registered were (LANCOM, AVL) the contents of carbon oxides (CO), hydrocarbons (HC), nitro oxides (NO_x) in fumes, motor oil temperature, rotational speed of the crankshaft, environment temperature, and fumes smoking.

Exploitation tests were realized in real conditions on a group of 20 randomly chosen vehicles with the engine S-359 throughout the period of 2 years in a military facility. The tests on toxic substances emission in fumes (CO, HC, NO_x and PM) of diesel engines during a hot start-up (oil and cooling liquid temperature – 70-80^{o}C) were performer at different environment temperatures, with a special consideration of run kilometers of vehicles, and operation-maintenance actions carried out during breaks in tests.

Average daily run of each car was about 70km, which with sustaining the regime of car operation suggested by the manufacturer gives on average about 14000-16000 km per car yearly.

3.2 Exploitation tests results

From the general number of 20 cars subjected to exploitation tests, 10 cars were chosen for the initial analysis, for which checked was the effect of the quantity of emissions of toxic fume components as well as the degree of smoking in relation to run kilometers in the testing period.

The chosen vehicles (num.4) were evaluated in respect of the contents of CO, HC, NO_x in fumes, and smoking of the hot engine, which is shown as an example in the Fig. 3.

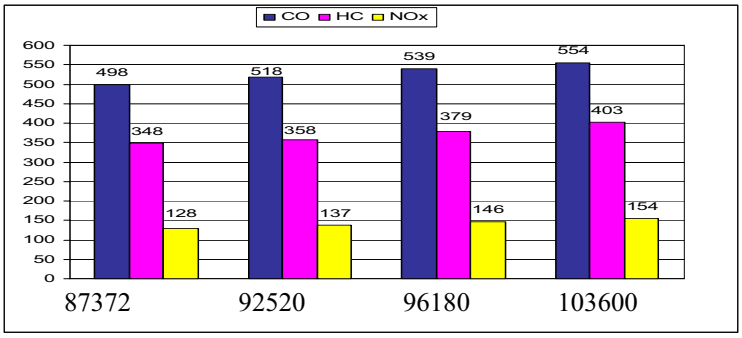

Fig. 3. Overall values of CO, HC, NO_x emissions engine 4 in relation to run km

The following Fig. 4 presents the juxtaposition of values of engine (vehicle num.4) fumes smoking for different km runs of the car.

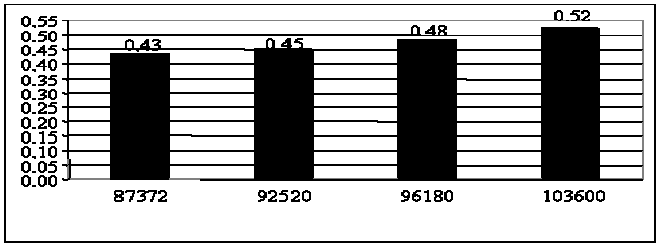

Fig.4. Smoking of 4 engine fumes depending on the km run

The vehicle (num.10) were evaluated in respect of the contents of CO, HC, NO_x in fumes, and smoking of the hot engine, which is shown on the Fig. 5.

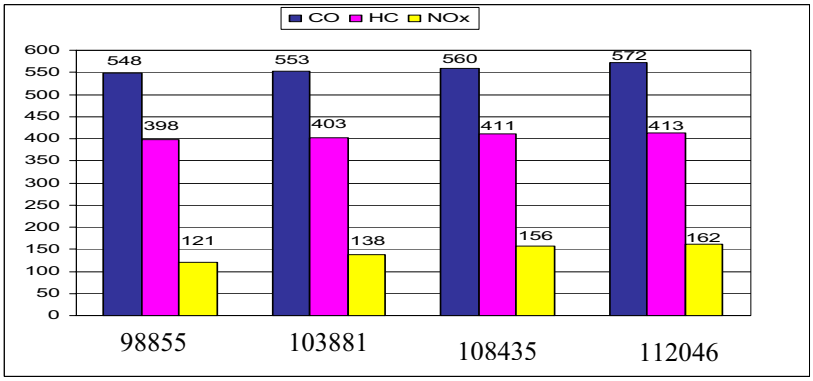

Fig. 5. Overall values of CO, HC, NO_x emissions engine 10 in relation to run km

The following Fig. 6 presents the juxtaposition of values of engine (vehicle num. 10) fumes smoking for different km runs of the car.

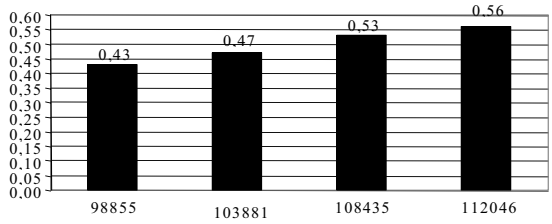

Fig. 6. Smoking of 10 engine fumes depending on the km run

Even brie analysis of the presented results of these tests indicates a visible increase of toxic fume components and engine smoking together with increasing mileage of the car. Other test results of the whole group of 20 cars confirm it visibly. It can be stated that together with the increase of the number of run kilometers, the quantities of carbon oxide (CO), hydrocarbons (HC), nitro oxides (NO_x), and smoking go up.

3.3 Results investigations regress for the exploational investigations

Analysis of the regress for results got in exploational investigations 10 cars were conducted stay for selected about the largest course. Put given these in the Tab. 2 and Fig. 7 represents the results of polynominal regressions, together with coefficient R^2.

Tab. 2 The results of exploitation investigations for chosen 10 vehicles

PARAMETR / NR VEHICLES	CO	HC	N_{ox}	k
1	0,567	0,797	0,978	1,010
4	0,141	0,135	1,000	0,945
5	0,096	0,151	0,389	1,000
8	0,053	0,101	0,153	1,000
9	0,064	0,132	0,101	1,000
10	0,311	0,638	1,000	0,989
11	0,169	0,191	0,311	1,000
15	0,021	0,056	0,044	1,000
18	0,059	0,156	0,250	1,000
19	0,173	0,195	0,461	1,000

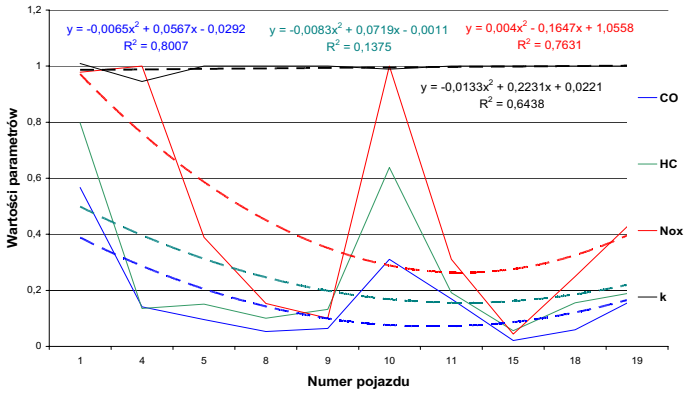

Fig. 7. The date for the polynominal regressions analysis of the studied group of cars

4. Fume test results for engine run on BIO-D10

The possibilities to satisfy increasingly strict regulations force vehicle manufacturers to search new solutions. One of the ways is looking for new, ecologically purer, fuels, among which galenic fuels begin to play a dominant role.

Vegetable oils in their pure form, also colza oil, are not suitable for engines with self-exciting fuse, mainly because of their increased density and viscosity, low cetane number, and insufficient immunity to low temperatures. These disadvantages are absent in products of chemical processes of vegetable oils, called methyl esters, which, combined with diesel oil in appropriate proportions, are called Bio-diesel.

Taking the above into account, quality comparison between diesel oil (ON) and the oil BIO-D10 was carried out during test realization. The comparison of qualities of BIO-D10 fuels with ON, used for tests, is shown in the Table 3. The characteristics of BIO-D10 fuel, produced in refinery Trzebinia are included in the certificate No. 5100634 from 7.10.2005, issued by the manufacturer.

Tab. 3. Comparison of chosen characteristics of test fuels of the engine S-359

Characteristics	Unit	Diesel Oil	BIO-D10
Density at temp. 15°C	g/m^3	0,836	0,841
Kinematical viscosity at temp. 40°C	mm^2/s	2,76	2,82
Fuse temperature	°C	63,5	72
Cetane number		51,1	52,4
Sulfur contents	mg/kg	6,9	4,8
Temperature of cold filter blockage	°C	-30	-25
Remains after incineration	%(m/m)	0,002	0,003
Water contents	mg/kg	68	93

Juxtaposition for easier comparison of emissions of toxic fume components of diesel oil and BIO-D10 during cold and hot start-ups of the engine in diversified environment temperature is presented in the following figures.

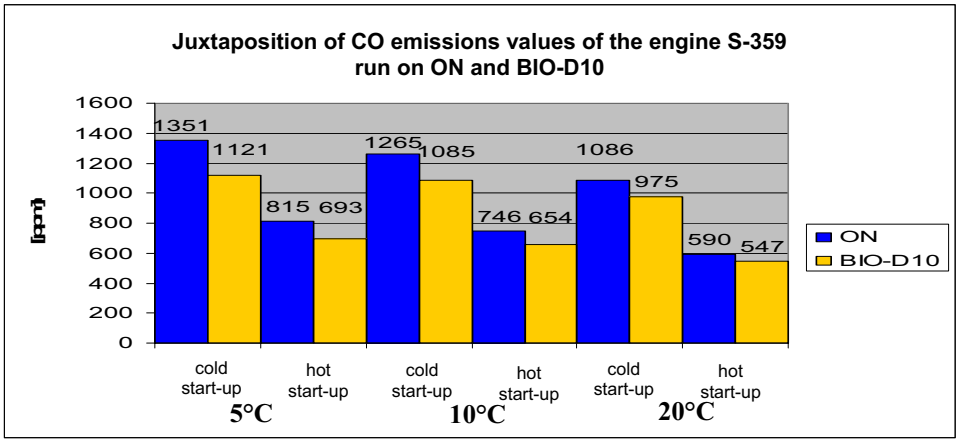

Fig. 8. Juxtaposition of CO emissions values of the engine S-359 run on ON and BIO-D10

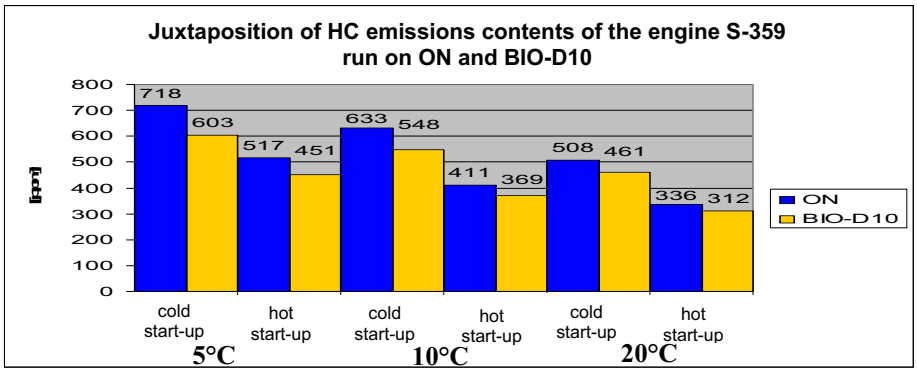

Fig. 9. Juxtaposition of HC emissions contents of the engine S-359 run on ON and BIO-D10

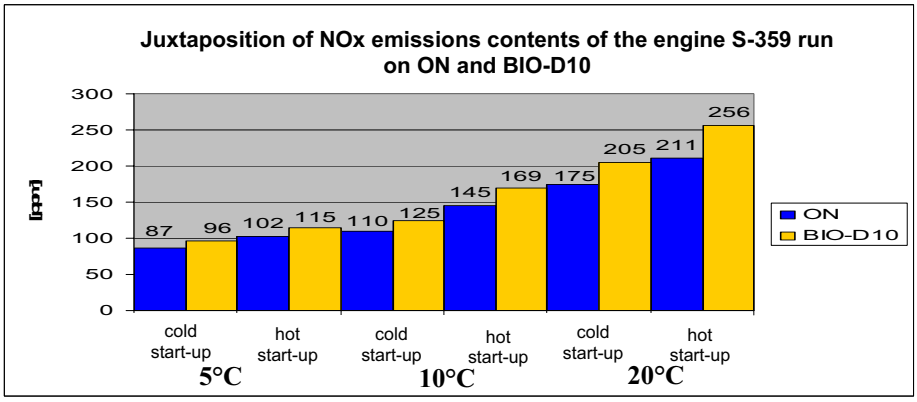

Fig. 10. Juxtaposition of NO_x emissions contents of the engine S-359 run on ON and BIO-D10

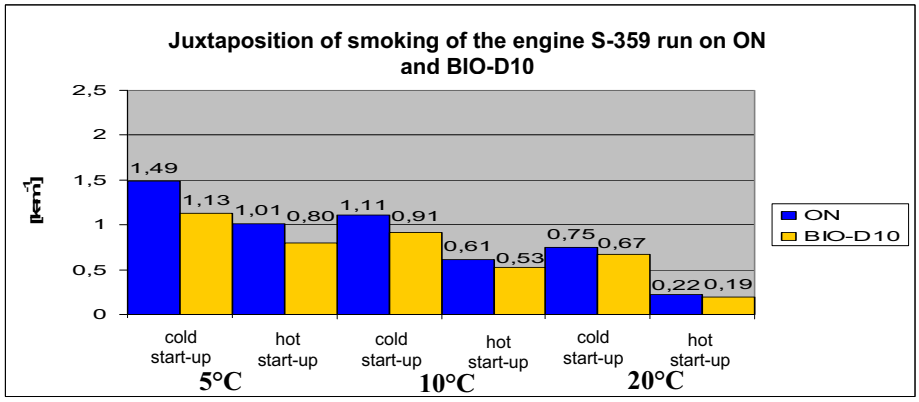

Fig. 11. Juxtaposition of smoking of the engine S-359 run on ON and BIO-D10

As the result of performed tests and result analysis, it was concluded that using the fuel BIO-D10 instead of diesel oil at cold engine start-up, at environment temperature of 5°C, causes

the decrease of emissions of CO with 16%, HC with 13% and smoking with 6%. Whilst the emission of NO_x grows with 10%.

It can also be stated that with the use of BIO-D10 at cold and hot start-ups at environment temperatures of 10°C and 20°C, the contents of CO, HC and smoking in fumes decreases. Whilst the contents of NO_x go up.

The presence of oxygen in the fuel causes the increase of nitro oxides with simultaneous decrease of carbon oxide and hydrocarbons, thus giving easier possibility to regulate toxicity of fumes by delaying the angle of fuel injection initiation. Steering the combustion process can be performer in a much wider range.

5. Summary

The need for detailed analysis of phenomena changes of state destruction of the examined engines, with a vast number of measuring data, requires the use of specialized methods of statistical concluding. The presented results were submitted to statistical analysis, where the methods OPTIMUM and AVD were used, as well as correlation and regression methods. It gave the possibility of quality and quantity comparison of results of fumes contents from stationary tests and exploitation researches. The results of this research allow a model (mathematical relations) determination of relations between smoking and the quantity of toxic fume components of a high-pressure engine.

The performed tests and analyses in his work's researches indicate to the conclusions:

1. In the engine of self-acting fuse (ZS), the emission of carbon oxide (CO), hydrocarbons (HC) and smoking are considerable, especially during start-up and engine warming.
2. Along with the decrease of environment temperature, the emission of CO, HC and smoking increase, whilst the quantity of NOx goes down, providing premises confirming the specified regulations of forming dangers on the side of engine fumes emission.
3. The phases of start-up and warming up of the ZS engine are characterized by increased fuel usage and increased emission of carbon oxide – CO, giving information and sensitizing vehicle users to these harmful for the engine working conditions.
4. The influence of environment temperature on the emission and smoking of fumes during hot start-ups is weaker than during cold start-ups.

References

[1] Kwiatkowski K., Żółtowski B.: *Manners of regeneration of solid particles filters* (in Polish). Materiały Konferencji Regeneracja. Bydgoszcz 2002.
[2] Kwiatkowski K., Żółtowski B.: *Ecological aspects of high-pressure engines affecting* (in Polish). Diagnostyka, vol.26, 2002.
[3] Kwiatkowski K., Żółtowski B.: *Combustion engines – environmental menace*. Teka Komisji Motoryzacji i Energetyki Rolnictwa, PAN, tom III, Lublin 2003.
[4] Kwiatkowski K., Żółtowski B.: *Combustion engines as the source of harmful fumes components* (in Polish). Diagnostyka, vol. 32, 2004.
[5] Kwiatkowski K., Żółtowski B.: *Measurements of fumes composition of combustion engines* (in Polish). Akademia Morska w Szczecinie, ZN nr 5(77), 2005.
[6] Merkisz J.: *Ecological problem of combustion engines*. Vol. 1 and 2 (in Polish). PP, Poznań 1999.
[7] Żółtowski B.: *High-pressure engine diagnosis* (in Polish). ITE, Radom 1995 (s.171).
[8] Żółtowski B., Cempel C. (red.): *Machine diagnostics engineering* (in Polish). ITE Radom, 2004 (s.1109).